OCTOBER, 1952

Journal of METALS

October JOURNAL OF METALS Highlights:

"Rare Earth Additions Improve Cast Steels" - p. 1024
"Century of Progress In Nonferrous Metallurgy" - p. 1033
"Research In Progress" - p. 1039

actual size
and color
LAN CER AMP = 1

this is Lan-cer-amp

—the ingenious combination of rare earth metals which is now conserving vital alloys and improving the physical properties of cast and wrought steel. Every day greater tonnage of Lan-cer-amp treated steel is being produced. Write or call. Let us discuss our latest developments with you.

American Metallurgical Products company

3600 Forbes Street · Pittsburgh 13, Pa.

Journal of **METALS**

VOL. 4, NO. 10 OCTOBER, 1952

Published to provide a continuing, authoritative, and up to date record of technological, engineering, and economic progress in all branches of the metals industry by the
Metals Branch
American Institute of Mining and Metallurgical Engineers, Inc.
29 West 39th Street, New York 18

COVER

An aluminum coating has been formed on this steel cylinder barrel at Fairchild Engine & Airplane Corp., Farmingdale, N. Y., developers of the Al Fin process, prior to casting an aluminum muff against the molten bond layer. Areas where bonding of aluminum is not desired are painted with Acheson Colloids Co.'s Prodag.

NEWS

Journal of Metals Reporter	1023	Employment Service	1008
Trends	1018	Books for Engineers	1014
Drift of Things	1021	Coming Events	1107
Industrial Notes	1019	AIME News	1101
New Products	1003	Personals	1103

TECHNICAL FEATURES

Properties of Cast Steels Improved with Rare Earth Element Additions 1024

Bethlehem Forges Giant Rotor Disks 1032

Nonferrous Metals Engineer Faces Challenge After Century of Progress 1033

New Process Permits Many Metals to Be Tungsten Carbide Coated 1036

Watertown Arsenal Testing Machine Has 72 Years History of Service 1038

Research In Progress—Abstracts of IMD Fall Meeting Papers 1039

TRANSACTIONS

Tungsten-Cobalt-Carbon System 1045

Role of the Binder Phase in Cemented Tungsten Carbide-Cobalt Alloys 1051

High Temperature Oxidation of Some Iron-Chromium Alloys 1057

Strain Patterns in Charpy Impact Specimens of 0.20 Pct C Mild Steel 1067

Intermediate Phases in the Mo-Fe-Co, Mo-Fe-Ni, and Mo-Ni-Co Ternary System 1071

Kinking in Zinc Single Crystal Tension Specimens 1076

Copper-Zinc Constitution Diagram, Redetermined in the Vicinity of the Beta Phase by Means of Quantitative Metallography 1079

Dynamic Formation of Slip Bands in Aluminum 1085

Mechanical Properties of Intermetallic Compounds at Elevated Temperatures 1093

TECHNICAL NOTES

Strain Sensitivity of Commercial Purity Titanium 1050

On the Reversal of the Strain-Induced Martensitic Transformation in the Copper-Zinc System 1065

Diffusion of Silicon in Iron 1070

Formation of Nitrides from Atmospheric Exposure During Creep Rupture of 18 Pct Cr-8 Pct Ni Steel 1083

War on waste!

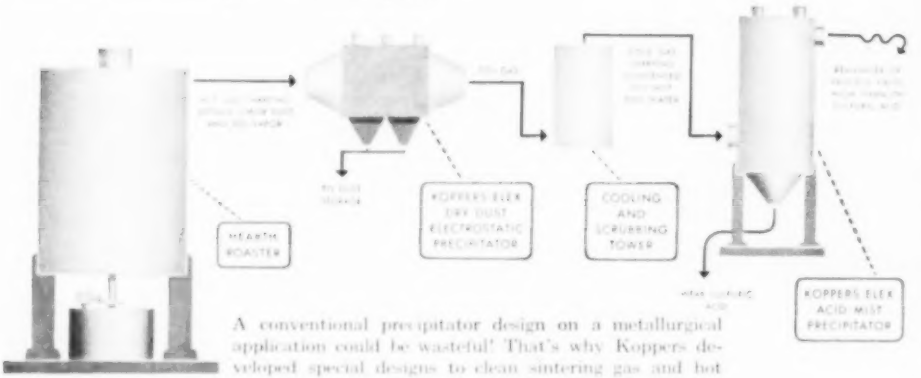
HEARTH ROASTER
KOPPERS ELEX DRY DUST ELECTROSTATIC PRECIPITATOR
COOLING AND SCRUBBING TOWER
KOPPERS ELEX ACID MIST PRECIPITATOR

A conventional precipitator design on a metallurgical application could be wasteful! That's why Koppers developed special designs to clean sintering gas and hot gases from hearth, flash and fluidized roasters. Other types are also available for removal of acid mists.

Koppers-Elex Electrostatic Precipitators offer Guaranteed Rates of Recovery and Nuisance Abatement!

HERE'S THE RECORD*

Koppers engineers analyze each metallurgical gas cleaning and recovery problem individually. Then, based on extensive experience, they give you a specific recommendation of the amount of recovery that can be economically combined with the degree of gas cleaning you require.

A PROFITABLE INVESTMENT . . . that's the report about Koppers-Elex electrostatic precipitators on zinc roaster and acid mist applications. Not only is recovery guaranteed to any efficiency you specify . . . but proper engineering protects you against failure during overloads and production peaks!

Only Koppers gives you the drag scraper which provides continuous dust removal and eliminates plugged hoppers and bothersome dust build-up. Separately energized multiple series fields provide maximum collection of very fine particles . . . and protect your investment because outage of one field does not halt the gas-cleaning action of the precipitator!

Hundreds of Elex precipitators are in use today all over the world. Koppers-Elex electrostatic precipitators are designed, engineered, fabricated and erected under one contract by the Koppers Company . . . and each installation comes complete with "packaged" mechanical or vacuum tube power packs. If you have a gas-cleaning problem, write to: Koppers Company, Inc., Precipitator Dept., 360 Scott St., Baltimore 3, Md.

*Guaranteed: Koppers-Elex precipitators are guaranteed to equal or better, under tests made by your own personnel, any efficiency or residual content you specify.

KOPPERS

Koppers-Elex ELECTROSTATIC PRECIPITATORS

Stokes Microvac Pumps...are basic to Vacuum Processing

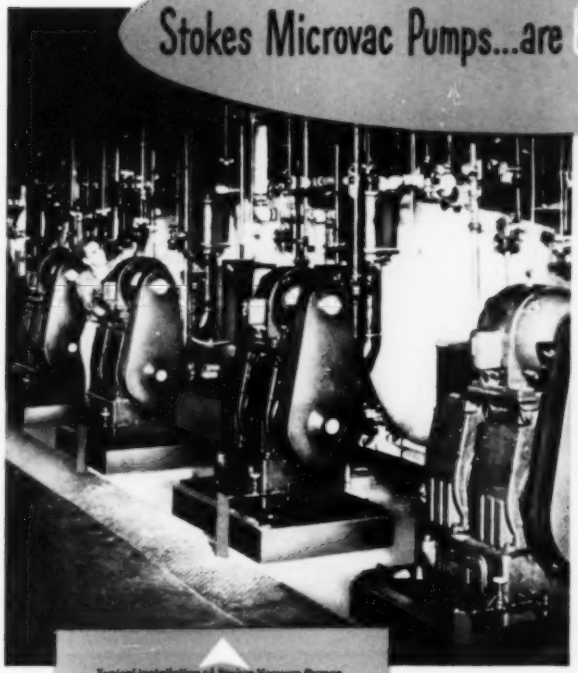

Typical installation of Stokes Vacuum Pumps.

Send for new Vacuum Calculator for rapid slide-rule calculations. Includes standard ABCD log scale. Also send for Catalog 700, "Stokes Microvac Pumps for High Vacuum" with copious reference material.

High volumetric and mechanical efficiency make these famous pumps economical and reliable units in any vacuum system.

Capacities of Stokes Microvac Pumps run from 15 to 500 cfm . . . pressures to 10 microns absolute. Power consumption is low and the top-mounted motor contributes to compact design requiring minimum floor space.

Lubrication of the four moving parts (including the exhaust valve of corrosion-resistant Teflon) is fully automatic. There are no stuffing-boxes or grease-fittings, and no packing.

Parts are precision-finished, standard and interchangeable. Freedom from wear assures years of trouble-proof service.

Stokes is the only manufacturer of equipment for complete vacuum systems, including Microvac mechanical pumps, oil diffusion pumps, McLeod Gages and Vacuum Valves.

Consult with Stokes on the application of vacuum to vacuum sintering, melting, de-gassing, heat treating, inert gas purging, vacuum metallizing, and to other purposes for which vacuum deserves exploration.

STOKES

STOKES MAKES

Plastics Molding Presses,
Industrial Tabletting
and Powder Metal Presses,
Pharmaceutical Equipment,
Vacuum Processing Equipment,
High Vacuum Pumps and Gages,
Special Machinery

F. J. STOKES MACHINE COMPANY, 5516 TABOR ROAD, PHILADELPHIA 20, PA.

IN THIS HEAVY-DUTY CULTIVATOR

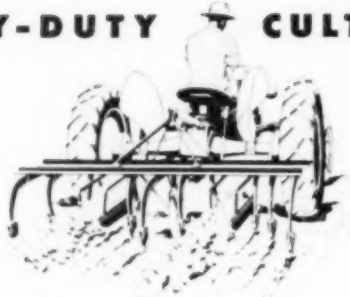

U·S·S CARILLOY steel effectively saves weight, increases durability,

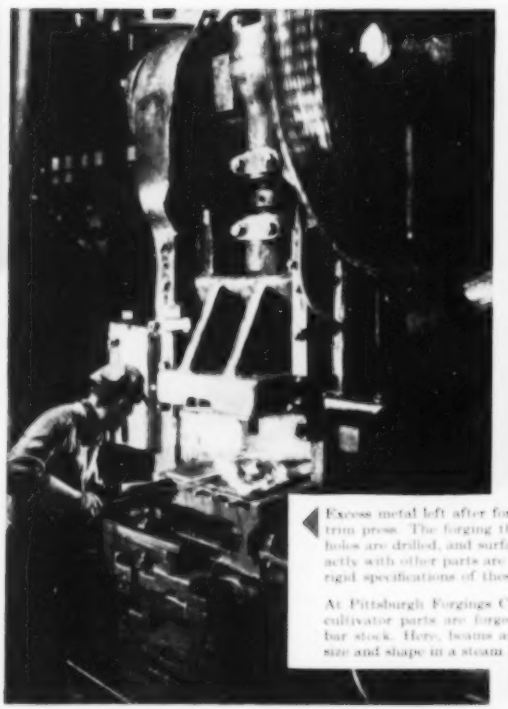

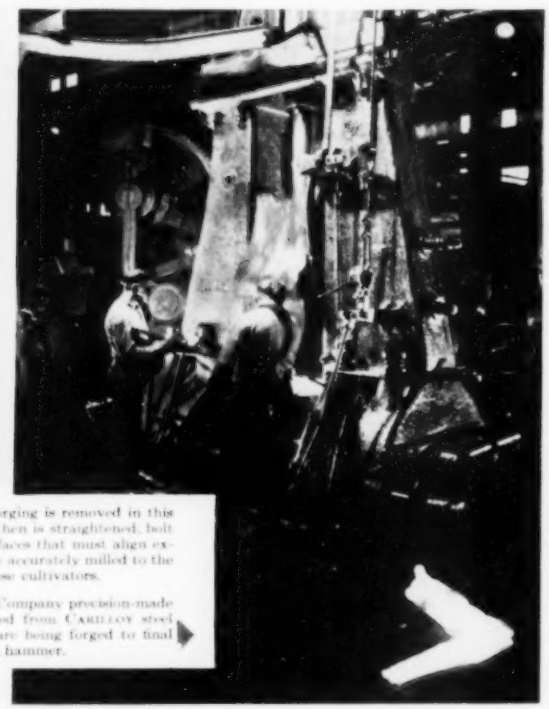

Excess metal left after forging is removed in this trim press. The forging then is straightened, bolt holes are drilled, and surfaces that must align exactly with other parts are accurately milled to the rigid specifications of these cultivators.

At Pittsburgh Forgings Company precision-made cultivator parts are forged from CARILLOY steel bar stock. Here, beams are being forged to final size and shape in a steam hammer.

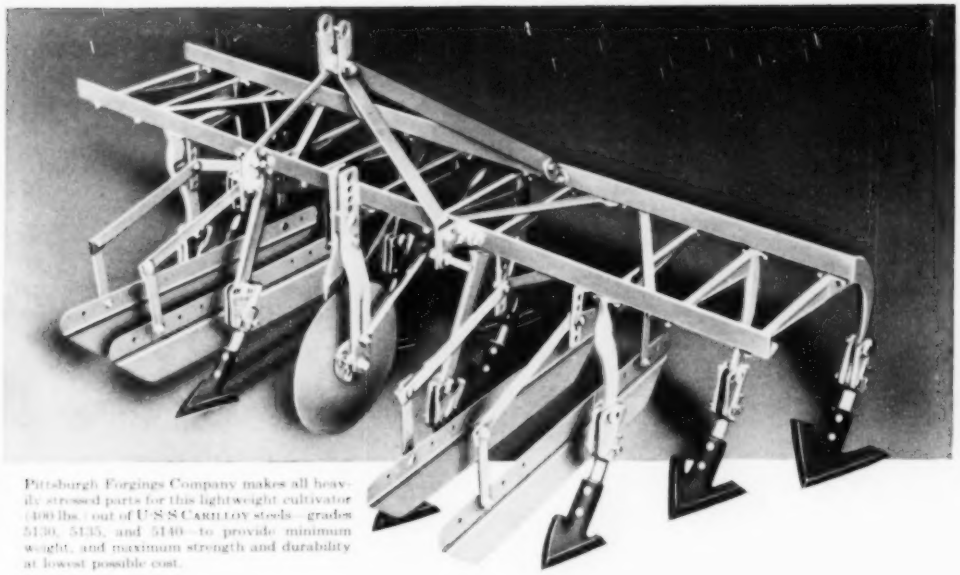

Pittsburgh Forgings Company makes all heavily stressed parts for this lightweight cultivator (400 lbs.) out of U·S·S CARILLOY steels—grades 5130, 5135, and 5140—to provide minimum weight, and maximum strength and durability at lowest possible cost.

and keeps costs down

TO pack the maximum strength into this heavy-duty lift-type cultivator and to keep its weight as low as possible, Pittsburgh Forgings Company of Coraopolis, Pa., has used U·S·S CARILLOY alloy steel in the shanks, beams, and main frame.

The excellent performance this equipment has been delivering is proof that many parts that must operate in extremely tough service can be made of alloy steels that do not contain critical elements. The three grades of U·S·S CARILLOY used here—CARILLOY 5130, 5135, and 5140—were selected by Pittsburgh Forgings Company years ago for the express purpose of providing minimum weight, maximum strength and durability at the lowest possible cost.

Strong and tough to permit speeds up to 6 miles per hour through heavy soil, CARILLOY steel construction has made it possible to reduce cultivator weight to only 400 lbs. This is about half that of comparable units made of ordinary carbon steel—well below the limit which the tractor lifting mechanism is designed to carry, light enough to be easily shifted on the ground by one man.

U·S·S CARILLOY alloy steel does more in this equipment than provide increased strength, greater durability, and added resistance to wear. It enables the manufacturer to safely decrease the size and weight of all heavily stressed parts, with the result that less steel is required and his costs can be kept well in line with competition.

Our metallurgists have had wide experience with similar applications in alloy steels and have developed special heat-treating procedures that make it possible to obtain maximum mechanical properties from them. We will be glad to assist you in selecting the steel and heat treating methods best suited to your product, and we believe we can help you. Just call the nearest District Sales Office, or write to United States Steel, 525 William Penn Place, Pittsburgh 30, Pa.

U·S·S Carilloy Steels

USS

UNITED STATES STEEL COMPANY, PITTSBURGH • COLUMBIA-GENEVA STEEL DIVISION, SAN FRANCISCO
TENNESSEE COAL & IRON DIVISION, FAIRFIELD, ALA. • UNITED STATES STEEL SUPPLY DIVISION, WAREHOUSE DISTRIBUTORS
UNITED STATES STEEL EXPORT COMPANY, NEW YORK

3-1459

UNITED STATES STEEL

MEET THE AUTHORS

H. W. MEAD

PEKKA RAUTALA

H. W. Mead (p. 1070) was born in Kettering, England. He graduated from Sheffield University and has B.Met. and Ph.D. degrees. A member of AIME, Dr. Mead is a research assistant at the Carnegie Institute of Technology. He holds memberships in the Iron and Steel Institute and Institute of Metals. As his hobbies, Dr. Mead enjoys gardening, music and camping.

Pekka Rautala (p. 1043), assistant professor at Massachusetts Institute of Technology, was born in Finland. He attended the Finland Institute of Technology and M.I.T. Prior to coming to the United States, Dr. Rautala had been employed by the Wuokanniska Steel Works in Finland. In 1946 he was a graduate student at M.I.T. and in 1947 was made an assistant professor.

D. K. Das (p. 1071), born in India, is presently working for his Ph.D. at the University of Notre Dame. He is a graduate of the Montana School of Mines (B.S.) 1938 and (M.S.) 1947. He has been employed by various companies in the west gaining mining, milling and smelting experience. As his hobbies he enjoys tennis and home movies.

G. A. Lillieqvist (p. 1024) was born in London and is a graduate of the University of Berne, Switzerland. Dr. Lillieqvist joined the Granite City works of American Steel Foundries in 1924 as a chemist. In 1927 he was transferred to the East Chicago office as research metallurgist, a position he held until 1940. He then was appointed chief metallurgist and located at the Indiana Harbor works. Since 1942 Dr. Lillieqvist has been research director for the firm. A member of the Chicago Section, AIME, he also holds membership in various other professional societies.

D. K. DAS

G. A. LILLIEQVIST

C. G. MICKELSON

J. E. REYNOLDS, JR.

C. G. Mickelson (p. 1024) has been associated with the American Steel Foundries since graduation from the University of Wisconsin (B.S. and M.S.). He has held the positions of chief metallurgist and research metallurgist and in 1951 was named assistant research director. Travel and photography are enjoyed by Mr. Mickelson.

James E. Reynolds, Jr. (p. 1063) is presently engaged in work for his D.Sc. in metallurgical engineering at the Massachusetts Institute of Technology. Born at Bessemer, Ala., he received his B.S. from the University of Alabama (1944) and M.S. from the Missouri School of Mines (1948). For approximately two years, Mr. Reynolds was working on electronics with the Navy. Prior to working for his doctorate at M.I.T., he had been an instructor at the Missouri School of Mines. Photography is the hobby of this AIME member.

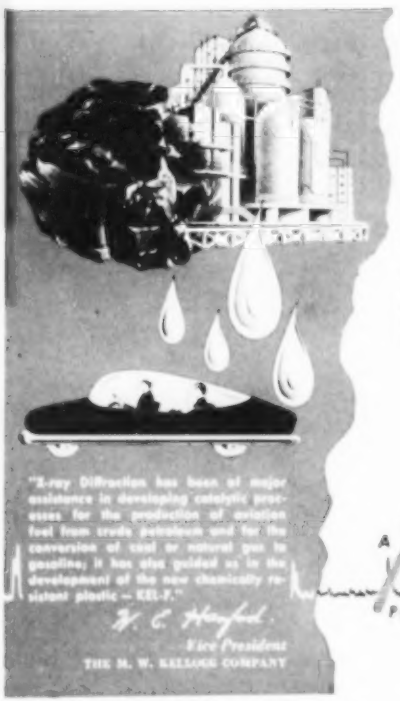
"X-ray Diffraction has been of major assistance in developing catalytic processes for the production of aviation fuel from crude petroleum and for the conversion of coal or natural gas to gasoline; it has also guided us in the development of the new chemically resistant plastic – KEL-F."
W. C. Hanford
Vice President
THE M. W. KELLOGG COMPANY

Synthetic Motor Fuels—New Plastics
Thanks to the *Atomic Third Degree*

Norelco X-ray Diffraction, X-ray Spectrometry, Fluorescence and Absorption Analysis equipment provide American industry with an atomic "third degree," enabling leaders to improve present products, develop amazing new ones.

Norelco X-ray Diffraction equipment is the new non-destructive research tool that permits results impossible for the cruder methods of traditional chemistry. It is the basic laboratory tool through which scientists probe the atomic structure of materials. It is an industrial tool for process control and product development.

Norelco X-ray Diffraction equipment may be the missing link in your own research process. Ask for a free consultation at Philips Applications Laboratories. Meantime, send for free booklet "What is X-ray Diffraction?"

Typical Users

Serving Science and Industry

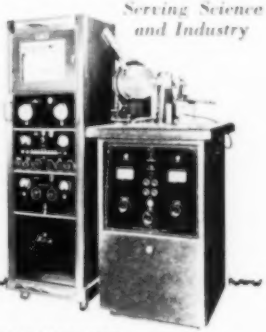

Norelco

A Norelco PRODUCT OF NORTH AMERICAN PHILIPS COMPANY, INC.

Dept. IG-10 • 100 East 42nd St., New York 17, N. Y.

In Canada: Rogers Majestic Electronics Ltd., 11-19 Brockville Road, Leaside, Toronto 17, Ontario

Serving up TONS of Vacuum Melted Metals

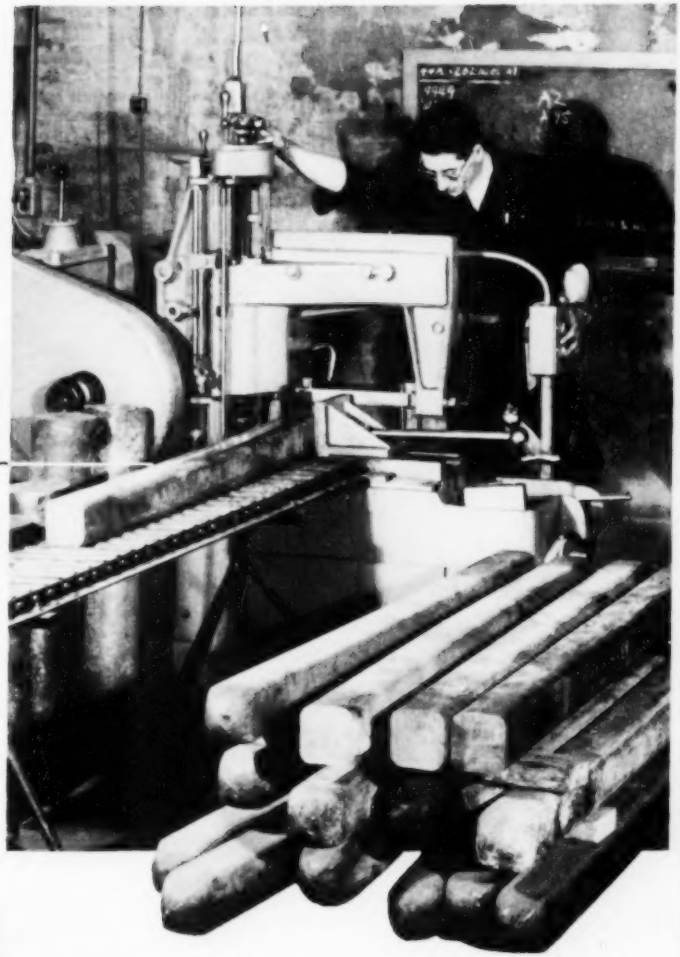

Preparing samples of vacuum melted metals for analysis.

PRODUCTION on vacuum melted metals that was formerly measured in pounds can now be measured in tons. Vacuum Metals' new expanded facilities are capable of producing 5 tons per day of Gas Free High Purity metals and alloys.

Vacuum melting techniques provide metals of higher purity . . . and alloys held to closer composition tolerances than ever before achieved commercially.

The unusual physical, chemical and electrical properties of these metals have proved of particular value for applications such as electronic and electrical parts, magnetic materials, bearing materials, diaphragms, instrument components, and Atomic Energy projects.

Metals now being vacuum melted include copper, nickel, iron, and molybdenum. Further information will be furnished gladly on request.

HIGH PURITY METALS
HIGH VACUUM CASTING
SPECIAL ALLOYS
GF (Gas Free) METALS

VACUUM METALS CORPORATION
Subsidiary of National Research Corporation
70 MEMORIAL DRIVE, CAMBRIDGE 42, MASSACHUSETTS

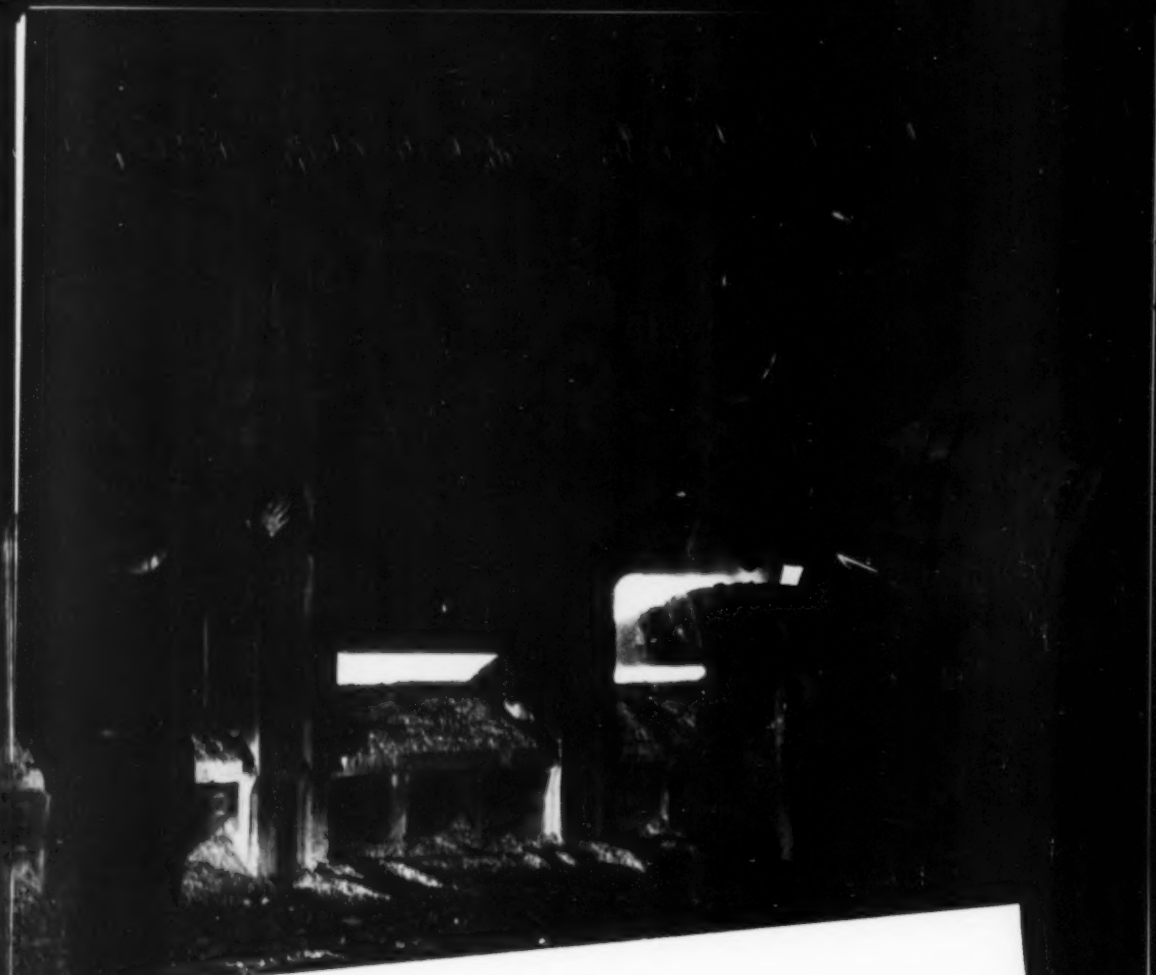

Harbison-Walker Refractories
for every type of furnace in the iron and steel industry

The conditions that affect the life and service of iron and steel furnaces are many and differ widely. To provide the exact kinds of refractories that will enable steel producers to maintain maximum production with greatest economy under all these varying conditions, Harbison-Walker offers the complete range of types and classes for every specific requirement.

Harbison-Walker Refractories Company

AND SUBSIDIARIES

WORLD'S LARGEST PRODUCERS OF REFRACTORIES

General Offices . . . . . Pittsburgh 22, Pennsylvania

HARBISON-WALKER

THE WORLD'S *Most Complete* REFRACTORIES SERVICE

SPECIALIZED REFRACTORIES

for IRON and STEEL producers

BLAST FURNACE REFRACTORIES

For more than half a century, Harbison-Walker Blast Furnace Refractories have been the leading choice of the industry. The major portion of linings currently installed in the United States, Canada, and Mexico are Harbison-Walker brands.

VARNON BF—extremely hard-fired, super-duty fireclay brick, having high strength and density, low porosity and permeability, immunity to disintegration by carbon monoxide, high refractoriness and resistance to slagging.

H-W 18 Pa. and H-W 18 Ky.—hard-burned, high-duty fireclay brick. Exceptionally resistant to abrasion, and to disintegration by carbon monoxide. H-W 18 brick are low in permeability and porosity, have high mechanical strength and excellent volume stability at working temperatures.

BENEZET BF and H-W Ky. BF—for many years the standard refractories for most blast furnaces—for hearth and bosh, inwall and top linings.

BLAST FURNACE STOVE REFRACTORIES

Harbison-Walker brands of high duty and super-duty fireclay refractories fulfill all the exacting requirements for stove linings, domes and checkers.

OPEN-HEARTH and ELECTRICAL STEEL FURNACE REFRACTORIES

STAR SILICA—The long established silica brick. Characterized by high refractoriness, rigidity under load at high temperatures, good resistance to abrasion and fluxing.

VEGA—the super-duty, high temperature silica brick especially suited for extremely severe operating conditions.

VEGA BOND—super-duty silica bonding mortar of excellent workability and super-duty refractoriness; thermal expansion entirely compatible with that of silica brick.

CHROMEX B—extremely hard burned chrome-magnesite brick with excellent volume stability and strength at high temperatures.

CHROMEX—a chemically-bonded chrome-magnesite brick having excellent spalling resistance.

METALKASE—a chemically-bonded metal-encased magnesite-chrome brick. Dense, strong, slag resisting and low spalling tendency.

H-W MAGNESITE—the standard burned magnesite refractory in the steel industry for more than fifty years.

H-W CHROME—a hard burned chrome brick especially adapted for various specific uses.

H-W MAGNAMIX—a magnesite ramming mixture for monolithic bottoms and for patching. Easily installed to the desired contour with great saving in time.

OTHER Iron and Steel Furnace REFRACTORIES

For the widely diversified furnace applications, Harbison-Walker provides refractories which meet every need. These include high-alumina brick of all classes; super-duty and other classes of fireclay refractories; insulating fire brick; high temperature bonding mortars and ramming mixtures; plastics and castables.

Harbison-Walker Refractories Company

AND SUBSIDIARIES

General Offices . . . . . Pittsburgh 22, Pennsylvania

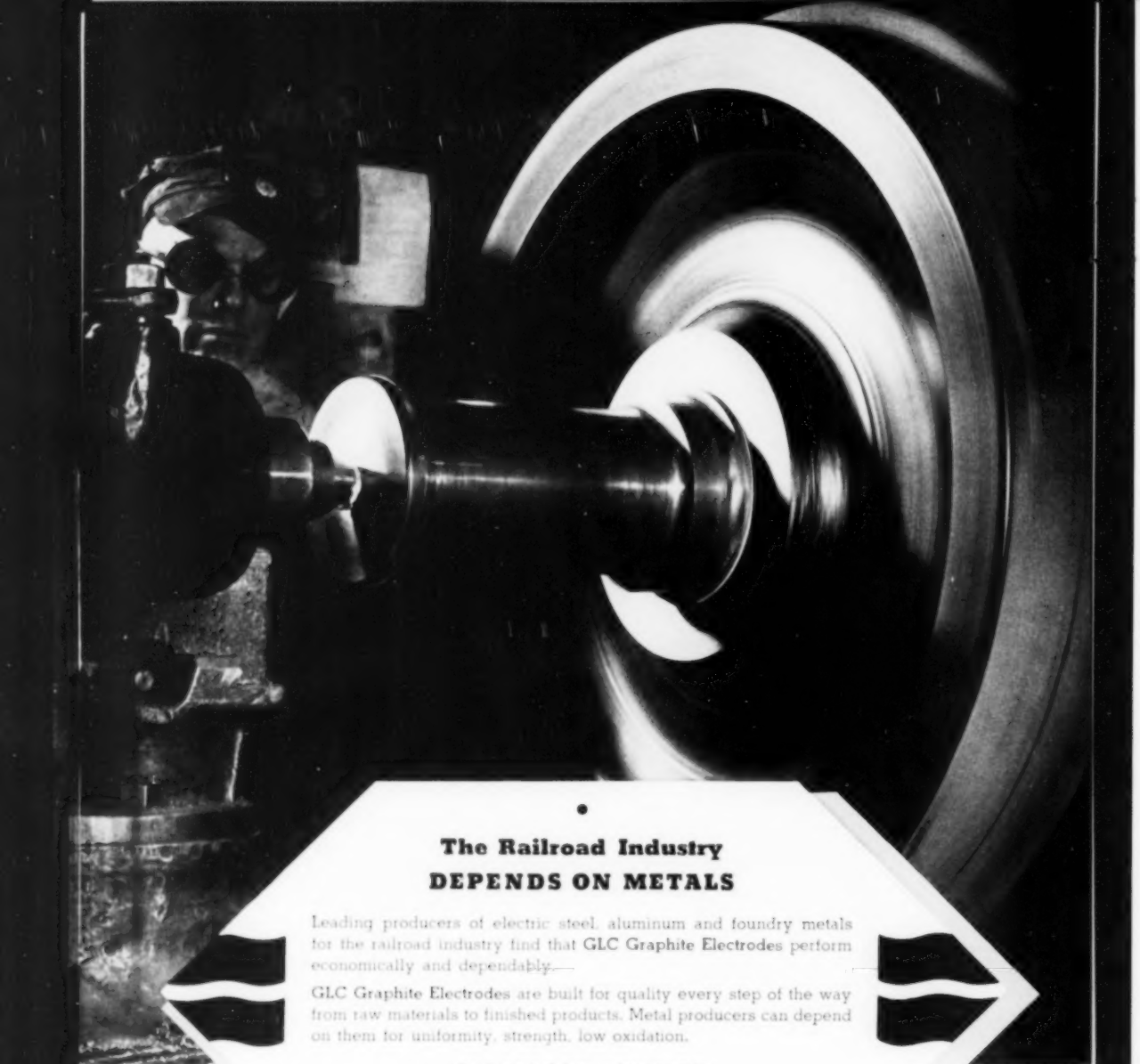

The Railroad Industry
DEPENDS ON METALS

Leading producers of electric steel, aluminum and foundry metals for the railroad industry find that **GLC Graphite Electrodes** perform economically and dependably.

GLC Graphite Electrodes are built for quality every step of the way from raw materials to finished products. Metal producers can depend on them for uniformity, strength, low oxidation.

ELECTRODE DIVISION

Great Lakes Carbon Corporation

Niagara Falls, N. Y. GLC Morganton, N. C.

Graphite Electrodes, Anodes and Specialties

Sales office: Niagara Falls, N. Y. **Other offices:** New York, N. Y., Chicago, Ill., Pittsburgh, Pa.

Sales Agents: U. S. Metals Company, Birmingham, Ala.; George W. Hark, Long Beach, Cal.; Great Northern Carbon & Chemical Co. Ltd., Montreal, Canada

1—SAFETY GUARD: A sheet of transparent, shatter-resistant Plexiglas ⅛ in. thick protects machine operators from flying chips without obstructing view of the work. A

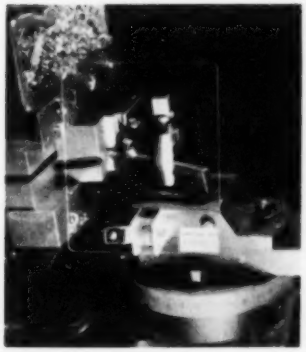

magnet holds the guard securely in any desired position on a machine base. The Alnico slug is surrounded with a Plexiglas ring. This outer surface of acrylic plastic prevents chips from collecting on the magnet. The guard is made in sizes from 6x8 to 12x16 in. *Dilley Mfg. Co.*

2—STEREOMICROSCOPE: Industrial stereomicroscope available from *Bausch & Lomb Optical Co.* embodies vertical eyepiece tubes with adjustments for interpupillary distance and balancing acuity of the observer's eyes, binocular dustproof prism bodies, and illuminator socket. When built into a machine, assembly, or inspection setup, it provides for continuing observation of the operation so that manufacturing and inspection standards can be adhered to.

3—AIR TRANSFORMER: Transformer introduced by *DeVilbiss Co.* has a built-in two stage regulating principle that provides easier adjustment of pressures. In tests, 97 pct of entrained water was removed from 100 cfm of air at 100 lb pressure.

4—GEAR MOTOR: A gear motor designed to simplify maintenance in case of electrical failure of the stator has been announced by the *General Electric Co.* The gear is available in speed ratings of 760 to 13.5 rpm. The new motor is available in ratings of 1 to 75 hp for standard applications and up to 200 hp for special applications.

5—CORROSION LIQUID: Protection of mild steel from corrosion after cleaning can be achieved by application of a recently developed homogeneous solution, Kelite M-2. By absorbing up to 11 pct of its own volume in water without impairment of efficiency, the drying operation prior to treatment is eliminated. *Kelite Products, Inc.*

6—CERAMIC COATING: A ceramic coating developed by the *California Metal Enameling Co.* protects mild steel ladles against molten aluminum.

7—SURVEY METER: A scintillation survey meter developed by *Nuclear Research Corp.* is a self-contained, portable instrument designed for field use in radioactive ore detection. It can be applied to any field in which a sensitive and rapid indication of a gamma ray flux is required. An all electronic high voltage supply is incorporated in the circuit. Instrument ranges for the device are 5.0, 0.5, 0.5 MR/HR. Meter accuracy is ±5 pct of full scale.

8—HYDRAULIC SHEAR: Activated by a 2 hp electric high pressure pump unit equipped with a 3 phase, 220/440 v, 60 cycle motor, this shear is operated by a hand or foot valve control. It is claimed that the new model cuts through steel strip 48 5/16 in. *Masco Mfg. Co.*

9—VARIDRIVE MOTOR: A lightweight Varidrive motor type 5 VA in fractional horsepower equipped with mechanical remote control has

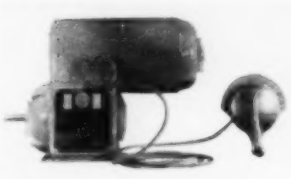

been developed by *U. S. Electrical Motors, Inc.* A control handwheel with indicator dial and a 5-ft flexible cable is included so the speed can be controlled away from the motor. It is available in 1/4, 1/3, 1/2, and 3/4 hp and in a speed ratio up to 10:1 over a range of 4 to 10,000 rpm.

10—DYNAMOMETER: This *W. C. Dillon & Co.* dynamometer does not depend upon springs but works upon the principle of deflecting a calibrated beam. It is not affected by extreme temperature changes. A 5 or 10 in. diam dial is optional and 13 different capacities from 0-500 lb up to 0-100,000 lb can be set.

11—FORMING PRESS: A 300-ton hydraulic press built for making plow beams has a special hydraulic circuit with two pressure cycles in one. The plow beams are bent to a specific angle at low tonnage and are then turned for flattening and high tonnage. A safety feature of the *American Steel Foundries* press, is a thermostat in the reservoir which will automatically stop press operation if the oil reaches a critical temperature.

12—SPEED CHANGER: A miniature adjustable speed changer has been announced by the *Metron Instrument Co.* Speed is controlled by an

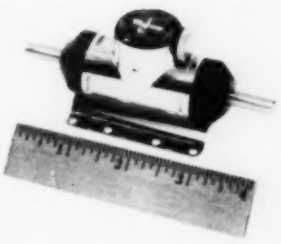

adjusting knob equipped with friction drag to prevent ratio wander. Ball bearings throughout, permanent high-low temperature lubricant, and operation in any position assure easy adaptation under rugged conditions.

13—OPTICAL LEVELER: Newly developed optical level for measuring flatness, straightness, and parallelism reads deviations from the horizontal of 0.00012 in. per ft of length or 0.00001 in. per in. of length. The optical system consists of three bubble phials and two prisms so arranged that twice the usual accuracy of level reading is obtained. *F. T. Griswold Mfg. Co.*

14—MILLING CUTTERS: Staggered tooth, indexable solid carbide blade, side milling cutters have been added to the *Detroit Milling Cutter Co.'s* line of Futurmill cutters. Straddle mills designed to cut on one side only can be made to a minimum thickness of 1 in. or more, depending on the size blade to be used.

15—MAT SWITCHES: A new line of Switchmats, extended area electrical switches in the form of sheets or thin mats, has been announced by the *Revere Co.* Foot pressure on any part of the area covered by the mat closes the circuit and release of pressure instantly opens it. Mats are hermetically sealed against moisture and weather between vinyl, rubber or neoprene. Switchmats can handle up to 1 amp at 110 v directly.

16—AIR DRY LUBRICANT: An air dry lubricant that can be sprayed or brushed on is available from *Electrosilm Corp.* Lubsol has excellent lubrication characteristics at temperatures from −70° to 300°F. It may be applied to steel, iron, stainless steel, lead foil, aluminum, wood, brass, cork, etc. It is resistant to hydraulic fluids, gasoline, lubricating oils, water, etc. Before applying Lubsol, the surface should be free of grease.

Free Literature

20—FLANGED HEADS: Bulletin issued by *Joseph T. Ryerson & Son, Inc.* lists sizes of ASME and standard types of flanged and dished heads available. Heads are suitable for pressure vessels, ladle and melting furnace bottoms, ends for annealing pots, and tanks.

21—INDUCTION MOTORS: Large wound rotor and squirrel cage polyphase induction motors are described in bulletin 37-200 available from *Electric Products Co.* Photographs show special designs of high horsepower motors.

22—ELECTROPOLISHER: A bulletin is offered providing information on the theory and practice of electrolytic polishing of metallurgical samples together with description of No. 1700 AB electro polisher. *Buehler Ltd.*

23—SURFACE GRINDER: Information on various attachments and accessories that can be supplied for the grinder are included in pamphlet obtainable from *Reid Brothers Co.* The grinder is also described in detail.

24—INSULATION: Industrial insulation materials covering temperature range from −150° to 1800°F are illustrated in catalog issued by *Baldwin-Hill Co.* Brief application descriptions with typical uses, sizes, and densities are included.

25—430 STAINLESS: Booklet that helps take much of the mystery out of the use of straight chromium type stainless steels is available from *Sharon Steel Corp.* Detailed fabricating instructions and illustrations of straight-chrome stainless are included.

26—TURBIDITY RECORDER: Data sheet 604 covers TR-6 for measuring amount of light cut off by undissolved substances suspended in fluids. Pertinent information relative to operating principles, and range of application of the turbidity instrument to main line of processing or sampling line is included. *Ess Instrument Co.*

27—HEAT RESISTANT ALLOYS: Publication of interest to users and potential users of stainless and heat resistant alloys in cast form is available from *International Nickel Co.* Charts compare creep strength of various alloys, resistance to corrosion in certain media, and to oxidation at elevated temperatures. Photographs illustrate applications of typical alloys by industry.

28—HACK SAW BLADES: Complete line of *DoAll Co.* hack saw blades is listed in brochure 50-823. Technical data is given on molybdenum blades, tungsten blades, and vanadium alloy steel blades.

29—TESTING MACHINES: Folder illustrating current Amsler machines for tests in tension, compression, torsion, shear, fatigue, bending and ductility may be obtained from *A. J. Buehler.*

30—SPECTROPHOTOMETERS: A new bibliography of applications for these instruments made by *Beckman Instruments, Inc.* is now available. More than 500 specific sources of application data for these analytical instruments are listed.

31—MEEHANITE CASTINGS: Illustrations of applications covering nearly every major industry and complete tables of the physical properties of the various types of materials available are contained in booklet *Meehanite Castings Serve All Industry. Meehanite Metal Corp.*

32—TONNAGE O PRODUCTION: A booklet has been published by the *Blaw-Knox Co.* describing oxygen and other low temperature separation processes as developed by Gesellschaft fuer Linde's Eismaschinen A. B. Included is a description and flowsheet of the Linde-Fraenkl process plus information on typical plant layouts.

33—SNAP ACTION SWITCHES: Catalog 82 published by *Minneapolis-Honeywell Regulator Co.* covers safety, limit, and interlock switches designed for switching ac circuits in industrial and commercial applications.

34—FABRICATED FITTINGS: Data on standard and special fabricated pipe fittings are contained in brochure announced by *Naylor Pipe Co.*

35—SURFACE ACTIVE AGENTS: Many metalworking applications where efficiency can be improved by addition of a small percentage of a surface active agent are discussed in bulletin from *E. F. Houghton & Co.* A chart outlines the physical properties of the leading surface active agents in Cerfak and Surfax that aids in selecting the proper product for various needs.

36—STAINLESS FASTENINGS: A 20-page catalog issued by *Star Stainless Screw Co.* provides detailed product specifications to aid in selecting stainless steel fastenings. All types of nuts, bolts, pins, rivets, studs, etc. are included.

37—METAL CLEANING: Illustrated brochure published by *Kelite Products, Inc.* explains scientific cleaning for modern metal finishing. Information on high speed phosphatizing, removal of heat treat scale, removal of carbon, grease, dyes or gums from aluminum, magnesium, cadmium, copper, zinc, diecast and ferrous metals by soaking in room temperature solutions is given.

Journal of Metals
29 West 39th St.
New York 18, N. Y.

October

1	2	3	4	5	6	7	8	9	10
11	12	13	14	15	16	17	18	19	20
21	22	23	24	25	26	27	28	29	30
31	32	33	34	35	36	37	38	39	40

Name Title

Company

Street

City and Zone State

Freyn-Design

BLAST FURNACES...

are contributing annually

20 million tons of pig iron

to the world need for metallics

METALLURGICAL PLANT DESIGN AND CONSTRUCTION

KOPPERS COMPANY, INC.

KOPPERS

Freyn Engineering

Department

109 NORTH WABASH AVENUE · CHICAGO 2, U.S.A. *Associated with* Ashmore, Benson Pease & Co., Stockton-on-Tees, ENGLAND; De Lattre & Frossard, Paris, FRANCE

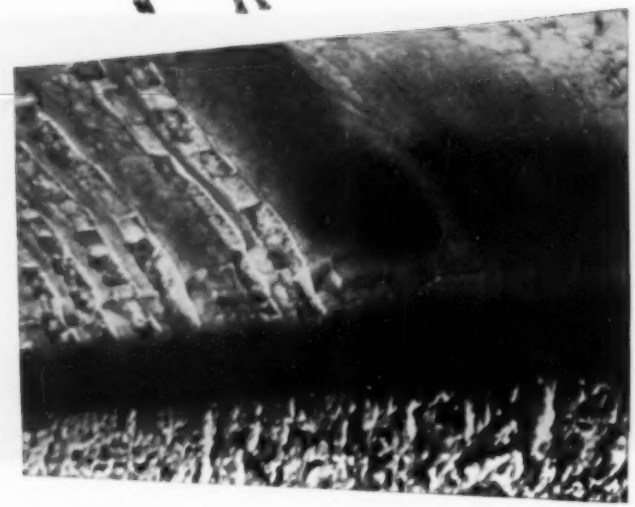

Revolutionary

"ZEBRA ROOFS", built with alternate rings of silica brick and patented STEELKLAD give top performance when open hearths are pushed for peak production. Unretouched photo shows marked superiority of ZEBRA section (on the left) over surrounding silica brick. Many operators report increased roof life despite higher tonnage. Others find reduced repairs to roof and backwalls. More and more plants are standardizing on ZEBRA roofs. Best results are obtained with 3" Silica Keys alternated with 3" or 6" of STEELKLAD.

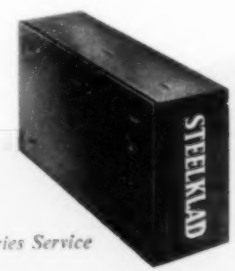

A Complete Refractories Service

GREFCO BASIC BRICK For All Industry

The metallurgical industry demanded furnace linings capable of withstanding extremely high temperatures under extraordinary operating conditions. To meet this challenge, Grefco research produced the famous REFEX unburned basic brick—one of the outstanding advances in the entire history of brick manufacture. REFEX brick possess great accuracy to specified dimensions. They are more resistant to thermal spalling . . . offer lower porosity, lower thermal conductivity, and higher hot strength. These properties insure increased service at reduced cost.

STEELKLAD For Tough Duty

For service too tough even for REFEX, Grefco offers STEELKLAD, an unburned basic brick, permanently jacketed in a patented steel shell. The brick will not slide from its shell in the construction of a furnace wall. When the furnace is heated the steel oxidizes and is absorbed by the brick. It provides an exceptionally efficient monolithic lining that outlasts all other brick in basic open-hearth steel furnaces, electric-arc furnaces, soaking pits, copper smelting and refining furnaces, and other basic metallurgical furnaces.

Take A Look At STEELKLAD

Shown at the left is a typical STEELKLAD basic brick, steel-jacketed on the four major faces, and containing Grefco unburned magnesite-chrome brick. The brick itself is exclusive and patented—as is the permanent steel shell. It may mean major savings in your operation.

Child's Play... *made with brick!*

• Skating down the sidewalk . . . thanks to bearings made with brick. Tiny steel bearings, little brothers to the precision-ground bearings that help move the wheels and shafts of American industry.

The production of steel for bearings—chemicals, glass, metals, for most everything else we use—depends largely on refractories to contain the high temperatures necessary in the furnaces of industry. Such products as Grefco silica brick, a favorite in electrical-steel and open-hearth furnaces, and in coke ovens.

General Refractories Company is one of the two largest producers of silica brick in the world.

Grefco silica brick are available in ever-increasing supply to meet the demands of American enterprise. And, like the thousands of other refractories products made by Grefco, they are the subject of constant research to assure their top quality.

If there's a smokestack in your business—call on the *complete refractories service* offered by Grefco.

GENERAL REFRACTORIES COMPANY

PHILADELPHIA

METALLURGIST

Steel fabricating manufacturer requires a metallurgist to aid in the practical solution of production problems in connection with the resistance welding, arc welding, submerged arc welding, forging, machining, cold forming, and heat treating of carbon, alloy and stainless steels as well as some nonferrous alloys. Should be qualified to advise management regarding the advisability of taking on new materials and products.

This is a new position due to increased use of alloy and stainless steel products. The man selected will have full opportunity to develop the position into an important part of our plant organization.

Applicants should be between the ages of 25 and 30, have an engineering degree in Metallurgy, and have a practical knowledge of steel fabricating methods, including stainless steel. Send resume of background, together with salary requirements, to Personnel Manager.

DRESSER MANUFACTURING DIVISION
Bradford, Pennsylvania
One of the Dresser Industries

A highly successful company located in southern New England is conducting progressive, forward looking research and development in copper, titanium, and other metals. We have a permanent position on our staff for a Physical Metallurgist or Physicist with a doctor's degree. While up to about 2 years' experience is desirable we are looking more for a man of high potentialities rather than experience. If this career opportunity appeals to you, please give us full details of your technical education, experience and interests.

Box H-21, JOURNAL OF METALS.

METALLURGIST (M.S., Ph.D.) or Engineer with interest, and preferably with experience, in X-ray diffraction investigations for application of preferred orientation studies to metallurgical processes.

Apply direct to Head, X-ray Laboratory, Division of Metallurgical Research, Kaiser Aluminum & Chemical Corporation, P.O. Box 1431, Spokane 10, Washington.

Personnel Service

The following employment items are made available to AIME members as a service feature by the Engineering Societies Personnel Service, Inc., operating in cooperation with the Four Founder Societies. Local offices of the Service are at 29 W. 39th St., New York 18; 57 Post St., San Francisco 4; 1 Wacker Dr., Chicago 1. Applicants should address all mail to the proper key numbers in care of the Service, 29 W. 39th St., New York 18, N. Y. Applications should be made on the forms provided by the Service. AIME members may secure a supply (limit of 6 forms available for $1.50 a quarter, $2.50 a year).

POSITIONS OPEN

Sales Engineer, 30 to 40, with thorough engineering training in the chemical-metallurgical fields, for new company organized to develop, manufacture and market super-refractory materials and compounds for industries engaged in metal production, abrasives, furnace linings, etc. Must be willing to travel. Salary open. Location, New York. Y-7478.

Engineers, (a) General superintendent, with broad supervisory experience in heavy metal fabrication involving welding, machining, and assembly operations. Must have proven ability to solve administrative and technical operating problems arising from plant expansion and revision of product. (b) Chief engineer with experience in all phases of engineering, preferably in heavy metal fabrication involving welding and machining operations. Position involves responsibility for production engineering, industrial engineering and layout and maintenance of plant buildings and manufacturing facilities. Write giving full details including salary requirements. Location, upstate New York. Y-7472.

Junior Chemical or Metallurgical Engineer interested in powder metallurgy, to perform tests with different binders on iron powders for transformer cores. Must be citizen. Salary, $3380 to $3900 a year. Location, New York. Y-7422.

Sales Engineers, preferably with one to two years' experience in industrial sales of electrometallurgical products. New York-New England territory. Salary, $4800 a year. Headquarters, New York. Y-7378.

Assistant Welding Engineer, 25 to 35, with metallurgical degree and several years' industrial experience dealing directly with welding problems of both a technical and production nature. Apply by letter stating qualifications, present employer, and salary requirements. Salary, $5400 to $7200 a year. Location, upstate New York. Y-7256.

POSITION WANTED

METALLURGIST, research, age 40. Recovery of molybdenum metals from refractory ores, sparing furnace, electrolytic and leaching methods. Experience with copper, silver, zinc, cadmium, selenium, tin, lead, and others. Also metal powders.
Box E-12, JOURNAL OF METALS.

METALLURGIST. A recent graduate is desired for research and development work in copper, titanium and other metals. This is an opportunity for a permanent position with a progressive and highly successful company in southern New England. Please give details of education, experience and interests.
Box H-20, JOURNAL OF METALS.

LITERATURE RESEARCH CHEMISTS

Needed for broad research programs in varied fields of chemistry, chemical engineering, and metallurgy. Degree in chemistry necessary. Some experience as literature chemist and reading knowledge of German desirable. Please send complete resume of background and experience to

Assistant Director for Personnel
Armour Research Foundation of
Illinois Institute of Technology
Chicago 16, Illinois

METALLOGRAPHER

Sylvania's metallurgy laboratories located at Sylvania Center, Bayside, Long Island, need a metallographer technician. 2 years' technical college highly desirable or sufficiently great experience in the field; must have 5 years' experience in industrial or academic metallography laboratory. Experience should be in more than one metal. Some supervisory experience desirable. Must be capable of investigating new techniques and putting them into operation.

Send complete resume to:
Manager of Personnel

SYLVANIA
Electric Products, Inc.
P. O. Box 6, Bayside, L. I., N. Y.

TECHNICAL RESEARCH ENGINEER

Experienced man with mechanical and chemical engineering background. Should have strong bent for converting research results into workable industrial equipment; should also be able to carry out essential research in this connection. Versatility and energy are prime requisites. Initial effort will be in the field of high vacuum continuous coating.

Please send resume to:

NATIONAL RESEARCH CORPORATION
70 Memorial Drive
Cambridge 42, Massachusetts

Metallurgists, junior, to participate in applied research in the field of high temperature metallurgy. Creep, fatigue, lean alloy development, and metal joining research and related problems. Salary, $3900 a year. Location, western New York. Y-7254.

Sales Engineer, 25 to 30, preferably married, with mechanical, chemical, electrical or metallurgical degree, and three to five years' experience selling industrial equipment for application and sale of industrial burner systems by mail and by direct personal solicitation. Field travel away from home frequently required. Salary, $4800 to $6000 a year depending on experience and qualifications. Location, Indiana. Company will pay fee. Y-7233.

Assistant Mill Superintendent at property using magnetic, gravity and flotation processes. Sound metallurgical and operating background required. Large progressive organization. Salary open. Location, upstate New York. Y-6200.

Metallurgist with engineering or physics and four years' experience in light metals and familiarity with Government specifications related to heat treating, plating, finishing, magnafluxing. Salary, $5200 to $5800 a year. Location, Michigan. Y-6176(c).

Metallurgist, recent graduate, for test work, preparation of material specifications, heat treatment, welding, annealing at heavy industry manufacturing plant. Location, central Pennsylvania. Y-6111.

Chemists, Chemical Engineers and Metallurgists, B.S., M.S., Ph.D., for process design, development and pilot plant, analytical laboratory and plant technical service. Position offers opportunity to become familiar with latest developments in ore processing, metal refining and fabrication. Salary open. Location, southern Ohio. Y-6042.

Concentrator Metallurgist, 30 to 35, graduate in ore dressing with practical experience, to take charge of laboratory testing for large mining company. Spanish helpful. Three year contract, transportation, living quarters. Location, South America. Y-6010.

Metallurgical Product Engineer, recent graduate, B.S. in metallurgy, for product engineering work on rod and wire. Excellent living conditions; housing available. Reply giving training, experience, age, salary desired, etc. Location, northern Pennsylvania. Y-5832.

Engineers. (a) Metal processing engineer familiar with metal processing equipment for smelting, forging and rolling. Liaison between research laboratory and production personnel. Emphasis is on the equipment aspects of processing, but appreciation of the metallurgical factors involved is important. (b) Junior research physical metallurgist, recent graduate, to work in research lab assisting experienced metallurgist in the physical metallurgy research of a series of new alloys. Liking and aptitude for laboratory work essential and experimental resourcefulness desirable. (c) Senior research physical metallurgist, to conduct alloy research on a new series of materials. Advanced degree in physical metallurgy or its equivalent in metallurgical research necessary. Location, Midwest Area. Y-5826.

Chief Engineer, to 45, training and experience in mining, chemical or metallurgical engineering. To administer and coordinate engineering for chemical operating company handling design and construction of new facilities. Salary to $20,000 a year. Employer may negotiate fee. Location, Chicago. R-9152.

Teacher to lecture in metallurgy. Salary open. Location, Israel. Y7209.

Metallurgist, at least five years' experience in nonferrous metallurgical work. Knowledge of electrical equipment helpful. Will do research and administration work on copper base and aluminum alloys used for electrical equipment. Salary, $7000 to $8000 per year. Employer may pay fee or negotiate same. Location, Alabama. T8663.

Cut Cost to a Minimum with

Wanted! ... for ...

THE DEMOLITION and REMOVAL EXPERTS

THE BEST EQUIPPED ORGANIZATION IN THE FIELD FOR DOING THE JOB QUICKER, BETTER AND AT LESS COST

- Furnace Tear Outs
- Salamander or Slag Removal
- Material Handling

24 Hour Service, 7 Days Per Week

World Wide Reputation

Consult Us on Your Next Removal Problem

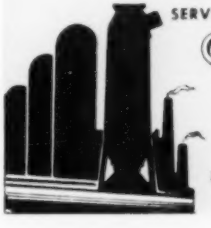

SERVING THE STEEL INDUSTRY FOR OVER 30 YEARS

CHICAGO CONCRETE BREAKING CO.

EDWARD GRAY, *President*

PITTSBURGH, PA.
530 Wm. Penn Place
ATlantic 1-4674

GENERAL OFFICES:
12233 Avenue O, Chicago 33, Ill.
BAyport 1-8400

NOW

You can afford a High Vacuum Furnace

This ONE

Versatile Unit lets you melt, pour, heat treat, degas

At last there is now available a single furnace that does away with the need to purchase equipment for each phase of your high vacuum, high temperature work. Because of its modest price, it will fall within the budget of most laboratories.

With this new furnace you can melt and solidify — melt and pour — add to the melt — stir — look into the hot zone — measure hot zone temperatures — introduce controlled atmospheres — degas — heat treat. It's a complete, versatile unit, capable of handling the widest variety of metallurgical research work. Write today.

FEATURES –

- Ultimate vacuum of less than 5×10^{-5} mm Hg.
- Heating element temperatures up to 2000° C.
- Temperature controllable within ± 5° C.
- Hot zone reaches temperature within one minute.
- No refractories used in hot zone.
- 4" purifying type diffusion pump insures high capacity for out gassing.
- Utilizes single turn low voltage resistance element of tungsten.
- Integral power supply.
- Either manual or automatic temperature control or both.

National Research Corporation

Equipment Division

Seventy Memorial Drive, Cambridge, Massachusetts

The burner block is the heart of your fuel-fired furnace

TASIL Burner Block installed in a No. 225-4 Dual Fuel Burner of the North American Manufacturing Co., Cleveland, Ohio, leading producers of industrial fuel-burning equipment. TASIL Burner Blocks are standard equipment on North American burners for high temperature applications.

The better burner block is TAYLOR SILLIMANITE!

PRE-FIRED BURNER BLOCKS of Taylor Sillimanite (TASIL) are preferred by North American and a majority of leading furnace and burner manufacturers for high temperature applications. TASIL is specified because the block must hold original contour and dimensions. Compared to blocks made of fireclay or most other refractory materials, TASIL has superior resistance to shrinkage, cracking or spalling. TASIL further qualifies because it is inert in either oxidizing or reducing atmospheres; has higher fusion point and resistance to corrosion by most industrial slags. For longer service from your heating, annealing or forging furnaces, specify TASIL burner blocks.

In an emergency, when a burner block failure occurs at the time your stocks of pre-fired shapes are depleted, you can ram your own TASIL Burner Blocks, on the job, with one of several TASIL Ramming Mixes *engineered* for this application. Burner Blocks which may be cast or poured in molds, air dried and placed in service can also be made from TASIL Hydrocast—the hydraulic-setting castable for use to 3000° F. Data on TASIL Ramming Mixes are given in Bulletin No. 515 . . . on TASIL Hydrocast, Bulletin No. 515. Write direct, or contact your Taylor field representative, for your free copies.

Exclusive Agents in Canada:
REFRACTORIES ENGINEERING AND SUPPLIES, LTD.
Hamilton and Montreal

The CHAS. TAYLOR SONS Co.
A SUBSIDIARY OF NATIONAL LEAD COMPANY
REFRACTORIES SINCE 1864 • CINCINNATI • OHIO • U. S. A.

For peak performance..

choose the control that suits *your furnace*

FOR STRAIGHT LINE TEMPERATURE RECORDS like this

When heat input should vary like this . . .

. . . choose **Electr-O-Line**

ELECTRIC PROPORTIONAL CONTROL

This position-proportioning control throttles the fuel valve in exact response to changes in heat demand . . . provides proportional action for quick correction of temporary upsets, plus automatic reset to take care of changes in load, fuel pressure, etc.

When heat input should vary like this . . .

. . . choose **Electr-O-Pulse**

ELECTRIC PROPORTIONAL CONTROL

Applicable to electric furnaces and to many fuel-fired units, this control delivers full heat input in pulses . . . varying the ratio of "heat on" to "heat off" time to control average input. It incorporates both proportional and reset actions.

. . . choose Manual Reset Control for less critical applications; has position-proportioning action with manually operated reset.

* *The difference in control action lies in this relay . . . an integral part of the* **ElectroniK** *Controller.*

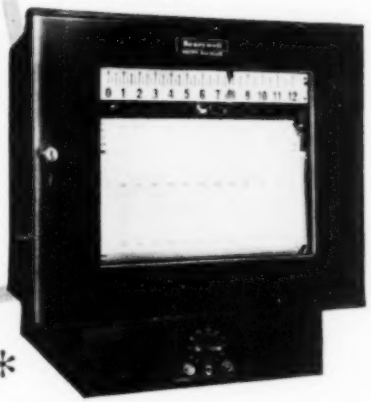

Whatever your type of furnace, Honeywell electric proportioning control will assure top quality performance and maximum output. Independent tuning adjustments, space-saving installation, plug-in construction, and approach rate adjustment are but a few of their plus values.

Your local Honeywell engineer will be glad to recommend the right control for your furnace. Call him today . . . he is as near as your phone.

MINNEAPOLIS-HONEYWELL REGULATOR CO., *Industrial Division*, 4573 Wayne Ave., Philadelphia 44, Pa.

MINNEAPOLIS **Honeywell**

BROWN INSTRUMENTS

First in Controls

● *Important Reference Data*

Write for Catalog 15-15, "ElectroniK Potentiometers with Electric Proportioning Control".

Banish the "Bite"

ON PICKLING AND PLATING EQUIPMENT

with these NATIONAL (TRADE-MARK) CARBON AND GRAPHITE AND KARBATE (BRAND) IMPERVIOUS GRAPHITE PRODUCTS

Pickling and tinning are messy, expensive – and *necessary*. However, you can *greatly reduce* equipment maintenance costs and improve plant housekeeping by making full use of these National Carbon products wherever service is dirty and tough. As is well known by manufacturers of your pickling and plating *solutions*, only carbon and graphite and impervious graphite withstand the "bite" of so wide a range of corrosive chemicals.

HERE'S WHERE THEY'RE USED:

STAINLESS PICKLING

Carbon brick tank linings with "Karbate" Plate-Type Heat Exchangers and drain lines offer powerful resistance to nitric-hydrofluoric solutions.

ELECTROLYTIC PLATING

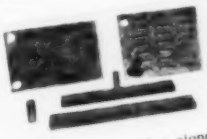

Graphite Anodes, either alone or in combination with dissolving-type anodes, are non-contaminating and long lasting.

Various immersion-type and shell-and-tube type "Karbate" Heat Exchangers are available to suit capacity requirements.

CARBON STEEL PICKLING

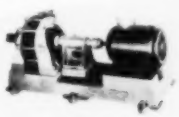

"Karbate" pumps and piping resist sulphuric and hydrochloric acid attack — protect solution from contamination.

"Karbate" Shell-and-Tube Heat Exchangers are often most economical where more than 50 square feet of heat transfer surface is required.

Graphite Tank Rolls provide an ideal combination of good electrical conductivity and resistance to acid attack in electrolytic pickling operations.

The terms "Karbate" and "National" are registered trade-marks of Union Carbide and Carbon Corporation

NATIONAL CARBON COMPANY
A Division of Union Carbide and Carbon Corporation
30 East 42nd Street, New York 17, New York

District Sales Offices: Atlanta, Chicago, Dallas, Kansas City, New York, Pittsburgh, San Francisco
IN CANADA: National Carbon Limited, Montreal, Toronto, Winnipeg

WRITE FOR CATALOG SECTION—S-5005

OTHER NATIONAL CARBON PRODUCTS

BLAST FURNACE LININGS • BRICK • CINDER NOTCH LINERS • CINDER NOTCH PLUGS • SKIMMER BLOCKS • SPLASH PLATES • RUNOUT TROUGH LINERS • MOLD PLUGS • TANK HEATERS

Books for Engineers

Ferromagnetic Properties of Metals and Alloys, by E. Houldin. *Oxford University Press*. $8.00. 317 pp., 1952.—The volume is one of a series using recent research results on materials. It gives a comprehensive account of theories of the magnetization curve, and attempts to demonstrate the connection between properties obtained in practice and existing theoretical explanations. The composition and properties of soft magnetic materials, as well as those of magnetically hard alloys, are fully described. The book also deals with methods of magnetic analysis for the determination of the constitution and structure of ferromagnetic metals and alloys, and with the potential application of magnetic methods to metallurgical problems.

Steel Defects and Their Detection, by Henry Thompson. *Sir Isaac Pitman & Sons, Ltd.* 15s, 65 pp., 1952.—The book gives a description of the characteristic common defects associated with steel ingots and with the rolling processes. Both macroscopic and microscopic tests are described and the microscopic constituents of steel are illustrated. The last chapter covers special methods; magnetic, fluorescent, electronic, and supersonic flaw detection; spark testing; and magnetic sorting.

Progress in Metal Physics, Vol. III, by B. Chalmers. *Interscience Publishers Inc.* $8.00, 334 pp., 1952.—It is the intention of this book to present authoritative reviews of the present state of knowledge in specialized aspects of the field that includes both physical metallurgy and metal physics. No one volume of the series is intended to form a complete textbook on these subjects. Much of the book is theoretical, dealing in such things as crystallography of transformations, properties of metals at low temperatures, recent advances in the electron theory of metals, and other subjects. The book contains a name and a subject index and is illustrated throughout with graphs and charts.

The Cold Working of Non-Ferrous Metals and Alloys. *The Institute of Metals*. $2.50, 207 pp., 1952.—Five papers are presented in the form of a symposium on the metallurgical aspects of the general subject: Fundamental aspects of the cold working of metals; lubricants for the cold working of nonferrous metals; cold rolling of nonferrous metals in sheet and strip form; wire drawing technique and equipment; and deep drawing and pressing of nonferrous metals and alloys. The current practices for the processes considered are outlined. The book also contains general discussions of the papers presented.

Soluble Silicates, Vol. I, by James G. Vail. *Reinhold Publishing Corp.* $9.00. Vol. I. 357 pp., 1952.—This two-volume monograph was written to replace the out-of-print *Soluble Silicates in Industry*, regarded as the bible of the silicate chemist. Vol. I is devoted to theoretical aspects, detailing past and present manufacturing processes, properties of homogeneous and heterogeneous systems of glasses, the formation of metallic silicates and other fundamental material. Vol. II is given over to more practical considerations involving application of soluble silicates to industry. Film forming properties of silicates and their uses in various industrial materials including adhesives, laminates, sizing, fire protection, and other items are described.

Annual Review of Nuclear Science, Vol. I. *Annual Reviews Inc.* $6.50, 645 pp., 1952.—This is the beginning of a series designed as a survey of the literature of nuclear science. Subjects range from meson physics to low temperature phenomena and radioisotopic uses. Authors were required to cover outstanding developments and to provide sufficient background material to make possible a critical appraisal of the current status of subject matter. A bibliography accompanies each article.

The Measurement and Control of Temperature in Industry, by R. Royds. *Chemical Publishing Co., Inc.* $5.00, 260 pp., 1952.—The book covers the most recent developments for maintaining high thermal efficiency as utilized in a wide variety of industries. The various methods and equipment available for the measurement of temperature in each particular range are described. A great deal of space is devoted to the standardization and automatic control of temperatures. Notice is given of improvement of product quality, increasing production rates, and fuel and labor saving by automatic temperature controls application.

Instrument Engineering, Vol. I. Methods for Describing the Situations of Instrument Engineering, by Charles Stark Draper, Walter McKay, and Sidney Lees. *McGraw-Hill Book Co., Inc.* $6.00, 269 pp., 1952.—The complete three volume set will eventually present a generalized view of attack on the problems of measurement and control as a comprehensive reference to the practicing engineer. Vol. I develops a system of concepts, notations, diagrams, and mathematical forms for describing the performance of physical devices and variations in physical quantities. Description of the physical circumstances under consideration is aided by diagrams, mathematical forms, curves, and numerical data.

ORDER YOUR BOOKS THROUGH AIME—Address Irene K. Sharp, Book Department. Ten per cent discount given whenever possible. Order Government publications direct from the agency concerned.

PROFESSIONAL SERVICES

Limited to AIME members, or to companies that have at least one AIME member on their staffs. Rates $40 per year per inch.

ST & CO. INC.
ENGINEERS
CONSULTANTS
METALLURGISTS
Small Jobs Welcomed
SAM TOUR & CO., INC.
Laboratories and offices
44 Trinity Place, New York 6, N. Y.
Testing—Certifying
American Standards
Testing Bureau, Inc.

LEWIS B. LINDEMUTH
Consulting Engineer
140 CEDAR STREET NEW YORK 6, N. Y.
STEEL PRODUCTION
DESIGN · OPERATION · CONSTRUCTION · METALLURGY

R. S. DEAN LABORATORIES, INC.
Consulting Research Development
Chemistry Electrochemistry & Metallurgy Laboratory Research on a Contract Basis
5810—47TH AVENUE AP. 2821
RIVERDALE, MD.

MAX STERN
Consulting Engineer
Expert for Spring Recovery and Improvement — Modernization of Plants and Tests for Furnaces and Boilerplate Alloy Steels
150 Broadway New York 7, N. Y.

T. STARLING WINTERS
Consulting Engineer
Specializing in Electric Arc Furnaces to 10,000 KVA
100 East Palisade Ave. Englewood, N. J.

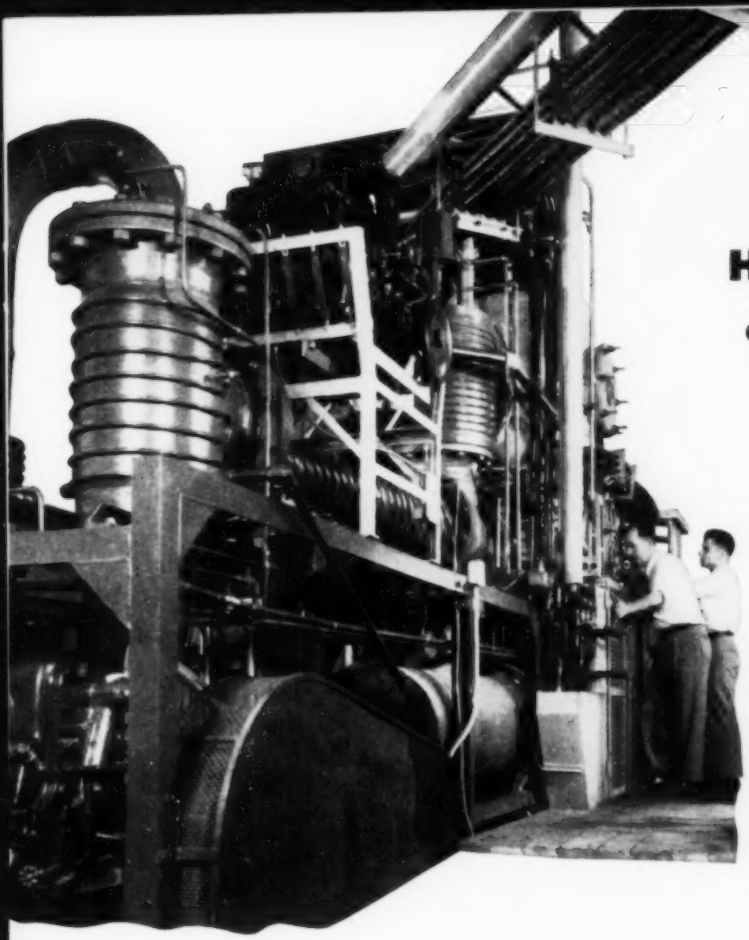

High vacuum develops muscles for "moly"

Pure molybdenum is sensitive to oxygen at the temperature it takes to melt it . . . and "moly" with oxygen is not much use. Jet engines, rockets, and other equipment need the pure metal because it stands up under heat that melts the strongest steels, but if there's oxygen in it the advantage vanishes.

High vacuum solves the problem. Climax Molybdenum Company of Detroit, Michigan, hydraulically compresses pure molybdenum powder and sometimes molybdenum chips with a little carbon. This mass is sintered into a crude stick which serves as a consumable electrode in an arc. The molten metal is caught in a pool which serves as the other electrode while it builds up into a half-ton ingot of malleable, ductile molybdenum.

The molybdenum turns out malleable and ductile because *high vacuum* gets rid of the injurious oxygen.

Why, you may ask, don't they just use an inert gas? Bear in mind that at the high vacuum under which these operations are carried out (.20 microns Hg) oxygen content is equivalent to about 0.0026%, at atmospheric pressure. Inert gas pure enough and in sufficient quantity to dilute atmospheric oxygen to this level would be staggering in cost. A DPi oil ejector pump, uniquely economical to operate, creates the vacuum in the sizable space needed for the whole series of continuous operations and gets rid of the gases evolved.

In supplying equipment for high vacuum metallurgy, DPi pools its own diversified experience in high vacuum technology with the experience of leading manufacturers of metallurgical furnaces.

In many other fields, too, where high vacuum processing has earned a useful role, DPi stands ready to help you with the vital details that add up to efficient, profitable production. Write to ***Distillation Products Industries,*** Vacuum Equipment Department, 607 Ridge Road West, Rochester 3, N. Y. (Division of Eastman Kodak Company).

DPi

high vacuum research and engineering

Also . . . vitamins A and E . . . distilled monoglycerides . . . more than 3500 Eastman Organic Chemicals for science and industry

Electro
TRADE MARK
Specific Purpose
Grinding Wheels
Only with specific purpose wheels engineered to your individual ways of working and to your objectives in each progressive step, can you hope to match competitive efficiency and economy. Let us send a technically trained Engineer without cost or obligation to you, to show you how the 3-way gains from use of Electro Specific Purpose Wheels can be introduced into your plant.
With them, you'll get more and better production and you'll reduce your production costs.

Industrial Notes . .

• The arrival of five huge castings from Duesseldorf, Germany at Aluminum Co. of America's Lafayette, Ind. works, signals a definite upward swing in the nation's heavy forging and extrusion press program. The castings will be part of a 13,200 ton extrusion press. The largest casting will form the cylinder housing for the press and weighs 107 tons. It measures 23 ft long, 8½ ft wide, and 14½ ft high. The second largest casting, weighing 103 tons, will form the platen of the press. Reloading the castings in New York and transportation inland to Lafayette required more than a month. They were moved by rail only during daylight and at speeds no greater than 30 mph.

• The AmForge div. of American Brake Shoe Co. has placed its new steel forging plant at Azusa, Calif. in operation. Eventually the 40,000 sq ft plant will produce from 1000 to 1200 tons of forgings per month. Initial output will be 57 mm and 75 mm shells. Other ordnance material, aircraft parts, and commercial forgings will be turned out in the future.

• Westinghouse Electric Corp. has been awarded a contract by Youngstown Sheet & Tube Co. for electrical equipment for a continuous pickling line and for two shearing lines at its Indiana Harbor, Ind. works. The new expenditure will reach $572,000, making a total of $3 million for electrical equipment Westinghouse has furnished the Indiana installation.

• *Foote Mineral Co., of Philadelphia is constructing a lithium processing plant at Sunbright, Va. Blaw-Knox Co. has already started work on the building. The projected plant's capacity is reported to be scheduled as the largest in the world. Combined with Foote's lithium ore mining, and quarrying and processing of limestone, it will double the nation's lithium output. The processing plant will reportedly be ready in one year.*

• For the third time in less than two years Youngstown Alloy Casting Corp. will expand its facilities. This time the firm plans to spend $100,000 for a 5400-ft plant addition and a new electric furnace. The new furnace will be a two-ton unit. A 1000 lb electric furnace is presently operating. Youngstown recently added 5400 ft to its new 15,000 sq ft plant.

• National Roll & Foundry Co. heat treating capacity at Avonmore, Pa. will be expanded by the

addition of a new car type heat treating furnace, installed by Russ Furnace Co. The new unit will be employed in the production of rolls and commercial castings, in addition to tank armor castings for national defense. The new furnace is similar to the five installed during World War II, but is not gas fired. A combination of fuel oil and natural gas will be used.

• High purity silicon powders specially processed for the manufacture of electronic crystals are available from the tungsten and chemical div. of Sylvania Electric Products, Inc., of Towanda, Pa. The purity of the new powders is reported at 99.85 to 99.95 pct Si.

• *A dock is being built in Texas to handle ore in Venezuela. U. S. Steel Corp. is constructing the installation at Orange, Texas, and the finished units will be towed by tugs to South America. When completed the three units will fit together to form a dock one fifth of a mile long. Months of work are being saved by the barge-like design of the units. The pier will connect by railroad and highway with Cerro Bolivar, 90 miles south. Each section measures 82 ft wide, 376 ft long, and 15 ft deep. Holes will be cut in each structure upon arrival to negate pressure exerted by buoyancy when the Orinoco River reaches flood stage.*

• **Mexico's Secretary of Hydraulic Resources, Ing. Adolfo Orive de Alba confirmed the report that an aluminum processing plant will be established in the valley of the Rapaloapan River at an initial cost of 100 million pesos. The plant will be near the Presidente Aleman Dam, scheduled to produce 100,000 kw of electrical power.**

• *The first of a battery of four new open hearth furnaces, to be constructed at a cost of about $10 million, will go into operation soon at the Lackawanna plant of Bethlehem Steel Co. All four furnaces are expected to be ready before the end of the year. They will raise the plant's capacity about 80,000 tons per month. Each furnace will have a capacity of 200 tons per heat.*

• The Longview, Wash., aluminum reduction plant of Reynolds Metals Co. is now turning out 100 million lb annually against its former output of 40 million lb annually. The 65 pct increase in production was attained by stretching the plant's 372 pots without extending the operation's floor area.

"Exceptionally Versatile" . . . that's why Pesco bought HEVI DUTY FURNACES

"We use our rugged Hevi Duty furnaces for carburizing, nitriding, hardening and normalizing parts for jet engine pumps," says Russ Fike chief metallurgist of the Pesco Products Co. "We can carburize one load and nitride the next by simply changing the atmosphere. Operating costs are at a minimum due to low ammonia consumption when nitriding, and our maintenance costs are negligible."

Learn how the versatile Hevi Duty vertical retort furnace can solve your production problems, write for your copy of bulletin HD-646 today.

HEVI DUTY®

HEVI DUTY ELECTRIC COMPANY

MILWAUKEE 1, WISCONSIN

Heat Treating Furnaces . . . Electric Exclusively

Dry Type Transformers *Constant Current Regulators*

Journal of Metals

BLAST Furnace Must Go—Blast Furnace Obsolete, But Due to Remain—Indicate Sponge Iron Process May Gradually Replace the Blast Furnace. These headlines appeared recently in newspapers, coming from reports presented in Geneva for the United Nations Economic Commission for Europe. To the average observer, it would seem that a major technological change was at hand. To the technician, it was confusing.

A careful analysis however, tempers these items. The two major replacements reported for blast furnace pig iron were the low shaft furnace employing oxygen, and the sponge iron process. It cannot be disputed that the reports leading to the headlines are true, and the conferees were all outstanding men in the industry. However, the reports apply to conditions peculiar to Europe, or more specifically, the country in which the report originated. The ores and fuels available in each country, as well as production rates, were the deciding factors. It cannot be inferred that a projection can be made for the conditions present in the United States.

The reduction of iron with oxygen in low shaft furnaces was advocated by Professor Durrer of the Zurich Polytechnicum, and director of the Louis de Roll Iron & Steel Works, Switzerland. He said that the process has been proven in principle, and should be worked out without delay, so that it can be adopted wherever new iron and steel plants are built or where circumstances are otherwise suitable. He asserted that the smelting of iron in blast furnaces must be replaced by better methods.

Even if the opinion is accepted that present blast furnaces are inadequate to cope with current problems in this country, it remains to be proven that the low shaft furnace is the answer. The International Research Project on Low Shaft Blast Furnace is just now constructing a furnace for research at Liege, Belgium. The many projects that await to be tried indicate that little has been proven in operation (JOURNAL OF METALS, September 1951, February 1952). Little interest was shown by American steelmakers when the project was inaugurated, although one or two may now be participating. H. Malcor, representing France at Geneva, said that the blast furnace will probably retain its supremacy for a long time to come. This from the president of the French Institut de Recherches de la Siderurgie and director of several French companies, who organized and is president of the directing committee of the research project on the low shaft furnace.

The story for sponge iron was ably presented by Professor Bo Kalling, director of research of Domnarvet, Sweden. Sponge iron is gaining a greater market as a raw material for steel production in Sweden, as mentioned by Professor Kalling, but it is mainly because of the shortage and high cost of pig iron and high grade scrap, and the need for high quality melting stock. Sponge iron also requires less fuel, and of a lower quality than that needed for the blast furnace. The need for better sources of electric furnace scrap in this country has directed attention toward the production of high grade concentrates, but production of sponge iron has not been a commercial success. It might be applicable for small tonnage consumers desiring an independent source of supply. Sponge iron here does have a good market as iron powder.

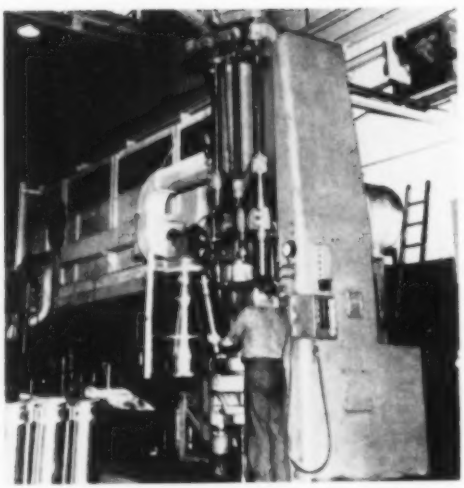

National Supply Co. reduced case hardening time from 4 hr to only 4 min on the inside surface of pump cylinder liners using this induction heat treater. Automatic controls hold properties within close limits.

◆◆◆◆◆◆◆◆

THE late steel strike resulted in an unusual reversal of field when Brazilian interests shipped steel to the United States to assure completion of a blast furnace under construction in Cleveland for the national Volta Redonda mill. The furnace is one of the key factors in an expansion program scheduled to raise Brazilian steel production by 280,000 tons, bringing annual output to 1 million tons. The first consignment shipped to Cleveland included 500 tons of slab and plate steel, and was followed later by another 300 tons. Brazil wants to blow in the furnace by July 1, 1953, and the restricted allocation system brought about by the steel shortage offered a real threat to the deadline. Volta Redonda, established during World War II by Brazilian and American financing, accounts for more than half of Brazil's steel production.

◆◆◆◆◆◆◆◆

THE Air Force envisions a big future for titanium and is going ahead with research plans which may lead to a lowering of production and selling costs. Wright-Patterson Air Force Base, Ohio, Air Materiel Command Headquarters, provided the backdrop for the first meeting of a committee whose job it will be to make recommendations to the AMC for the efficient application of titanium to aeronautic products.

The committee will collect all available information on machining, forming, welding, drawing and other metallurgical aspects of the use of titanium in airplane construction. Industry will be asked to lend assistance in the program, and though Government may finance development, actual production and fabrication will be the job of private organizations.

Meanwhile, Republic Steel Corp. announced that it is producing titanium and titanium alloys at its Canton and Massillon, Ohio steel plants. Republic has been supplying titanium and titanium alloys in ingot, sheet, plate, strip, bar, and wire forms for the last two years for aircraft and defense programs.

Titanium is melted by Republic at the Canton plant by arc and induction methods. Several small furnaces are in experimental production, and additional equipment for melting and processing is projected. Induction melting is carried out in a dense grade of graphite under an atmosphere of inert gas—either argon or helium. In arc melting, specially prepared sponge is fed continuously into a water cooled copper crucible, under an inert atmosphere and melted with a direct current graphite, tungsten, or other type electrode. The arc melted product appears likely to find the most widespread applications. Alloy content of titanium alloys are not likely to exceed 15 pct, with most high strength grades running about 4 to 10 pct. Alloys include iron, chromium, manganese, aluminum and others.

◆◆◆◆◆◆◆◆

SOVIET Russia recently took the rest of the world into her confidence and announced her industrial plans for the next five years. While no exact numerical goals are stated, the percentage figures indicate that this will be a maximum effort to close the gap between the USSR and the western capitalists. Even if she reaches the established marks, Russia will be a long way from equaling the free world. Indicated in the plan is a steel production increase of about 62 pct. Estimated soviet steel production for 1950 was 27.6 million metric tons, which would mean 44.7 million metric tons by 1955, when the latest five year plan matures. Russia also aims at a coal production of 374 million metric tons and a pig iron goal of 34 million metric tons.

Possibly the greatest single effort will be in aluminum production, with the plan calling for an increase of 176 pct. French economists estimate that 1950 production reached 200,000 tons. Copper is scheduled to rise 90 pct, zinc 150 pct, lead 170 pct, nickel 53 pct, and tin 80 pct. The labor force increase is expected to be only about 15 pct, which means that the USSR will have to intensify its use of every available manhour. Increase in automobile production will be only about 20 pct and tractors 19 pct, indicating that Russia will stress arms production over that of consumer goods. Yet, one of the stated aims of the new plan is reduction of prices to instrument raising of the buying power of industrial and farm workers. If consumer goods production is raised only a little, the increased buying power is meaningless. The betterment of standard of living can only be nominal—and not actual.

For the first time in automotive history, a plastic die is being used in actual factory production to shape major steel panels. The die is being used by Chrysler Corp. at its Dodge Trucks div. A standard 100-ton press, with a draw die made of plastic instead of steel has already turned out several hundred steel cowls.

ALCOA seems to have stolen a march in the race of cheaper power for the aluminum industry. Its proposed Alaskan project appears to be rooted in the cheap hydroelectric energy which will come from Canadian water power sources. Power will be generated by damming the Yukon River at Miles Canyon near Whitehorse. Several legislative barriers remain in the way of the Taiya Valley undertaking. First, Canadian Government permission will be needed for obtaining water power. Second, the project requires about 20,000 acres to accommodate the Alaskan smelting facilities and the electric power developments needed to operate them. Presently, there is no means under the law for Alcoa to acquire that much land. Thus, Congress will have to pass special legislation if the project is to go through to completion.

Alcoa will finance the entire project privately, without guarantees of any kind from Government and without special accelerated amortization arrangements. The time needed for completion is estimated at approximately four years and will provide year round employment for about 4000 people when in full operation.

Alcoa has made some attempt to use power sources other than hydroelectricity. Along with several aluminum producing companies Alcoa has been using natural gas, but the cost factor has been far from easy to assimilate. Thus, despite the inconvenience of location, and the accompanying higher transportation costs, Alcoa may have decided that Alaska is the most logical area for future operations. One Alcoa executive summed up the situation with:

"The most important single ingredient in aluminum production is power. Hydroelectric power is the best and cheapest."

In the meantime Alcoa will continue experimenting with other power sources. Its Rockdale, Texas works, now under construction, will be the first aluminum plant to use lignite.

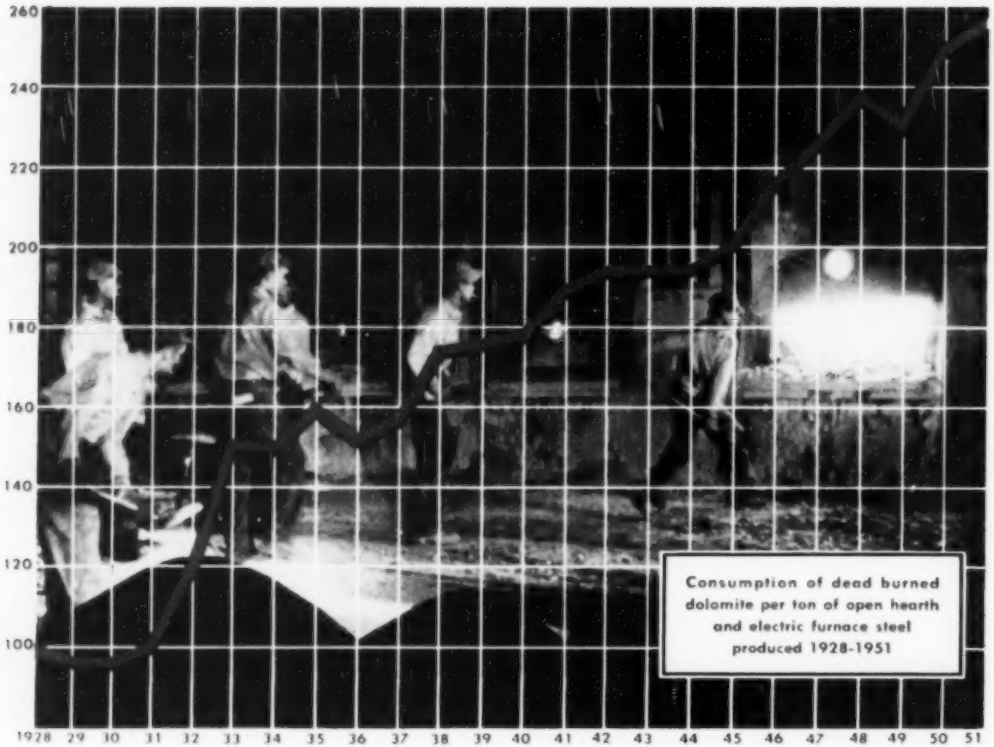

just what is dead burned dolomite?

It is a hearth maintenance refractory made from a relatively inexpensive raw material (dolomite). Under properly controlled manufacturing processes, dead burned dolomite develops certain inherent qualities advantageous to efficient, low cost maintenance—qualities which have led to a steadily widening acceptance by the steel industry.

Typically, dolomite suitable for dead burning shows a chemical analysis of lime 30.4%, magnesia 21.6%, silica 0.3%, other oxides 0.2% and carbon dioxide 47.5%. Prior to dead burning, quarried dolomite is classified to proper sizes and the very fine particles, along with clay and silt, are removed by washing.

The sized, washed dolomite granules, proportioned with a small percentage of iron oxide, travel through rotary kilns heated to above 3000°F. As they pass through the hot gases, the particles are first calcined, giving up approximately half their weight of carbon dioxide, and then sintered and shrunk to dense, hard clinkers. High temperature reactions convert calcium oxide to crystalline lime and magnesium oxide to periclase. Some lime also combines with iron oxide and silica to serve the refractory as a bonding agent.

The resultant product has been variously called "double burned", "roasted", "sintered", "clinkered", "prepared", "black" and "dead burned" dolomite. Of these designations, dead burned is now the generally accepted term, indicating as it does the characteristic hard, dense, inert, crystalline, highly refractory quality of the material.

Dependable dead burned dolomite, marketed under the well-known trade names Magnefer and Syndolag, is manufactured by Basic Refractories at its Ohio Works—recently expanded to meet the industry's ever increasing use of this refractory.

Basic Refractories Incorporated

845 HANNA BUILDING, CLEVELAND 15, OHIO

Exclusive Agents in Canada: REFRACTORIES ENGINEERING AND SUPPLIES, LTD., Hamilton and Montreal

THE DRIFT OF THINGS

by Edward H. Robie

A Company's Stake in the AIME

At a recent meeting of the AIME Board there was considerable discussion of a suggestion that companies should be more interested in promoting AIME membership among their employes. The advocate of this idea argued that companies benefit greatly if their employes are active AIME members, so even on purely a selfish basis they should use various means to encourage membership. Also he argued that companies in general make no contribution to the support of the AIME although benefiting from its work, so should not object to making more of a contribution, financial or otherwise, than they do.

One Director stated that an investigation had developed the fact that a large majority of members felt it unwise for employers to pay the initiation fees or dues of employes. They felt that AIME membership should be on a purely personal basis; that the rewards of active membership were sufficient so that it is a good investment for a man in developing his own professional stature, presumably resulting in an increase in salary sooner, or in greater amount, than would otherwise be the case. If an employer paid a member's dues or initiation fee the member would take less interest in the Institute. But this Director felt that an employer should otherwise encourage his employes to join the Institute, attend its meetings, and write papers based on company work for presentation and publication. Another Director reported that his company pays the expenses of AIME members in its employ to meetings; the company also encourages nonmembers to attend AIME meetings but does not pay their expenses unless they present papers of interest to the company. Another Director, representing a supplier, stated that his company's policy was to send some of its staff to all AIME meetings at which papers of interest were to be presented or at which valuable contacts could be made.

The consensus seemed to be that an employer should preferably not pay the initiation fee or the dues of a member except in special cases. Such a special case might be that of a technical librarian whose company might thereby obtain technical publications at less expense than if purchased at the nonmember price. Another special case might be that of a company which wished to keep in touch with AIME activities in a certain field which might be only a fringe field for the employe for whom the membership was taken out. But companies should encourage their men to attend AIME meetings, and pay their expenses thereto. They should also help Local Sections in their territory to put on good meetings. They could do this by such means as encouraging the writing of papers; by contributing a part of the cost of dinners for Junior Members and Student Associates; by contributing transportation for a group in a company car; and by permitting and encouraging inspections of their plants on field trips, perhaps providing a luncheon for a group.

The Directors of the Institute have never looked with favor on company memberships in the AIME. But they do not frown on passing the hat for voluntary contributions for special and occasional purposes, such as contributing souvenirs to an Annual Meeting, or perhaps to financing a general cocktail party in preference to individual hospitality in hotel suites; or to contributions to worthy funds, such as for student prizes or scholarships, for awards or medals.

Members of the Institute who have risen to top rank in their companies can well give thought to ways in which they can further the operation of their professional society. Their employes, as members, will benefit, as will the companies themselves.

"The People" Are of Good Will

By the time this appears in print, the Olympic Games in Helsinki (pronounced with the accent on the first syllable the Finns tell us) will have been largely forgotten, but their success affords a lesson that should be remembered. It was not the many world's records that were broken. Rather it was a congress of people from all over the world that met in peaceful contest, with a spirit of good will and cordial fellowship. The hospitality of the Finns and their conduct of the meeting, with the meager resources of their little but much admired country, brought much favorable comment. But this atmosphere could not have been maintained had there been exhibitions of international and interracial enmity by the contestants. All got along beautifully with one minor exception and the fellowship between the two leading groups of contestants, the Russians and Americans, was most cordial.

The wrong people are running the world. If the athletes were put in power, or the Quakers, the ministers, the doctors, or the engineers, specially the mining engineers, we venture to say that wars would be less frequent and that people would lead happier lives. The politicians and the diplomats have a sorry record of ineptitude so far in the twentieth century. But do they ever apologize or admit their mistakes? No. They rather talk about increasing our facilities for what they euphemistically call our defense and security. Defense is too often merely another name for war; and there is no such thing as security in the measures commonly adopted to attain it.

Intelligence Test

Some of the young ladies who are compiling our Directory are being forced to learn something about geography, a subject, like grammar, so largely neglected in our schools. About a sixth of the AIME membership lives outside of the United States. Often it is a problem, never completely and successfully solved by those who work on our Directory, whether a country is independent or merely a state or province in another country. Geographical ignorance even enters the door of the Secretary's office. We read the other day that Viet-Nam is the eleventh country to ratify the UNESCO pact to remove tariffs on the importation of educational, scientific, and cultural materials. Among the other ten countries that have ratified it are Cambodia and Laos. Now we have not the slightest idea where Viet-Nam is, nor have we any recollection of ever having heard of the country before. Our ignorance of Laos is almost equally great and we are not at all sure about Cambodia.

Negroes in Engineering

Engineering careers are being increasingly opened to Negroes. RCA-Victor has been scouting for Negro engineering talent for more than three years, has hired 16, nine of them this year, and reports that probably every reasonably qualified Negro engineering graduate has received at least one attractive offer of engineering employment in American industry. Negro engineers are practically if not entirely absent in American mining but there are a few Negro metallurgists and chemists and at least one is an AIME member.

GIANT NICKEL STEEL SHAFT installed as a replacement on a 54" crusher, to assure maximum service life for The International Nickel Co., at Copper Cliff, Canada. Overall length 21'6", maximum diameter 13'8", bore 9".

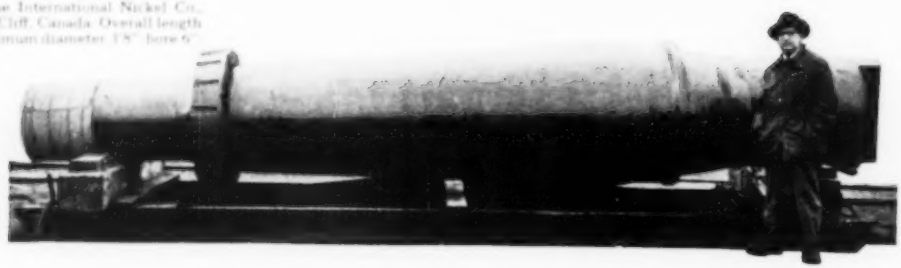

How Nickel Helps a Crusher

PUT THE SQUEEZE ON COSTS

Many forgings are so large that only part of the mass can be worked under the press before the steel has to be reheated. These large sections of steel, typified by this crusher shaft, so limit the cooling rate as to make liquid quenching ineffective.

Consequently, improved strength, hardness and other properties that prolong life of large forgings are much more dependent upon wise selection of alloy content than is the case with small forgings.

Because of these facts, the large crusher shaft shown above was forged from a 160,000-pound ingot of 2¼ per cent nickel steel... produced, rough-turned and heat-treated by the Bethlehem Steel Company, and finish-machined by the Traylor Engineering Company of Allentown, Pa.

After normalizing and tempering, two tests on longitudinal specimens, taken from a prolongation at mid-radius, averaged as follows:

Tensile Strength	80,000 p.s.i.
Yield Strength	51,000 p.s.i.
Elong. in 2"	28.0%
Red. of Area	58.3%

The strengthening effect of nickel on ferrite is independent of carbon content or heat treatment of the steel, and its effectiveness in reducing the rate and temperature of the upper transformation, induces better response to the necessarily milder heat treatments used.

Nickel alloy steels may help you obtain peak performance from vital parts of your products or equipment. Send us the details of your problems for our suggestions. Write us now.

At present, most of the nickel produced is being diverted to defense. Through application to the appropriate authorities, nickel is obtainable for the production of engineering alloy steels for many end uses in defense and defense supporting industries.

INCO

THE INTERNATIONAL NICKEL COMPANY, INC. 67 WALL STREET NEW YORK 5, N. Y.

Investigations of rare earth element additions to cast steels indicate that these elements may well be the penicillin for steel castings and help eliminate many production difficulties. See story p. 1024.

Anaconda Copper Mining Co. is set to proceed with construction of a $45 million aluminum metal producing plant at Columbia Falls, Flathead County, Mont. Alumina for the new plant will be obtained from the Reynolds Metal Co. plant at Corpus Christi, Texas. The Anaconda project will be privately financed.

A new germanium extraction method has been developed in Britain by Johnson Matthey & Co. It is understood that the new method, for extraction of germanium from flue dusts, will give Britain as much of the metal as she can sell. Germanium is found in most British coals to the extent of about 0.1 pct.

Washington officials have expressed the belief that Bolivia needs a beneficiation plant rather than a tin smelter as has been discussed. They feel that if the South American country can clean up her ore, she will be able to offer much more competition to other tin producing nations. The change in plan has been suggested to the Bolivian Government.

Manufacture of alloy steel is increasing more rapidly than is the consumption of alloying elements. Alloy steel output rose 18 pct to more than 10 million tons, while consumption of alloying elements rose 16 pct to 418 million lb during 1951. The spread was partly because the use of boron made leaner alloy content possible.

Zinc production in Canada reached $1.33 million in dollar value in 1951, setting a new high. The actual increase in volume was 20,700 tons. The increase was the result of operations of the Consolidated Mining & Smelting Co., at Trail, B. C., and Hudson Bay Mining & Smelting Co., at Flin Flon, Man.

Australia's steel production may increase 200,000 tons this year, bringing total anticipated output to 1.35 million tons. Production in 1951 was 1.15 million tons. The National Development Ministry claims Australia will be producing another 900,000 tons per year by 1955.

Substantial quantities of columbium and cobalt are being saved in the production of the world's most powerful qualified turbojet engine by Westinghouse Electric Corp. The two metals have been eliminated in production of the J40, as the engine is called, according to Westinghouse.

Chairman Jack Gorrie of the National Security Resources Board has organized a committee to further study the now controversial Paley report. Recommendations in the report will be reviewed by representatives of 25 major Government departments and agencies.

Properties of Cast Steels Improved With Rare Earth Element Additions

This excellent systematic survey reveals that the addition of rare earth elements to cast steels had a beneficial effect on almost all properties, and in no case was any detrimental effect experienced. Improvements were noted in ductility, impact strength, inclusions, hot tears, fluidity, sulphur reduction, porosity, weldability, and feedability.

by G. A. Lillieqvist and C. G. Mickelson

INVESTIGATIONS of rare earth element additions to steel have led to interesting and fascinating results. While considerable information has been reported by American and British authors regarding the use of cerium in the production of nodular cast iron and by Carpenter Steel Co. listing the advantages of using rare earth elements in stainless steels, little information has been reported regarding the effects of rare earth elements on common cast steels. An interesting editorial article¹ referred to the befuddled and confused condition surrounding the use of these elements. The experiences American Steel Foundries had with these elements when adding them to steel may be of interest to the casting industry and may throw some light on the subject of rare earth additions to steel.

About the only information presented thus far regarding the use of rare earth elements in common cast steels was reported by C. D. Berry and A. A. Dorvel.² This information dealt primarily with the effect of improvement in ductility properties with the use of cerium in cast steels. While the possibility of using rare earth elements as an addition to steel has been under investigation for some time, American Steel Foundries research and development work since November 1950 has been concentrated on this subject and interesting and astonishing properties were obtained. These elements may well be the penicillin for steel castings and help eliminate many production difficulties.

At the present time there are a number of different rare earth alloys sold on the market; however, investigations have been concentrated on one alloy that appeared most promising. This alloy contains various percentages of rare earth elements such as cerium, lanthanum, praseodymium, neodymium, samarium, etc., and is known as LanCerAmp produced by American Metallurgical Products Co.

Table 1. Normalized Physical Properties of 1.50 Pct Manganese Manganese Steel with Rare Earth Additions at Various Times

Rare Earth Addition	Strength, Psi Yield	Strength, Psi Tensile	Elongation, Pct	Red. Area, Pct	Charpy, Ft-Lb Room	Charpy, Ft-Lb 0°F
No Rare Earths	73,000	131,000	23.0	28.0	22.0	16.0
At Melt Down	68,500	132,500	30.0	34.0	44.0	34.0
After Ladle	69,000	128,000	30.0	34.0	44.0	34.0
After Al	70,000	130,000	29.0	30.0	37.0	25.0
After Ca-Si Mn	70,500	131,000	27.0	30.0	34.0	20.0

At the present time there are a number of different rare earth alloys sold on the market; however, investigations have been concentrated on one alloy that appeared most promising. This alloy contains various percentages of rare earth elements such as cerium, lanthanum, praseodymium, neodymium, samarium, etc., and is known as LanCerAmp produced by American Metallurgical Products Co.

Physical Properties

The usual procedure when investigating a new addition to steel is to determine its effect on physical properties. Naturally the first problems involved were the questions of how much alloy should be used and in what state of deoxidation the steel must

G. A. LILLIEQVIST is Research Director and C. G. MICKELSON is Assistant Research Director, American Steel Foundries, East Chicago, Ind. This paper will be presented at the Electric Furnace Steel Conference, Iron & Steel Div., AIME, in Pittsburgh, Dec. 4 to 6, 1952.

Table II. Physical Properties of Various Steels as Normalized

Steel Composition, Pct						Strength, Psi				Charpy, ft-lb	
C	Mn	Si	P	S	Special Addition	Yield	Tensile	Elongation, Pct	Red. Area, Pct	Room	-40°F
Grade B steel					No Rare Earths	45,000	72,000	29.4	58.5	53.8	11.8
0.26	0.70	0.40	0.021	0.038	Rare Earths	44,000	70,500	29.1	57.8	49.6	7.8
1040 Steel					No Rare Earths	55,000	91,000	24.1	52.6	23.4	5.4
0.41	0.70	0.40	0.021	0.038	Rare Earths	54,000	88,500	25.4	57.8	23.4	5.4
High Tensile Steel					No Rare Earths	61,000	97,500	27.6	59.3	46.6	15.1
0.30	1.60	0.40	0.021	0.038	Rare Earths	64,500	95,000	29.8	60.6	52.2	40.1

be at the time of the LanCerAmp additions. In the investigation of physical properties, the SFSA standard test block was used in all laboratory experiments. In later work at some of the plants, larger blocks were used because of the difficulties involved in bottom pouring a small size test piece from a large ladle.

Numerous heats were produced in high tensile steel (0.30 pct carbon, 1.60 pct manganese) in which the amounts of aluminum, LanCerAmp and calcium-manganese-silicon additions were varied. The best all around results were obtained in the laboratory when the aluminum addition was maintained at 1½ lb per ton of charge, when the LanCerAmp addition was 2 lb per ton of charge and when the calcium-manganese-silicon addition was 3 lb per ton of charge. Results indicated that either calcium-manganese-silicon, calcium-silicon or Graphidox could be used interchangeably. There were indications that while the Graphidox produced slightly higher ductility properties in the pull bars, the calcium-manganese-silicon produced the highest low temperature impact properties. Because of the interest in low temperature impact work, it was decided to use the latter in all experiments.

In some cases investigations in the shops under production conditions indicated it was desirable to increase the aluminum addition to 2 lb per ton of charge. The larger aluminum addition required was attributed to the greater possibility of aluminum loss when added under production conditions, or because of variation in oxygen content of the bath.

The other problem to be solved before too much work could be started was the best time to add the LanCerAmp. It also was important to know whether or not the benefits of the rare earth materials would be lost on remelt and if there would be a possibility of a detrimental buildup in the scrap. In this study five heats were produced wherein the time of the LanCerAmp addition was varied.

In the first study the 2 lb LanCerAmp addition was made in the charge; in the second case it was made at melt down; in the third case it was added just after the ferrosilicon addition but before the aluminum and calcium-manganese-silicon additions. In the fourth and fifth cases the rare earth additions were made after the aluminum and after the calcium-manganese-silicon additions respectively. The results of the physical properties of this study are shown in Table I.

It can be observed that when the LanCerAmp addition was made in the charge or at melt down, few beneficial results were obtained, especially in impact properties both at room temperature and -40°F. This also indicated that the material would be oxidized easily and would not buildup in the scrap during remelting. When the LanCerAmp was added after the silicon addition, some improvement resulted although best results were obtained when it was added after the aluminum. This indicated the steel must be fairly well deoxidized before the LanCerAmp addition is made. When discussing future heats in this paper, unless otherwise stated, the laboratory heats were produced with the normal alloy additions of ferrosilicon and ferromanganese, followed by 1½ lb of aluminum per ton of charge, then 2 lb of LanCerAmp per ton of charge, and last, 3 lb of calcium-manganese-silicon per ton of charge.

All production basic open hearth heats were treated in a similar manner except that 2 lb of aluminum per ton of charge were added in place of 1½ lb. In these heats it was necessary to add silico-manganese to the bath. Sufficient silico-manganese was added to bring the silicon content up to the desired 0.40 pct. The use of this material through the furnace caused considerable phosphorus reversion unless the addition of lime to the charge was increased to about 6 pct. The LanCerAmp itself was added by wiring it to a bar of steel about 1½ in. diam and 12 in. long and throwing the bundle into the ladle at a point where the metal stream joins the metal in the ladle.

Three American Steel Foundries compositions were investigated both in the normalized and quenched condition. These compositions were Grade B steel containing 0.26 pct carbon, 0.70 pct manganese and 0.40 pct silicon; high tensile steel containing 0.30 pct carbon, 1.60 pct manganese and 0.40 pct silicon; and 1040 steel containing 0.40 pct carbon, 0.70 pct manganese and 0.40 pct silicon. Results in the normalized condition are given in Table II.

These steels were normalized at 1650°F for 20 min and tempered at 950°F for 2 hr and air cooled. All ductility and impact properties were improved with the LanCerAmp additions. Table III shows these

Table III. Physical Properties of Various Steels as Quenched and Tempered

Steel Composition, Pct						Strength, Psi				Charpy, ft-lb	
C	Mn	Si	P	S	Special Addition	Yield	Tensile	Elongation, Pct	Red. Area, Pct	Room	-40°F
Grade B steel					No Rare Earths	57,000	104,000	24.2	58.5	53.1	20.5
0.26	0.70	0.40	0.021	0.038	Rare Earths	55,000	103,000	24.2	58.5	52.5	18.2
High Tensile Steel					No Rare Earths	68,000	120,000	21.2	56.5	47.8	17.5
0.30	1.60	0.40	0.021	0.038	Rare Earths	67,000	120,000	21.2	57.5	52.5	19.0
1040 Steel					No Rare Earths	61,000	104,000	23.2	58.5	47.8	16.0
0.41	0.70	0.40	0.021	0.038	Rare Earths	60,000	104,000	23.2	57.5	47.8	17.5

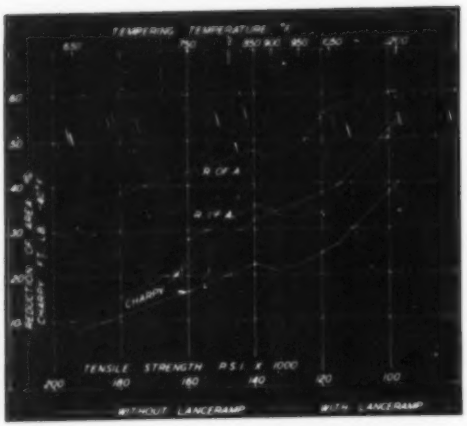

Fig. 1—Average ductility, low temperature impact properties and tensile strength of a 0.30 pct C 1.60 pct Mn steel are shown after various tempering treatments. It can easily be seen that rare earth treated steels are superior.

same steels in the quenched and tempered condition.

In this case all steels were quenched in water from 1550° to 1600°F after holding 20 min. The Grade B steel was tempered to 200 Bhn, the high tensile steel to 250 Bhn, and the 1040 steel to 300 Bhn. The effects of the rare earth elements on ductility and impact properties of these steels in the quenched and tempered condition were even more pronounced than in the normalized condition. This improvement, especially in low temperature impact properties, also was observed in various low alloy grades of steel. In most cases this improvement was over 50 pct.

Temper Brittleness

Under certain conditions a steel may, as determined by the tempering temperature, exhibit a phenomenon called temper brittleness. This condition is undesirable although it normally occurs in most quenched and tempered steels. Usually this undesirable condition occurs when the tempering temperature is around 800° to 1000°F, although this temperature range may vary somewhat depending upon the composition of the steel.

During the tempering of a normal steel as the temperature is increased in small steps between 650° and 1200°F, hardness and tensile strength decrease with the increase in temperature. As the hardness and tensile strength decrease ductility and impact properties increase. However, at certain tempering temperatures even though the hardness and tensile strength decrease, the ductility and impact properties also decrease. This is referred to as the temper brittle zone. It was hoped that the addition of LanCerAmp might have a beneficial effect toward elimination of this undesirable condition.

Studies were conducted on a 0.30 pct carbon, +1.60 pct manganese steel produced with and without LanCerAmp. Test bar sections about $\frac{7}{8}$ in. thick were given the standard heat treatment and water quenched from 1650°F. Tempering treatments in steps of 50° or 100°F from 650° to 1200°F were used. Pull bar and Charpy specimens were machined and tested. Charpy results were obtained both at room temperature and −40°F. Fig. 1 illustrates the average ductility, low temperature impact properties and tensile strength obtained after the various tempering treatments.

It can be seen that both steels exhibit similar temper brittle conditions in reduction of area and low temperature impact properties. A similar condition to a lesser degree was noticeable in the elongation and room temperature impact properties. The temper brittle range for these steels was between 850° and 950°F with the poorest results around 900°F.

Table IV. Comparison of Low Temperature Impact and Ductility of Various 1.60 Pct Manganese Steels as Quenched and Tempered

Steel	Tensile Strength, Psi	Charpy, Ft-Lb at −40°F	Red. Area, Pct
Regular	130,000	23.5	39.0
Selenium	130,000	27.0	40.5
LanCerAmp	130,000	32.5	48.0
Regular	110,000	31.0	44.0
Selenium	110,000	34.0	47.0
LanCerAmp	110,000	40.5	58.0

While LanCerAmp did not aid in the elimination of the temper brittle condition, the results at all hardnesses were far superior to those from the heats without the rare earth additions.

Inclusions and Microstructure

After obtaining improvement in physical properties, the next step was to try and determine what changes took place in the steel itself. Investigations under the microscope showed that when 2 lb of LanCerAmp per ton of charge were added to the steel in addition to the regular aluminum and calcium-manganese-silicon, the normal crystalline or Type III inclusions were changed to round or Type I inclusions. This is shown in Fig. 2. The crystalline inclusions on the left are from a heat deoxidized only with aluminum and calcium-manganese-silicon, while the round duplex inclusions on the right are from a heat deoxidized with aluminum, LanCerAmp and calcium-manganese-silicon. In the many heats produced in the laboratory and in the basic shops, a predominate number of round inclusions in the LanCerAmp treated steels was always obtained.

It is known that when cast steels have predominately Type I inclusions, normally superior properties are obtained. There is no doubt that the addition of the rare earth elements to steel has an effect on the melting point and solubility of the sulphur

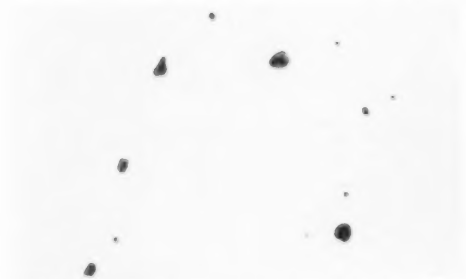

Fig. 2—When LanCerAmp was added to a steel deoxidized only with Al and CaMnSi, the crystalline Type III inclusions, shown at the left, were changed to the round Type I inclusions at the right.

containing nonmetallic inclusions. Most of the round Type I inclusions are in duplex form indicating a complex refractory structure.

It is not believed, however, that the change in nonmetallic inclusions is entirely responsible for the remarkable increase in ductility and impact values. This assumption is based on the fact that by other combinations of deoxidizers, it is possible to change the type of inclusions from Type III to Type I without obtaining the marked improvement in physical properties, especially in the low temperature impact properties. This is demonstrated with the heats made with aluminum and selenium. These heats had globular Type I inclusions but did not have the high ductile and impact properties exhibited by the LanCerAmp treated steel.

Table IV gives the average Charpy values at —40° F and reduction of area properties obtained with: 1—The regular 1.60 pct manganese steel deoxidized with aluminum and calcium-manganese-silicon, 2—the selenium-1.60 pct manganese steel deoxidized with aluminum and selenium; and 3—the LanCerAmp-1.60 pct manganese steel deoxidized with aluminum, LanCerAmp and calcium-manganese-silicon.

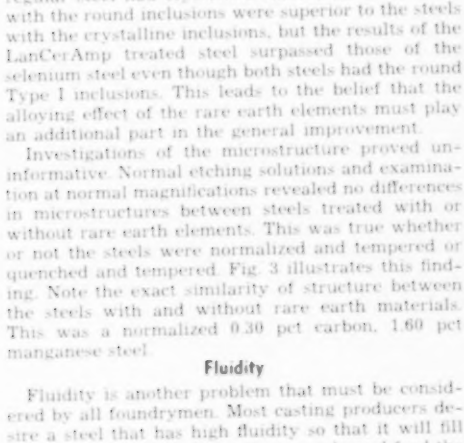

Fig. 3—In these photomicrographs of a normalized 1.60 pct Mn steel, no difference in structure can be seen between the plain steel at the left, and the steel with rare earth additions at the right.

These steels were quenched and tempered at about 925° and 1125° F. The selenium and LanCerAmp steels had predominately round inclusions, while the regular steel had crystalline inclusions. Both steels with the round inclusions were superior to the steels with the crystalline inclusions, but the results of the LanCerAmp treated steel surpassed those of the selenium steel even though both steels had the round Type I inclusions. This leads to the belief that the alloying effect of the rare earth elements must play an additional part in the general improvement.

Investigations of the microstructure proved uninformative. Normal etching solutions and examination at normal magnifications revealed no differences in microstructures between steels treated with or without rare earth elements. This was true whether or not the steels were normalized and tempered or quenched and tempered. Fig. 3 illustrates this finding. Note the exact similarity of structure between the steels with and without rare earth materials. This was a normalized 0.30 pct carbon, 1.60 pct manganese steel.

Fluidity

Fluidity is another problem that must be considered by all foundrymen. Most casting producers desire a steel that has high fluidity so that it will fill all portions of the mold cavity properly and feed the

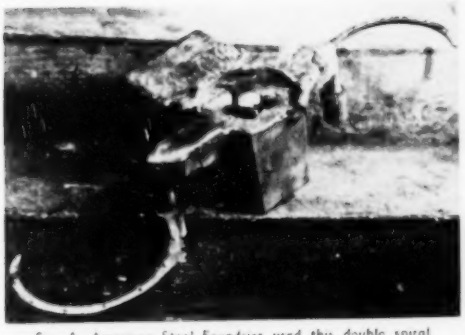

Fig. 4—American Steel Foundries used this double spiral test casting to determine fluidity characteristics. High fluidity steels are desirable for proper filling of mold cavities and to feed the casting successfully.

casting successfully. It is possible solidification and feedability may be closely connected with fluidity but this will be discussed separately. The test casting used in determining fluidity characteristics at American Steel Foundries is the double spiral and is shown in Fig. 4. The assembly of the core mold and the temperature measuring equipment is shown in Fig. 5.

A 32 gage platinum-platinum 10 pct rhodium thermocouple is inserted at an angle of 45° into the pouring cup and shielded by a fused quartz tube 6 in. long with 4 mm OD and ½ mm wall thickness. If the pouring of the steel is continuous for a period of 7 to 12 sec, this method produces accurate and reproducible pouring temperatures. The casting weighs approximately 90 lb and the large reservoir between the two spirals has been provided as an aid in controlling the rate of feeding the spirals. Satisfactory results have been obtained with this equipment under laboratory and shop conditions.

With this type of test, comparisons were conducted on the intermediate manganese steel with and without additions of LanCerAmp. Heats of 0.30 pct carbon, 1.60 pct manganese, 0.40 pct silicon, 0.015 pct phosphorous and 0.035 pct sulphur were produced and

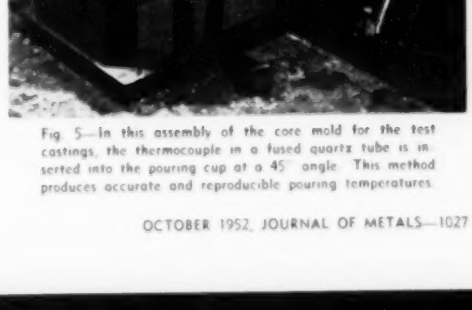

Fig. 5—In this assembly of the core mold for the test castings, the thermocouple in a fused quartz tube is inserted into the pouring cup at a 45° angle. This method produces accurate and reproducible pouring temperatures.

Fig. 6—Use of LanCerAmp improved the fluidity of the 1.60 pct Mn steel. The test casting used in these experiments is that shown in Fig. 4.

poured into the test casting at various temperatures. The curves developed are shown in Fig. 6.

It is easy to see that LanCerAmp improved the fluidity of the 1.60 pct manganese steel, especially in the lower pouring ranges most common in basic open hearth shops and in acid electric shops. Here again was another property of steel improved with the use of LanCerAmp.

Hot Tears

A thorough investigation was undertaken determining the effect of LanCerAmp regarding resistance to hot tearing using the ASF standard hot tear test casting. Fig. 7 illustrates the core assembly of this test casting, while Fig. 8 illustrates the test casting itself.

The wall thickness of the test casting used was ¼ in. Temperature readings were taken with a platinum-platinum 10 pct rhodium thermocouple fitted into the bottom of the cup in the downgate. After the castings were poured at various temperatures, they were blasted and etched in hot 1:1 muriatic acid for 1 hr. An evaluation of the severity of hot tearing was made on all castings and curves plotted.

A hot tear rating of 0 indicated the casting was free of hot tears. The ratings of 1 to 8 indicated a relative increase in the severity of the cracking. Fig. 9 illustrates the rating of 1 and Fig. 10 demonstrates the rating of 8. In all of this comparative work the center core was maintained as uniform as possible. The mix used in the production of this core was: Linseil, 1 pct; Mogul, 1 pct; ASF #85 sand, 99 pct, and water, 3 pct.

Grade B steels were produced with and without LanCerAmp and again the rare earth elements appeared beneficial. The curve shown in Fig. 11 illustrates the hot tear ratings at the various pouring temperatures. Note the lower hot tear ratings for the rare earth treated steels. Similar curves were observed on other grades of steel. It is again believed that the change in inclusions from Type III to Type I is partly responsible for the improvement in resistance to hot tearing. This information in general parallels reported results from the stainless steel producers who found that rare earth elements greatly reduce the possibility of cracking during hot working and forging.

Sulphur Removal

All steel producers whether they melt basic or acid are at some time or other troubled with sulphur. Its reduction or limitations are of interest to everyone. LanCerAmp was actually discovered in a survey and investigation of various materials that might be useful for sulphur reduction.

Initial laboratory experiments in a basic lined induction furnace were discouraging as no sulphur reduction was observed; however, the physical properties of these LanCerAmp treated steels were so far superior to the untreated steels that work was continued with this material. Thus far, and many hundreds of heats have been produced in the laboratory, no sulphur reduction has been observed on steel produced in basic lined induction heats.

In production heats under operating conditions using the basic open hearth furnace, the condition is different. Sulphur reduction has been obtained on all heats. When tapping out basic open hearth heats at about 0.018 to 0.019 pct sulphur, a 4-point

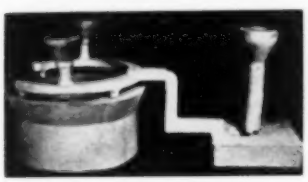

Fig. 8—This is the actual test casting shown schematically in Fig. 7.

Fig. 9—This casting illustrates a hot tear rating of 1, being relatively free of hot tears.

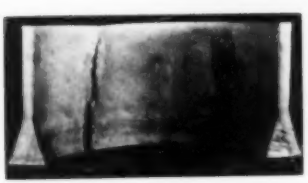

Fig. 10—This severe hot tear indicates a hot tear rating of 8, the highest number of the scale.

Fig. 7—The gating system in this assembly of cores for hot tear test casting is so arranged that 1 to 4 test castings can be poured.

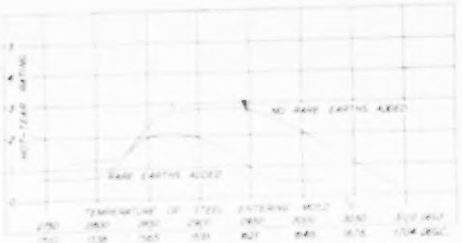

Fig. 11—Rare earth additions to this Grade B steel containing 0.035 pct S reduced hot tear ratings. Similar curves were obtained on other grades of steel.

drop is obtained when the steel is treated with LanCerAmp in the ladle. This condition has been observed on hundreds of heats in four different basic open hearth shops. Table V shows the normal sulphur drop obtained in ten consecutive regular basic open hearth heats. The tap sulphur was taken on a sample poured just before tapping and the final sulphur was taken from the regular ladle analysis test poured in the middle of the heat. No kick back in sulphur was observed between the beginning and end of the pour.

Experiences under production conditions with an eight-ton acid electric furnace have not been too consistent, although drops in sulphur as high as 17 points have been obtained. Normally the drop was approximately 4 points. It is believed the acid slag is responsible for considerable sulphur reversion. The use of LanCerAmp in a basic electric furnace appears considerably more promising with more consistent results.

Solidification Temperature

It was believed that the LanCerAmp treated steel might have a somewhat lower final solidification point that might explain the higher fluidity characteristics and possible better feedability. To check this phenomenon, blocks of steel 4x4x10 in. were poured, with a platinum-platinum 10 pct rhodium thermocouple protected by a thin quartz tube inserted into the center of the section. Cooling curves were obtained on high tensile steels produced with and without LanCerAmp. The analysis of the high tensile steel follows: 0.30 pct C, 1.60 pct Mn, 0.42 pct Si, 0.015 pct P, and 0.032 pct S.

Results showed the LanCerAmp treated steel had a slightly lower final solidification temperature than the untreated steel. The final solidification temperature for the LanCerAmp treated steel was 2640 F as against 2660 F for the untreated steel. This is shown in Fig. 12. Reports from other sources indi-

Table V. Sulphur Reduction with LanCerAmp in Basic Open Hearth Steel

Tap Sulphur Pct	Sulphur After LanCerAmp Additions, Pct	Sulphur Drop, Pct
0.020	0.016	0.004
0.017	0.013	0.004
0.018	0.015	0.003
0.018	0.013	0.005
0.018	0.014	0.004
0.020	0.014	0.006
0.019	0.014	0.005
0.019	0.014	0.005
0.021	0.017	0.004
0.020	0.015	0.005

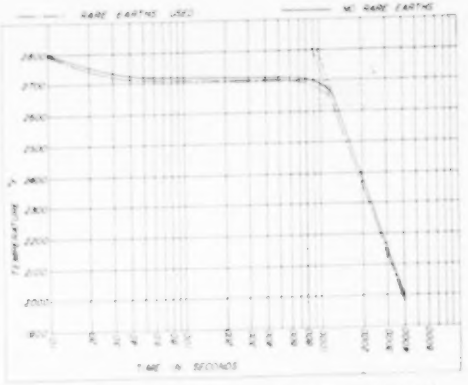

Fig. 12—Solidification temperature of 1.60 pct Mn steel was lowered from 2660 to 2640 F by addition of rare earths. This might be a contributing factor toward improved fluidity and feedability.

cated this difference might be as high as 35 F on other grades of steel. It is possible that this difference might be a contributing factor toward improved fluidity and feedability. Again this is another factor favoring the use of LanCerAmp treated steels.

Hardenability

Because of the exceptional improvement in physical properties, especially in the quenched and tempered condition, it was believed that the addition of LanCerAmp may have increased the hardenability characteristic of the steel. To check this factor Jominy hardenability tests were conducted on the high tensile steel. Regular end quenched hardenability specimens were machined from 0.30 pct carbon, 1.60 pct manganese steels treated with and without LanCerAmp. After the standard end quenching, Rockwell C readings were taken and curves plotted for the two steels. Results can be observed in Fig. 13.

Note that the two curves are practically identical. This indicated that LanCerAmp had no effect on the hardenability characteristics of the cast steels. Additional checks were made with medium and low alloy steels. These results, too, were similar in that no apparent increase in hardenability was obtained

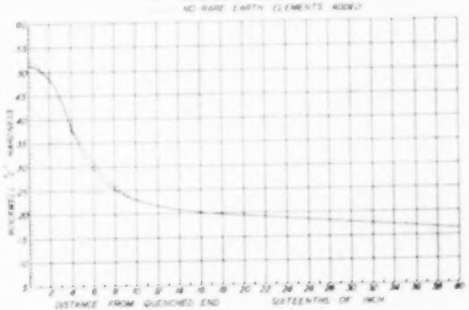

Fig. 13—Almost identical hardenability results were obtained on this 1.60 pct Mn steel whether or not rare earth additions were made.

with this special addition. From these results it was concluded that even though a marked improvement in low temperature impact properties was obtained, it was not caused by increased hardenability properties. Microstructures of some of the alloy steels also seem to bear out this point. While extreme improvements in low temperature impact properties were obtained, the microstructures showed no changes. These steels in areas where the structure was not completely martensite but contained some intermediates did, however, exhibit exceptionally high impact properties at −40 F. Whenever any free ferrite was present, however, the results were greatly inferior, although even then the LanCerAmp treated steels were superior to the untreated material.

Porosity

In previous work it was noted that LanCerAmp was readily oxidized or, in other words, it had a great affinity for combining with any oxygen present.

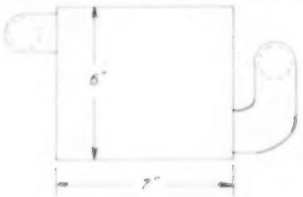

A S F POROSITY TEST PLATE CASTING

Fig. 14—The ASF standard porosity test plate, gated into one corner and with a pop riser on the opposite corner, is very sensitive to the formation of pinhole porosity.

This indicated that LanCerAmp might have powerful deoxidizing properties. To check this property, heats were produced in which LanCerAmp was the only deoxidizer added outside of the normal ferrosilicon addition. The degree of deoxidation was checked using the ASF standard porosity test plate shown in Fig. 14.

This test casting consists of a flat plate approximately $^{7}/_{8}$ in. thick, 6 in. wide and 7 in. long. It is gated into one corner and has a pop riser on the opposite corner. This casting is exceedingly sensitive to the formation of pinhole porosity and has been used successfully for the evaluation of various types of deoxidizers. Steel produced with no special deoxidizers except the 50 pct ferrosilicon produces a test casting containing large amount of pinhole porosity. This porosity is not always noticeable on the surface and is most often found under the surface. The test casting must be examined either by X-ray methods or by machining.

Proper aluminum additions will completely eliminate all traces of pinhole porosity, as shown in Fig. 15. Results of this investigation showed that porosity in the test casting was eliminated when 2 lb of LanCerAmp per ton of charge was used. Results were similar when aluminum was used.

LanCerAmp must, therefore, be considered a good

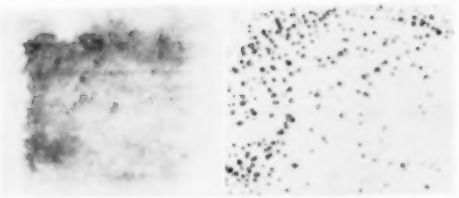

Fig. 15—All traces of pinhole porosity are eliminated with aluminum or LanCerAmp as a deoxidizer as shown at left. Pinhole porosity resulting when no special deoxidizer was used can be seen at right.

deoxidizer and could be used in place of aluminum if economics allowed. At the present time the cost would not warrant its use as a replacement for aluminum in the deoxidation of steel. It is, therefore, imperative that to obtain the maximum benefits from this alloy, it must be protected from traces of oxygen in the steel by proper additions of aluminum.

Weldability

In the development of any new steel or with the use of radically new additions to steel, its weldability characteristics must be considered both from a repair and fabrication standpoint. While all physical property results pointed to the possibility that no difficulties would be encountered in welding this material, welding experiments were performed.

Two types of tests were conducted on medium alloy steels produced with and without LanCerAmp additions. In one case single beads $^{1}/_{2}$, 1, and 8 in. in length were laid on cast and machined surfaces of 2x10x12 in. plates. This type of test produced drastic cooling conditions which might be responsible for certain types of cracking. The welding rods used were of similar composition as the parent metal and were low hydrogen or lime coated rods. These tests were performed at room temperature and 20 F. After welding, the plates were etched in hot muriatic acid and carefully examined. One small crack was observed starting in the heat affected zone on the machined plate produced with no additions of LanCerAmp. Fig. 16 illustrates the manner in which the welds were made and the location of the one crack. No cracks were observed on the plates when the steel was treated with LanCerAmp. No special welding process or techniques were used and no porosity was observed when the plate was welded with the standard lime coated rods.

Sections were removed through the various welded areas and Rc hardness readings were taken in the heat affected zones. There was absolutely no difference in hardness values in the heat affected zones of the steels made with and without LanCerAmp.

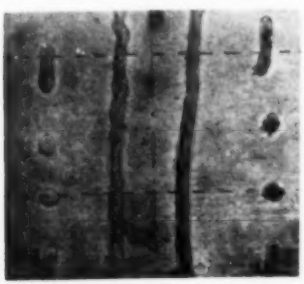

Fig. 16—The one small crack starting in the heat affected zone on the plate containing no addition of LanCerAmp is shown. No cracks were observed on the steel plate treated with rare earths.

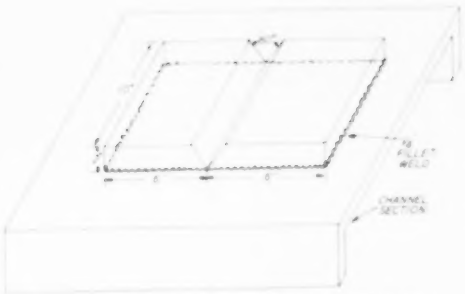

Fig. 17—The diagram shows how halves of beveled plates were first welded to a heavy channel section to prevent warping during the main welding operation

The depth of the heat affected zones was also identical. This again proved that the LanCerAmp addition had absolutely no effect on the initial hardness or hardenability characteristics. An examination under the microscope showed no difference in the structure in the heat affected zones of the two steels.

In the second section of the weldability investigation, halves of a 2x10x12 in. plate, beveled to give a 60° included angle groove, were welded under restraint. Fig. 17 shows how the halves of the plates were first welded rigidly to a heavy channel section. This was done so the sections could not warp during the main welding operation. After welding to the channel, the two halves were welded together at room temperature using a similar rod as described in the first welding experiment. The fillet welds were chipped off and the welded plate removed from the channel section. The plates were quenched and tempered followed by a careful radiographic and macroetching examination. No defects or any indication of cracking was observed.

These tests indicated that no special difficulties would be encountered in welding LanCerAmp treated steels. In fact indications were that the LanCerAmp treated steels were actually more weldable than the steels containing no LanCerAmp.

Feedability

To study the possibility of increased feedability of production castings, a feedability test casting developed by the Naval Research Laboratory was used. Because of the slightly lower final solidification temperature of the LanCerAmp treated steel and the appearance of a denser macrostructure in the standard test coupons, it was believed the LanCerAmp treated steel might feed better than the regular deoxidized steel.

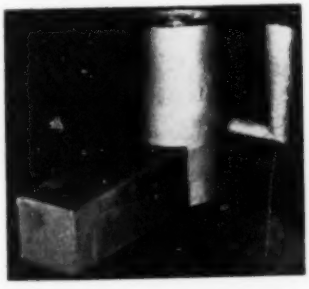

Fig. 18—This feedability test casting, developed by the Naval Research laboratory, was used for all tests.

Fig. 18 illustrates the Naval Research Laboratory test casting used. The riser was 4½ in. diam and poured to a height of 6 in. The lengths of the test section of the casting were 10 in. in one case and 16 in. in another. The width and height of the test sections were 3 in. The casting was gated tangentially into the riser. Heats of the 1.60 pct manganese steel were produced with and without LanCerAmp. Mold entering temperatures for both steels were 2860° F and the pouring rate was carefully controlled. One inch vertical slabs were sawed out of the center of the test sections. The surfaces were ground and an X-ray examination made. Following this examination the slabs were machined to ½ in. thickness so that the center line of the test section was now one of the surfaces. This surface was etched in hot muriatic acid for 30 min. Results between the X-ray and macro etch examination were similar, although the etching was considerably more critical. The slabs from the 10 in. test sections of both steels with and without LanCerAmp showed no shrinkage except for a very slight center line weakness brought out during etching.

The 16 in. test sections showed some shrinkage or lack of feeding in both steels. The slab from the

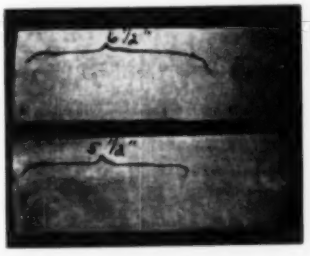

Fig. 19—Rare earth treated steel, above, had solid metal for a longer distance from the opposite end of the riser than the untreated steel.

LanCerAmp treated heat appeared slightly superior. Fig. 19 illustrates this comparison. Note that from the opposite end of the riser, the LanCerAmp heated steel had solid metal for a distance of 6½ in. as compared to 5½ in. for the slab from the heat with no LanCerAmp added. These results fall in line with those regarding solidification and fluidity.

While the difference is slight, results again favor the LanCerAmp treated steels. It is expected experiments on this subject will be continued.

Conclusions

At the present time, it can be observed from the preceding information that, while the rare earth addition of LanCerAmp is not a complete cure for all steel problems, it has helped improve many of them and thus far has shown no detrimental effects to the steel itself.

There is no doubt that the use of LanCerAmp or similar alloys in the steel casting industry can be compared to some of the wonder drugs in the medical profession. There is a good possibility that this new addition will open new fields to the casting industry which heretofore have been classified as impractical, and at the same time open new phases for research and development.

References

1. D. I. Brown: *Iron Age*, January 1952.
2. C. D. Berry and A. A. Dorvel: *American Foundryman*, December 1951.

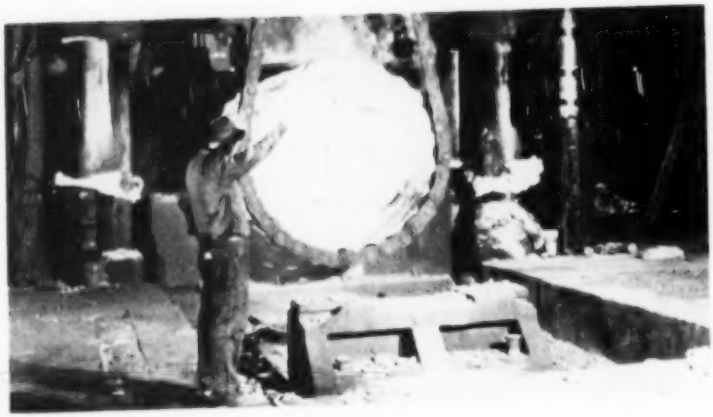

Initial operation in fabricating the rotor disk from a 92-in. ingot takes place in the 7500-ton forging press at the Bethlehem, Pa., plant of Bethlehem Steel Co. Ingot mold corrugations are still visible.

Bethlehem Forges Giant Rotor Disks

BETHLEHEM STEEL CO. is forging 11 giant rotor disks to be used for compressors in supersonic wind tunnels to be employed by the NACA for experimental air development. The disks are approximately 18 ft in diam, 9 in. thick, and weigh almost 50 tons. The disks are being forged from 92-in. ingots, and delivered in heat treated and rough machined condition. The diameter of the forgings and the limited distance between press columns and positioning of the forging under the 7500-ton press required partial forging of two disks simultaneously to avoid unequal loading of the press. One of the largest heat treatment furnaces in the nation is being used in the operation. The rotor discs are wider and heavier than those forged at the Bethlehem plant for the Columbia University and University of Chicago Cyclotrons.

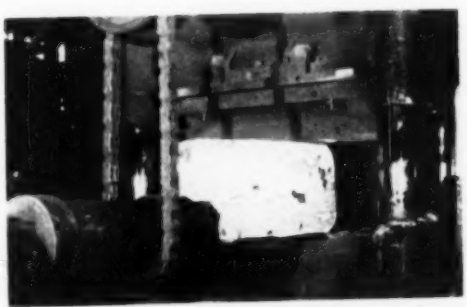

At this point the ingot has been cropped and upset. Its diameter is being compressed and grain refined by kneading action of the press.

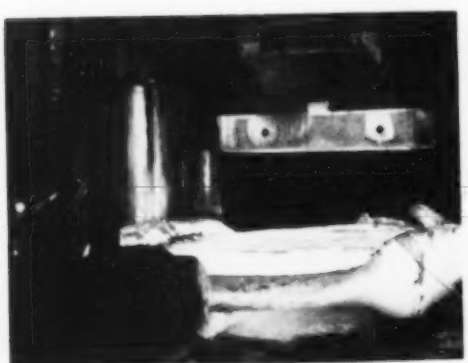

The greater part of the piece is finished to required thickness in a lengthwise path during this stage of the forging. Lips are left on each side because of the limited spread of the press columns, preventing forging the entire piece to exact thickness. Piece was returned for reheating. The last operation reduced lips to thickness.

The 18 ft diam forging could not be transported from shop to shop by ordinary means, necessitating a specially rigged railway car permitting it to be tilted. The rotor disk was heat treated and rough machined at the Bethlehem plant before being shipped to the NACA. Materials handling problem was one of the most serious encountered.

Nonferrous Metals Engineer Faces Challenge After Century of Progress

The engineer occupies a proud place in history. His contributions to civilization have been immeasurably great. His is the spirit of progress, the spirit which responds to the challenge of difficulties. He has taken the forces and raw materials of nature and put them to use, one by one, for the benefit of mankind, so, in effect, creating new natural resources. This he will continue to do, and, by advancing techniques, will make our resources virtually inexhaustible. But he must now contribute in a greater way than ever before to maintain the present position and to build upon it a still better civilization. The impact of scientific and technological developments on society has created a multitude of great and ever-increasing problems in the social, political, and economic fields. To deal with these, the engineer is needed by America, in fact by the world, to take an ever broadening view of his profession, and to develop sound philosophies and objectives of the widest scope. The engineer now faces his greatest challenge.

by R. W. Diamond and B. P. Sutherland

ONE hundred years ago, annual world production of copper was less than 100,000 tons, and in North America the copper industry was just getting under way in the Lake Superior region. About 1880, copper production began in Montana. Shortly after the turn of the century important copper deposits were found in Chile and Africa, and improved methods made possible the economic treatment of porphyry ores. World copper production grew at an accelerating rate. In 1911 the million-ton per year mark was passed. Present world production is nearly 3 million tons, over 40 pct of which comes from North America.

Similarly, production of lead and zinc has increased about 20 times in the same 100-year period. Present world output is about $1^3/_4$ million tons of lead, and approaching $2^1/_2$ million tons of zinc per year. In each case North America contributes about half the total.

The copper smelter of only 50 years ago was a place of dust and smoke, heat and hard labor. Twelve-hour shifts, or their equivalent, and 7-day weeks were the rule. Piles of ore might be seen in the open, burning and smoldering for weeks and giving off clouds of fumes, destroying all vegetation for miles around. There were rows of small roasting furnaces, where men raked the ore in the heat and in an atmosphere of sulphurous gas. There were other small furnaces for producing copper matte. To convert this matte to crude copper was a complicated business. Even after crude copper was obtained, there was further heating and scorifying to remove impurities, in attempts to produce commercially acceptable refined metal.

In contrast, modern practice has been reduced to three basic steps. A plant formerly having about 200 furnaces might now have from five to ten. Manual labor has been reduced to the minimum, and working conditions are relatively pleasant. Copper concentrate from flotation of sulphide ore is mixed with fluxes and fed directly to huge reverberatory furnaces, which may treat as much as 2000 tons of charge per day. Copper matte is produced and transferred to large converters, where crude copper results from blowing air into the molten bath, burning off the sulphur and slagging the impurities. The crude copper is then cast into anodes for electrolytic refining. In this process, under the impelling force of electric potential, and precisely by the law worked out by Faraday over 100 years ago, the copper in the anode is dissolved and the pure metal invisibly transported to cathodes. The silver and gold, arsenic and antimony, selenium, tellurium, and other impurities in the crude copper remain as a black mud, which is collected and treated for recovery of these valuable constituents. The copper cathodes are removed from the cells and cast into bars of pure copper for market.

These tremendous advances achieved in copper metallurgy have been paralleled by great developments in lead and zinc smelting and refining.

It should be observed that very pure metal results from modern refining processes for copper, lead, and zinc. This is most important because a small impurity content has a remarkable effect on the properties of the metal. For example, the total

R. W. DIAMOND is Executive Vice President and B. P. SUTHERLAND is Technical Assistant to the Executive Vice President, Western Region, the Consolidated Mining & Smelting Co. of Canada Ltd., Trail, B. C. This is an abstract of an address presented at the Mineral Industries Symposium of the Centennial of Engineering, Chicago, Sept. 8 and 9, 1952.

impurities in copper for electrical purposes must be less than 1 part in 20,000.

The economic recovery, as byproducts, of the impurities contained in the crude metal is another important feature of present day refining of the principal nonferrous metals. For example, cadmium is recovered from zinc operations, and gold and silver from the refining of lead and copper. An important part of the world's supply of antimony, arsenic, and bismuth comes from lead refineries. So with many other minor metals, such as gallium, germanium, indium, and thallium, which are byproducts of zinc and other operations.

Another development of recent years is the economic use of sulphur dioxide gas which is given off from roasting of sulphide ores. This gas is now used in many modern plants for making sulphuric acid. Almost 15 million tons of acid a year are made in this way in North America, or about 11 pct of the total production of this continent. It is hardly necessary to point out that this improves the atmosphere as well as adding to the reserves of sulphur.

It should not be forgotten that, while smelters and refineries have progressively made more and better metals, science, engineering generally, and industry, have been finding new uses for these metals. Large tonnages of copper, lead, and zinc are now being put to uses not thought of 100 years ago.

In retrospect, it becomes apparent that the progress achieved by the engineer in the metallurgy of copper, lead, and zinc, in the past 100 years, was made possible only by the use of ever advancing scientific and technological knowledge. It is interesting to observe that the advance was along three general lines: First, the increasing scale of operations made possible by mechanization; next, the production of metals and alloys of ever increasing purity; and, finally, the economic recovery of numerous byproducts.

Nickel, one of the newer metals, was no doubt accidentally present with other metals and alloys from very early times, but was not recognized as a distinct element until about 200 years ago. Its discovery was the result of an unsuccessful attempt of miners in Saxony to smelt copper ore which, unknown to them, contained nickel. The problem was investigated by the Swedish scientist Cronstedt, who in 1751 discovered that the bad actor was a new metal to which he gave the name nickel (after "Old Nick" who, according to their superstition, had corrupted their copper). Its recognition gradually led to production on a small scale. However, the total world production of nickel was less than 1000 tons per year when mining for copper began in the Sudbury district of Ontario in 1886.

At that time most of the world's nickel was coming from New Caledonia, where the ores did not contain copper, and no one in North America knew much about separating nickel and copper. When the first batch of Sudbury copper ore was smelted, the same thing happened that had happened in Saxony years before. Something was wrong with the copper, making it unsaleable. Again analysis revealed that nickel was the cause of the trouble, but the men concerned were not easily daunted and saw in the difficulty an opportunity for new and greater success in the production of a new metal. While one group started work on the problem of producing nickel, another set out to find uses for the great quantities which they foresaw might be produced. It was not long before experimental work was fruitful in developing the Orford process, which continued in use for 60 years and has only recently been superseded. At about the same time the unique Mond, or carbonyl distillation process was developed, which was the first to produce nickel free from cobalt and is still being used in one or two plants.

Outstanding success also was achieved in finding outlets for nickel. One important example was in nickel-steel for armor plate. The first world war created a great demand for nickel for military purposes. Plants were expanded as rapidly as possible so that in 1917 a new peak production of more than 50,000 tons was reached. But, as had been foreseen, the end of the war in 1918 brought about a drastic drop in demand, so that production fell to about 10,000 tons. Research to develop new uses for nickel was pressed. So successful was this work that, within ten years, peacetime uses of nickel had brought consumption up to previous wartime peaks. Within another ten years, production had more than doubled again, and then the second world war created a demand for as much nickel as could be made available. Today the world's output is about 200,000 tons annually, with further increases planned.

Nickel has become such a versatile metal that it is impossible to catalog all its uses. When comparing the uses of nickel with those of other metals, it is worth recalling that the present world production is something like one tenth that of either copper, lead or zinc, and only a fraction of 1 pct of that of iron. Nevertheless, nickel has won for itself an almost universal usefulness.

It is interesting to note that, in the modern process for refining nickel, the impurities which are separated constitute the raw material from which about half the world's supply of platinum metals is obtained. This group includes not only platinum itself, but also iridium, osmium, rhodium, ruthenium, and palladium.

The early history of aluminum is a real *united nations* effort and shows the benefit of the free exchange of scientific information between different countries. In 1808, Davy published a paper in England in which he discussed his unsuccessful attempts to produce the metal, which he was convinced existed, in oxide form as alumina. In 1825 Oersted first made aluminum metal in Denmark. The next step was in Germany where Wöhler in 1845 first made coherent particles of metal, although they were only the size of a pin's head. Ten years later in France, St. Clair Deville exhibited the first bar of aluminum metal which he had made by his new process. Finally, in 1886, Hall in America, and Heroult in France, independently developed the electrolytic process which is the basis of the present industry.

A great forward step was taken when this new process was invented, but the few little buttons of metal made by Hall in the family woodshed in Pittsburgh, Pa., were in themselves no guarantee of a major new industry. The next step was to build and operate on a larger scale and that required more money than Hall could provide. Difficulties and disappointments beset him, but he managed to transfuse some of his unquenchable assurance and enthusiasm into a little group of men, who scraped together $20,000. With this they formed the Pittsburgh Reduction Co. and built a plant which could, on good days, make 50 lb of metal. Within two or three years North American capacity alone will be

well over 10 million lb a day, and aluminum will lead the nonferrous group in world production.

The first plant had $20,000 in capital behind it; today, there is about $15,000 investment behind every employee in the industry. Also back of every aluminum plant is an electric power plant, for every 100 lb of this metal represents as much electrical energy as would supply a modern household for two months. This is 80 times as much energy as is needed to refine 100 lb of copper, or about six times as much as to make the same amount of zinc by electrolysis. No wonder aluminum has been called *packaged power*.

In many ways magnesium is similar to aluminum. It is lighter in weight than aluminum, so that, although it usually costs a little more per pound, magnesium is comparable to aluminum on a unit volume basis. Other points of similarity are the large quantity of power used for production and the abundance of the raw material. In fact, probably the most economical process for the production of magnesium is its recovery from sea water. One cubic mile of ocean contains about 4½ million tons of magnesium, which is more than the world's consumption of the metal up to the present time. That supply will not soon be exhausted.

Much could also be said about sodium, lithium, tungsten, cerium, mercury, calcium, beryllium, cobalt, manganese, chromium, vanadium, molybdenum, columbium, and thenium. Each of these, and others whose names are unknown to the layman, represent the work of scientist and engineer.

Future Trends

This sketch of nonferrous metallurgy over the last 100 years has revealed an almost unbelievable rapidity of growth and development, and is still continuing. A few among many recent metallurgical advances may suggest the trend of the future.

First, there are the metallurgical methods. No doubt there will be new processes, more push-button operation, more mechanical hands, and more electrical brains, with less arduous labor and better working conditions. There will be much more science employed in engineering and in smelting and refining. Higher efficiencies and better products will result. As examples, three new techniques might be mentioned.

One is the use of oxygen in smelting, not as slightly enriched air, but as substantially pure oxygen. There is a copper smelter already operating in Canada along these lines. In one step, copper concentrates are flash smelted with oxygen right through to blister copper. This development seems to point the way to what might be almost a new type of high temperature smelting. Another process is a new hydrometallurgy. Ores, suspended in water, are treated with oxygen under pressure, whereby the metal sulphides are dissolved. By subsequent controlled reduction, the individual metals can be recovered one by one in pure form. Such a plant, with no roasters, no furnaces, no electrolysis, would present a strange contrast to most present day operations. As the third example, there is the new invisible crucible. Metals with very high melting points have long been difficult to handle, because it is almost impossible to find suitable crucibles to hold them. Lately a scheme has been used whereby the metal is literally suspended in mid-air by electromagnetic force, while being melted by induced electric current.

Next there are some outstanding new metals, whose possibilities are just being grasped. Titanium, while a really abundant constituent of the earth's crust, is scarce and expensive in refined form because of technical difficulties. However, it is looked upon as the next major metal. For equal strength, a weight less than that of aluminum or stainless steel can be used. For resistance to salt water corrosion, it is better than either. Its properties at high temperatures are outstanding. Titanium is only at the beginning of its career and the familiar pattern of ever increasing quantities of metal at decreasing costs may be repeated. Similar to titanium in many ways is zirconium, another metal of the future, just coming into production. Uranium must also be mentioned. Physically and chemically, uranium metal showed no particularly striking features and, although not rare, had only a limited application, mainly in special steels, until its possibilities as a basic fissionable material were discovered. It then became almost priceless. Normal economic considerations went by the board and all the skill and industry of metallurgical and chemical engineers were brought to bear on the problem of recovering pure uranium and putting it to use. Having unlocked the secret of its nuclear energy, uranium is now wanted, not as a metal in the ordinary sense, but as a source of energy, a fuel. Theoretically, 1 lb of uranium is equivalent to burning 1500 tons of coal. Undoubtedly a substantial part of its energy will become available not only in atomic weapons but in industrial plants supplying the needs of mankind.

Some of the great changes applied science has brought about in the nonferrous metallurgical industry over the last century have been outlined. Because of these, and similar changes in other fields of activity, many new and great problems have been created for governments, their people and their industries.

One hundred years ago capital requirements of metallurgical plants were relatively modest. Labor requirements were high and productivity in terms of metal output was low. Today such plants tend toward ever larger units, with more mechanization and higher capital costs. Hourly wage rates and labor productivity have multiplied many times. In 1948 the average overall productivity for all employees in the domestic copper, lead and zinc industry in the United States, was about 25 tons of refined metal per man per year. In spite of this high productivity, labor costs have risen to about 8¢ per lb of metal, which is twice the selling price of lead and zinc as of 50 years ago. Capital investment per man has risen to approximately $10,000. Corporation income taxes have increased from virtually nothing in 1850 until, today, they are most onerous. All in all, in spite of the great technical advances in nonferrous metallurgy, this industry, in common with others, faces greater economic problems today than ever before. Moreover, from political or disruptive motives, there has recently been a tendency to bring discredit on industry, to induce mistrust in management, and to condemn big business simply because it is big. There has been gross misrepresentation as to the meaning of profits. Not only are such attacks unjustified, but they contribute seriously to unrest, and otherwise are to the detriment of society. Yet it remains true that the progress already achieved could have been realized only under the free enterprise system, and only in that way can progress be continued.

New Process Permits Many Metals To Be Tungsten Carbide Coated

WEAR resistant parts can be made from almost any metal with the application of a thin coat of tungsten carbide. This is possible with a new process, Flame-Plating, developed by Linde Air Products Co., capable of plating tungsten carbide in thicknesses of 0.0005 to 0.020 in. Other refractory metals have been deposited by the Flame-Plating process, but only tungsten carbide coatings are available now. Steels of all types, cast iron, aluminum, copper, brass, bronze, titanium, and magnesium have all been successfully coated with tungsten carbide. Chromium plate, sintered tungsten carbide, and ground Flame-Plated surfaces cannot as yet be coated.

One of the basic advantages of the process is that the temperature of the base metal does not exceed 400 F during the plating operation. Thus, the base metal is not damaged in any way, and there is little tendency for the part to warp. Flat areas, cylinders, holes, and parts having various shapes and contours can be coated. Surfaces up to 6 in. wide and 40 in. long can be handled, and the plated part used as-coated or finish ground.

In the majority of applications to date, parts Flame-Plated with tungsten carbide have shown wear resistance equal to or greater than sintered tungsten carbide, and by far superior to cast alloys, hard chromium plating, and tool steels. These parts have all the desirable properties of sintered tungsten carbide such as resistance to abrasion and frictional wear, and in addition have a lower modulus of elasticity and greater resistance to impact and thermal shock.

Flame-Plated parts can be used wherever an undiluted coating of tungsten carbide is required for protection from severe abrasion and frictional wear. Cotton picking spindles, dies, seaming rolls, and furnishing tools are examples of parts exposed to this type of wear.

Precision parts can be protected by Flame-Plating, where the wearing away of a few thousandths of an inch would make the part useless. These parts, many of which are made of sintered tungsten carbide, are scrapped when worn. Flame-Plated parts may be an economical answer to the problem. When wear does occur, the tungsten carbide coating can be removed down to the steel base, and a new coating applied. Plug and thread gages and arbors fall into this category.

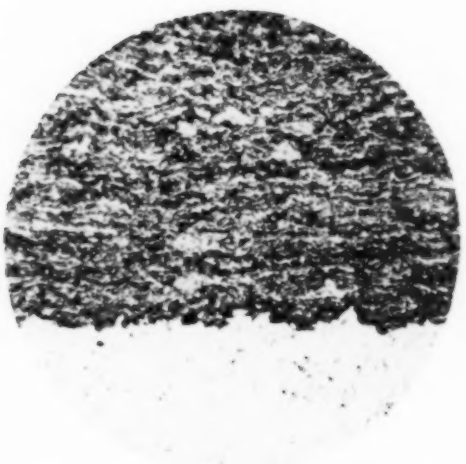

The dark area of this photomicrograph represents the Flame Plated tungsten carbide surface. The mild steel base is shown in the lighter zone. The jagged bond line between the two materials indicates the cleaned, slightly roughened, coated surface. No mixing or dilution of the coating with the base takes place.

Core rods used in powder metallurgy are good applications for Flame-Plating. Sintered tungsten carbide core rods in use are brittle, whereas the plated core rod combines the wear resistance of the coating with the toughness of the base metal.

The wide selection of base metals offers many design possibilities. Parts requiring good electrical conductivity and resistance to wear can be obtained by Flame-Plating copper. Weight of wearing parts can be reduced by coating aluminum with tungsten carbide.

The tungsten carbide applied in the process differs from sintered tungsten carbide. The elements tungsten, carbon, and 8 pct cobalt are present as WC,

and Co_3W_3C, Co_6W_6C, or Co_4W_2C. There is no free cobalt. The particles forming the coating are elongated and flattened into disks, the diameter of each particle being many times its thickness.

The bond between the coating and the base metal is an interlocking mechanical bond and not a welded bond. The coating does not mix with or dilute the base metal, and no visible oxide layer appears. Deformation of the base metal will crack or separate the coating, depending on the thickness of the coating. The thinner the coating, the less tendency toward separation.

Parts to be Flame-Plated should be undercut deep enough to allow for the desired thickness of the coating. It is usually desirable to leave a small protective lip at any edge where the part may be subjected to abuse or where two Flame-Plated surfaces are at right angles to each other. A coating thickness of a few thousandths of an inch will resist mechanical and thermal shock more than a coating of 0.010 or 0.020 in. A coating thickness of 0.001 in. over the allowable wear tolerance is sufficient in most instances. If the part is to be finish ground an excess coating of 0.004 in. is deposited. The as-coated parts have a surface of 125 micro in. rms.

Finish grinding will produce a surface of 2 micro in. rms. Resinoid bonded diamond wheels should be used for finish grinding; a 100 mesh wheel for rough grinding, and a 400 mesh wheel for finishing when no more than 0.0005 in. is to be removed. The part to be ground should be flooded with coolant, such compositions as 50 pct water-50 pct soluble oil,

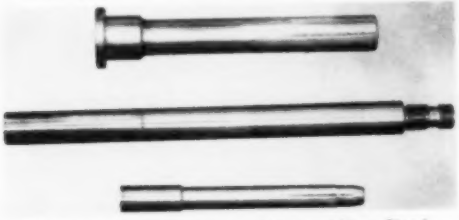

These samples represent sizes and shapes of Flame Plated core rods used in powder metallurgy. Core rods must be able to take severe abrasion, in addition to being tough enough to withstand a certain amount of loading and deformation. A hard coating of Flame-Plated tungsten carbide over a strong steel base provides ideal combination of properties for this application.

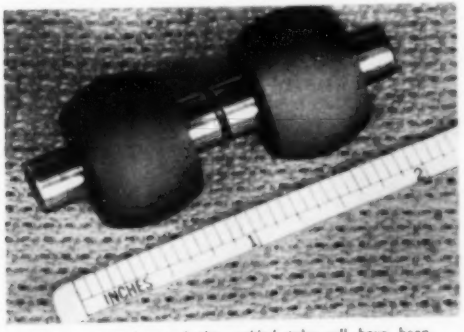

The wear surfaces of this welded tube roll have been Flame Plated. After finishing the coatings will be 0.010-in. thick. Other parts now being tested for flame coating are valve plugs, seat rings, balls, mill hammers, cut-off dies, punches and other items.

Specifications and Properties of Flame Plated Tungsten Carbide Coatings

Composition:	92 pct tungsten carbide, 8 pct cobalt
Hardness:	1200 to 1300 Vickers (300 g loads); R_A 89.3
Coating Thickness:	0.020 in. max, 0.0005 in. min
Surface:	As coated — 125 micro in. rms Finish Ground — 2 micro in. rms
Base Materials:	All steels; cast iron, aluminum, copper, brass, bronze, titanium, magnesium
Process:	Application temperature is less than 200°C
Part Size:	Rounds — ¼ to 6 in. OD. to 40 in. long Flats — As coated, 6x40 in. Finish ground, ¾x40 in.
Part Shape:	Externals — Any area at no greater than 45° from a horizontal datum Inside Cylinder walls — Coating can be deposited to a depth equal to diameter of the hole Irregular shapes — Any shape within above limitations, such as saw teeth
Applications:	Core rods, plug gages, burnishers, saws, shafts and bearings, draw dies, thread gages, paper cutter knives, valve plugs, balls, mill hammers, etc.
Modulus of Elasticity:	35 million psi
Porosity:	Less than 0.5 pct
Corrosion Resistance:	Attacked by most acids and strong alkalies. Resistant to mild alkalies, detergents in lubricating oils, atmospheres free from acid fumes
Thermal Shock Resistance:	Good below 2000°F
Mechanical Shock:	Can absorb moderate amount of deformation

or 50 pct kerosene-50 pct spindle oil have proved satisfactory.

At the present time parts to be Flame-Plated must be sent to Speedway Laboratories of Linde Air Products Co., Indianapolis, a time consuming and expensive procedure. Other facilities in various parts of the country will be established in time. In most instances, the company does not perform finish grinding. This is either performed by the customer or contracted out. Cost of plating varies with the size and shape of the part, number of parts to be plated, and thickness of coating. The cost of a Flame-Plated part will probably fall somewhere between the cost of a hard faced part and a sintered carbide part. Service life of the part will be the deciding factor as to the economic advantage of the process.

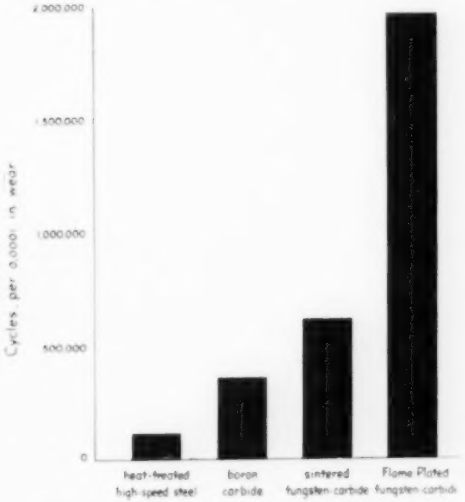

An extensive wear test on 14 different materials conducted over a two year period showed that a Flame Plated gage out-wore all other materials. The wear medium was cylinder block cast iron. The Flame Plated gage showed a life of about 5 to 1 over a gage made of boron carbide and 3 to 1 over sintered tungsten carbide.

Watertown Arsenal Testing Machine Has 72 Year History of Service

SEVENTY-TWO years of history are written into the U. S. Testing Machine at Watertown Arsenal, Watertown, Mass. The 1 million lb capacity machine is entering into the second phase of its life, refitted with four new Emery hydraulic load cells and a Tate-Emery control system with three-range load indicator dial. The electric motor-driven oil pump in the control cabinet replaced accumulator type hydraulic equipment occupying 200 sq ft of floor space.

With the new equipment, loads are automatically indicated on a large dial instead of the slow manually balanced lever system, and load changes are followed instantly under changing load conditions.

The machine was constructed for the testing of steel, which began to emerge in the 1870's as a competitor of cast iron in gun manufacture. Congress appropriated money to build the machine to take compression specimens up to 30 ft long, and A. H. Emery was awarded the contract. A report to Congress on June 30, 1879 stated, "The machine is more perfect than we had any right to expect from the terms of the contract." Fulfillment of the contract cost Emery twice the $31,500 called for by the agreement, and the board appointed by Congress to oversee construction recommended that relief be granted to Emery.

A forged link of wrought iron, 3 in. diam, was broken at 722,800 lb as part of the acceptance tests. A horse hair 0.007 in. diam was slowly strained and stretched 50 pct before breaking under a 1 lb load.

The machine is the same as it was in 1879. The hydraulic load cells and the use of flexure bars or plates where very small movements are necessary are still features of Baldwin testing machines built today. The hydraulic load cell is basically a shallow cylinder with a loose fitting piston and metal diaphragm arranged so that the load on a test specimen must pass through a thin film of liquid trapped between the diaphragm (backed by the piston) and the bottom of the cylinder. Piston movement is almost negligible. The only significant change in the Emery cell design is a bridge ring, which supports the diaphragm over the clearance space between piston and cylinder, and centers the piston so that it does not touch the cylinder wall.

The original Emery cells on the testing machine were connected with a smaller Emery cell in the load weighing cabinet, thus providing a hydraulic lever giving the first load reduction to the mechanical lever system. Use of flexures instead of knife edge pivots is one of the design features of the lever system.

The testing load is applied through two 8½ in. diam screws. The screws are 48 ft long and threaded for a length of 38 ft with a truncated thread, two per in. The loading cylinder and one set of specimen grips travel on rail carriages driven by a keyed gear that slides on a horizontal shaft near the floor level. The grips are positioned by four nuts on the two horizontal screws, turned by a gear train.

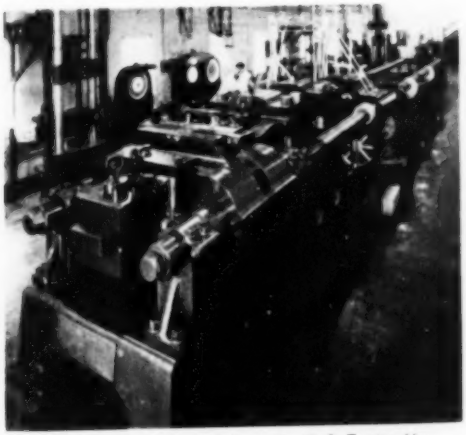

Original hydraulic Emery Cells on the U. S. Testing Machine, installed at Watertown Arsenal in 1879, were replaced by cells of advanced design. The cells are held between the stationary crossheads by flexure bars on the side of the machine. When the test specimen is loaded in tension or compression (up to 800,000 lb) the cells are squeezed, and resultant hydraulic pressure is transmitted to the Tate Emery null balance indicator.

A double acting piston in the loading cylinder has a 20 in. diam head and 10 in. diam piston rod forged in one piece, providing 800,000 lb in tension and a little more than 1 million lb in compression, with oil at 3400 lb pressure.

The machine once tested the thesis of naval officers at Massachusetts Institute of Technology, advocating an improved arrangement of rivets for joints in ship plates. Plates 1¼ in. thick, joined together by seventeen 1½ in. rivets started to come apart when a load of 783,000 lb was applied. Rivets shot across the shop floor in all directions. Less impressive, but very interesting, was the test of the main cylinder used to hold a new type of alloy steel mast on the racing vessel Enterprise, runner of several cup races against England, in 1930.

During the past 11 years, seven Baldwin testing machines of smaller capacity have been installed in the Arsenal's laboratory. Operation of the old testing machine is identical with that of the later models because of the new accessories added.

Research In Progress

There is a vast amount of research work for both Government and private industry now underway in the industrial, Government, and university laboratories. JOURNAL OF METALS brings you a summary of some of the outstanding projects, with abstracts or summarizations of the progress thus far on such work, prepared by scientists in charge of the activities. Descriptions of these research projects will be given in greater detail at the Fall Meeting of the AIME Institute of Metals Div., Adelphia Hotel, Philadelphia, at 2 pm Monday, Oct. 20, 1952. The papers will be presented in the same order as they appear here.

Magnetic Transfer of 18-8 Stainless Steel Recording Wire

by Samuel Storchheim

ONE of the phenomena accompanying magnetic wire recording is that of magnetic transfer. This condition involves the magnetization of unrecorded turns of wire by adjacent turns of recorded wire, the wire usually being made of 18-8 stainless steel.

Tests were conducted in which 0.004 in. diam wires having different magnetic properties, i.e., remanence and coercive force, were magnetized with increasing recording currents. The resultant transfer was measured in decibels and plotted against the log of the recording currents used. The curves obtained showed that transfer first increased, then reached a peak and finally started to decline, all with increasing recording currents.

It was found that increasing remanence displaced the peak of the curves upward while higher coercive forces shifted the peak of the curve towards increasing current inputs.

Additional tests using wires of finer size, 0.0036 in. diam, indicated that the maximum transfer attained was less than for the heavier sized wires.

S. STORCHHEIM, formerly with Wilbur B. Driver Co., Newark, N. J., is now Senior Metallurgical Engineer, Atomic Energy Div., Sylvania Electric Products Inc., Bayside, N. Y.

Effect of Cycle-Sintering in the Powder Metallurgy Process

by H. H. Hausner

ORDINARY sintering occurs by heating the metal powder compact at a certain heating rate up to the sintering temperature, keeping the compact at this temperature for a predetermined time, and then

cooling it. Cycle-sintering is distinguished from the ordinary sintering by a certain variation of the temperature above and below the sintering temperature in a predetermined cycle. In the tests to be described, fine electrolytic iron powder of high purity was compacted at various pressures between 10 to 40 tsi into small compacts. Some of the compacts were sintered by keeping them 2 hr at temperature and other compacts were sintered by cycling them every 5 min from 15 C above to 15 C below the various sintering temperatures. Some of the cycle-sintered samples were cycled through the alpha-gamma transformation temperature. In general, no difference in the properties of the compacts could be observed whether the sintering occurred at temperature or by cycling through the temperature. However, the samples cycle-sintered through the transition temperature showed certain remarkable differences compared with the other samples: 1—The linear shrinkage was less in the compacting direction but considerably greater perpendicular to this direction; 2—The grains of the cycle-sintered specimens were substantially larger than that of any other specimen; 3—The cycle-sintered specimens contained fewer but larger voids than the regularly sintered specimens.

Cycle-sintering may be considered as a valuable method for the analysis of the sintering process.

H. H. HAUSNER is Manager, Atomic Energy Engineering, Sylvania Electric Products Inc., Bayside, N. Y. and Adjunct Professor at Polytechnic Institute of Brooklyn, Brooklyn, N. Y.

The Initial Phase of Sintering

by H. H. Hausner and J. L. Zambrow

TO follow up on the early stages of sintering, tests were made with carbonyl nickel powder compacts heated to 100 C in argon and hydrogen, respectively. The nickel powder was used in the as-received state, that is, slightly surface oxidized. The effect of the various heat treatments on the electrical resistivity of the compacts was studied.

Heating in argon to 100 C resulted in an extremely slight decrease in electrical resistivity which may be explained as a result of stress relief. Considerable decrease in resistivity (up to 40 pct and more) was observed when heating occurred in hydrogen at temperatures as low as 50 C. The decrease in electrical resistivity after heating was greater with fine powder compacts than with compacts made from coarse powders.

It can hardly be assumed that reduction of the slightly oxidized powder particle surface took place at this low temperature, although a certain state of readiness for reduction or an induction period for reduction must have taken place. Any lattice change such as involved in the reduction of an oxide starts with lattice disturbances and imperfections. These imperfections appear to be the cause of the migration and exchange of atoms resulting in a low degree of bonding between powder particles and therefore in a lowering of the electrical resistivity.

H. H. HAUSNER is Manager and J. L. ZAMBROW is Section Head, Atomic Energy Engineering, Sylvania Electric Products Inc., Bayside, N. Y.

Effect of Grain Size and Density on Mechanical Properties Of Sintered Carbides

by W. G. Lidman and H. J. Hamjian

IT has been shown that with powder metallurgical methods it is possible to closely control grain size of sintered materials. To evaluate this advantage over conventional melting, casting, and forging practices, this investigation was conducted to determine the effect of grain size on the physical properties of sintered carbides. Since varying the sintering temperature and time at temperature resulted in different densities as well as grain sizes, both structural variables were studied.

The results showed that increasing grain size and density caused improvements in room temperature strength and hardness. Highest values of both properties were measured for specimens below maximum density. Further increases in density did not yield better properties, since apparently the effects

of the accompanying coarser grains overshadowed the improvements that would be expected. Additional evaluations however indicated that the coarse grains may not be detrimental to elevated temperature strength. Since grain size increases with increasing density, other studies are necessary on the mechanism of grain growth for sintered materials which provide an understanding of the influence of other variables.

W. G. LIDMAN is Senior Engineer, Atomic Energy Div., Sylvania Electric Products Inc., Bayside, N. Y., and H. J. HAMJIAN is Research Metallurgist, Utica Drop Forge & Tool Co., Clayville, N. Y.

Origin of Spiral Eutectic Structures

by R. L. Fullman and D. L. Wood

EUTECTIC structures in which the two phases appear spiralled about each other in cross-section have been observed in the systems zinc-magnesium[1] and aluminum-thorium.[2] It is proposed that this type of structure is produced when one phase grows faster in all directions lying in the plane of the spiral, and the other phase is the faster growing one in the direction perpendicular to the plane of the spiral. Observations of the three-dimensional shape of the spirals in an alloy of zinc + 3 pct magnesium are in agreement with predictions based on this hypothesis.

[1] E. Scheil: *Z. fur Metallkunde* (1946) 37, 1.
[2] H. Buckle: *Z. fur Metallkunde* (1946) 37, 42.

R. L. FULLMAN and D. L. WOOD are associated with General Electric Co., Schenectady, N. Y.

Growth of Cadmium Iodide Crystals

by R. L. Fullman and D. L. Wood

FRANK[1] proposed that at low supersaturation, crystals may grow without the necessity for two-dimensional nucleation of surface layers if the growing surface is intersected by one or more dislocations with Burgers vector components normal to the surface. The spirals and loops of surface steps required by this hypothesis have been observed on a number of materials, including metals.[2,3] A color motion picture has been prepared that shows the manner in which these surface steps move as cadmium iodide crystals grow from solution.

[1] F. C. Frank: *Discussions Faraday Society* (1949) 5, 49.
[2] S. Amelinckx: *Comptes Rendus* (1952) 234, 113.
[3] A. J. Forty: *Phil. Mag.* (1952) 43, 481.

R. L. FULLMAN and D. L. WOOD are associated with General Electric Co., Schenectady, N. Y.

Growth Spirals Originating from Screw Dislocations On Electrolytically Produced Titanium Crystals

by M. A. Steinberg

IN the course of work on the production of titanium by fused salt electrolysis (ONR Contract Nonr-394 [01]), a number of large hexagonal titanium flakes were obtained which are single crystals as revealed by X-ray examination, and have flat (0001) plane surfaces. On further examination using a metallographic microscope and employing known techniques, growth spirals originating from screw dislocations have been observed on these surfaces. This is the third reported instance wherein direct visual evidence of screw dislocations has been obtained on metal crystals and is the first case of

screw dislocations being responsible for crystal growth in electrolysis.

The average step height, measured by two-beam interference fringes of the Fizeau type, obtained with parallel, monochromatic light at normal incidence, was 240 ± 100A.

It is evidence that most of these spirals cannot be caused by dislocations of unit strength but are generated by groups of dislocations all having the same sign and having a resultant Burgers vector with a component normal to (0001) of approximately 100A. However, in some cases, no deviation of the fringe system could be seen, proving that the steps are less than 100A.

Besides multiple spirals originating at the same dislocation centers, spirals of opposite sign, interacting so as to form closed loops have been observed in accordance with theory.

M. A. STEINBERG is associated with Horizons Inc., Cleveland.

Nucleation of Isothermal Martensite

by J. C. Fisher

CECH and Hollomon reported an isothermal martensite transformation in an iron-nickel-manganese alloy. They state that the transformation proceeds by isothermal nucleation and rapid growth of martensite plates, so that the rate-limiting step is nucleation. New nuclei are required to continue the transformation, for a martensite plate does not grow beyond the austenite region in which it is nucleated.

Using a simple extension of classical nucleation theory to include the effects of elastic strain energy, the experimental data on the isothermal formation of martensite can be accounted for quantitatively. In the process of making this comparison, the rate of nucleation of martensite plates per unit volume of untransformed martensite was deduced from the overall transformation rate by assuming that martensite plates compartmentalize the austenite as they form, restricting the volume in which they can nucleate.

R. F. Cech and J. H. Hollomon. To be published.
J. C. Fisher, J. H. Hollomon, and D. Turnbull. Trans. AIME (1949) 185, p. 691.

J. C. FISHER is associated with General Electric Research Laboratory, Schenectady, N. Y.

Time Duration of the Formation of a Martensite Plate And the Influence of Metallurgical Variables

by R. F. Bunshah and R. F. Mehl

SEVERAL reactions in the solid state in metals and alloys occur in very short periods of time, of which the martensite transformation is an important example. The characteristics of the formation of martensite, including the time-rate, were determined by measuring the type and duration of the signal resulting from the change in electrical resistance of a sample of steel during the formation of a single plate of martensite, using highly sensitive electronic equipment.

The time of formation of a single martensite plate in an iron-30 pct nickel alloy was found to be 10⁻⁷ sec, the sensitivity of the method was 10⁻⁷ sec. The plot of martensite plate length vs time of formation was found to be linear, from the slope of which the velocity of propagation of the martensite plate may be calculated as 3300 ft per sec, which is roughly of the same order of magnitude as the velocity of propagation of elastic waves in the solid.

The signal from the unit martensite transformation consists of two parts. An initial rise followed by a fall in resistance, leading to the conclusion that the unit martensitic transformation consists of two steps or distortions. The time of formation and the wave form of the signal are the same irrespective of whether the martensite forms athermally or isothermally. The velocity of martensite propagation is also virtually independent of the transformation temperature, between −30° and −195° C. Consequently, the activation energy for the propagation of martensite is extremely small, possibly zero.

This method is being used to study other transformations, and also to study slip, twinning, and cleavage.

R. F. BUNSHAH is Research Associate and R. F. MEHL is Director, Metals Research Laboratory, Carnegie Institute of Technology, Pittsburgh.

Quantitative Determination of Preferred Orientation

by J. H. Bach and J. B. Burnham, Jr.

FOR a randomly oriented sample of known structure and symmetry the ratio of intensities of any two lines can be calculated. If there exists a family of planes whose total diffracting power remains constant, no matter what the orientation of the sample, the intensity ratio of all other sets of planes to that of such a standard plane can be calculated and the quotient of the measured ratio with calculated ratio can be taken as a measure of orientation.

If I and I_0 represent the calculated intensities of any reflection (hkl) and of the reflection of the chosen standard plane (HKL) respectively

$$r = \frac{I}{I_0} \quad [1]$$

let i equal the measured intensity of (hkl) and i_0 the measured intensity of (HKL), then

$$r = \frac{i}{i_0} \quad [2]$$

and

$$\frac{r}{r} = 1 \quad [3]$$

- becomes a measure of orientation by its deviation from unity since for a randomly oriented sample

$$r = \frac{i}{i_0} = \frac{I}{I_0} = r$$

By correlating - with the position in space of the surface examined, the orientation of the crystallites can be determined; a large - would of course indicate that the plane under examination tends to lie parallel to the surface examined. The examination of three or four surfaces will usually suffice for a fairly good determination of the preferred orientation.

The foregoing technique was employed on uranium samples when it was discovered that the (111) reflection remained nearly constant in intensity no matter what the orientation of the sample was. Experiments are in progress to determine whether such constant intensity planes can be found in other metals as well.

J. H. BACH is Section Head, Atomic Energy Div., Sylvania Electric Products Inc., Bayside, N. Y., and J. B. BURNHAM, JR. is with the Phillips Petroleum Co., Arco, Idaho

Twinning in Single Crystals of Titanium

by T. S. Liu and M. A. Steinberg

CLOSE examination of titanium flakes produced by fused salt electrolysis revealed their single crystal nature. X-ray examination and etch pits established that the flat surfaces correspond to (0001) basal planes. It has appeared that profuse twinning shows up in these crystals in their handling.

Two sets of mutually perpendicular twin traces can be distinguished on the basal plane. The traces in each set make perfect 60° angles with each other.

Knowing the traces of twinning planes on the basal plane, two techniques were used for the preliminary identification of these twinning planes: 1—Sectioning the flakes along different prismatic planes and observing the twin traces, and 2—Calculating the angles of the twinning planes by comparing the dimension and shape of etch pits in the twinned portion and in the matrix.

Using a stereographic plot and comparing with a standard (0001) projection for titanium (c/a = 1.5873), it was found that the {1012}, {1121}, {1122}, {1123} and {1124} planes were responsible for twinning. The angles calculated from etch pit measurements checked within 2°.

These results are based on observations of some thirty single crystals and are believed to be representative.

T. S. LIU and M. A. STEINBERG are associated with Horizons Inc., Cleveland

Plastic Deformation of Silicon and Germanium

by R. G. Treuting

THE first experimental evidence of the plasticity of the diamond-structured semi-metals was obtained by H. C. Theuerer,[1] who in 1950 bent a twinned single crystal prismatic bar of ⅛ in. square section under a static compressive load of 10 lb at 900°C. The first announcement thereof was by C. J. Gallagher,[2] who reported on the plasticity of germanium, ascribing this to slip on the {111} plane and giving electrical properties of slipped planes.

The work to be discussed describes the bending of germanium and silicon single crystals at temperatures of 900°C and 1170°C respectively. Traces in priorly polished surfaces confirm Gallagher's report of a {111} slip plane, and displacement of scratches at the point of traverse with slip lines shows gliding.

Laue photograms of deformed germanium crystals show streaks having coagulated into discrete spots suggestive of polygonization, and also streaks of reticulated pattern suggestive of other possible flow mechanisms than slip. Silicon, at less extensive deformation, shows neither of these conditions, but the spots become slightly elongated and of discontinuous intensity.

Experiments to strain germanium in uniaxial tension are in progress and it is hoped to report on the slip direction.

[1] H. C. Theuerer, Private Communication.
[2] C. J. Gallagher, To be published in *Physical Review*.

R. G. TREUTING is associated with Bell Telephone Laboratories, Inc., Murray Hill, N. J.

Specific Heat, Latent Heat of Fusion, And Melting Point of Germanium

by E. S. Greiner

THE specific heat, between 600° and 900°C, and the latent heat of fusion of germanium were determined by the constant heat flow method described by Smith.[1] The specific heat of germanium (10 ohm-cm electric resistivity at 25°C) increases from 0.080 to 0.085 cal per g per °C as the temperature increases from 600° to 900°C. Extrapolation of this data to lower temperatures shows that it agrees with the results for the range 0° to 300°C reported by Nilson and Pettersson.[2]

The latent heat of fusion of germanium was observed to be 8100 ± 800 cal per g-atom. This is larger than the value of 7300 ± 300 cal per g-atom obtained by other thermal measurements.[3]

Three determinations of the melting and freezing point of germanium (~20 ohm-cm resistivity at 25°C) showed this quantity to be 936 ± 1°C. The rates of heating or cooling were such that 15 to 20 min were required for the phase change.

[1] C. S. Smith, *Trans. AIME* (1948) 175, p. 236.
[2] L. F. Nilson and O. Pettersson, *Zeits. Physik. Chem.* (1887) 1, p. 27.
[3] O. Kubaschewski, *Zeits. Elektrochem.* (1950) 54, p. 275.

E. S. GREINER is Member of the Technical Staff, Bell Telephone Laboratories, Inc., Murray Hill, N. J.

Constitution of Germanium Rich Germanium-Gallium Alloys

by E. S. Greiner

THE liquidus of the germanium-gallium system decreases linearly from 936° to 860°C between 0 and 20.4 atom pct gallium.

The lattice constant of germanium is 5.6575 ± 0.0001 A at 25°C. Gallium has a limited solid solubility in germanium. The lattice constant of the germanium phase is increased 0.0004 A per atom pct gallium.

Small pieces of two-phase alloys (germanium phase plus liquid) were equilibrated at various temperatures for periods of 4 to 26 days, drop-quenched, and ground to powder for the X-ray examination. The lattice constants of the germanium phase were determined, then by comparison with the values for the single-phase alloys the solid solubility limits at the respective quenching temperatures were obtained.

The results show that germanium dissolves 2 pct gallium at 600°C and 2.5 pct at 780°C.

E. S. GREINER is a Member of the Technical Staff, Bell Telephone Laboratories, Inc., Murray Hill, N. J.

Tungsten-Cobalt-Carbon System

by Pekka Rautala and John T. Norton

The phases and equilibria in the W-Co-C system have been studied by X-ray diffraction methods, metallographic technique, and thermal analysis. In addition to the η phase, two double carbides, called θ and κ, have been revealed. The compositions correspond to Co_3W_3C and Co_2W_4C. The reactions leading to these phases have been explained and tentative diagrams of stable and metastable equilibria proposed. The basic reactions in sintering cobalt cemented tungsten carbides are discussed.

THE W-Co-C system is of fundamental importance in practical carbide manufacturing as well as for the understanding of the sintering mechanism. Surprisingly little is known about this system, for the probable reason that all the important alloys are of two-phase structure and that the diagram Co-WC has been treated as a quasi-binary. This obviously is incorrect, because WC decomposes before melting.

One ternary phase, η, of composition Co_3W_3C has long been known. It was first studied by Adelskold, Sundelin, and Westgren,[1] although the isomorphous iron-tungsten carbide was known earlier. There have been in the literature several reports of two η phases.[2,3] Also the η phase has been considered unstable by Takeda[4] and Westgren.[1]

The Co-WC diagram has been studied by Wyman and Kelley[5] and a quasi-binary diagram has been published by Sandford and Trent.[6] Takeda has published a tentative Co-W-C diagram, considering both metastable and stable equilibria. However, the lines of two-fold saturation are shown only partially and it seems impossible to complete the diagram without violating the phase theory. Therefore it seemed desirable to examine the system in more detail.

Experimental Procedure

The alloys used in the present investigation were made of powders of tungsten, tungsten monocarbide, cobalt, and carbon and were of the grade used in manufacture of commercial cemented carbides. The powders were ground and mixed in small stainless steel ball mills, using balls of the same material. Benzene was used as a dispersing agent. The mixing period was 1 hr, since this was shown to give sufficiently good mixing of the powders without too great a contamination from the mill. After ball milling, the specimens were pressed in cylindrical or rectangular dies. No paraffin or other lubricant was used and the small compacts had sufficient green strength to be handled without difficulty.

Several sintering furnaces were employed. The most satisfactory arrangement was a vacuum furnace based on the Arsem principle which employed a graphite helix as the resistance heating element. Specimens were placed on graphite stands and there was generally a slight carburization or decarburization of the specimen surface, depending on the carbon content of the alloy. The evaporation of the cobalt at a sintering temperature of 1400°C was not significant, but became severe at 1500°C and higher. The sintering time was 1 hr at 2000°C and 2 to 4 hr at lower temperatures. It was not possible to quench the specimens, but the cooling rates were rather fast, greater than 300°C in the first minute. In the system under investigation, the reactions are sluggish, and it is believed that the high temperature structures are satisfactorily retained.

The principal method of investigating the sintered specimens was X-ray diffraction by the Norelco recording spectrometer. Approximate determinations of the phase boundaries were made by the disappearing phase method.

Ternary Phases

To study the phase formation in W-Co-C system, a series of specimens was sintered at 1400°C. In this experiment two ternary phases, called here θ and κ were formed in addition to the well-known η phase. The η phase, which has been completely described by Westgren,[1] showed a range of homogeneity from 7 to 20 pct C and from 38 to 48 pct Co. At 1400°C the η phase was found to be in equilibrium with monotungsten carbide, θ, tungsten, δ, β, and liquid. The boundaries toward β and liquid were difficult to determine and appeared to be very temperature sensitive. The other boundaries are believed to be well fixed. The homogeneity range of η, as measured in this work, is considerably smaller than the one

P. RAUTALA is Assistant Professor of Metallurgy and J. T. NORTON, Member AIME, is Professor of Metallurgy, Massachusetts Institute of Technology, Cambridge, Mass.

Discussion on this paper, TP 3360E, may be sent, 2 copies, to AIME by Dec. 1, 1952. Manuscript, April 15, 1952. Philadelphia Meeting, October 1952.

This paper is based on a thesis by P. Rautala submitted in partial fulfillment of requirements for the degree of Doctor of Science in Metallurgy at Massachusetts Institute of Technology, May 1951.

This Transactions paper appearing in the Journal of Metals during 1952 will subsequently appear in AIME Transactions Volume 194, and may be permanently referenced to that volume.

Table I. X Ray Patterns of η, η', and ε Phases
Plane Spacings (d) and Relative Intensities (I) of Reflections

	d	I
η Phase		
400	2.540	0.24
331	2.314	0.26
422	2.070	0.93
511,333	1.955	1.00
440	1.797	0.36
η' Phase		
400	2.572	0.09
331	2.344	0.41
422	2.096	0.93
511,333	1.979	1.00
440	1.819	0.44
ε Phase		
10.0, 10.1	2.290	0.10
00.2	2.235	0.14
10.2	2.178	0.08
10.3	2.026	0.80
20.0, 11.0	2.004	0.75
11.2, 21.1	1.947	0.80
20.1	1.900	0.40
00.4, 11.3	1.734	1.00
21.2	1.705	1.00
20.2, 21.0	1.674	0.80
10.3, 21.1	1.662	0.40
20.3	1.604	0.60
11.4	1.556	0.10
21.3, 30.0	1.538	0.10
00.5, 11.4	1.511	0.50
30.1	1.454	0.70
10.5, 20.4	1.392	0.10
30.2, 22.0, 00.4	1.364	0.60
40.1	1.291	0.60
30.3, 00.6	1.260	0.15
40.2, 20.5, 21.4	1.240	0.60
22.3, 31.2, 20.5	1.230	0.60
41.0, 00.6	1.204	0.10
41.1, 31.3	1.194	0.10
00.7	1.193	0.20
40.3, 20.6	1.123	0.20
31.4, 22.3	1.111	0.30
41.2, 31.4	1.097	0.30
30.5, 00.7	1.081	0.30
40.4, 20.7, 10.6	1.051	0.40

reported by Brownlee.[7] The two η phases, assumed to be Sandford and Trent,[1] are the limiting compositions of η saturated by cobalt and tungsten.

The composition of θ phase corresponds to formula Co_3W_3C. It has cubic symmetry and its structure is closely related to the η structure. The axial length of the face-centered cubic lattice was measured as 11.25A. The order of the diffraction lines was similar to those of η, but the relative intensities were slightly different. The characteristic X-ray patterns of η and θ are given in Table I. The composition range of the η phase was narrow, about 2 pct. At 1400 C, θ was in equilibrium with monotungsten carbide, η, tungsten, and α. There was a well-defined two-phase field between η and θ. A series of specimens, which had their composition in this field, showed a gradual transition of the relative intensities from the η to the θ pattern, without any change in the lattice constants. Fig. 1 shows the X-ray pattern of an alloy in the middle of the two-phase field $\eta + \theta$. There is no mention in the literature of a phase of composition Co_3WC. However, the phase Co_2WC, proposed by Kislovkova,[8] has the same Co-W ratio but 4 pct less carbon.

The ε phase corresponds to the formula Co_6W_6C. Its range of homogeneity was very narrow, less than 1 pct. The lattice was found to be hexagonal and the lattice constants a and c were both equal and measured as 7.940A. The diffraction lines of the ε phase are given in Table I and a typical X-ray pattern is reproduced in Fig. 2. The ε phase was found to be

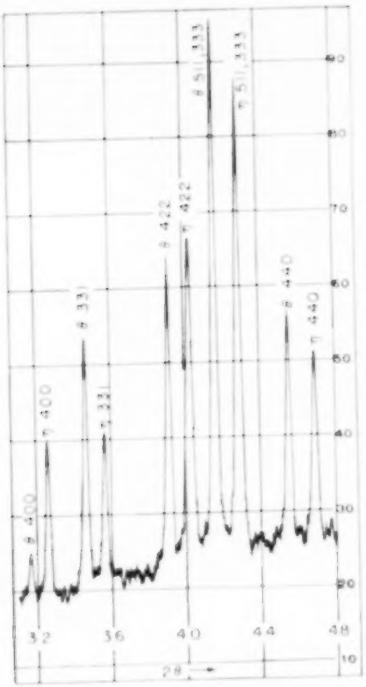

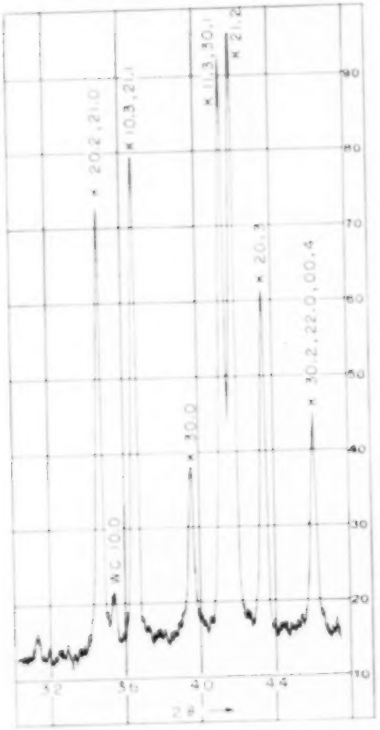

Fig. 1 (top) — X ray spectrometer pattern of η and θ phases.

Fig. 2 (bottom) — X ray spectrometer pattern of ε phase.

in equilibrium at 1400°C with monotungsten and ditungsten carbides, tungsten, and θ.*

* The ϵ and ζ phases were readily formed in the Fe-W-C and in the Ni-W-C systems with the same compositions and lattices.

Isothermal Section at 1400°C

By combining the results of this experiment with 1400°C isothermal lines from the adjoining binary diagrams it was possible to construct an isothermal section of W-Co-C diagram. This 1400°C isothermal section is illustrated in Fig. 3. The equilibria in the tungsten-rich part of the section have been described in connection with the ternary phases. Of special interest is the two-phase field, WC + liquid, which extends across the isothermal section. After cooling to room temperature, specimens in this field showed a two-phase structure, β + WC. Occasionally, depending on the carbon content, η or graphite was found in addition. The two-phase field β + WC was very narrow, less than 1 pct in width. The WC phase seems to have a very small solubility for cobalt. All attempts to measure any changes in the lattice constant of WC failed. The boundaries of the liquid phase are known only approximately. This phase extends from the eutectic of the Co-C binary toward the η phase.

Ternary Reactions

The invariant temperatures of the reactions leading to three-phase equilibria β + WC + graphite and β + η + WC were determined by thermal analysis. The measurements were made by a modified inverse-rate technique. Alloys in equilibrium with graphite showed a thermal arrest at 1298°C, whereas alloys in equilibrium with η had a thermal arrest at 1357°C.

To establish the reactions which lead to the formation of the η, θ, and κ phases, a series of alloys which consisted of one or two of these phases was heated to temperatures of 1700° and 1880°C. The specimens were first prepared by sintering at 1400°C. After rapid cooling from 1700°C, the θ and κ phases showed no changes, but the specimens containing η indicated increasing amounts of θ. The η specimens were melted and full of large gas holes, apparently due to evaporation of cobalt. After heating to 1880°C both θ and κ showed decomposition. A specimen, originally pure θ, recorded X-ray lines of κ and tungsten in addition, whereas a specimen of κ composition showed strong lines of θ, κ, and W_2C, and weaker lines of tungsten.

These observations suggest the following peritectic reactions:

$$\theta + \text{liquid} \rightleftharpoons \kappa + W$$
$$\kappa + \text{liquid} \rightleftharpoons W_2C + W$$

In the case of θ, the cobalt-rich liquid probably decomposed by evaporation. Traces of W_2C found in the θ specimen support this assumption. The liquid from the κ decomposition probably solidified under nonequilibrium conditions into θ and κ. Because the amount of the liquid, as indicated by the intensities of the θ lines, was large, the composition of this liquid apparently was not far from the κ composition. The small amounts of tungsten found were in accordance with this view.

Tentative Metastable Diagram W-Co-C

The experimental evidence described permits the construction of a tentative model of the W-Co-C diagram. It will be shown later that this diagram is of metastable nature. The model is illustrated in Fig. 4, which shows the basal projection of the lines of two-fold saturation. The notation used refers to this figure. The simplifications made in designing the model are that all the allotropic transformations which occur in the components tungsten, graphite, cobalt and possibly in the phase W_2C are omitted, that the complications caused by the γ phase Co_3W have not been considered, and the vapor phase of cobalt is not included. It is believed that these simplifications are justified, because the allotropic phase transformations as well as the γ formation occur at temperatures which are outside of the range of the primary interest.

The general appearance of the diagram is determined by the very high melting points of carbon and tungsten. The liquidus surface slopes sharply toward the cobalt corner. A valley of low melting extends

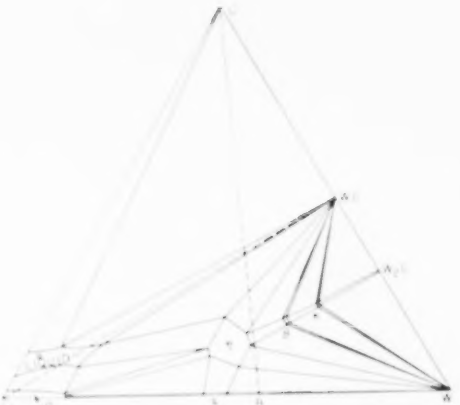

Fig. 3—1400°C isothermal section of W-Co-C equilibrium diagram. The dotted lines *B-C* and Co-WC correspond to the vertical sections of Figs. 5 and 7.

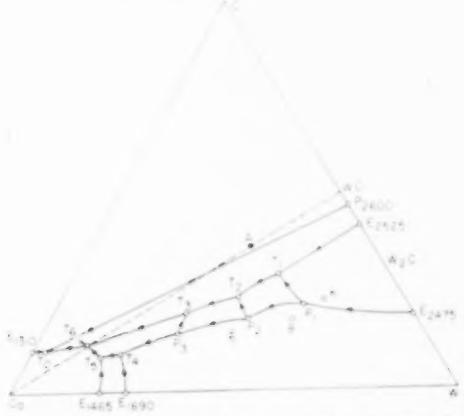

Fig. 4—Metastable equilibrium diagram W-Co-C, representation by basal projection.

P—Liquid + WC ⇌ W + κ	T—Liquid + θ ⇌ η + WC
T—Liquid + WC ⇌ κ + WC	T—Liquid + W ⇌ η + δ
P—Liquid + κ + W ⇌ θ	T—Liquid + δ ⇌ β + η
T—Liquid + κ ⇌ θ + WC	T—Liquid + η ⇌ WC + β
P—Liquid + θ + W ⇌ η	T—Liquid + WC ⇌ β + graphite

Fig. 5—Vertical section through carbon corner of metastable W-Co-C diagram. W-Co ratio is 57:43. The dotted line A corresponds to the composition of the cemented carbide of 18 wt pct Co content.

from the eutectics on the W-C binary across the diagram.

The invariant temperature of the four-phase equilibrium, liquid-β-WC-graphite, was measured as 1398°C, which was the lowest reaction temperature found. The average temperature of the lowest melting in sintering commercial two-phase alloys, β + WC, seems to be about 1320°C. The invariant reaction at 1398°C then has to be a eutectic reaction:

$$\text{Liquid} \rightleftharpoons \beta + \text{WC} + \text{C}$$

The ϵ phase can be formed only by a peritectic reaction. Because no WC was found in the decomposed ϵ, the reaction must be:

$$\text{Liquid} + \text{W} + \text{W}_2\text{C} \rightleftharpoons \epsilon$$

The composition of the liquid, indicated by the letter P_1, is not far from the ϵ composition. The reaction temperature is near 1880°C because of the three ϵ specimens heated to 1880°C, two decomposed and one did not. Since the accuracy of the temperature measurement in this range is about ±15°C, this means that the invariant temperature is between 1865° and 1895°C. The reaction provides the two-phase equilibria ϵ + W$_2$C and ϵ + W, which were found at 1400°C.

To obtain the ϵ-WC equilibrium, also found, a ternary transition:

$$\text{Liquid} + \text{W}_2\text{C} \rightleftharpoons \epsilon + \text{WC}$$

has to occur at somewhat lower temperature T_1.

The formation of the θ phase is similar to the ϵ

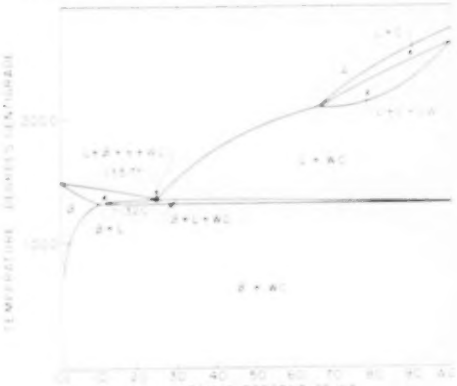

Fig. 7—Vertical section of Co-WC. Because experimental data is lacking, a special case is illustrated.

reaction, and in accordance with the experiments the peritectic reaction is:

$$\text{Liquid} + \text{C} + \text{W} \rightleftharpoons \theta$$

The reaction temperature P_2 is in the neighborhood of 1700°C, but is not known accurately. This reaction furnishes the experimentally found two-phase fields θ + C and θ + W. The ternary transition:

$$\text{Liquid} + \epsilon + \text{C} \rightleftharpoons \theta + \text{WC}$$

provides the two-phase field θ + WC. This reaction temperature T_2 has to be lower than P_2.

There is not much experimental support for the nature of the η reaction. The various attempts made were upset by the evaporation of cobalt. It is believed that the temperature of the invariant reaction of the ϵ formation is about 1600°C. The peritectic reaction, Liquid + θ + W $\rightleftharpoons$ ϵ is considered the only possibility.

The reaction, Liquid + θ + W $\rightleftharpoons$ η would give the two-phase fields η + θ and η + W, and the transition, Liquid + θ + η $\rightleftharpoons$ WC at a lower temperature supplies the field η + WC.

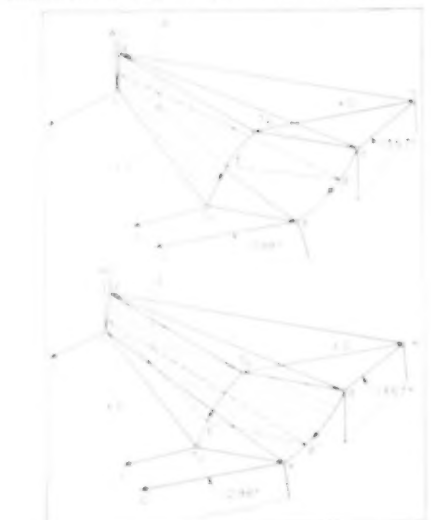

Fig. 6—Perspective illustration of solidification of cobalt cemented tungsten carbides. The composition of the alloy is given by vertical line A. Points D and E indicate the approximate compositions of the thermal analysis specimens.

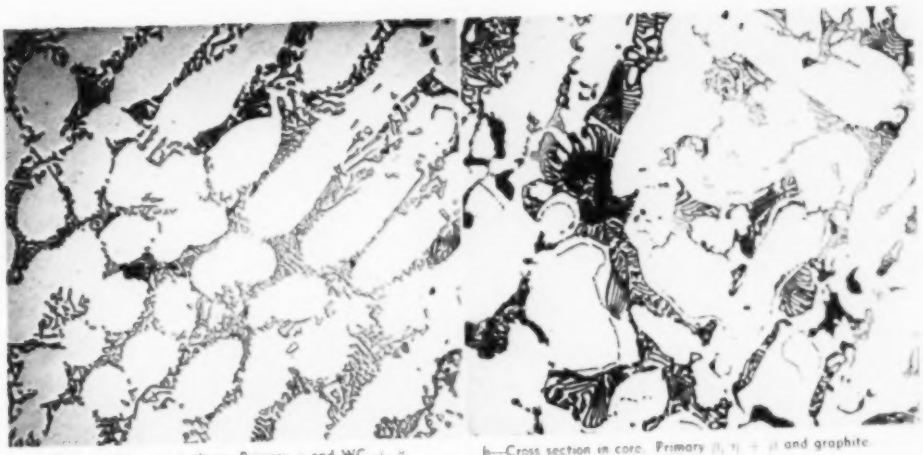

a—Cross section near surface. Primary γ and WC + β

b—Cross section in core. Primary β, η + β and graphite

Fig. 8—Microstructure of 9 pct W 81 pct Co 10 pct C alloy. Etched by alkaline $K_3Fe(CN)_6$. X250

The experimentally verified η-δ field is a product of ternary transition, Liquid + W = η + δ. The η-β equilibrium, which exists at 1400°C and below, is formed by a ternary transition, Liquid + δ = η + β. At 1357°C a ternary transition reaction, Liquid + η = β + WC, forms the important two-phase equilibrium β-WC.

Not much has been said as to the compositions of the reacting phases. This is especially true with the compositions of the saturated liquids. The solid phase compositions are, in general, well fixed. It has been revealed in this study that the homogeneity ranges of all participating phases are very narrow. The only exception is the η phase.

It is possible to locate the ternary eutectic to within a few percentage points by pure speculation. The ternary eutectic temperature was measured as 1298°C. The binary eutectic reaction, Liquid = β + C has been reported between 1300° and 1315°C. The difference is very small, as a matter of fact within the experimental errors. It is unlikely that the ternary eutectic composition would be far from the Co-C binary. But on the other hand, there is cumulative evidence that the maximum solubility of WC in cobalt is about 10 pct. Yet the eutectic point has to be within the three-phase field corner and not far from the section Co-WC because toward the carbon corner the liquidus surface is almost vertical.

One point of great practical importance is the composition of the liquid phase in the reaction: Liquid + η = β + WC. Fig. 5 represents a vertical section through the carbon corner of the diagram for constant W-Co ratio of 57/43. This is a section which includes cemented carbides of 18 wt pct Co content. An alloy of this composition, which at low temperatures would have a two-phase β + WC structure, is represented by line *A*. It is evident that the extension of the invariant plane at 1357°C will determine whether or not η phase is formed during heating or cooling of the specimens. The question is important because it will form the basis of understanding the sintering mechanism of the cemented carbides.

The reactions occurring during cooling from the sintering temperature can be followed by Fig. 6. The common sintering temperature is about 1400°C. The specimen at this temperature consists of solid WC and liquid. During cooling WC precipitates, and the composition of the liquid follows the surface of one-fold saturation until the line T_c-T_e is encountered. During further cooling, WC and β precipitate simultaneously. The composition of the precipitating β follows the curve *d*-*e*. When the line WC-β intersects the vertical *A*, all liquid has been consumed and solidification is complete. Depending on the cooling rate, various amounts of WC will precipitate out of the β solid solution during subsequent cooling to room temperature.

If the invariant plane g-T_c-d-η extends completely over the two-phase field WC + β, the two-fold precipitation will be WC + η until the invariant temperature is reached.

The vertical section, Co-WC is illustrated in Fig. 7. Because it is not known whether or not the 1357°C invariant plane extends over the two-phase field, β + WC, a compromise has been made by drawing a special case represented by a point at 1357°C. If the carbon content of the saturated liquid at 1357°C is higher than indicated, two three-phase fields and one two-phase field will be generated from the point at 1357°C. In the opposite case the four-phase equilibrium will disappear.

Instability of Carbides

The instability of η phase has been reported by Takeda[1] in the Fe-W-C system. The basis of Takeda's hypothesis seems to be a micrograph of an annealed η grain, which according to Takeda, shows a rim of WC formed by decomposition of η. However, it is believed here that the rim was nothing but η, from which a heavy layer of etching stain had been chipped off. If a more careful etching technique would have been applied, probably no such rim would have been visible. Takeda's instability hypothesis was accepted by Westgren.[2] To verify it, Westgren annealed a specimen of composition Ni_6W_6C for ten days at 1000°C and the result was WC. It is believed here that carburization took place in this experiment. It will be shown by the following experiment that the η phase is stable.

A specimen of composition 81.0 pct Co, 9.0 pct W, and 10.0 pct C was heated to 1500°C in an alundum crucible by induction. At 1500°C the alloy was ex-

pected to consist of liquid phase only. The specimen was then furnace cooled. A section through the solidified specimens showed two types of structures. The surface layer, shown in Fig. 8a, consists of primary β surrounded by a fine structure of β and WC. The center of the specimen, shown in Fig. 8b, also shows primary β but now surrounded by γ-β eutectic and numerous graphite flakes. The condition in the furnace was only slightly carburizing, if at all. The alundum crucible was enclosed in a graphite crucible, which was completely packed in nickblack. The cooling rate on the surface of the specimen is expected to be faster than inside. The surface structure is in accordance with the metastable diagram. During the cooling from the liquid state the precipitation of β starts first and during subsequent cooling simultaneous precipitation of WC and β takes place. The composition of the specimen is such that all liquid is consumed before the eutectic temperature 1298 C has been reached.

The structure of the specimen core, apparently cooled slower, cannot be explained by means of the metastable diagram, which has no γ-graphite equilibrium. Apparently the core has approached true equilibrium conditions more closely and thus the combination Co-γ-graphite is the stable one. It will be noted that the composition of the specimen was not changed. The free graphite amounts to the difference between the carbon contents of WC and γ.

Tentative Model of Stable Diagram W-Co-C

A stable system may be developed from the metastable by omitting the ternary transition at 1357 C. Above this temperature the stable and the metastable diagrams are essentially the same. In the stable system the ternary transition

$$\text{Liquid} + \text{WC} \rightleftharpoons \gamma + \text{C}$$

produces the γ-graphite equilibrium.

At a lower temperature a eutectic reaction[1]

$$\text{Liquid} \rightleftharpoons \beta + \gamma + \text{C}$$

produces the three phase field β-γ-graphite.

[1] The composition of the eutectic reaction was not measured in the Harvard institute described. Apparently the thermocouple protecting tube contributed sufficient iron to cause the crystals of the specimens that are liquid at 1298 C. It is believed that the composition of the eutectic reaction in the stable system is lower than in the metastable system.

A model of the stable equilibrium diagram W-Co-C is illustrated in Fig. 9.

The characteristic feature of the metastable diagram is the two-phase field β-WC, which extends across the diagram. The cemented carbides should

Fig. 9—Stable equilibrium diagram of W-Co-C. Representation by basal projection. The reactions P_1 to T_1 are the same as in Fig. 4. T_1—Liquid + WC $\rightleftharpoons$ γ_1 + graphite. T_2—Liquid $\rightleftharpoons$ β + γ_2 + graphite.

have this structure. In the stable system this important two-phase equilibrium is destroyed. From the viewpoint of technical applications it is clear that the stable equilibrium is most undesirable. Therefore slow cooling rates from the sintering temperatures must be avoided.

Acknowledgment

Part of this work was sponsored by the Ordnance Dept. of the United States Army, Contracts No. W-19-020-ORD-6489 and No. DA-19-020-ORD-10, under the technical supervision of the Watertown Arsenal Laboratory. Permission to publish the results is gratefully acknowledged.

References

1. V. Adelskold, A. Sandelin, and A. Westgren: *Ztsch. anorg. allgem. Chem.* (1933) **212**, p. 401.
2. E. J. Sandford and E. M. Trent: Symposium on Powder Metallurgy. Iron and Steel Inst. *Special Report* 38, (1947) p. 54.
3. E. N. Kislyokova: *Zhur. Fiz. Khim.* (1943) **17**, p. 108.
4. S. Takeda: *Technol. Repts. Tohoku Imp. Univ.* (1931) **9**, pp. 463, 627, and (1931) **10**, p. 42.
5. L. L. Wyman and F. C. Kelley: *Trans.* AIME (1931) **93**, p. 260.
6. A. Westgren: *Jernkontorets Ann.* (1933) **117**, p. 1.
7. L. D. Brownlee: Unpublished Report, Vickers Electrical Co. Ltd., Manchester, England.

Technical Note

Strain Sensitivity of Commercial Purity Titanium

By James L. Wyatt

THE strain sensitivity, K, a property of metals defined as the unit change in electrical resistance per unit strain, was measured for commercial purity titanium wire to determine its usefulness as a strain gage material. A Kelvin double bridge, accurate to 0.00001 ohm, was used to make measurements from 0 to 1 pct total strain. A positive value of 0.17 for K was found. This compares with 2.15 for constantan and 3.5 for cold-worked invar, two of the more common strain gage materials.

The effect of temperature also was determined. It was found that a change in temperature of 30 F caused the same resistance change as 1 pct strain. It is therefore concluded that titanium would have utility as a strain gage only if the thermal fluctuations in the specimen could be controlled to a high degree and in applications of very large total strain.

J. L. WYATT, Junior Member AIME, is National Lead Co. Fellow, Massachusetts Institute of Technology, Cambridge, Mass.

TN 125E. Manuscript, April 29, 1952, revised, Aug. 5, 1952.

Role of the Binder Phase in Cemented Tungsten Carbide-Cobalt Alloys

By Joseph Gurland and John T. Norton

IN spite of the extended use and high state of practical development of the cemented tungsten carbides, the structure of these alloys is still a matter of considerable controversy. The characteristic high rigidity and rupture strength of sintered compacts have been attributed to a continuous skeleton of tungsten carbide grains, formed during the sintering process. This view is based mainly on the work of Dawihl and Hinnuber,[1] who reported that a sintered compact of 6 pct Co maintained its shape and some of its strength after the binder was leached out with boiling hydrochloric acid. After leaching, only 0.04 pct Co was reported to remain in the compact. They also showed that the assumed increasing discontinuity of such a skeleton, as the cobalt content is increased, could be made to account for the observed discontinuous increase of the coefficients of thermal expansion, the loss of rigidity, and the impaired cutting performance of alloys of more than 10 pct Co.

Contradictory evidence was cited by Sanford and Trent,[2] who mentioned that a sintered compact was destroyed by reacting the binder with zinc and leaching out the resulting Zn-Co alloy. The skeleton theory also does not account for the observed change of strength of sintered compacts as a function of cobalt content. If the skeleton is responsible for the strength, the latter would be expected to decrease with increasing binder content. Actually, the strength increases and reaches a maximum around 20 pct Co. In addition, tungsten carbide is brittle and undoubtedly very notch sensitive. The highest value found in the literature for the transverse rupture strength of pure tungsten carbide prepared by sintering is 80,000 psi.[3] Therefore, such a skeleton does not easily account for a rupture-strength value of 300,000 psi and higher, commonly found in sintered tungsten carbide-cobalt compacts.

In view of the conflicting data present in the literature, experiments were undertaken to determine whether the sintering of tungsten carbide-cobalt alloys leads to the formation of a carbide skeleton or whether the densification behavior and the properties of cemented compacts are consistent with a structure of isolated carbide grains in a matrix of binder metal.

The specimens were prepared from powders of commercial grade. Tungsten carbide powder ranged in particle size from 0 to 5×10^{-4} cm. Mixtures of tungsten carbide and cobalt were ball milled in hexane for 48 hr in tungsten carbide lined mills. After milling, the specimens were pressed in a rectangular die (1x1/4x3/4 in.) at 16 tons per sq in. No pressing lubricant was used.

Sintering of the tungsten carbide-cobalt compacts was carried out in a vertical tube furnace equipped with a dilatometer (Fig. 1), by means of which the change of length of the powder compacts could be followed from room temperature to 1500°C. An atmosphere of 20 pct H, 80 pct N was maintained inside the furnace. Decarburization of the samples was prevented by the presence of small rings of graphite inside the furnace tube. The temperature of the sample was measured by a platinum-platinum-rhodium thermocouple, which also was part of a temperature control system able to maintain a constant temperature within ±10°C.

Pure tungsten carbide compacts were prepared by sintering the carbide without binder or by evaporating the binder from sintered compacts in vacuum at 2000°C. Since complete densification of these samples was not desired, they were sintered only to 60 or 80 pct of the theoretical density of tungsten carbide.

The specimens were prepared for metallographic examination by polishing with diamond powders and etching with a 10 pct solution of alkaline potassium ferricyanide. Cobalt etches light yellow and the carbide gray. The amount of porosity is exaggerated since it is difficult to avoid tearing out carbide particles, especially from incompletely sintered samples.

Experimental Observations

A number of specific experiments were carried out in order to study some particular aspect of the sintering problem. The details of these experiments, together with their results, are as follows:

Electrolytic Leaching. The binder was removed by electrolytic leaching from sintered tungsten carbide-cobalt compacts for the purpose of determining the continuity of the carbide phase. The method used was based on the work of Cohen and coworkers[4] on the electrolytic extraction of carbides from annealed steels. If the sample is made the anode, using a 10 pct hydrochloric acid solution as the electrolyte, the binder is dissolved, but the rate of solution of tungsten carbide is negligible. A current density of 0.2 amp per sq in. was applied. As shown in Fig.

J. GURLAND, Junior Member AIME, is associated with Firth Sterling Steel and Carbide Corp., Pittsburgh, and J. T. NORTON, MEMBER AIME, is Professor of Metallurgy, Massachusetts Institute of Technology.

Discussion on this paper, TP 3359E, may be sent, 2 copies, to AIME by Dec. 1, 1952. Manuscript, April 15, 1952. Philadelphia Meeting, October 1952.

This paper is based on a thesis by J. Gurland submitted in partial fulfillment of the requirements for the degree of Doctor of Science to Massachusetts Institute of Technology.

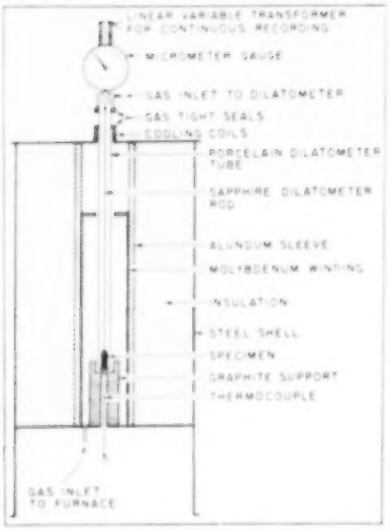

Fig. 1—Sintering dilatometer.

2, the samples containing cobalt were strongly attacked. The loose carbide particles remained on the surface as a powdery layer which could be easily removed by washing with water. A pure tungsten carbide compact, sintered to 64 pct of its theoretical density, remained intact.

Coefficients of Thermal Expansion. The coefficients of expansion of sintered tungsten carbide-cobalt alloys were measured with the dilatometer of Fig. 1 and are reported in Table I. Fig. 3 compares the measured coefficients (20° to 800°C) with those calculated for a mechanical mixture, assuming the law of mixtures to hold, and using 5.4×10^{-6} and 16.2×10^{-6} in. per in. per °C as the coefficients of thermal expansion of tungsten carbide and cobalt.

Dilatometric Cooling Curves. A clue to the high temperature structure of tungsten carbide-cobalt alloys is given by the continuously recorded dilatometric cooling curves, which show discontinuities between 1350° and 1320°C, Fig. 4. The magnitude of the discontinuities changes gradually with composition, from a contraction at high cobalt content to an expansion at low cobalt content. Zero, on the change of length scale of Fig. 4, corresponds to the length of the fully sintered specimens at the sintering temperature. The specimens were 1 in. long, as pressed, before sintering.

Infiltration. The behavior of a carbide skeleton in the presence of liquid binder metals was demonstrated by infiltration experiments. A pure tungsten carbide compact, sintered to 80 pct of its theoretical density, was infiltrated with liquid cobalt. The change in length of the carbide block, standing vertically in the furnace tube in contact with a measured amount of cobalt powder, was followed dilatometrically (Fig. 5) during the heating and infiltration process. The compact first expands uniformly to 1320°C, then a noticeable contraction sets in, followed by a sudden expansion and collapse of the specimen.

The same experiment, performed with copper as the infiltrant, showed none of the discontinuous changes. This sample expanded uniformly on heating and maintained its shape. The microstructures of sintered tungsten carbide compacts, infiltrated with cobalt and copper, are shown in Figs. 6 and 7.

Sintering Behavior. The effect of composition, temperature, and time on the densification of tungsten carbide-cobalt compacts is shown by the sintering curves at a constant rate of heating (5°C per min) of Fig. 8 and by the isothermal sintering curves of Fig. 9. The specimens with 1 and 15 pct Co attained, respectively, 86 and 98 pct of their theoretical densities during heating at a constant rate to 1500°C. Microstructures of cemented compacts sintered at 1300° and 1325°C, Figs. 10 and 11, show that porosity is almost completely eliminated in that temperature range.

Considerable grain growth takes place at the sintering temperature. In a sample of 15 pct Co held 20 hr at 1350°C, the average particle length increased by 17 pct from 1.8×10^{-4} to 2.1×10^{-4} cm. The smallest particles tend to disappear, the percentage of those of length of 1×10^{-4} cm or less decreasing from 50 to 20 pct during this holding time. The particle length was determined by measuring the length of the carbide particles along arbitrary straight lines across the photographic prints. Approximately 1000 particles were measured on each sample and averaged.

Wettability. The properties of the solid-liquid interface in tungsten carbide-cobalt compacts may influence the sintering behavior of the compacts, since the carbide particles are of almost colloidal dimensions and present a great surface area to the action of the liquid. The most important of these properties is the wettability of tungsten carbide by liquid cobalt. The wettability was determined by the drop-shape method, which consists of measuring the angle of contact of a liquid drop on a solid surface. The smaller the angle, the greater is the wetting ability of the liquid.

A small piece of cobalt was placed on a level tungsten carbide block and was heated in a horizontal tube furnace in an atmosphere of hydrogen at 85 mm pressure. The cobalt spread freely over the available surface and soaked into the porous block at 1420°C, although melting at the interface was first

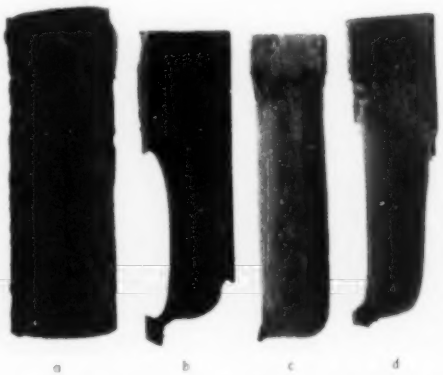

Fig. 2—Sintered compacts after electrolytic leaching experiments. a—100 pct WC leached 56 hr. b—85 pct WC, 15 pct Co leached 24 hr. c—90 pct WC, 10 pct Co leached 24 hr. d—92.5 pct WC, 7.5 pct Co leached 48 hr. Length of samples, approximately 1 in.

observed at 1375°C. It was concluded that the angle of contact of liquid cobalt on solid tungsten carbide is infinitely small. The same experiment was repeated with copper. Liquid copper did not spread on solid tungsten carbide. It maintained an angle of contact of 29° at a temperature of 1405°C.

Discussion of Experimental Observations

Structure: The disintegration of sintered compacts by electrolytic leaching demonstrates that a continuous skeleton is not formed as a result of the sintering process. The previously reported strength of acid-leached specimens may be attributed to an insufficient penetration of leaching solution into the fine capillaries between adjacent carbide particles.

The observed depression of coefficients of thermal expansion of low cobalt alloys below those of a corresponding simple mixture, Fig. 3, was attributed by Dawihl and Hinnuber to the restraining influence of a tungsten carbide skeleton. However, the coefficients of thermal expansion of a mixture are not only a function of the coefficients of expansion and the proportions by volume of the components, but also of their relative moduli of elasticity. Since the value of Young's modulus of tungsten carbide is about three times as high as that of cobalt, the carbide will depress the coefficients of the mixture below the average value when the composition is such that it restrains the free expansion of the binder; namely, at the high carbide end of the composition range. Consequently, the observed deviation of the coefficients of thermal expansion from the law of mixtures are to be expected in sintered compacts, without having to suppose the existence of a carbide skeleton.

The discontinuous dilatometric changes at the solidification temperature of the binder, Fig. 4, can only be explained by a structure of isolated carbide grains, each of which is surrounded by a film of liquid. The expansion on cooling of low cobalt alloys cannot be attributed to the effect of the latent heat of freezing of the binder on a carbide skeleton, since it was not observed on cooling a copper infiltrated carbide skeleton. The heats of fusion of copper and cobalt are of comparable magnitude. It is possible to account for the discontinuities of the dilatometric cooling curves by considering the physical changes which take place at the freezing temperature of the binder; namely, the sudden growth of the carbide particles by precipitation as the solubility of tungsten carbide in cobalt is reduced from 38 to 17 pct by weight, and also the volume shrinkage of the binder as it freezes. If the amount of binder is small, the carbide particles will be quite closely packed. Only that thin layer, required to satisfy the tungsten carbide-cobalt interfacial energy, will surround each grain and separate it from its neighbors. The freezing contraction of the binder cannot force the particles closer together, but the precipitation of carbide, taking place on all faces of the particles, forces the

Table I. Thermal Coefficients of Expansion, 10^{-6} In. per In. per °C

Temperature Range, °C	Composition						
	100% WC	5% Co	7.5% Co	10% Co	12.5% Co	15% Co	25% Co
20 to 800	5.4	7.6	7.9	7.8	7.6	7.9	11.3
800 to 1300	9.2	10.4	10.5	12.4	12.7	13.0	*

* Specimen deforms at high temperatures.

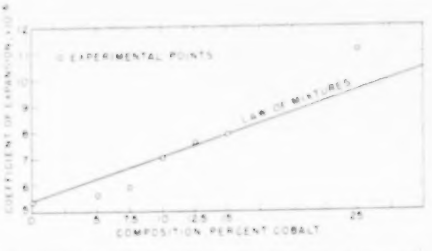

Fig. 3—Coefficient of linear thermal expansion of cemented WC-Co alloys.

centers of the growing grains apart and the specimen expands. With a greater content of binder, the structure approaches more nearly that of dispersed carbide grains in a matrix of cobalt. The contraction of the binder freezing is able to bring the carbide particles closer together, without causing them to abut against each other, and the specimen as a whole shrinks.

The infiltration experiment proves that liquid cobalt breaks up and destroys an already existing tungsten carbide skeleton. The first contraction of the dilatometer curve, Fig. 5, at 1320°C is probably due to a reaction between the carbide specimen and the cobalt where the sharp corners of the specimen rest on the rounded bottom of the dilatometer tube. As the cobalt melts and infiltrates the compact, an expansion occurs because the liquid metal attacks the skeleton at the grain boundaries and separates the carbide particles. For this reason, the compact loses its strength, deforms, and eventually collapses. In the case of copper as the infiltrating metal, the

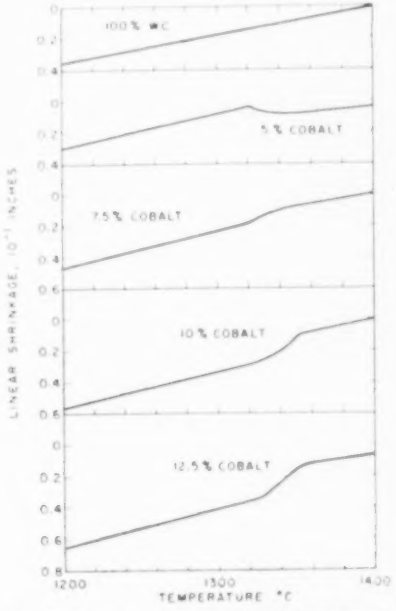

Fig. 4—Discontinuous change of length on cooling of sintered WC-Co alloys of different compositions.

compact did not lose its shape. The microstructures of Fig. 6 and 7 illustrate the action of cobalt and copper as binders. The cobalt tends to surround each grain of tungsten carbide, destroying the existing skeleton, while copper preserves the sintered skeleton. The solubility of tungsten carbide in copper is insignificant compared to that in cobalt. The wettability of tungsten carbide by cobalt is also appreciably greater than that by copper.

The experimental evidence presented shows that the structure of the sintered compact is one of tungsten carbide particles dispersed in a matrix of cobalt. A carbide skeleton does not form during sintering or on cooling from the sintering temperature. This also follows from theoretical considerations.

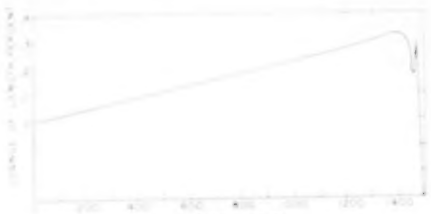

Fig. 5—Infiltration with cobalt dilatometric curve.

Smith has pointed out that a liquid will penetrate indefinitely along the grain boundaries of a solid if the liquid-solid interfacial energy is sufficiently low. In such a case, a polycrystalline aggregate of the solid will be disintegrated by the liquid. If the amount of liquid is relatively small, its surface tension will hold the mass together.[7] Although the solution of tungsten carbide in cobalt at the sintering temperature could alone lead to the elimination of carbide particle to particle contact, it is the low interfacial energy of the liquid-solid boundary which effectively prevents a sintering together of the tungsten carbide particles in the presence of liquid cobalt.

Cementing Action of the Binder. The sintering curves show that shrinkage becomes noticeable at relatively low temperatures, approximately 800 C, and reaches a maximum rate between 1300° and 1350 C. The beginning of shrinkage coincides with the effective sintering temperature of pure cobalt, 800 C. Rate and extent of shrinkage increase with

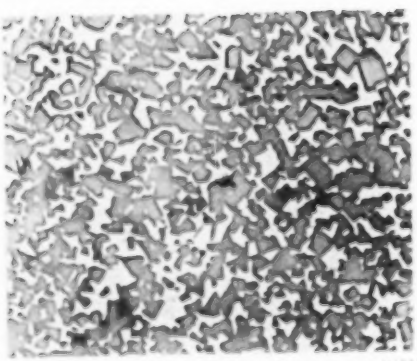

Fig. 6—Microstructure of cobalt infiltrated WC compact. X1500.

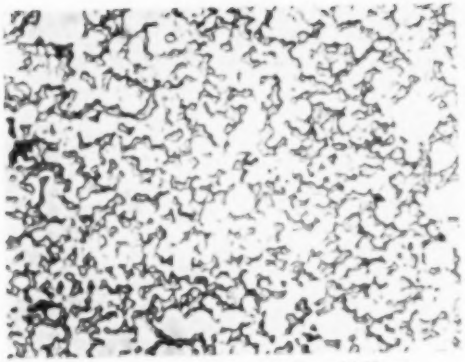

Fig. 7—Microstructure of copper infiltrated WC compact. X1500.

temperatures and with cobalt content.

The disappearance of porosity between 1300° and 1325 C, Figs. 10 and 11, is associated with the appearance of a considerable amount of liquid phase. Published temperatures for the formation of a liquid binder range from 1275 ° to 1350 °. Sandford and Trent report 1320 C.

The characteristic angular grains of tungsten carbide indicate that considerable solution and redeposition of carbide takes place during sintering. This leads to grain growth; the smallest particles dissolve in the liquid and are reprecipitated on the larger ones, so as to minimize the interfacial tension of liquid and solid. In practice, it is observed that different batches of tungsten carbide exhibit different degrees of grain growth during sintering, so that the grain growth reported is characteristic only of the powder batch under discussion.

The volume of a cemented tungsten carbide-cobalt compact, of low binder content, is determined by

Fig. 8—Sintering curves constant rate of heating change of length vs. temperature.

the packing of the carbide aggregate. But it has been shown that a continuous tungsten carbide skeleton is not formed during the sintering operation. Densification, therefore, does not take place by the usual sintering processes encountered with homogeneous solid powder compacts, namely, by diffusion or flow of material within the solid particles or across the contact bridges between them. It seems more likely that the densification of tungsten carbide-cobalt compacts takes place by a rearrangement of the carbide particles under the influence of the surface tension forces of the binder, which tend to eliminate pores present in the compact. Appre-

ciable stresses are introduced by surface tension. Shaler[7] calculated that, for the sintering of copper, they range from 35 to 35,000 psi in the vicinity of pores of diameters from 10^{-4} to 10^{-6} cm at 1200°C. It may be assumed that the surface tension of cobalt is of a similar magnitude as that of copper. In heterogeneous tungsten carbide-cobalt alloys, such stresses are transmitted by the binder, either solid or liquid, to the carbide particles and force them to move in the direction of the pore exerting the greatest stress; thereby, in effect, producing a rearrangement of the packing of the carbide aggregate, and reducing the dimensions of the specimen. Densification at the sintering temperature is a result of the ability of cobalt to dissolve and wet tungsten carbide.

The wetting property of the binder is essential to the process, because it forces the liquid to surround all particles and thereby allows the surface tension stresses to act upon them. As shown by capillarity phenomena, liquids may sustain very high tensile stresses if present as very thin films.[7] The solubility of tungsten carbide in the binder indirectly helps this rearrangement by breaking up existing carbide

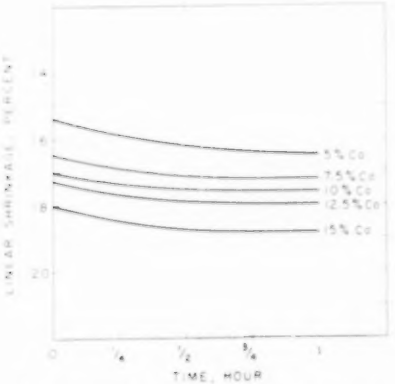

Fig. 9—Sintered WC Co alloys isothermal sintering curves at 1400°C

to carbide bridges, and by eliminating surface and shape irregularities, decreasing the resistance to movement, and allowing a denser packing. In addition, the solution effect directly contributes to the densification by reducing the size of the particles and permitting their geometrical centers to approach each other without altering their relative positions. The effect can be approximately calculated: For a sample of 10 pct Co, assuming a uniform particle size of 3×10^{-4} cm, a close-packed arrangement of particles, and a solubility of tungsten carbide in cobalt of 40 pct, the solution shrinkage amounts to about 2 pct, compared to a total linear shrinkage of about 18 pct at 1400°C.

Grain growth will also result in shrinkage since, for equal volumes of carbide dissolved and reprecipitated, the decrease of diameter of small grains is greater than the increase of diameter of large grains. At the sintering temperature, the shrinkage due to solution of tungsten carbide in cobalt will reach a limit as the particles abut against each other. Probably only the grain growth mechanism will permit densification as long as any porosity is present.

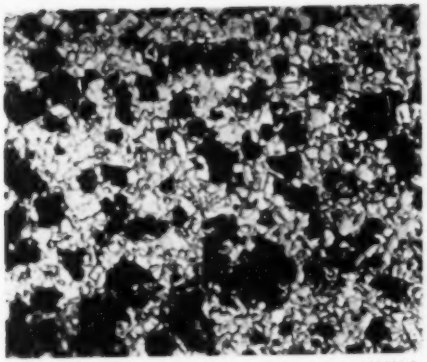

Fig. 10—Sintered WC Co alloy. 7.5 pct Co. 3 hr at 1300°C. X1500

The double role of the binder phase during the sintering of cemented tungsten carbide may be summarized as follows: It supplies the driving force towards densification, namely, its surface tension, and it increases the mobility of the carbide particles, allowing them to achieve a closer packing. The characteristic properties which make cobalt such an effective binder metal for cemented tungsten carbide are: 1—the relatively low melting temperature of the cobalt-tungsten carbide solid solution; 2—the solubility of tungsten carbide in cobalt, and 3—the wetting of carbide particles by the liquid binder.

Relation of Structure and Strength. The maximum strength of cemented tungsten carbide-cobalt alloys is found in compacts of approximately 20 pct Co, for which transverse rupture strengths in excess of 300,000 psi are commonly observed.[7] The binder, constituting a continuous phase, must be responsible for the strength and brittleness of sintered compacts. Cobalt is normally a reasonably ductile metal of a tensile strength of 40,000 psi. Even considering a ratio of two between the transverse rupture strength and the tensile strength of brittle materials, such as cemented carbides,[7] an increase of strength of the binder by a factor of approximately four has to be accounted for.

In sintered compacts, the thin films of binder metal surrounding the carbide grains are in a condition of severe restraint when a tensile stress is

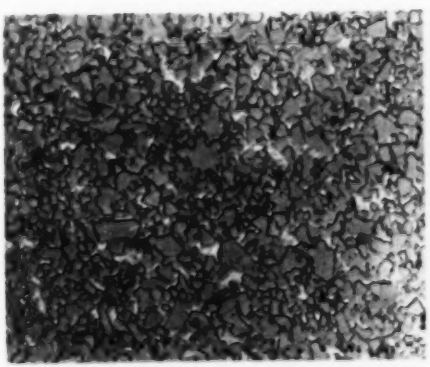

Fig. 11—Sintered WC Co alloy. 7.5 pct Co. 2 hr at 1325°C. X1500

applied externally. The high elastic modulus of the carbide, together with its high yield strength, effectively prevents any plastic flow of the binder and as a result, high strength and low ductility are observed. If the plastic yielding of a metal is restrained, its flow stress is greatly increased and may approach the fracture strength. The stress system in the binder is essentially triaxial when a uniaxial load is applied to the compact, and the situation is very similar to that found in soldered or brazed joints. In the latter case, the thin layer of soft metal between the two pieces of much harder material is prevented from contracting laterally when under tensile load. Under certain conditions, the strength of such a joint is increased as much as 5.5 times over that of the pure joining metal.[17] Failure takes place, usually, not through the joint, but at the boundary layer between the two metals, or even through the parent metal. The strength of a brazed or soldered joint varies with the thickness. It reaches a maximum at a certain thickness, decreasing radically with thinner joints and more gradually with thicker joints. Similarly, the strength of cemented carbides shows a maximum at a certain composition. This may be attributed to the change of strength with the thickness of the cementing layer between carbide particles. With larger amounts of binder, the thickness of the binder layers increases and the triaxial restraint decreases so that there is a greater and greater opportunity for plastic deformation. As the cobalt content exceeds about 15 pct, the sintered compacts begin to show a small ductility prior to fracture, and this increases markedly with increasing cobalt content.

The same argument applies to the theoretical effect of particle size on the strength of sintered compacts. For a given composition, the layer of cementing material becomes thinner as the particle size decreases and the strength increases until the particle size becomes so small that the amount of binder present is insufficient to cover all the available surface and achieve full density.

An additional factor contributing to the strength is the presence after cooling of residual stresses, which are caused by the difference in coefficients of thermal expansion and elastic properties of the constituents. Such stresses of high magnitude have been found to exist in the binder by magnetic measurements and have been reported by Ritzau.[18] Their magnitudes can be evaluated by the method of Laszlo for tesselated stresses.[19] The stresses, both tensile and compressive, normal to the carbide-cobalt interfaces, were estimated to have theoretical values of the order of 100,000 psi. The actual magnitude of the stresses are, of course, limited by the flow stress of the binder under conditions of complex stress. The signs of the stresses in the binder are a function of the carbide distribution; both tensile and compressive stresses are present in adjacent microscopic regions. Although the fracture strength may be locally reduced, the net effect will be an increase of the yield strength of the binder. In addition, the strength of the binder may be increased by such factors as the solid solution of tungsten carbide in cobalt at room temperature and the stresses introduced by the transformation of cobalt on cooling.

Conclusions

1—Densification of cemented tungsten carbide-cobalt alloys takes place by a rearrangement of the carbide particles, which achieves a denser packing under the influence of the surface tension forces of the binder. The disappearance of small grains and the growth of large grains of tungsten carbide also contribute to densification.

2—The resulting structure is one of carbide particles embedded in a cobalt-rich matrix. A continuous tungsten carbide skeleton is not formed during the sintering treatment.

3—This structure accounts for some of the characteristic properties of the cemented compacts. Their high strength and lack of ductility can be attributed to the mechanical restraint exerted by the carbide particles upon the thin films of the binder, the yield strength of which is correspondingly raised, and to the complex state of stress resulting from the presence of residual stresses of thermal origin.

4—The following are the essential characteristics required of an effective binder for cemented tungsten carbide compacts: it must supply a liquid phase at relatively low temperatures; tungsten carbide must be soluble in the binder; and the liquid binder must wet the solid carbide particles.

Acknowledgments

This project was carried out under sponsorship of the Ordnance Dept., Dept. of the Army, contracts No. DA-19-020-ORD-10 and No. W-19-020-ORD-6489. The authors gratefully acknowledge this sponsorship and permission to publish the results. It is also a pleasure to acknowledge the assistance of William Campbell and Kenneth Carlson.

References

[1] W. Dawihl and J. Hinnuber: Ueber Den Aufbau der Hartmetallegerungen. *Kolloid Ztsch.* (1943) **104**, p. 233.

[2] E. J. Sandford and E. M. Trent: The Physical Metallurgy of Sintered Carbides. Iron and Steel Inst., Symposium on Powder Metallurgy. Special Report No. 38 (1947) p. 84.

[3] C. G. Goetzel: *Treatise on Powder Metallurgy* (1950) Vol. 2, p. 81. New York. Interscience Publishers.

[4] D. J. Blickwede and M. Cohen: The Isolation of Carbides from High Speed Steels. *Trans.* AIME (1949) **185**, p. 578; JOURNAL OF METALS (September 1949).

[5] P. S. Turner: Thermal Expansion Stresses in Reinforced Plastics. *Journal of Research*, National Bur. Standards (1946) **37**, p. 241.

[6] C. S. Smith: Grains, Phases and Interfaces, An Interpretation of Microstructure. *Trans.* AIME (1948) **175**, p. 15; METALS TECHNOLOGY (June 1948).

[7] J. S. McFarlane and D. Tabor: Adhesion of Solids and the Effect of Surface Films. *Proc.* Royal Soc. (1950) **202A**, p. 224.

[8] S. Takeda: A Metallographic Study of the Action of the Cementing Material for Cemented Tungsten Carbide. *Science Reports*, Tohoku Imperial Univ., Hondu Anniversary Vol. (1936) **193**, p. 864.

[9] L. L. Wyman and F. C. Kelley: Cemented Tungsten Carbide, A Study of the Action of Cementing Material. *Trans.* AIME (1931) **93**, p. 208.

[10] A. J. Shaler: The Kinetics of the Sintering Process. Sc.D. Thesis (1947) Dept. of Metallurgy, Massachusetts Institute of Technology.

[11] A. Nadai: *Plasticity* (1931) p. 13. New York. McGraw-Hill Book Co.

[12] C. J. Smithells: *Metals Reference Book* (1950) p. 58. New York. Interscience Publishers.

[13] E. Orowan, J. F. Nye, and W. J. Cairus: Notch Brittleness and Ductile Fracture in Metals. Theoretical Research Report No. 16/45, Ministry of Supply, London (1944).

[14] C. Ritzau: Beitrag Zur Magnetischen Analyse von Hartmetallen. *Stahl und Eisen* (1940) **60**, p. 891.

[15] F. Laszlo: Tesselated Stresses. *Journal* Iron and Steel Inst. (1943) **147**, Part I, No. 1, p. 173.

High Temperature Oxidation of Some Iron-Chromium Alloys

by D. Caplan and M. Cohen

The scaling characteristics of three Fe-Cr alloys have been investigated by determining their weight gain vs. time curves at 1600 to 2000 F. The scales formed thereby have been examined using the techniques of X-ray diffraction and spectrographic and metallographic analyses in an attempt to explain the discontinuities in the curves and to elucidate the mechanism of scaling.

DESPITE the considerable number of investigations that have been carried out on heat resistant alloys, the characteristics of the scales formed at high temperatures are not fully known. The research reported here was undertaken in an attempt to ascertain the mechanism of scaling of the stainless steels. Scaling experiments were carried out first, the weight increase of the specimens being followed continuously with time. It was observed that, as well as showing the expected decrease in oxidation rate with time, the oxidation curves showed breaks corresponding to intermediate periods of accelerated oxidation, after which protectiveness again increased. This phenomenon was observed with austenitic stainless steels (types 302, 309, and 330) and with Fe-Cr alloys (types 410, 430, and 446), but only the latter are treated in this report. An examination of the scales was made using the techniques of X-ray diffraction and spectrographic and metallographic analyses in an attempt to obtain a correlation between the nature of the scales and the oxidation curves.

A search through the literature revealed only a very few previous reports of such periods of accelerated oxidation. Dunn[1] found breaks in the oxidation-time curves of some Cu-Si alloys but saw no rational explanation of the phenomenon. Heindlhofer and Larsen[2] attributed a discontinuity in the weight gain-time curve of iron at 1290 F to the formation of blisters, the subsequent cracking of which exposed an unprotected surface and permitted rapid oxidation until a new protective scale had been reestablished. They advanced no explanation, however, for what they termed the peculiar behavior of a 27 pct Fe-Cr alloy at 2000 F which gained weight very rapidly in between two periods of very slow weight gain. Portevin, Pretet, and Jolivet[3] in describing breaks in the weight gain-time curves of Fe-Al alloys suggested that they might be associated with the occurrence of localized and deeply oxidized areas on the specimens. Bandel[4] in a general discussion of oxidation curves of heat resistant alloys considered that the discontinuities were due to a local disruption of the protective layer by the growth of iron-rich oxides. Day and Smith[5] in their report on the scaling of a large number of iron alloys noted but did not explain occasional relatively rapid changes in oxidation rate at higher temperatures. Chevenard and Wache[6] found breaks, often two per specimen, in the oxidation curves of an 18-8 type alloy. They suggested that the cause might be a depletion in chromium of the surface layer of metal due to its selective oxidation, the resultant high concentration of iron and nickel in the scale leading to a poorly protective scale. McCullough, Fontana, and Beck[7] explained the breaks in the oxidation curves of types 304, 430, and 410 alloys as due to mechanical ruptures.

Table I. Chemical Compositions of Specimen Materials

Element, Pct	Type 410	Type 430	Type 446
Carbon	0.10	0.10	0.20
Manganese	0.34	0.40	0.40
Silicon	0.26	0.37	0.44
Nickel	0.21	0.43	0.32
Chromium	11.44	15.78	26.54

Experimental Work

Table I lists the chemical compositions of the materials used. Cylindrical specimens $\frac{1}{4}$ in. in diam and $1\frac{1}{2}$ in. long were machined from cold rolled $\frac{3}{8}$ in. rod. After a fine finish cut with a sharp tool, the specimens were abraded while still mounted on the lathe with Nos. 2, 1, 0, and 00 metallographic grade emery papers. A 3/64 in. hole was drilled at a distance of $\frac{1}{8}$ in. from one end to permit suspension in the furnace. Specimen Nos. 1, 2, and 3 were tested with this surface preparation. All others, after being similarly prepared, were electropolished in a perchloric-acetic electrolyte, electrical contact being made by pressing a tapered platinum hook into the drilled hole. The specimens were then washed in hot water, rinsed with distilled water, rinsed with methanol, dried at 120 F, and weighed. Thereafter,

D. CAPLAN and M. COHEN are associated with the Division of Applied Chemistry, National Research Council, Ottawa, Ont., Canada.

Discussion on this paper, TP 3366E, may be sent, 2 copies, to AIME by Dec. 1, 1952. Manuscript, April 3, 1952. Philadelphia Meeting, October 1952.

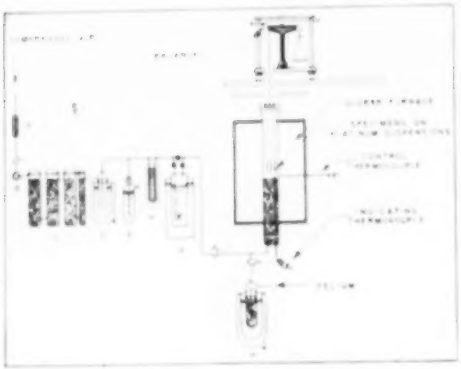

Fig. 1—Diagram of scaling apparatus

A—Glass wool filter
B—Reducing valves
C—Absorption towers of calcium chloride, soda lime, ascarite, magnesium perchlorate
D—Liquid air trap
E—Constant pressure regulator
F—Flowmeter—n butyl phthalate
G—Water saturator in constant temperature bath
H—Activated charcoal in liquid air trap

thick were handled only with forceps or rubber gloves. Measurements of the length and diameter were made with micrometer calipers and the apparent surface areas calculated.

The apparatus for carrying out the oxidation runs is shown in Fig. 1. Three specimens were suspended by means of platinum wires in a vertical tube furnace of 1¼ in. ID. Temperature measurements were made with a shielded platinum-platinum-rhodium thermocouple located in the tube ¾ in. below the specimens. The temperature was controlled to within 2°F at 2000°F by means of a temperature controller actuated by a bare chromel-alumel thermocouple located outside the furnace tube and able to "see" the global heating elements. The 9 in. heating section of the elements gave a working zone that varied by no more than 1°F over the length of the specimens. An analytical balance, protected from the heat of the furnace by interposed baffle plates, was mounted on a rolling table so that it could be located directly over the vertical tube or rolled to one side to permit the introduction or removal of specimens. The method of suspension was such that the three specimens could be weighed alternately at 2 min intervals. The prepared air stream was admitted to the bottom of the furnace tube at a rate of 200 ml per min, which amounted to a linear rate of flow of 12 in. per min in the 1¼ in. ID tube. Packing of the lower part of the tube with ceramic rings served to preheat the air.

Air from a compressed air line at 80 psi was passed through a glass wool filter (*A* in Fig. 1) and reduced to ¾ psi by two reducing valves (*B*). The greater part of the water and carbon dioxide was removed by calcium chloride, soda lime, ascarite, and magnesium perchlorate in the absorption towers (*C*); the liquid air trap (*D*) removed the last traces of moisture and carbon dioxide. The rate of flow was adjusted and controlled by the constant pressure regulator (*E*), the level of the concentrated sulphuric acid being modified as required to give the desired reading on the flowmeter (*F*). Some runs were conducted with air prepared and dried in this way. In the others, this dry air was saturated with water vapor at 90°F by passing it through the water saturator (*G*). Provision was also made for flushing the furnace tube with helium purified by passing through activated charcoal held at liquid air temperature (*H*).

Method of Measurement. After the furnace had been brought to the required temperature and the gas flow adjusted to the correct rate, the three specimens were lowered into the furnace, the balance rolled into position and weighing begun. Zero time was taken as the time of introduction of the specimens. Zero weight was determined by weighing the specimens at room temperature prior to the start of the run and adding the correction (1.1 mg) for the change in buoyant force at the testing temperature.

In an alternative procedure which was used in some of the runs to prevent oxidation during the heating up period, the specimens were brought to temperature in helium. The furnace tube was flushed out with helium at 500 ml per min for 30 min, the specimens put in, and the initial weight determined, corrections being made for the difference in buoyant force between helium and air (0.3 mg). Zero time was when the helium was turned off and the prepared air stream turned on.

At the end of a run the specimens were removed singly and one end dipped immediately into a button of molten silver. By freezing around the hot specimen this silver prevented the scale from flaking off on cooling and proved useful in the metallographic examination of scales which spalled badly.

Examination of the Specimens. As soon as the silver button described above had solidified, the hot specimen was placed in a quartz dish and examined during cooling by means of a low power stereoscopic microscope for spalling, cracking, color, texture, and inhomogeneities of the scale. In some cases, this was the only way a knowledge of the scale structure could be obtained, since after cooling, the scale might all have disintegrated to a coarse powder. When cold, further examination was made with this microscope and a cross-sectional sketch drawn of the apparent structure. Tiny pieces of the various layers, as uncontaminated as possible with other layers, were picked out under the microscope with a needle and mounted for X-ray diffraction analysis. After

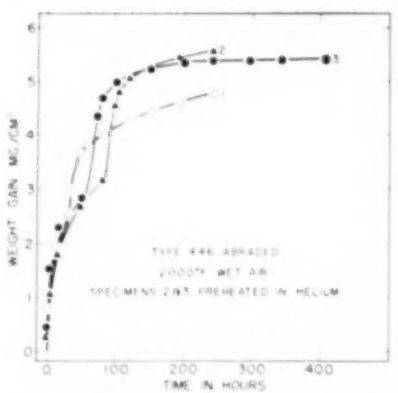

Fig. 2—Oxidation of type 446 stainless steel (abraded) at 2000°F in moist air, with and without preheating in helium

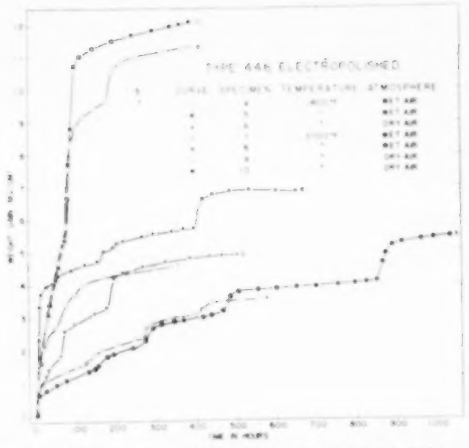

Fig. 3—Oxidation of type 446 stainless steel (electropolished) at 1800° and 2000° F in moist and dry air.

diffraction the same samples were used for spectrographic analysis.

Considerable effort was applied to the development of an impregnation and mounting technique in order that as true a cross section as possible could be prepared for metallographic examination. The method finally adopted was a double vacuum impregnation, first with bakelite lacquer and then with methyl methacrylate monomer. The plastic was kept frozen in a side tube of the vacuum apparatus while the system was evacuated, then warmed and allowed to flow over the specimen. By first coating the whole specimen with the lacquer, the scale was prevented from breaking up when the microspecimens were sawed out. The less viscous monomer then penetrated along the tiny passages from the cut edges. After polymerizing the monomer with slow heating to prevent the formation of vapor bubbles within the scale, the specimens could be mounted as usual in molding powder. Wet grinding and polishing with silicon carbide and diamond instead of with the softer abrasives gave less relief polishing of the extremely hard oxide layers and less rounding of the edges. Polarized light was used in the metallographic examination to distinguish between isometric and nonisometric oxide crystals.

Results

Scaling Runs: The weight gain vs. time curves in moist air at 2000° F of three type 446 (27 pct Cr) abraded specimens are shown in Fig. 2. In order to make the graphs less confusing many of the experimentally determined points have been omitted from Figs. 2, 3, and 4. Specimen No. 1 was introduced into the furnace with the air stream flowing, while Nos. 2 and 3 were brought to temperature in helium. This latter procedure was not used for any of the subsequent runs, since it was observed that the specimens slowly lost weight (2 mg in 30 min) during the helium pretreatment. Austenitic alloys tested at the same time slowly gained weight during this period (1 mg for type 302 and 0.5 mg for type 309) indicating that a small amount of oxidizing gas was present, due possibly to moisture in the furnace tube or ceramic packing rings.

Fig. 3 shows the oxidation curves of seven type 446 electropolished specimens. These represent runs carried out at 1800° and 2000° F, in dry and in moist air. The very coarse time scale necessarily used in plotting Figs. 2 and 3 tends to misrepresent the high degree of protectiveness of the scales in the periods between the breaks. For instance, the apparently steep flat before the last break in curve No. 9 denotes a weight gain of only 1.4 mg per specimen per day, and a more protective flat, such as the one before the last break in curve No. 5, a gain of only 0.15 mg per specimen per day. The addition of moisture leads to an unexpected result: at 1800° F specimens 4 and 5, in moist air, gained less weight than No. 6, in dry air, and at 2000° F Nos. 7 and 8, in moist air, gained less than Nos. 9 and 10, in dry air. This is at variance with previous work which has shown[7] that the addition of moisture to the oxidizing atmosphere results in increased oxidation (except for two cases[7] where the experiments were carried out at quite low temperatures).

Comparison of curves 7 and 8 in Fig. 3 with the curves in Fig. 2 indicates that the surface preparation used for the specimens is unimportant, probably because the conditions of oxidation are too severe for this relatively minor variable to have an effect.

Fig. 4 shows the oxidation curves of four type 410 (12 pct Cr) and 430 (16 pct Cr) electropolished specimens at 1600° F in moist and in dry air. In contrast to type 446 at 1800° and 2000° F, these specimens show a greater weight gain in moist air than in dry. Breaks appear in the curves but are not of the same type as those in Figs. 2 and 3. The nature of these breaks and the effect of moisture are treated in the discussion.

Examination of Scales on Type 446: Fig. 5 is a representation of a typical scale cross section on the 27 pct Cr alloy as estimated from the stereoscopic microscope examination. (Specimen 8 is the scale actually drawn.) There is an outer black layer or in some cases two such layers (*A* and *C*) finely wrinkled, poorly adherent, and fragile. Beneath this is a greenish-black, glassy layer (*E*), very hard and

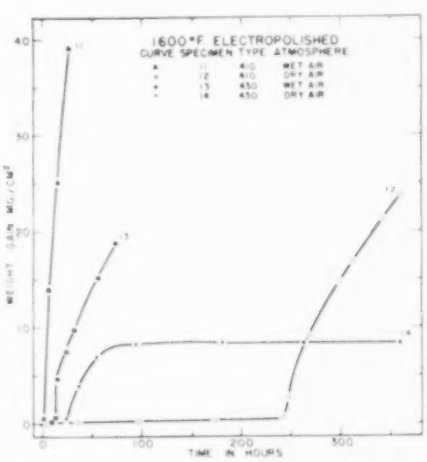

Fig. 4—Oxidation of types 410 and 430 stainless steels (electropolished) at 1600° F in moist and dry air.

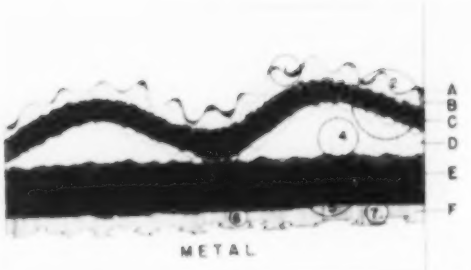

Fig. 5—Type 446. Specimen 8. Diagrammatic representation of scale cross section. Layers B, D, and F are silica. Layers A and C mostly spinel. Layer E mostly Cr_2O_3. The numbered circles show where samples were taken for X-ray diffraction and spectrographic analysis. See Table II.

Table II. Analyses of Scale Layers on Specimen 8

Fraction	Layer	Diffraction data*			
		Spinel (M.O.)	Rhombohedral (M.O.)	Silica	Metal
1	A, B	100	0	20	0
2	A, B, C, D	100	10	40	0
3	C	100	30	0	0
4	D	20	5	100	0
5	E, F	5	100	60	0
6	F	10	25	100	40
7	F	20	15	100	50

* The numerical values are the relative intensities of the strongest lines to each of the four patterns.

abrasion resistant. White crystals (*B* and *D*) exist between all the scale layers and between the scale and the metal (*F*). The crystals between the outer layers are usually masses of tiny needles, sometimes with white or gray granular material as well. The crystals between the scale and the metal are in the form of a rough crumbly grayish-white layer, some of which is adherent to the metal and some to the underside of the glassy layer. At higher magnifications tiny metallic spheres can be seen embedded in this layer *F*.

The accuracy of the spectrographic analysis is low because the samples used only weighed from 0.01 to 0.1 mg; these very small amounts of any one fraction uncontaminated with other fractions were all that could be separated under the microscope. The analyses show that the scales are made up mainly of chromium oxide with silica the next largest constituent. Iron and manganese are present in lesser amounts. Aluminum and copper are detectable but nickel is not. The ratio of chromium to iron is about 20 to 1.

The numbered circles on Fig. 5 represent where samples were taken for X-ray diffraction and spectrographic analysis; the areas falling within the circles indicate the anticipated contaminants of each fraction. Table II shows the X-ray diffraction data for these fractions.

The diffraction data show that the scales on the 27 pct Cr alloy oxidized either at 1800° or 2000° F, in moist or in dry air, are made up of four phases:

1—A spinel of lattice parameter about 8.40A which, considering the accuracy of the technique, fits either of the spinels $FeO \cdot Cr_2O_3$ (8.40), $FeO \cdot Cr_2O_3$ (8.35), or $MnO \cdot Cr_2O_3$ (8.42), all of which are possible on the basis of the spectrographic analysis.

2—A rhombohedral oxide, the diffractogram fitting a Fe_2O_3 or Cr_2O_3 or solid solutions of these two

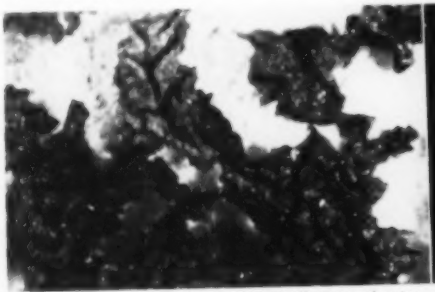

Fig. 6—Type 446. Specimen 5. Flaked off pieces of outer layer of scale showing extensive wrinkling and gray silica clinging to underside. X50.

Fig. 7—Type 446. Specimen 10. Underside of outer scale layer showing needle like silica crystals. X250.

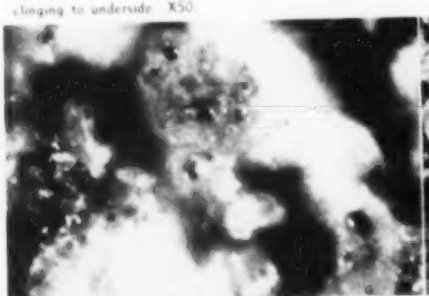

Fig. 8—Type 446. Specimen 7. Metallic spheres embedded in the silica layer adhering to the metal specimen. Compare with Fig. 10. X750.

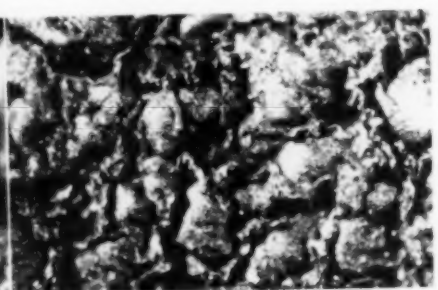

Fig. 9—Type 446. Specimen 7. Plan view of outer side of outer layers of scale showing severely wrinkled layer lying in troughs of undulating layer. Compare with Fig. 10. X90.

An attempt was made to determine the approximate composition by comparing the relative line intensities with those reported in the literature[7,8] and with the patterns obtained from known α Fe_2O_3 and Cr_2O_3 but without success. The difference in relative line intensities between Fe_2O_3 and Cr_2O_3 was found to be too small for our purpose.

3—Silica in the α-cristobalite form.

4—Elemental metal which, according to the diffraction pattern, could be iron, chromium, or the Fe-Cr alloy.

The outer black wrinkled layer, or layers, is made up of spinel and rhombohedral oxide. The dark green glassy layer is mainly rhombohedral. The white or gray material is α-cristobalite, whether it appears as needles or granules. The pattern of elemental metal appears in fractions containing the tiny metallic spheres, layer *F* in Fig. 5.

The scale structures on the 27 pct Cr alloy are illustrated in Figs. 6 to 13. The fact that many of the scales spalled badly on cooling made it difficult to obtain good metallographic cross sections and, while the silver button technique was useful for specimens which spalled completely, it was only partly successful since it crushed the fragile outer layers considerably. In many of the cross sections the scale is separated from the metal by a gray layer of methacrylate plastic. This separation probably resulted from the differential contraction of scale and metal on cooling. The dark areas seen in some of the figures are holes where the plastic did not completely fill the voids.

Because the optical contrast between the silica and plastic is low and the needle-like silica crystals are extremely fragile, silica is poorly depicted in the cross sections. It can be faintly discerned as a layer against the metal in Figs. 10 to 13 and, on the microscope, the silica needles under the outer layers can be detected by focusing down into the plastic. The plan views in Figs. 6 to 8 give a truer impression of the large masses of silica present. Metallic spheres similar to those which appear in the silica in Fig. 8 can be seen in cross section adjacent to the metal in Figs. 10 to 13. Their location indicates that they are the remains of intergranularly oxidized grains.

The marked wrinkling of the outer layer is shown in plan in Figs. 6 and 9 and in section in Figs. 10 to 13. The wrinkled layer lying in the troughs of an undulating layer in Fig. 9 is seen in cross section in Fig. 10.

Fig. 11 of specimen 10 shows an outer wrinkled layer, the glassy inner layer, silica against the metal and clinging to the underside of the glassy layer, and the metallic spheres in this silica. The silica needles under the outer layer can only be detected by focusing down into the plastic. The local enlargement included in this field is seen at higher magnification in Fig. 12a and in polarized light in Fig. 12b. The glassy layer is seen to be optically active, indicating Cr_2O_3, except for the grayer islands in it. This optical activity of the lighter scale and inactivity of the grayer scale was observed generally not only with type 446 but with types 410 and 430 as well.

Examination of Scales on Types 410 and 430: Examination of the scaled specimens of the 12 and 16 pct Cr alloys with the stereoscopic microscope shows them to be markedly different from the 27 pct Cr alloy. There is no evidence of any white crystals; except for an occastonal local area, the outer surface is not wrinkled; and the scales are generally redder than those on the type 446 speci-

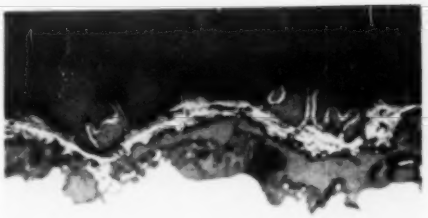

Fig. 10—Type 446. Specimen 7. Metallographic cross section of same scale as Fig. 9 showing severely wrinkled layer lying in troughs of undulating layer. Compare with Fig. 9. Note also silica between metal and scale and remains of intergranularly corroded metal grains in this silica. Unetched. X250.

mens, indicating a higher iron content. The scales are stratified but not as on type 446; the layers are more like those which form on unalloyed iron.[9,10,11]

The structure of the scales on these lower chromium alloys is shown in Figs. 14 to 16. It can be seen that the scale in contact with the metal is the reduced, gray, optically inactive $(Fe, Cr)_2O_3$ form, while that in contact with the air has been oxidized to the whiter, optically active, rhombohedral $(Fe, Cr)_2O_3$ form.

Discussion

Comparison of the oxidation curves and scale structures indicates that the character of the oxidation process for the 27 pct Cr alloy is different from that of the lower chromium alloys. A different scaling mechanism is proposed for each case.

Scaling Mechanism for Type 446: It is evident from the examination of the scales on type 446 stainless steel that silica as a separate phase is a major constituent, even though the silicon content of the original alloy is only 0.44 pct. Silicon has long been recognized along with chromium and aluminum as one of the elements which contribute oxidation resistance to metals. Oxides of chromium and aluminum, because they can combine with iron oxides

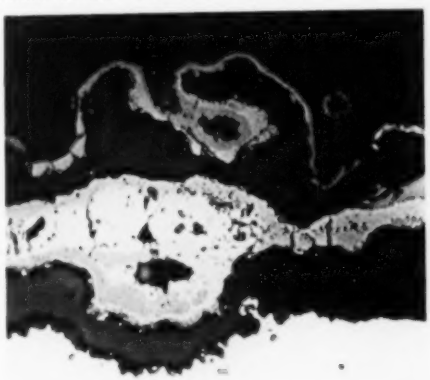

Fig. 11—Type 446. Specimen 10. Metallographic cross section of the scale layers, the field including a local enlargement of the glassy layer. Note extensive wrinkling of outer layer. Unetched. X250.

Fig. 12—Part of Fig. 11 at higher magnification. Unetched. X500.

a—Showing silica layer "F" against metal and clinging to underside of glassy layer; remnants of metal grains in both these silica areas; darker gray islands in highly reflecting glassy layer "E". Letters correspond to lettered layers of sketch shown in Fig. 5.

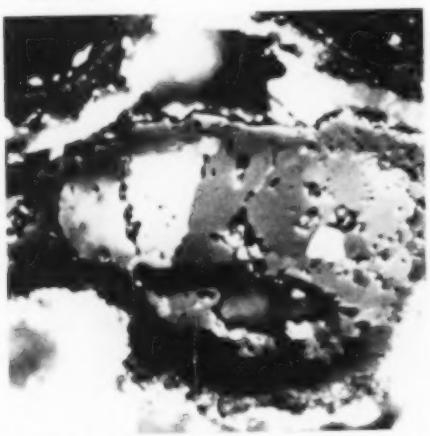

b—Same field in polarized light showing optical activity of glassy layer, indicating Cr_2O_3, and inactivity of darker gray islands in glassy layer, indicating isometric oxide.

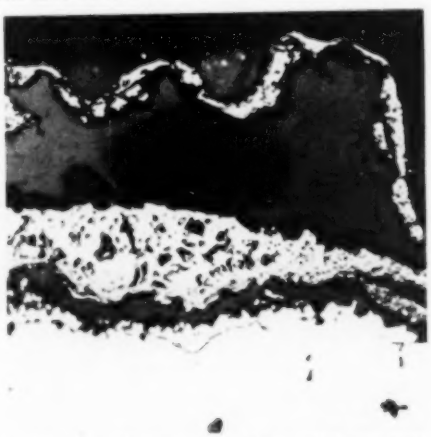

Fig. 13—Type 446. Specimen 9. Note wrinkled outer layer, silica against metal, intergranularly corroded metal and gray non optically active band in main scale layer. Unetched. X250.

to form either mixed oxides by isomorphous substitution or spinels,[15] affect the mechanical properties or the electrical conductivity of the scales and thus decrease the rate of oxidation. Silicon, however, does not form such complex oxides nor is fayalite, Fe_2SiO_4, detectable in any of the X-ray diffraction patterns. It follows, therefore, that silicon must confer protectiveness in some other way.

The numerous reports in the literature of improvement in oxidation resistance due to the presence of silicon in the metal[1, 2, 3, 4, 5] have not shown direct evidence of the mechanism by which this improvement is effected. In some instances[1, 2, 3, 4, 5] silica has been observed to concentrate at the metal/scale interface. Dewey and Jenkins[2] and Hickman and Gulbransen[3] concluded that the silicon in Ni-Cr alloys did not change the bulk structure of the oxides but affected the metal/scale boundary. Griffiths[4] and Lustman[5] ascribe an improvement in scale adhesion and consequently in oxidation resistance to the roughness of the metal/scale interface resulting from the oxidation of silicon.

In the case of the scales on type 446 stainless steel which have been examined here, the authors believe the part played by the silica to be as follows:

Fig. 17 is an idealized oxidation curve of the 27 pct Cr alloy similar to the curves of Figs. 2 and 3.

1—In the first stage of the oxidation process, represented by section *OA*, a scale of chromium oxide containing minor amounts of iron oxide builds up and the rate falls off parabolically as the film increases in thickness.

2—In section *AB* silica gradually accumulates between metal and scale, silicon apparently being capable of reducing chromium oxide under the conditions obtaining, and also being insoluble in the chromium oxide lattice. This is in agreement with the data of Lustman[5] who shows that the dissociation pressure of silica is lower than that of chromium oxide over the full range of temperatures. As a result of this accumulation of silica the transfer of cations across the metal/scale interface is impeded and consequently the rate of oxidation decreases more rapidly than would be predicted by the parabolic law, which is the result of the rate being controlled by the diffusion reaction through the scale layer. This leads to the very low weight gains observed during these periods.

3—As the quantity of silica increases with time, the degree of insulation of the scale from the metal becomes so great that (a) cations are no longer being supplied to the scale, enabling the state of oxidation of the scale to increase to an equilibrium value, and (b) the scale, no longer constrained by attachment to the metal, wrinkles under the force of the

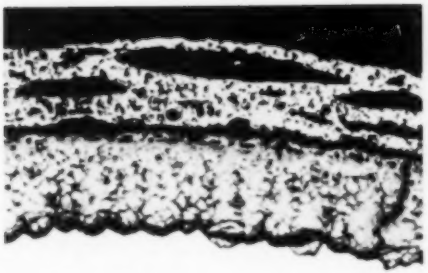

Fig. 14—Type 410. Specimen 11. Showing layered structure of scale of a type more like scale on unalloyed iron than on the type 446 specimens. Note whiter (optically active) outer portion of outer layer indicating Fe, Cr, O. Unetched. X100.

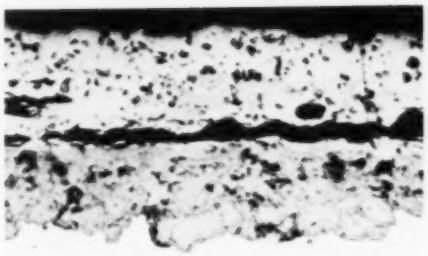

Fig. 16—Type 430. Specimen 13. Showing layered structure after the fashion of scale on unalloyed iron. Outer layer is mostly Fe, Cr, O (optically active) except for darker islands. Outer surface of inner layer is Fe, Cr, O. Unetched. X250.

compressive stresses resulting from the fact that the natural area of the scale is greater than the area of metal surface on which it grows. For either or both of these reasons cracks form in the scale and oxygen is permitted to penetrate to the bare metal underneath. The rate of oxidation now increases sharply as indicated in section *BC*.

4—Section *CD* represents the building up of a second layer of scale, essentially chromium oxide again, underneath the outer layer of scale, now wrinkled, and under the silica layer. Section *CD* is thus equivalent to section *OA*.

5—Another layer of silica accumulates with time, insulates the new scale layer from the substrate, section *DE*, and the break is repeated.

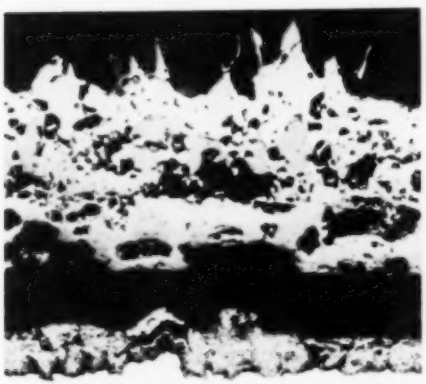

Fig. 15—Type 410. Specimen 12. Showing white Fe, Cr, O outer portion of outer layer. Note faceted crystalline outer surface. Unetched. X250.

This mechanism accounts for the mass of silica observed between all the scale layers in the examination of the scales on type 446 and for the fact that the outer layers are greatly wrinkled and cracked and the inner one still monolithic.

The number of layers of scale as seen in the metallographic cross section of a specimen would be expected to correspond to the number of breaks in the oxidation curve and in a number of cases they do, but in the others the number of layers is less than the number of breaks. This may be accounted for by assuming that the scale becomes unprotective over only a part of the specimen at a time. In the duplicate specimens 9 and 10 (Fig. 3) it appears that No. 9 broke in two steps while No. 10 became unprotective over the entire specimen at one time. In the case of the lower chromium alloys the number of layers is often more than the number of breaks (if breaks can be spoken of as existing at all) but these extra layers are due to the stratification normal to the scale on unalloyed iron rather than the result of insulation by silica.

Another deduction from the mechanism of the breaks as outlined here is that the thickness or mass of the various layers in a specimen should be proportional to the heights of the breaks or, more correctly, to the vertical distances between the ends of the protective periods. That is, in Fig. 17 the ratio of the mass of the outer layer to that of the next layer should be proportional to the ratio of x to y. Estimation of the relative masses is difficult because of the wrinkling and disintegration of the outer layers but it does appear that the outer layer is usually less massive than the ratio of break heights would predict. Two reasons may be advanced to resolve this apparent diversity: 1—A larger proportion of the weight gain indicated for the first layer may have gone into internal oxidation than for the later layers, and 2—the outer layer loses mass by the volatilization of chromium as discussed later.

Scaling Mechanism for Types 410 and 430. The discontinuities in the oxidation curves of the lower chromium alloys (Fig. 4) are of a different type from those of the 27 pct Cr alloy. Whereas the type 446 specimens (oxidized at 1800 and 2000 F) initially gained weight rapidly before developing a protective layer, the 12 and 16 pct Cr specimens (oxidized at 1600 F) show an extraordinarily low initial rate, the break in the curves is due to the departure from this low rate. Evidently, for Fe-Cr alloys containing 12 pct Cr or more, the thin oxide film which forms at low temperature, and which is already present at the beginning of the run, is exceptionally protective and is able to remain so at 1600 F for some time (the scale on specimen 12 remained in this highly protective condition for 240 hr). This thin film is a combination of the oxides formed by the electropolishing process, room temperature air oxidation, and oxidation while the specimens are heating up in air to the testing temperature. When this film is destroyed, either by

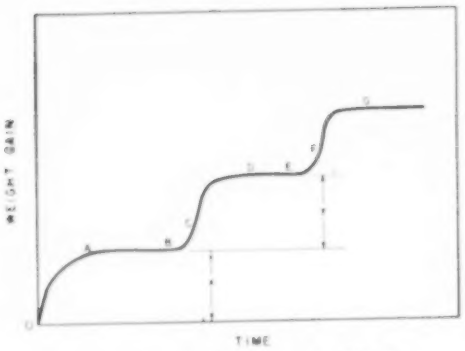

Fig. 17—Idealized oxidation curve for type 446 alloy

mechanical rupture or by recrystallization or by a change in composition (by dilution with different cations from the metal), the specimens gain weight at the fastest rate normal to the testing conditions to which they are exposed until the thickening oxide layer causes the rate to decrease again in accordance with the now generally accepted theory.[20] Since it is to be expected that the type 446 alloy forms a low temperature film at least as protective as that on the lower chromium alloys, and yet the type 446 specimens do not display this initial exceptional degree of protectiveness (at 1800° and 2000 F), it follows that the thin film, although protective at 1600°F, is unable to protect at 1800° and 2000 F. Further, the low temperature film on the lower chromium alloys is probably of the same type and composition as that on the 27 pct Cr alloy.

Effect of Moisture. A possible explanation of the anomalous effect of moisture on the scaling rate of the 27 pct Cr alloy can be based on a consideration of the defects in the oxide lattice. It has been shown[21] by electrical conductivity measurements that Cr_2O_3 is a metal deficiency conductor and that the greater the number of cation vacancies, the faster will be the rate of cation diffusion.[22] If hydrogen ions resulting from the decomposition of water molecules on the scale surface were to occupy some of the vacancies, the diffusion rate and hence the scaling rate would be lessened. On the other hand, Fe_2O_3 is a metal-excess oxide.[23] Therefore, the more iron in the $(Fe, Cr)_2O_3$ oxide the less cation deficient the lattice will be. For the lower chromium specimens then, where the relatively rapid scaling rate leads to a higher iron content in the scale, the diffusion rate should be little affected by hydrogen ions and the normal increase in oxidation rate with the addition of moisture can be expected, as is seen in Fig. 4.

Composition of the Spinel Phase. The spinel-type oxide which forms a major part of the scale on the 27 pct Cr alloy is shown by the spectrographic analysis to have a very high chromium to iron ratio—from 15 to 1 to as high as 30 to 1. The spinel chromite, $FeO \cdot Cr_2O_3$, which is the one to be expected on Fe-Cr alloys, has a chromium to iron ratio of only about 2 to 1. Therefore, the spinel observed must either be Cr_2O_3, which the known instability of chromous ion makes improbable, or a spinel structure with additional divalent lattice sites vacant. This is equivalent to a γ form of Cr_2O_3 analagous to γ Fe_2O_3, which is a known low temperature oxidation product of iron and which has a diffraction pattern practically indistinguishable from that of Fe_2O_3. However, γ Cr_2O_3 has not been previously described, although this difficulty of a spinel-type structure associated with a high chromium content has been encountered before.[24]

Volatilization of Chromium. As noted above, type 446 specimens lost weight while soaking in helium, whereas austenitic alloys under the same conditions slowly gained weight. It was observed, also, that at the end of a run the platinum suspension wires were discolored, and, in longer runs, were coated with dark green crystals as shown in Fig. 18. X-ray diffraction and electrographic analysis showed these to be Cr_2O_3. Since similar crystals were observed on the wall of the furnace tube, it is apparent that chromium has in some way been transported away from the specimens through the gas phase. A calculation based on thermodynamic data given by Dushman[25] shows that a sublimation process as suggested by Bandel[1] cannot nearly account for the quantities of Cr_2O_3 observed on the wires and tube. However, by estimating the amount of carbon lost from a specimen from the depth of the decarburized ring seen in the metallographic cross section, it can be shown that more than sufficient chromium could be volatilized from the specimen as a result of the decarburization reaction:

$$Cr_2O_3 + 3C \rightleftharpoons 2Cr + 3CO$$

which has recently been discussed by Gulbransen, Wysong, and Andrew.[26] The vapor pressure of elemental chromium is relatively high at 2000 F (approximately 1 micron[27]—about 100 times the vapor pressure of iron or nickel) and, once reduced, a sufficient percentage might escape into the gas phase before being reoxidized.

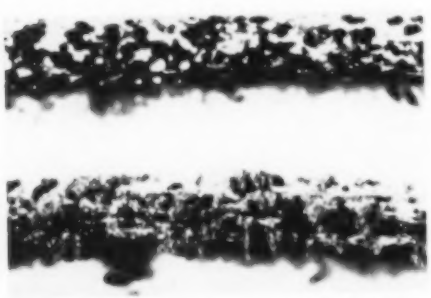

Fig. 18—Sections of platinum suspension wire from specimen 9. X40.
a (top)—Section showing mostly Cr_2O_3 crystals.
b (bottom)—Section closer to specimen (and therefore at higher temperature) showing mossy growth of platinum as well as Cr_2O_3 crystals.

Summary

1—The oxidation of a 12, 16, and 27 pct Cr stainless steel is studied in dry and in moist air, the 12 and 16 pct alloy at 1600 F and the 27 pct at 1800° and 2000 F. The oxidation curves of the 27 pct alloy are found to exhibit periods of accelerated oxidation intermediate between periods of high protectiveness. Examination of the scales indicates that this may be due to the accumulation of silica at the scale/metal interface.

Discontinuities in the oxidation curves of the 12 and 16 pct Cr alloys result from the extraordinary protectiveness (at 1600 F) and subsequent destruc-

tion of the thin oxide film which forms at low temperature.

2—The 27 pct Cr specimens unexpectedly gain more weight in dry than in moist air. This may be due to the filling of cation vacancies in the Cr_2O_3 lattice with hydrogen ions.

3—The scale on the 27 pct Cr alloy is mainly chromium oxide, with silica the next largest constituent. Iron and manganese are present in lesser amounts. Aluminum and copper are detectable but nickel is not.

Crystallographically, the scale consists of a spinel (Cr_2O_3 or some equivalent), a rhombohedral oxide Cr_2O_3 with some FeO in solid solution, and silica in the α-cristobalite form. Grains of elemental metal in the scale are the result of intergranular oxidation of the specimens.

4—Chromium is found to volatilize from the 27 pct Cr specimens, being observed as Cr_2O_3 crystals on the suspension wires and furnace tube. Carbon from the alloy is believed to reduce Cr_2O_3 on the outer surface of the scale, some of the resultant elemental chromium volatilizing into the gas stream.

5—The scaling process is not affected by a change in surface preparation (abraded or electropolished) for the 27 pct Cr alloy, probably because the oxidation conditions are too severe for this relatively minor variable to have an effect.

Acknowledgment

The authors wish to thank Mrs. Helen Sheppard and Dr. W. H. Barnes of the Division of Physics for carrying out the X-ray diffraction analyses, and P. E. Beaubien for preparing the metallographic specimens.

References

[1] J. S. Dunn: *Journal* Inst. Metals (1931) **46**, pp. 25-48.

[2] K. Heindlhofer and B. M. Larsen: *Trans.* Amer. Soc. Steel Treat. (1933) **21**, pp. 865-895.

[3] A. M. Portevin, E. Prétet, and H. Jolivet: *Journal* Iron and Steel Inst. (1934) **130**, pp. 219-271.

[4] G. Bandel: *Arch. Eisenhüttenwesen* (1941) **15**, pp. 271-283.

[5] M. J. Day and G. V. Smith: *Industrial and Engineering Chemistry* (1943) **35**, pp. 1098-1103.

[6] P. Chevenard and X. Wache: *Revue Metallurgie* (1948) **45**, pp. 121-128.

[7] H. M. McCullough, M. G. Fontana, and F. H. Beck: *Trans.* A.S.M. (1951) **43**, pp. 404-420.

[8] R. Griffiths: *Journal* Iron and Steel Inst. (1934) **130**, pp. 377-384.

[9] C. A. Siebert and H. G. Donnelly: *Trans.* A.S.M. (1940) **28**, p. 372.

[10] W. H. Hatfield: *Journal* Iron and Steel Inst. (1927) **115**, pp. 483-522.

[11] W. E. Campbell and U. B. Thomas: *Trans.* Electrochem. Soc. (1947) **91**, pp. 623-639.

[12] A. B. Winterbottom: *Journal* Iron and Steel Inst. (1950) **165**, pp. 9-22.

[13] W. O. Milligan and L. Merten: *Journal of Physical and Colloidal Chemistry* (1947) **51**, pp. 521-528.

[14] L. Passerini: *Gazz. Chim. Ital.* (1930) **60**, pp. 544-558.

[15] N. B. Pilling and R. E. Bedworth: *Journal* Inst. Metals (1923) **29**, pp. 529-582.

[16] R. Griffiths: Iron and Steel Inst. *Carnegie Scholarship Memoirs* (1937) **26**, pp. 165-174.

[17] L. B. Pfeil: *Journal* Iron and Steel Inst. (1931) **123**, pp. 237-258.

[18] B. W. Dunnington, F. H. Beck, and M. G. Fontana: *Corrosion* (1952) **8**, pp. 2-13.

[19] A. F. Wells: *Quarterly Reviews* (1948) **2**, No. 3, pp. 185-202.

[20] O. Krause and W. Thiel: *Ber. deutsch. keram. Ges.* (1934) **15**, pp. 101-110.

[21] I. I. Kornilov and A. I. Spikelman: *Doklady Akad. Sci. U.R.S.S.* (1946) **54**, pp. 511-514.

[22] D. M. Dovey and I. Jenkins: *Journal* Inst. Metals (1950) **76**, pp. 581-596.

[23] J. W. Hickman and E. A. Gulbransen: *Trans.* AIME (1949) **180**, pp. 519-533; METALS TECHNOLOGY (June 1948).

[24] A. E. White, C. L. Clark, and C. H. McCollam: *Trans.* A.S.M. (1939) **27**, pp. 125-148.

[25] B. Lustman: *Trans.* AIME (1950) **188**, pp. 995-996; JOURNAL OF METALS (August 1950).

[26] L. S. Darken: *Journal* Amer. Chem. Soc. (1948) **70**, pp. 2046-2053.

[27] B. Lustman: *Metal Progress* (1946) **50**, pp. 850-860.

[28] C. Wagner: *Corrosion and Material Protection* (1948) **5**, No. 5, pp. 9-11.

[29] D. J. M. Bevan, J. P. Shelton, and J. S. Anderson: *Journal* Chem. Soc. (1948) pp. 1729-1741.

[30] C. Wagner: *High Temperature Properties of Metals* (1951) pp. 93-132. A.S.M.

[31] E. M. Mahla and N. A. Nielsen: *Trans.* Electrochem. Soc. (1948) **93**, pp. 1-15.

[32] S. Dushman: *Scientific Foundations of Vacuum Technique.* (1949) p. 778. New York. John Wiley and Sons.

[33] E. A. Gulbransen, W. S. Wysong, and K. Andrew: *Trans.* AIME (1949) **180**, pp. 565-578; METALS TECHNOLOGY (September 1948).

Technical Note

On the Reversal of the Strain-Induced Martensitic Transformation in the Copper-Zinc System

by J. E. Reynolds, Jr. and M. B. Bever

IN several alloys of iron, copper, and lithium as well as in some pure metals, martensite formed on cooling reverts to the parent phase upon heating to a temperature below the equilibrium temperature at which the parent phase becomes stable.[1] These martensitic transformations, therefore, are thermally reversible, although appreciable hysteresis may be involved. The martensitic reaction has long been

J. E. REYNOLDS, Jr., Junior Member AIME, is Instructor and M. B. BEVER, Member AIME, is Associate Professor, Dept. of Metallurgy, Massachusetts Institute of Technology, Cambridge, Mass.

TN 124E. Manuscript, June 20, 1952.

recognized as sensitive to plastic straining, while elastic strains have commonly been thought to have little or no effect upon this type of reaction. Kulin, Cohen, and Averbach,[1] however, have recently shown that elastic strains raise the temperature of initial martensite formation (M_s temperature) in an iron-base alloy. Greninger and Mooradian found that martensite in a Cu-Zn alloy containing 39.21 pct Zn forms first on cooling to between −30° and −40°C and that it reverts to the β phase upon heating to room temperature. They were able to induce the formation of martensite at room temperature by straining, but made no mention of the effects of removing the applied stress. They determined (155), or (166), as the habit plane.

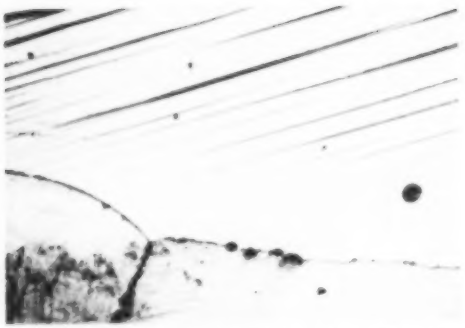

Fig. 1—Plates of martensite in metastable β brass held in compression. X200

In the work reported here specimens of Muntz metal analyzing 60.12 pct Cu, 0.75 pct Pb, 0.02 pct Fe, and 39.71 pct Zn (by difference) were solution treated at 870°C for 45 min and quenched into a brine-ice mixture. After mechanical polishing the specimens were polished and etched electrolytically in dilute orthophosphoric acid. The structure consisted almost entirely of β with slight precipitation of α in the grain boundaries. The grain size was coarse with a minimum grain diameter of approximately 1 mm.

A specimen measuring 6x8x8 mm was compressed in a vise in a direction parallel to the polished surface. A change in the appearance of this surface could be observed without magnification. Microscopic investigation, while the specimen was still in compression, revealed long narrow plates. When the stress was released by loosening the vise, many of the plates disappeared while others decreased in length and width. Figs. 1 and 2 illustrate these observations for an identical field. This behavior was confirmed with several specimens, all of which exhibited considerable hysteresis. In the areas where plates disappeared, the surface showed a slight residual disturbance. When specimens were stressed and unstressed in successive cycles, the plates appeared in the same locations.

The following additional observations were made: When the stress was increased in steps, some plates grew in length and width and new plates also appeared. Some wide bands were made up of clusters of parallel thin plates. When the specimen surface was observed microscopically while the stress was increased slowly and continuously, the plates seemed to grow smoothly at the magnification used. After a specimen had been deformed by bending and the stress removed, some residual plates disappeared when the specimen was slightly bent in the opposite direction.

Although the deformation was carried into the plastic range in most of these experiments, the dimensional changes were not measured. The essential feature of these experiments lies in the fact that the plates tended to disappear when the applied force ceased to act. This fact indicates the important role of elastic stresses associated with plastic deformation.

The microstructural appearance of the plates was identical with the structures which Greninger and Mooradian[2] showed to be associated with the martensitic transformation of metastable β to the face-centered tetragonal transition lattice. A further confirmation of the nature of the transformation product was sought by cooling in liquid nitrogen one of the specimens that had been stressed previously and contained residual strain-induced plates. As the specimen was cooled below room temperature, some of these plates increased in length

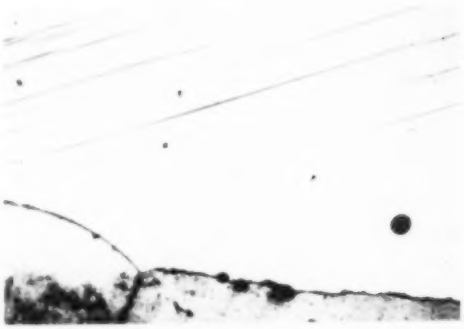

Fig. 2—Same location as Fig. 1 after release of compressive stress. X200

and thickness and additional plates formed. The thermally induced and strain-induced plates had a similar metallographic appearance.

Orientation relations of the plates with respect to the β matrix were examined briefly in the work reported here. The orientation of a large β grain was determined by a Laue back-reflection pattern and the angle between two sets of plates in the surface of this grain was measured. This angle agreed closely with the angle at which the (155), and the (1$\bar{5}$5), planes should intersect each other in the plane of polish according to a stereographic plot. This finding was thus consistent with one set of habit planes found by Greninger and Mooradian.[2]

In summary, it is concluded that martensite, strain-induced in metastable β brass at room temperature, is mechanically reversible with considerable hysteresis and that elastic stresses are operative in this reversal.

References

1. Morris Cohen. *Phase Transformations in Solids*. Edited by Smoluchowski, Mayer, and Weyl. (1951) Chap. 17, p. 620 ff. New York. John Wiley and Sons.
2. S. A. Kulin, Morris Cohen, and B. L. Averbach. JOURNAL OF METALS (June 1952), *Trans.* AIME, p. 661.
3. A. B. Greninger and V. G. Mooradian. *Trans.* AIME (1938) **128**, p. 337.

Strain Patterns in Charpy Impact Specimens Of 0.20 Pct C Mild Steel

by E. S. Bumps

A series of macrographs are presented for the purpose of graphically recording the strain phenomenon that accompanies the energy transition in the Charpy impact testing of a mild steel that is susceptible to strain aging.

STRAIN patterns in mild steel Charpy impact specimens were obtained in order to determine whether, on the first appearance of plastic strain during deformation, the initial fracture cracks appear in the region of plastic strain or in the elastically deformed regions between. Although this attempt to locate the initiation of cleavage was not successful, the observed strain patterns illustrating various stress conditions in partially deformed Charpy specimens are presented along with a discussion of the possible dependence of transition energy on the yield phenomenon.

Earlier work on the development of strain patterns in mild steel have been reported by Fry[1] and later by Jevon.[2] Harris, Rinebolt, and Raring[3] observed characteristic strain markings on the surface of Charpy V-notch impact specimens fractured above and below the transition temperature which they presented schematically. It is intended that the strain figures presented here will add to the literature a graphic correlation of strain with transition energy in impact specimens.

Samples of $\frac{3}{8}$ in. round hot rolled, 0.20 pct C steel were machined to standard 0.394 in. sq. V-notch Charpy impact specimens. Preliminary testing involved determination of transition temperature, Fig. 1, using a Sontagg impact tester. These data were subsequently used to select temperatures above, within, and below the transition range at which specimens were partially deformed. Partial deformation was obtained by either varying the energy or the testing temperature, see Table I.

Macroscopic strain figures shown in Figs. 2 to 19 were produced by several metallographic repolishing and etching steps. The macroetchant used was as follows:[4] 120 g HCl, concentrated; 100 ml water; and 90 g cupric chloride. Strain figures were obtained on the outer surface and on sections through the central portion of the impact specimens in order to determine an approximation of the volumetric strain pattern. In the tensile strain figures reported by Jevon, it was found that strain etching would not work immediately following strain unless the material was heated to 200° C. The impact strain patterns presented here were obtained without this heating, but the specimens were not etched until ten months after straining. This confirms a discussion of Jevon's paper, in which it was pointed out that strain figures can also be developed after aging for long periods of time at room temperature. Hardness of the strained and unstrained portions, revealed by the etched pattern, was explored using R_c impressions converted to R_c hardness values.

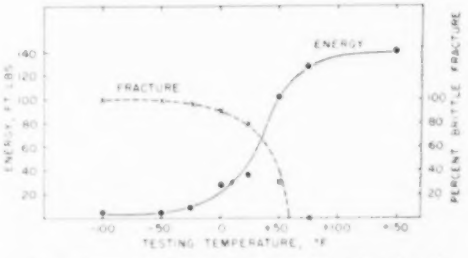

Fig. 1—Energy and fracture curves for 0.20 pct C mild steel

Discussion of Results

In the impact test, as in the tensile test, some parts of the specimen yield and deform plastically, while other regions are deformed only elastically. The plastic deformation bears a relation to the imposed stress pattern. In the strain figures presented here, the plastically deformed regions are the dark etching ones. The strain figures are always symmetrical because the stress state in the Charpy-type specimen under impact loading is symmetrical.

The difficulties encountered to produce initial cracks are intimated in Figs. 2 and 4. At a temperature of −75° F, the stress was not sufficient to pro-

Table I. Testing Conditions for Partially Deformed Mild Steel Charpy Impact Specimens

Specimen No.	Capacity	Testing Temperature, °F	Angle of Deformation	Fig. No.
XA3-9	Hammer raised approximately 12 in.	75	0°	2
XA3-2	Hammer raised 12½ in.	75	Broke	4
XA3-1	25 ft lb	12	2°	5-9
XA3-4	25 ft lb	0	14°	10-14
XA3-8	60 ft lb	−27	33°	15-19

E. S. BUMPS, Junior Member AIME, formerly Research Metallurgist, Armour Research Foundation, Chicago, is now Metallurgist, Studebaker Corp., South Bend, Ind.

Discussion on this paper, TP 3357E, may be sent, 2 copies, to AIME by Dec. 1, 1952. Manuscript, April 4, 1952. Philadelphia Meeting, October 1952.

Fig. 2—Strain pattern in a 0.20 pct C mild steel Charpy impact specimen partially deformed at −75° F. X2½.

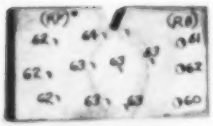

Fig. 3—Same specimen as Fig. 2 showing R_c hardness (Rockwell C impressions converted to Rockwell B hardness number). X2½.

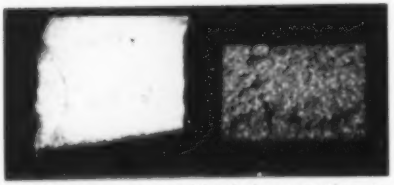

Fig. 4—Strain pattern and brittle fracture surface in specimen broken at −75° F. Hammer was lifted approximately ½ in. higher than for partially deformed specimen shown in Fig. 2. X2½.

Fig. 5—Partial deformation in a mild steel Charpy impact specimen tested at −112° F, 25 lb capacity. X2. Area reduced approximately 40 pct for reproduction.

Fig. 6—Strain pattern near the surface of specimen shown in Fig. 5. X2½.

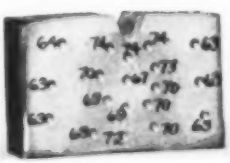

Fig. 7—Same as Fig. 6 showing R_c hardness. X2½.

Fig. 8—Strain pattern in a section through central portion of specimen shown in Fig. 5. X2½.

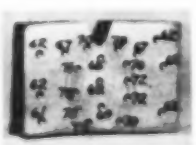

Fig. 9—Same as Fig. 8 showing R_c hardness. X2½.

Fig. 10—Partial deformation in a mild steel Charpy impact specimen tested at 0° F, 25 lb capacity. X2. Area reduced approximately 40 pct for reproduction.

Fig. 11—Strain pattern near the surface of specimen shown in Fig. 10. X2½.

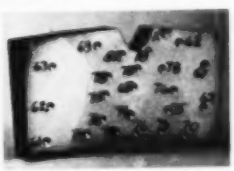

Fig. 12—Same as Fig. 11 showing R_c hardness. X2½.

Fig. 13—Strain pattern in a section through central portion of specimen shown in Fig. 10. X2½.

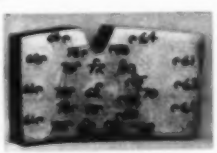

Fig. 14—Same as Fig. 13 showing R_c hardness. X2½.

duce initial cleavages or break the specimen, Fig. 2, but by slightly increasing the impact load a similar specimen broke with 100 pct brittle fracture, Fig. 4. The strain patterns in both specimens are essentially alike. Experience on many attempts was that the specimens either partially deformed without initial cracks or fractured completely. Any cracks that did develop were always ductile tears near the notch.

The series of strain patterns in Figs. 2 to 19 showed good correlation with the amount of bending or plastic deformation to which the specimen had been subjected. Also significant was the fact that higher stresses, and consequently more strain, existed near the longitudinal surface normal to the notch than in the corresponding center portion of the partially deformed specimens. Not only was there a difference in the amount of strain at the surface and center of the specimen, but the shape of the strain figure also changed, see Figs. 6, 8, 11, and 13. This illustrates the already known stress distribution in Charpy-type impact specimens wherein the stresses are more biaxial at the surface and triaxial near the center.

The sequence of strain in the Charpy-type impact specimen is also indicated. A small amount of initial plastic flow extends in a symmetrical convex manner from the bottom of the specimen to the base of the notch, Fig. 2, while the strain-free central por-

tion is probably stressed within the elastic limit. With increasing load and further bending, the strain pattern becomes more complex. Finger-like strain markings branch out and downward from the notch, the strained region at the bottom of the specimen increases due to compressive stresses, Fig. 8; and a band conforming to the shape of the notch, Fig. 13, appears. Finally, with very severe deformation, the entire region from the bottom of the specimen to the notch and a broad area following the contour of the notch shows plastic flow, Fig. 16.

The hardness of the dark etching region was determined and plotted directly on the various strain figures. There was little or no hardness increase with initial plastic flow, Fig. 3, but further deformation was accompanied by correspondingly higher hardness values, Figs. 9, 14, and 19. The hardness of the light etching, elastically deformed regions in the central portion of some of the strain figures was of the same order as the unstrained base metal at either end of the sectioned specimens, Figs. 3, 7, and 14.

The dependence of impact transition energy on the yield phenomenon has been discussed previously.[5] It was pointed out that within the region of greatest triaxiality of stresses, located somewhat back of the notch, the restraint to deformation and the temperature of the steel are such as to cause cleavage within the ferrite grains when the tensile stress normal to cleavage planes reaches an appropriate value. Microscopically, it was shown that flat "brittle" cleavages exist in the 100 pct brittle specimens tested at temperatures below the transition, Fig. 20. Within the transition range the "brittle" cleavages are restricted to the central portion of the fractured surface, Fig. 21, while above the transition, Fig. 22, no "brittle" portion exists and all the fracture facets were shown by subsequent micrographic examination to be distorted by cold work. The amount of brittle cleavage that is observed on fractured surfaces agrees with the observed strain patterns, in that below the transition, plastic flow is divorced from the area in which brittle fracture takes place, while within the transition, the amount of plastic deformation has increased as the elastically stressed regions where "brittle" cleavages could occur have become restricted. Above the transition, all the area under the notch showed plastic flow, as revealed by the strain figures, while microscopically, it was shown that the fracture facets were distorted.

Summary

Strain patterns can be developed to show the regions of plastic flow and elastic stress in Charpy-type impact specimens of mild steel. An increase in hardness with increased plastic flow, as indicated by the strain etching, was shown. The strain patterns revealed more deformed metal near the surface than on a section through the central portion of the specimen, which illustrates the effect of a biaxial stress distribution at the surface and triaxial stresses at the center.

The amount of strain was correlated with the type of fracture over the transition energy range as follows:

1—A small amount of initial plastic flow extends in a convex manner from the base to the bottom of the notch, with strain free, elastically stressed metal between the symmetrical markings. This condition is representative of specimens tested at low tem-

Fig. 15—Partial deformation in a mild steel Charpy impact specimen tested at 27 F, 60 lb capacity. X2. Area reduced approximately 40 pct for reproduction.

Fig. 16—Strain pattern near surface of specimen shown in Fig. 15. X2½.

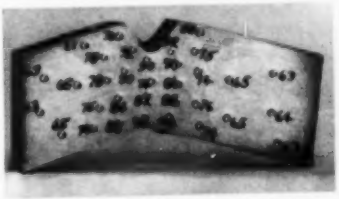

Fig. 17—Same as Fig. 16 showing R_c hardness. X2½.

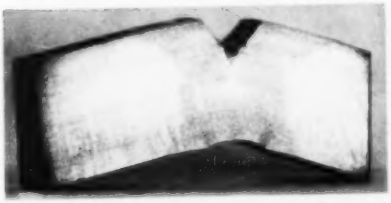

Fig. 18—Strain pattern in a section through central portion of specimen shown in Fig. 15. X2½.

Fig. 19—Same as Fig. 18 showing R_c hardness. X2½.

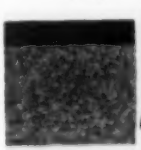

Fig. 20 — 100 pct "brittle" cleavage.

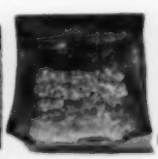

Fig. 21 — 30 pct "brittle" cleavage.

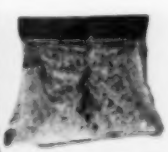

Fig. 22 — 0 pct "brittle" cleavage.

peratures, below the transition where fractures are 100 pct brittle.

2. Within the transition range, the increased deformation results in strain markings which branch out from the notch, and a larger strained area at the bottom of the specimen due to compressive stresses is obtained. The correspondingly smaller elastically stressed portion is characteristic of partially "brittle" fractures within the transition energy range.

3. Above the transition temperature, the entire region from the bottom of the specimen to the notch, and a broad area following the contour of the notch, shows plastic flow. The 100 pct "ductile" fractures are characteristic of this energy level.

Acknowledgment

The author acknowledges his indebtedness to M. Baeyertz, who conceived and initiated this study, and to Walter Craig, who supervised and encouraged the experimental work. Thanks are due to J. F. Sheehan for assistance, and to M. Hansen and the Armour Research Foundation for permission to publish these results.

References

1. A. Fry: *Stahl und Eisen* (1921) **41**, p. 1093.
2. J. D. Jevon: *Journal* Iron and Steel Inst. (1925) **111**, pp. 191-294.
3. W. J. Harris, Jr., J. A. Rinebolt, and R. Raring: *Welding Journal* (September 1951) p. 417-S.
4. *Metals Handbook* (1948) p. 391. Cleveland, A.S.M.
5. M. Gensamer: *Strength of Metals Under Combined Stresses* (1941) pp. 18-20. Cleveland, A.S.M.
6. M. Baeyertz, W. F. Craig, Jr., and E. S. Bumps: *Trans.* AIME (1949) **185**, pp. 481-490; JOURNAL OF METALS (August 1949).

Technical Note

Diffusion of Silicon in Iron

By W. Batz, H. W. Mead, and C. E. Birchenall

AT temperatures between 1095° and 1347° C, 13 runs have been made on the diffusion of silicon in iron. In two of the runs the couple compositions were entirely within the γ loop of the Fe-Si system, the face alloys containing 0.0 and 1.0 wt pct Si. The other runs in which the couples consisted of a 2.3 wt pct Si alloy welded to a 3.7 pct Si alloy were α phase throughout. The alloys were made by melting electrolytic iron and commercially pure silicon. Trace impurities were not determined.

The butt welded couples were diffused in an inert atmosphere of argon or hydrogen. After cooling, cuts of two mils or greater thickness were machined parallel to the weld interface. The chips were analyzed for silicon. When the concentration and distance data were examined on the conventional probability plot,[1] no marked variation of the diffusion coefficient with concentration was indicated over the narrow composition ranges employed. Therefore, a single diffusion coefficient is recorded for each run in Table I. The temperatures and atmospheres of the diffusion anneal are listed along with the compositions of the base alloys.

For α iron the silicon diffusion coefficient is given by the equation

$$D = 0.44\, e^{-49{,}000/RT}$$

where R is the gas constant and T, the absolute temperature. However, since the scatter in the data is fairly large, the activation energy may be in error by as much as 6000 cal per g-atom.

The two γ iron points do not permit estimation of the activation energy with any reasonable certainty. They do indicate that the coefficients reported by Smithells[2] and Jost,[3] based on the work of Fry,[4] are much too high.

Although very dilute solutions in iron of manganese,[5] nickel,[6] cobalt,[7] and molybdenum[8] give diffusion coefficients quite close to those obtained for self-diffusion in iron, the silicon values are considerably higher, though of the same order of magnitude. This seems to be consistent with the fact that the silicon atom is the only one of those listed here which is appreciably smaller than iron.

Table I. Diffusion Coefficients of Silicon in α and γ Iron

Composition Range Wt Pct	Annealing Atmosphere	Temperature, °C	Diffusion Coefficient, Sq Cm per Sec
0.0-1.0	Hydrogen	1296	4.0×10^{-8}
0.0-1.0	Hydrogen	1293	3.7×10^{-8}
2.3-3.7	Argon	1095	1.3×10^{-8}
2.3-3.7	Argon	1194	2.4×10^{-8}
2.3-3.7	Argon	1251	4.2×10^{-8}
2.3-3.7	Argon	1292	5.2×10^{-8}
2.3-3.7	Hydrogen	1249	5.0×10^{-8}
2.3-3.7	Hydrogen	1295	5.7×10^{-8}
2.3-3.7	Hydrogen	1294	7.3×10^{-8}
2.3-3.7	Hydrogen	1300	9.0×10^{-8}
2.3-3.7	Hydrogen	1309	7.1×10^{-8}
2.3-3.7	Hydrogen	1344	1.2×10^{-7}
2.3-3.7	Hydrogen	1347	1.3×10^{-7}

The authors are grateful to the Office of Naval Research for their support of this work under Contract N6ori-47, Task Order IV, Project NR 031-184, to J. K. Stanley and the Westinghouse Research Laboratories for the silicon alloys used, to several steel companies for the silicon analyses, and to C. Wells, of the Metals Research Laboratory, Carnegie Institute of Technology, for numerous suggestions during the course of the work.

References

1. C. Wells: *Atom Movements* (1951) Chapter 2. A.S.M.
2. C. J. Smithells: *Metals Reference Book* (1949) p. 405. Interscience Pub. Co.
3. W. Jost: *Diffusion* (1952) p. 223. Academic Press.
4. A. Fry: *Stahl und Eisen* (1923) **43**, p. 1039.
5. C. Wells and R. F. Mehl: *Trans.* AIME (1941) **145**, p. 315.
6. C. Wells and R. F. Mehl: *Trans.* AIME (1941) **145**, p. 329.
7. M. F. Hawkes and R. F. Mehl: *Trans.* AIME (1947) **172**, p. 467; METALS TECHNOLOGY (August 1947).
8. J. L. Ham: *Trans.* A.S.M. (1945) **35**, p. 331.

W. BATZ, formerly Research Assistant, Metals Research Laboratory, Carnegie Institute of Technology, is now with the Research Laboratories, Jones & Laughlin Steel Corp., Pittsburgh. H. W. MEAD, Junior Member AIME, is Research Associate, Metals Research Laboratory, Carnegie Institute of Technology, Pittsburgh, and C. E. BIRCHENALL, Junior Member AIME, formerly Member of Staff, Metals Research Laboratory, is now Assistant Professor of Chemistry, Princeton University, Princeton, N. J.

TN 123E. Manuscript, June 27, 1952.

Intermediate Phases in the Mo-Fe-Co, Mo-Fe-Ni, and Mo-Ni-Co Ternary Systems

by D. K. Das, S. P. Rideout, and Paul A. Beck

IN a previous publication[1] 1200°C isothermal phase diagram sections were given for the Cr-Co-Ni, Cr-Co-Fe, Cr-Co-Mo, and Cr-Ni-Mo ternary systems, in which the σ phase formed narrow, elongated solid solution fields. The present investigation is concerned with the 1200°C isothermal sections of the Co-Ni-Mo, Co-Fe-Mo, and Ni-Fe-Mo ternary systems. A prominent feature of these systems is the presence of narrow, elongated μ phase fields.

The crystal structure of the phase designated as μ both here and in the previous publication[1] was determined by Arnfelt and Westgren.[2] For the $(Co, W)_\mu$ phase, named by them Co$_7$W$_6$ (and also frequently designated as δ), these authors found that the crystal system is hexagonal-rhombohedral and the space group is $D^5_{3d} - R\bar{3}_m$. Westgren and Magneli[3] later found that isomorphous phases exist in the Fe-W and the Fe-Mo systems (these phases are often referred to as γ and κ, respectively). Henglein and Kohsok[4] stated that the phase described by them as Co$_7$Mo$_6$ (otherwise frequently designated as ϵ) is also isomorphous with the above three.

The Co-Fe-Mo system was investigated at 1300°C by Koester and Tonn,[5] who found a continuous series of solid solutions between $(Co, Mo)_\mu$ and $(Fe, Mo)_\mu$. Koester[6] also indicated similar uninterrupted solid solutions in the Ni-Fe-Mo system. However, since the Ni-Mo binary system does not have a phase isomorphous with μ, Koester's diagram is expected to be erroneous. No data appear to be available in the literature concerning the Co-Ni-Mo system.

The face-centered cubic (austenitic) solid solutions of iron, nickel, and cobalt, which are quite extensive in all three systems at 1200°C, are here designated as the α phase. The body-centered cubic (ferritic) solid solutions, based on iron, are designated in this report as the ϵ phase, in conformity with the nomenclature used previously.[1]

Experimental Procedure

The alloys were prepared by vacuum induction melting in zirconia and alumina crucibles. The lot analyses for the metals used have been given.[1] The number of alloys prepared was 46 for the Co-Ni-Mo system, 65 for the Co-Fe-Mo system, and 113 for the Ni-Fe-Mo system. The compositions of these alloys were selected with due regard to maximum usefulness in locating phase boundaries.

D. K. DAS, Associate Member AIME, is associated with the University of Notre Dame, Notre Dame, Ind.; S. P. RIDEOUT is associated with the Du Pont Co. Argonne National Laboratory, Chicago; and P. A. BECK, Member AIME, is Research Professor of Physical Metallurgy, University of Illinois, Urbana, Ill.

Discussion on this paper, TP 3372E, may be sent, 2 copies, to AIME by Dec. 1, 1952. Manuscript, March 17, 1952. Philadelphia Meeting, October 1952.

This paper represents part of a thesis by D. K. Das submitted in partial fulfillment of requirements for the degree of Doctor of Philosophy to the University of Notre Dame.

The alloy specimens were annealed at 1200°C in an atmosphere of purified 92 pct helium and 8 pct hydrogen mixture. Alloys consisting almost entirely of the face-centered cubic austenitic α phase, or of the body-centered cubic ferritic ϵ phase were double-forged with intermediate annealing. The double-forged specimens were then final annealed for 90 hr at 1200°C and quenched in cold water. Alloys containing considerable amounts of any of the other phases could not be forged. Such specimens were annealed for 150 hr at 1200°C and quenched. Microscopic specimens of all alloys were prepared by mechanical polishing, in many cases followed by electrolytic polishing. Description of the polishing and etching procedures used and tabulation of the intended compositions of the alloys prepared are being published in two N.A.C.A. Technical Notes.[7,8] Many of the alloys were analyzed chemically and, in general, the results are in excellent agreement with the intended compositions. X-ray diffraction samples were prepared by filing or crushing homogenized alloy specimens and by reannealing the obtained powders in evacuated and sealed quartz tubes. After annealing for 30 min at 1200°C the tubes were quenched into cold water. X-ray diffraction patterns were made with unfiltered chromium radiation at 30 kv, using an asymmetrical focusing camera of high dispersion. X-ray diffraction and microscopic methods were used jointly to identify the phases present in each specimen. The amounts of the phases in each alloy were estimated microscopically. The phase boundaries were located by the disappearing phase method. The results were used to construct 1200°C isothermal sections for the three ternary phase diagrams. The accuracy of the location of the phase boundaries determined in this manner is estimated to approximately ±1 pct of each component.

The portion of the three phase diagrams lying between the μ, P, and δ phases on the one hand, and the molybdenum corner on the other, has not been investigated. Recently Metcalfe reported[9] a high temperature allotropic form of cobalt on the basis of dilatometric results and of cooling curves. In the present work no attempt was made to search for the new phase in the cobalt corner of the Co-Fe-Mo and Co-Ni-Mo systems. No alloy was prepared with more than 80 pct Co; the alloys used were intended to locate the boundary of the α phase saturated with μ. The microstructures of the quenched α alloys near the cobalt corner gave no suggestion of an insuppressible transformation on quenching.

The location of the boundaries of the $\alpha + \epsilon$ two-phase fields in the Fe-Ni-Mo and Fe-Co-Mo systems was determined entirely by the microscopic method. The face-centered cubic α alloys near the ϵ field transform partially or wholly into the body-centered cubic ϵ phase on quenching from 1200°C to room temperature. The ϵ formed in this manner has an

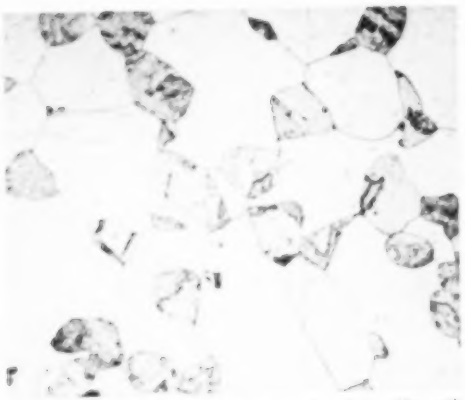

Fig. 1—Transformed α grains in a matrix of ϵ phase. Alloy with 17.2 wt pct Co, 12.8 wt pct Mo, and 70 wt pct Fe, annealed 48 hr at 1200 C, water quenched. Etched with CuCl$_2$ in HCl-ethyl alcohol solution. X100.

acicular martensitic structure and it can be thus readily distinguished macroscopically from ϵ grains that exist at 1200 C and remain unchanged on quenching (Fig. 1). The α phase can be recognized microscopically by its typically irregular, ragged grain boundaries, as shown in Fig. 2. Positive identification is easily done by X-ray diffraction; the diffraction lines have been published.[7]

Results

The experimental results are shown in Figs. 3 to 5. It is seen that the α phase forms narrow, elongated fields in all three diagrams. In the Co-Fe-Mo system, the α phase field completely traverses the ternary system from $(Co, Mo)_\beta$ to $(Fe, Mo)_\alpha$, Fig. 3. In the Ni-Fe-Mo system, Fig. 4, and in the Ni-Co-Mo system, Fig. 5, the α phase field extends approximately half-way across the ternary diagram. The boundaries of the binary $(Fe, Mo)_\alpha$ and $(Co, Mo)_\beta$ phases, as determined in the present work, are somewhat different from those given by other authors.[8]

It is interesting to note that in the Co-Ni-Mo system, Fig. 5, the α phase directly coexists with δ, while in the Fe-Ni-Mo system, Fig. 4, the P phase is interposed between them, so that α and δ do not coexist. The P phase, of unknown crystal structure, is isomorphous with the Cr-Ni-Mo ternary phase of the same name, described previously,[9] which was found there interposed between the α and δ phases. The X-ray diffraction lines for the P phase have been given.[9] Even though in both ternary systems the composition range of the P phase field is relatively small, it is quite possible that in the quaternary Fe-Ni-Cr-Mo system, which was not investigated, an elongated P phase field extends from (Ni, Cr, Mo)P to (Fe, Ni, Mo)P.

Discussion

In the previous publication[1] an empirical correlation was described between the composition of the α phase in various binary and ternary alloy systems of the transition elements and the electron vacancy concentration, N. For alloys, N was calculated on the assumption of simple additivity from the electron vacancy numbers for the 3d subbands of the components. The N values used for transition elements of the first long period from chromium to nickel were those given by Pauling.[10]

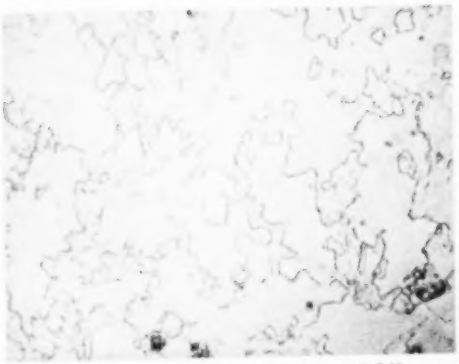

Fig. 2—Typical microstructure of α phase. Alloy with 9.89 wt pct Ni, 34.69 wt pct Fe, and 55.42 wt pct Mo, annealed 96 hr at 1200 C, water quenched. Etched electrolytically in a phosphoric acid solution and stained in an alkaline potassium permanganate solution. X500.

For the 4d subband of molybdenum, N_v was assumed to be the same as that for the 3d subband of chromium, namely 4.66; however, in certain ternary alloy systems an empirical value of $N_v = 5.6$ for molybdenum was found to fit the data better. Accordingly, N_v was calculated for binary and ternary alloys from:

$$N_v = 4.66\,(Cr + Mo) + 2.66\,(Fe) + 1.71\,(Co) + 0.61\,(Ni) \quad [1]$$

or from:

$$N_v = 5.6\,(Mo) + 4.66\,(Cr) + 2.66\,(Fe) + 1.71\,(Co) + 0.61\,(Ni) \quad [2]$$

where the bracketed chemical symbols stand for the atomic fractions of the corresponding metals in the alloy and the numerical coefficients are the N_v values for the elements. It was found that, while the composition in terms of the atomic percentages of the various α phases varies considerably (as shown for example by the following approximate formulas for a series of binary α phases: CrMn, CrFe, and CrCo), the electron vacancy number remains within a relatively narrow range, approximately 3.36 to 3.60. The elongated α fields in the Co-Cr-Mo and the Ni-Cr-Mo ternary systems also gave fairly good alignment with the lines of constant electron vacancy, provided that the latter were determined according to eq. 2.

In the present investigation the elongated α phase fields appearing in the three ternary systems studied are also found to be well aligned with the lines of constant electron vacancy (Figs. 6, 7, and 8). As stated above, in general, the electron vacancy numbers accepted for the transition elements in the previous publication[1] were those given by Pauling.[10] It was, however, noted (p. 875 of ref. 1) that for α alloys with manganese the correlation can be improved if the vacancy number used for this metal is smaller than Pauling's value of 3.66. A vacancy number of 3.2 for manganese appears to fit best the binary α phases with manganese so far investigated. Similarly, the present work shows that in the Fe-Co-Mo system much better correlation is achieved for the composition range of the ternary μ phase field, Fig. 3, by using a vacancy number of approximately 2.2 for iron, instead of the value 2.66. As seen in Fig. 6, with this value for iron and with the electron vacancy number of 4.66 for molybdenum, both the

Fig. 3—1200 C isothermal section of the Fe-Co-Mo phase diagram

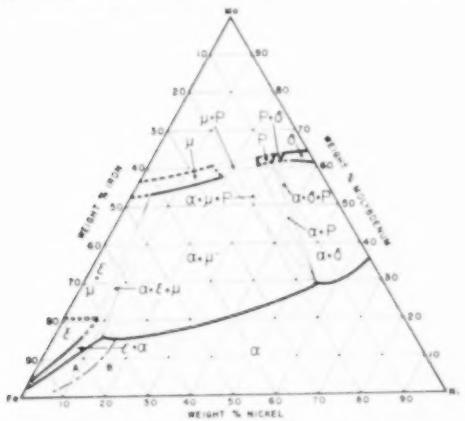

Fig. 4—1200 C isothermal section of the Fe-Ni-Mo phase diagram

μ phase field across the Fe-Co-Mo ternary diagram and the dash-dot line connecting the two binary σ phases (and presumably corresponding to ternary σ solid solutions) are quite well aligned with the constant electron vacancy lines.

In the Fe-Ni-Mo and the Co-Ni-Mo systems good alignment of the μ phase field can be achieved by using the electron vacancy number of 4.66 for molybdenum and 1.6 for nickel, Figs. 7 and 8. The latter value may appear unreasonable, since ferromagnetic saturation measurements for nickel give a value for the magnetic moment of 0.61 Bohr magnetons per atom. However, the assumption of an effective N_v value of 1.6 for nickel in these alloys not only gives satisfactory results in the two ternary diagrams (Figs. 7 and 8), but also improves the alignment of the σ phase in the Co-Ni-Cr system,[7] as seen in Fig. 9 in comparison with Fig. 6 of ref. 1. Furthermore, it was noted previously that the electron vacancy number corresponding to the composition range of the (Ni, V)σ phase given by Pearson, Christian, and Hume-Rothery[8] is unusually low, if calculated on the basis of eqs. 1 or 2. With the N_v value of 1.6 here proposed for nickel, the electron vacancy concentration for this σ phase is 3.29 to 3.59 in good agreement with the usual range. These facts all suggest that the electron vacancy value of 1.6 for nickel is empirically justified in these alloy systems.

The assumption of simple additivity of electron vacancy numbers for both the σ and the μ phases has proved to be adequate to a rather surprising degree. The electron vacancy numbers discussed above for the various transition elements reproduce

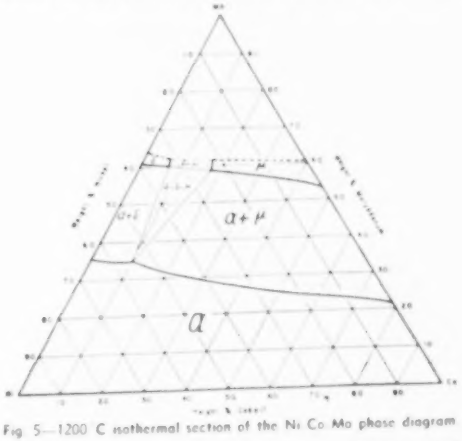

Fig. 5—1200 C isothermal section of the Ni-Co-Mo phase diagram

fairly well the compositions of many binary and ternary σ and μ phases. Thus:

$$N_v = 4.66\,(\mathrm{Mo} + \mathrm{Cr} + \mathrm{V}) + 3.2\,(\mathrm{Mn}) + 2.2\,(\mathrm{Fe}) + 1.71\,(\mathrm{Co}) + 1.6\,\mathrm{Ni} \quad [3]$$

in most cases leads to fairly sharply defined N_v ranges for these phases, as shown in Table I. However, there are now data available which suggest that the N_v numbers obtained for alloys on the basis of simple additivity from fixed electron vacancy values for the components may not always satisfactorily determine intermediate phase compositions. Apparently, the σ phases in the three ternary systems containing both chromium and molybdenum (Fe-Cr-Mo, Co-Cr-Mo, and Ni-Cr-Mo), which have been so far investigated, represent anomalies. In the Co-Cr-Mo system the narrow, elongated σ solid solution field found at 1200°C,[7] which is based on (Co, Cr)σ, leads to a composition of approximately 44 to 48 atomic pct Mo, when extrapolated to the Co-Mo binary, while the binary (Co, Mo)σ phase recently discovered by Goldschmidt[9] is actually located at about 60 atomic pct Mo. As shown previously,[7] the position of the elongated ternary σ field requires a N_v number for molybdenum of about 5.6, whereas Goldschmidt's binary (Co, Mo)σ composition is in accord with a N_v number for

Table I. Electron Vacancy Concentration Ranges for Various σ and μ Phases, as Calculated from Eq. 3

Phases	Alloy System	Temperature, °C	N_v
σ	Co-Cr	1200	3.45–3.57
σ	Co-Cr-Ni	1200	3.45–3.57
σ	Fe-Cr	800	3.33–3.35
σ	Mn-Cr		3.44–3.61
σ	Co-Mo	1200	3.5
σ	Fe-Mo		3.44
σ	Co-V		3.2
σ	Fe-V		3.57
σ	Ni-V		3.29–3.59
σ	Mn-V		3.55
σ	Fe-Mo-Ni	1200	3.15–3.25
σ	Fe-Mo-Co	1200	2.95–3.25
σ	Ni-Mo-Co	1200	2.94–3.19
μ			

Fig. 6—1200 C isothermal section of the Fe-Co-Mo phase diagram plotted in atomic percentages. Lines of constant electron vacancy concentrations of 2.9 to 3.6 are indicated. Dash-dot line connects two binary σ compositions and indicates compositions along which ternary σ solid solutions presumably exist at 1300 C and above.

Fig. 7—1200 C isothermal section of the Fe-Ni-Mo phase diagram plotted in atomic percentages. Lines of constant electron vacancy concentrations of 3.0 to 3.4 are indicated.

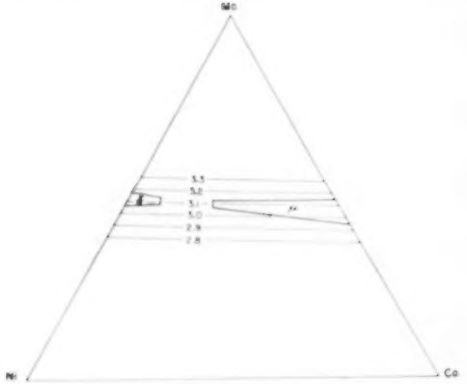

Fig. 8—1200 C isothermal section of the Ni-Co-Mo phase diagram plotted in atomic percentages. Lines of constant electron vacancy concentrations of 2.8 to 3.3 are indicated.

molybdenum of 4.66. So also is the newly discovered binary (Fe, Mo)$_7$C phase.[7] It appears then that the effective N_v number for molybdenum is the same as that for chromium (as might be expected from their relative positions in the periodic table), except when molybdenum occurs together with chromium in the same alloy. Apparently, if the amount of chromium is approximately equal to or larger than that of molybdenum, the latter contributes a larger number of vacancies, namely about 5.6. It seems likely that a similar interpretation might help in explaining the unusual width of the ternary σ field in the Fe-Cr-Mo system.[5,6] The wide range of molybdenum content for the σ phase would then be the result of the variability in the electron vacancy contribution of molybdenum as a function of composition. Whether or not this explanation will be adequate to account for the surprising position of the μ phase field in the Fe-Cr-W system, reported recently by Goldschmidt,[7] cannot be decided at this time. (In Goldschmidt's work this phase is designated as δ).

The analogy in the behavior of the σ phase and of the μ phase is so complete, that it suggests the possibility of finding still other intermediate phases exhibiting this behavior. One of the phases that might be investigated from this point of view is (Fe, W)$_3$ which, according to available information, appears to be isomorphous with (Co, W)$_7$ and with (Ni, Mo)$_7$, all three being close-packed hexagonal, with c_0 in the order of 7.7 kX. The electron vacancy numbers for these phases, calculated from eq. 3 and by assuming $N_v = 4.66$ for tungsten, are as follows: 2.36 for (Mo, Ni)$_7$, 2.34 for (W, Co)$_7$, and 3.0 for (W, Fe)$_3$. It might be expected that these phases form with each other elongated continuous solid solution fields across the corresponding ternary systems. The type of phase, like σ and μ, whose boundaries are largely determined by electron vacancy values, might be termed "electron vacancy phase," in analogy with the term "electron compound."

An advantage of using ternary phase diagrams rather than binaries for investigations of this kind is the possibility of determining the effective electron vacancy contribution of elements which do not form the phase in question in the corresponding binary alloys. A case in point is the Cr-Co-Ni system, Fig. 9 (also refs. 1 and 17), from which the electron vacancy contribution of nickel to (Cr, Co)σ could be roughly determined even though nickel is not known to form the σ phase in the Cr-Ni or Co-Ni systems. This scheme might be useful in studying the effect of elements other than those of the transition group. For instance, in the Cr-Co-Cu and Cr-Mn-Cu systems it would be expected that the elongated ternary σ field, if it occurs, would point toward a composition of 20 atomic pct Cu + 80 atomic pct Cr ("hypothetical (Cr, Cu)σ"), even though no σ phase is known to exist in the Cr-Cu binary system. This composition was calculated on the assumption that one valency electron per copper atom is being contributed toward filling the 3*d* vacancies of chromium, i.e., that $N_v = -1$ for copper. Similar calculation for zinc, with $N_v = -2$, gives 17.4 atomic pct Zn + 82.6 atomic pct Cr as the "ideal composition" of a hypothetical (Cr, Zn)σ.

Although the real physical meaning of the empirical correlation of the σ and μ phase boundaries with electron vacancy concentration has not as yet been clarified, the correlation itself has been quite definitely established. The same correlation was also found independently by Sully[18] at about the

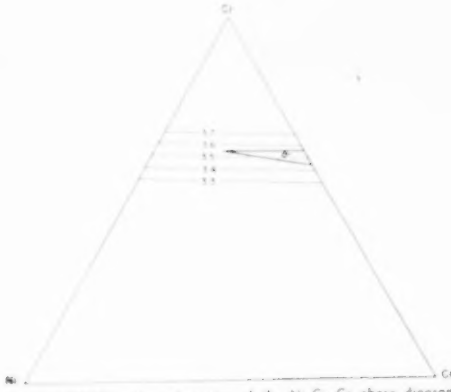

Fig. 9—1200 C isothermal section of the Ni-Co-Cr phase diagram plotted in atomic percentages. Lines of constant electron vacancy concentrations of 3.3 to 3.7 are indicated.

same time, for binary σ phases. In search of a deeper meaning behind the empirical correlation, Sully sought to establish an analogy with Hume-Rothery's rules for electron compounds. On the basis of the empirical correlation, and by assuming that the vacancies in the atomic orbitals are filled with electrons from the bonding orbitals, Sully found that for various binary σ phases the number of the remaining bonding electrons (that of the bonding electrons in excess of the number of vacancies) is about 2.25 per atom. On the further assumption that the 4s electrons take no part in bonding and do not contribute to the Brillouin zone, the number of excess bonding electrons per atom for σ phases was calculated by Sully to 1.7. This number is in good agreement with the number of electrons accommodated by the first Brillouin zone of the σ phase, as calculated independently by Douglas,[21] Heal and Silcock,[22] and Shoemaker,[23] in Sully's view the excess bonding electrons completely fill the first Brillouin zone. Although several of the assumptions on which the above interpretation is based are rather doubtful theoretically, and a completely filled Brillouin zone is unlikely in view of the strong paramagnetism and ferromagnetism of σ alloys,[6] definite experimental proof or disproof of Sully's views is difficult to obtain. As far as the description of composition limits of intermediate phases is concerned, the empirical correlation referred to can be equally well stated either in terms of the number of vacancies, or of the number of excess bonding electrons, the two being fully equivalent. The former method of expression, which is frankly empirical, has the advantage of not requiring the far-reaching assumptions underlying the latter.

Conclusions

1—In the Co-Fe-Mo, Co-Ni-Mo, and Ni-Fe-Mo ternary systems at 1200 C the μ phase forms narrow, elongated ternary solid solution fields. In the first named system the μ field extends all the way across the ternary diagram, in the other two systems approximately half-way across.

2—If the electron vacancy numbers assigned to molybdenum, iron, cobalt, and nickel are 4.66, 2.2, 1.71, and 1.6, respectively, the elongated μ phase fields in the above ternary systems correspond quite well to a constant electron vacancy range of about 2.95 to 3.25.

3—The alloying behavior of the μ phase is entirely analogous to that previously found for the σ phase. It is quite likely that there are still other "electron vacancy phases" of this type among the intermediate phases in alloys of the transition elements. The study of ternary phase diagrams is highly effective in disclosing such properties.

Acknowledgment

This work was carried out at the University of Notre Dame under the sponsorship and with the financial assistance of the National Advisory Committee for Aeronautics.

References

[1] S. Rideout, W. D. Manly, E. L. Kamen, B. S. Lement, and Paul A. Beck: Intermediate Phases in Ternary Alloy Systems of Transition Elements. *Trans.* AIME (1951) **191**, p. 872; JOURNAL OF METALS (October 1951).

[2] W. Arnfelt and A. Westgren: *Jernkontorets Ann.* (1933) **119**, p. 185.

[3] A. Magneli and A. Westgren: Roentgenuntersuchung von Kobalt-Wolframlegierungen. *Ztsch. anorg. allgem. Chem.* (1938) **238**, pp. 268-272.

[4] E. Henglein and H. Kohsok: La determination de la phase Co-Mo. *Revue de Metallurgie* (1949) **46**, p. 366.

[5] W. Koester and W. Tonn: Das System Eisen-Kobalt-Molybdaen. *Arch. Eisenhuettenwesen* (1932) **5**, pp. 627-630.

[6] W. Koester: Das System Eisen-Nickel-Molybdaen. *Arch. Eisenhuettenwesen* (1934) **8**, pp. 169-171.

[7] S. P. Rideout and P. A. Beck: Survey of Portions of the Cr-Co-Ni-Mo Quaternary System at 1200 C. *NACA Technical Note No. 2683.*

[8] D. K. Das and P. A. Beck: Survey of Portions of the Fe-Ni-Mo and of the Co-Fe-Mo Ternary Systems at 1200 C. Prospective NACA Technical Note.

[9] A. G. Metcalfe: The Allotropy of Cobalt. *Proc.* World Metallurgical Congress, Cleveland (1952).

[10] L. Pauling: The Nature of the Interatomic Forces in Metals. *Physical Review* (1938) **54**, p. 899. See also a recent summary report by G. V. Raynor in: *Progress in Metal Physics* I. Edited by Bruce Chalmers (1949) p. 48. London.

[11] W. B. Pearson, J. W. Christian, and W. Hume-Rothery: New Sigma Phases in Binary Alloys of the Transition Elements of the First Long Period. *Nature* (1951) **167**, p. 110.

[12] H. J. Goldschmidt: A Further High Temperature Sigma Phase and a Note on Sigma-Xi Relations. *Research* (1951) **4**.

[13] H. J. Goldschmidt: A Molybdenum Sigma Phase. *Research* (1949) **2**, p. 343.

[14] H. J. Goldschmidt: Phase Diagrams of the Ternary Systems Fe-Cr-W and Fe-Cr-Mo at Low Temperatures. Symposium on High-Temperature Steels and Alloys for Gas Turbines. London (1951).

[15] J. W. Putman, R. D. Potter, and N. J. Grant: The Ternary System Chromium-Molybdenum-Iron. *Trans.* A.S.M. (1951) **43**, pp. 824-847.

[16] Spencer R. Baen and Pol Duwez: Constitution of Iron-Chromium-Molybdenum Alloys at 1200 F. *Trans.* AIME (1951) **191**, pp. 331-335; JOURNAL OF METALS (April 1951).

[17] Paul A. Beck and W. D. Manly: The Sigma Phase in Ternary Cr-Co-Fe and Cr-Co-Ni Alloys. *Trans.* AIME (1949) **185**, p. 354; JOURNAL OF METALS (June 1949).

[18] A. H. Sully: Sigma Phase in Transitional Metal Alloys. *Nature* (1951) **167**, p. 365.

[19] A. H. Sully: The Sigma Phase in Binary Alloys of the Transition Elements. *Journal* Inst. Metals (1951) **80**, pp. 173-179.

[20] A. M. B. Douglas: British *Journal of Applied Physics* (1951) **2**, p. 305.

[21] T. J. Heal and J. M. Silcock: Personal communication from A. H. Sully.

[22] D. P. Shoemaker: Personal communication.

[23] Paul A. Beck: Magnetic Behavior of Intermediate Phases in Alloys of Transition Elements. JOURNAL OF METALS (April 1952), *Trans.* AIME, p. 420.

Kinking in Zinc Single-Crystal Tension Specimens

By Jack Washburn and Earl R. Parker

Kinking in zinc single-crystal tension specimens was observed under conditions of low stress and high temperature. Kinking is discussed in relation to other plastic bending phenomena on the basis of dislocation theory. Experiments on the stress-induced motion of small angle boundaries are reported.

KINKING was first reported by Orowan as a new deformation mechanism. He observed the phenomenon in cadmium single crystals loaded in compression. Glide lamellae in a local region of the rod were observed to snap over suddenly to a tilted position, resulting in a sudden shortening of the specimen. Between the tilted portion and the rest of the crystal there were fairly sharp boundaries, with the slip plane assuming approximately mirror image positions on opposite sides of these boundaries. Orowan considered the boundaries to be regions where dislocations had concentrated. Hess and Barrett[2] observed the formation of kinks in critically oriented zinc compression specimens. It was found that the sudden snapping over of the tilted region was not an essential part of the kinking phenomenon but rather was associated with the method of loading. Kinking was explained on the basis of the accepted mechanisms of slip and flexural glide. It was also suggested that a kink can be considered as a special type of deformation band.

During a recent investigation of the effect of surface condition on creep of zinc single crystals,[3] a similar phenomenon was observed in crystals which were loaded in tension. The specimens were 0.4 in. diam cylindrical rods with a free length of 4 in. between end connections. All of the crystals were tested at a constant load, adjusted to give an extension rate of approximately 0.05 pct per hr. Kinking, as shown in Fig. 1, occurred in some of the tests performed at temperatures above 200 C. Kinking was observed in specimens varying widely in initial orientation, scattering about a 45° angle between the slip plane and the specimen axis. The condition leading to kinking in tension appeared to be nonuniform distribution of flow along the gage length combined with the restraint imposed by the tensile load. At low temperatures and fast strain rates, the distribution of strain throughout the midsection of tension specimens was generally quite uniform; therefore, bend planes developed only near the ends as described by Miller.[4] However, at high temperatures under creep conditions it was difficult to obtain specimens in which the distribution of flow was uniform. Some of the factors which may have caused differences in flow stress along the length of the crystals are: Nonuniform distribution of impurities, accidents of growth (lineage structure), slight bending or other damage during handling, surface conditions, and strain-aging characteristics due to dissolved nitrogen.[5] Plastic flow, once started in a local region, often continued to a relatively large strain before other parts of the gage length became active. Under these conditions a series of kinks, such as those in Fig. 1, were produced.

Fig. 2 illustrates how a nonuniform distribution of slip produces bending moments which are responsible for kink formation. If no plastic bending were to occur while the rod extended by pure slip in two separate sections of the rod, it would assume a shape such as that in Fig. 2a. A specimen having this shape and being subjected to a tension load would have concentrations of stress at the concave surfaces C and lower than average stress would exist at the convex surfaces D. Therefore a bending moment is superimposed on the average stress in the regions between C and D. The positions of potential bend planes under these conditions are shown as dotted lines. Actually no such shape as Fig. 2a develops because plastic bending in the region C-D occurs simultaneously with pure slip in the intervening regions. The observed structure of a tension kink is indicated by Fig. 2b.

Perhaps the best approach to an understanding of kinking as well as other related plastic bending phenomena, such as the bend planes discussed by Miller,[4] cell formation studied by Wood et al.,[6] and polygonization,[7] is consideration of the dislocation model of a bent lattice.

Current theories of the slip process postulate generation or multiplication of dislocations at certain lattice imperfections. The mechanism proposed by Frank and Read[8] results in continuous generation of concentric dislocation loops which spread out

J. WASHBURN is Research Metallurgist and E. R. PARKER, Member AIME, is Professor of Metallurgy, University of California, Berkeley, Calif.

Discussion on this paper, TP 3362E, may be sent, 2 copies, to AIME by Dec. 1, 1952. Manuscript, March 4, 1952. Philadelphia Meeting, October 1952.

Fig. 1 (left)—Zinc single crystal creep specimen showing kinks produced by tension loading. Original orientation: angle between tension axis and normal to slip plane, 62°; angle between tension axis and active slip direction, 28°.

Fig. 2 (right)—Formation of kinks in tension specimens due to nonuniform distribution of strain. a—Nonuniform slip without bending. Stress is concentrated at C and decreased at D. b—Observed structure of kinked specimen showing formation of bend planes.

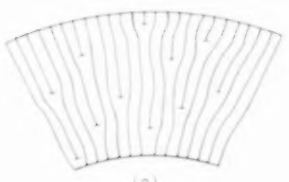

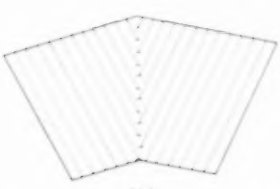

Fig. 3—Distribution of dislocations in a region of bent crystal. a—Random distribution. b—Collected into a sharp boundary.

from the source. In a crystal subjected to bending, a shear stress gradient may exist along the slip direction. Dislocation loops originating at active Frank-Read sources are distorted by such a gradient. The part of the loop having a component of motion in the direction of increasing stress has a high probability of expanding and ultimately reaching the surface of the crystal. However, the remainder of the loop moving in the negative direction of the shear stress gradient may reach a position where the shear stress is insufficient to move the dislocation further and hence becomes stopped. A large excess of inactive edge dislocations of one sign satisfies the geometrical conditions for a bent crystal lattice. The distribution of dislocations in a bent crystal probably depends on the temperature and the stress conditions during bending. Two extreme cases are illustrated by Fig. 3a and b. Single zinc crystals formed into smooth curves at low temperatures produce elongated but apparently continuous Laue spots. This indicates that a somewhat random distribution of dislocations may be produced. Polygonization, which occurs when such bent crystals are heated, demonstrates that this dispersed array of dislocations is an unstable configuration. Upon annealing, dislocations tend to collect into planar arrays forming small angle boundaries between large volumes of relatively perfect crystal. In zinc, apparently sharp boundaries can be formed directly by bending at high temperatures, or at low temperatures under conditions where a very sharp shear stress gradient exists. For example, at −196° C when a thin wafer is cleaved from a large zinc crystal by introducing

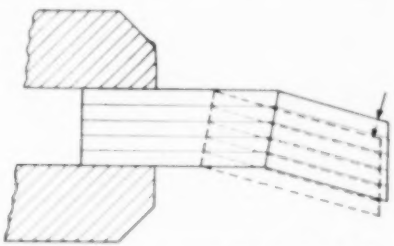

Fig. 4—Sketch showing motion of a boundary by application of a stress.

a wedge at one surface, a sharp boundary is formed which follows the base of the advancing cleavage crack.

There is at present no way of knowing the degree of perfection of the dislocation array in an apparently sharp boundary. A 2° boundary, for example, could be composed of one dislocation every 30 atomic distances, as shown in the bubble model of Lomer and Nye,[7] or it could be composed of 100 dislocations about every 3000 interatomic distances. The theory that small angle boundaries in metals do consist of arrays of like dislocations is supported by the fact that these boundaries can, under certain conditions, be made to move by the application of a shear stress. This behavior has been predicted by Burgers,[8] Bragg,[9] and Shockley[10] and has recently been demonstrated for similar boundaries in bubble rafts by Lomer and Nye.[7] The conditions for motion are illustrated in Fig. 4. The specimen consisted of a plate-shaped crystal $\frac{1}{8}$ in. thick containing a 2° boundary of the type discussed. The horizontal lines in the figure represent the slip direction for the dis-

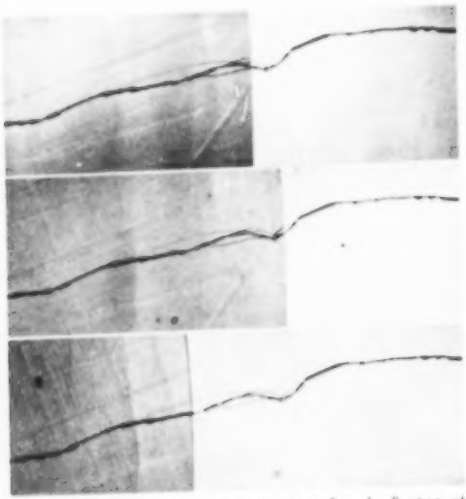

Fig. 5—Top surface of specimen shown in Fig. 4. Position of boundary is apparent on (0001) cleavage surface under vertical illumination due to 2° angular change in the surface at the boundary. Irregular horizontal line is a small step in the cleavage surface which serves as a reference mark. Top, original position of boundary center, moved 0.1 mm to the right; bottom, moved back 0.4 mm. X50. Area reduced approximately 40 pct for reproduction.

locations of which the boundary is composed and also the traces of the slip plane (0001), which is at right angles to the plane of the paper. When one side of the wafer was clamped as shown in the figure and a force was applied at a point on the opposite side of the boundary, motion occurred as indicated by the dotted lines. Motion of the boundary apparently took place by a cooperative motion of the dislocations in the array, each moving an equivalent distance on its own slip plane. Opposite top and bottom intersections of the boundary with the surface were observed to move approximately the same amount. Fig. 5 shows the top surface of the specimen just described, which is on (0001) plane. The picture was taken using vertical illumination; the change in brightness indicates the angular change of the surface at the boundary. The irregular horizontal line is a small step in the cleavage surface which serves as a reference mark for the position of the boundary. The boundary was first moved to the right approximately 0.1 mm and then, by reversing the direction of the stress, moved back about 0.4 mm. Only a small segment of the boundary, which extended as a somewhat irregular line across the entire 14 mm width of the specimen, is shown.

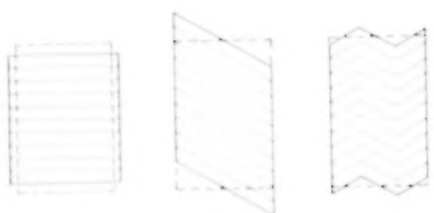

Fig. 6—Lattice bending as related to a general change in shape during deformation. a—Original shape of grain with required change in shape shown by dashed lines. b—Approach to deformed shape by slip alone on indicated slip plane. c—Closer approach to required shape by slip and bending.

The conditions under which sharp kink boundaries form during creep of single-crystal tension specimens appear to be similar to the conditions causing individual grains of a polycrystalline specimen to break up into cells. The high temperature and low applied stress result in a process which can be considered as simultaneous bending and polygonization, an excess of dislocations of one sign becoming trapped because of shear stress gradients. Thermal energy aided by the applied stress brings about collection of the dislocations into sharp boundaries. In the case of single crystals, the shear stress gradients may be produced by the restraint imposed by tension loading. In the case of an individual grain in a polycrystalline sample, a similar restraint may be imposed by neighboring grains. Fig. 6 illustrates in two dimensions how bend plane formation can aid in the conformity along grain boundaries of a polycrystalline specimen. Experiments with bicrystals of zinc have shown that plastic bending can and does occur near the boundary when such specimens are deformed. Thus it becomes evident that continuity at crystal boundaries during deformation is aided by the occurrence of lattice bending. Under these conditions a general change in shape is possible with less than the five slip systems discussed by Taylor.[7]

Acknowledgment

The support of this work by the Office of Naval Research and in particular the sustained interest of Julius Harwood, of the ONR, are gratefully acknowledged.

References

1 E. Orowan: A Type of Plastic Deformation New in Metals. *Nature* (1942) **149**, p. 643.

2 J. B. Hess and C. S. Barrett: Structure and Nature of Kink Bands in Zinc. *Trans.* AIME (1949) **185**, p. 599; JOURNAL OF METALS (September 1949).

3 M. R. Pickus and E. R. Parker: Creep Behavior of Zinc as Modified by Copper in the Surface Layer. *Trans.* AIME (1951) **191**, p. 792; JOURNAL OF METALS (September 1951).

4 R. F. Miller: Influence of a Grain Boundary on the Deformation of a Single Crystal of Zinc. *Trans.* AIME (1934) **111**, p. 135.

5 H. L. Wain and A. H. Cottrell: Yield Points in Zinc Crystals. *Proc.* Physical Soc. (1950) **63**, p. 339.

6 G. R. Wilms and W. A. Wood: Mechanism of Creep in Metals. *Journal* Inst. Metals (1949) **75**, p. 693.

7 R. W. Cahn: Recrystallization of Single Crystals After Plastic Bending. *Journal* Inst. Metals (1949) **76**, p. 121.

8 F. C. Frank and W. T. Read, Jr.: Multiplication Processes for Slow Moving Dislocations. *Physical Review* (1950) **79**, Series 2, No. 4, p. 722.

9 W. M. Lomer and J. F. Nye: A Dynamical Model of a Crystal Structure, IV, Grain Boundaries. *Proc.* Royal Soc. (1952) **212A**, p. 576.

10 J. M. Burgers: Geometrical Considerations Concerning the Structural Irregularities to be Assumed in a Crystal. *Proc.* Physical Soc. (1940) **52**, p. 23.

11 W. L. Bragg: Discussion of a Series of Papers on "Slip in Single Crystals." *Proc.* Physical Soc. (1940) **52**, p. 54.

12 W. Shockley: Dislocation Theory. *Cold Working of Metals* (1948) p. 131, Cleveland, A.S.M.

13 G. I. Taylor: Plastic Strain in Metals. *Journal* Inst. Metals (1938) **62**, p. 307.

Copper-Zinc Constitution Diagram, Redetermined In The Vicinity of the Beta Phase by Means Of Quantitative Metallography

by L. Hall Beck and Cyril Stanley Smith

KNOWLEDGE of the Cu-Zn constitution diagram was critically examined in 1944 by G. V. Raynor, who suggested the diagram reproduced in Fig. 1 as the best evaluation of available data. No pertinent work on the constitution has been published since that time, although a number of authors have discussed transformation kinetics and theory. Despite the large amount of work that has been done on the constitution of these industrially important and scientifically interesting alloys, minor uncertainties still exist. For example, it is still not possible to say definitely whether a two-phase region exists between the ordered and disordered forms of the β phase. A careful re-examination of the phase boundaries in this part of the diagram was therefore undertaken.

Two methods were selected for the new investigation—quantitative metallography for the higher temperatures and precision lattice parameter measurement for lower temperatures. Because of the relatively narrow two-phase regions flanking the β phase in these alloys, quantitative metallography is particularly suited for their examination, since the relative amounts of the two phases are very sensitive to their compositions. The method, however, is useless below about 350 C because of the inadequate resolution of the two constituents. Below 400 C, however, the X-ray diffraction method is applicable, although it is of somewhat lower sensitivity in this system. The changes of composition that occur during quenching from above about 500 C entirely vitiate X-ray measurements at room temperature though they do not affect metallographic area measurements. The two methods overlap and supplement each other admirably. Both methods depend on the attainment of equilibrium composition of the two phases in a more or less intimate mixture and thus avoid the difficult problems of nucleation and long range diffusion involved in the conventional metallographic bracketing method.

The alloys were melted from a master alloy made from re-electrolyzed cathode copper and Horsehead 99.99 pct Zn. Melting was done under a cover of either borax or charcoal and the alloys cast into a $\frac{7}{8}$ in. sq graphite mold for the α-β alloys or a $\frac{3}{8}$ in.

L. H. BECK, formerly with the Institute for the Study of Metals, is now at Champaign, Ill., and C. S. SMITH, Member AIME, is Director, Institute for the Study of Metals, University of Chicago, Chicago.

Discussion on this paper, TP 3380E, may be sent, 2 copies, to AIME by Dec. 1, 1952. Manuscript, April 15, 1952. Philadelphia Meeting, October 1952.

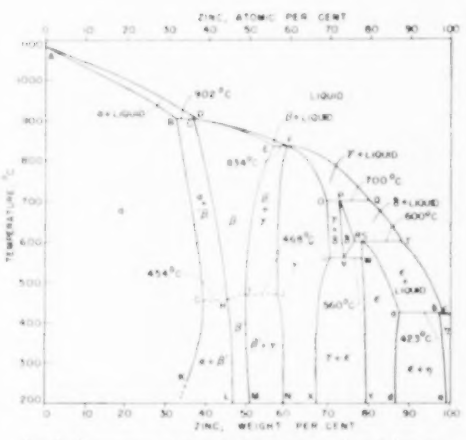

Fig. 1—Constitution of the Cu-Zn alloys according to Raynor.

diam cylindrical graphite mold for the β-γ alloys. The α-β alloys were rolled at 750 C to $\frac{3}{8}$ in. sq, annealed for 24 hr at 800 C and quenched; then rolled and swaged at 200 C to $\frac{3}{8}$ in. diam rods, annealed 24 hr at 200 C, quenched and cold rolled 2 pct reduction. This treatment was intended to obtain a small grain size and to produce many nuclei of the minor phase for growth on subsequent heat treatment.

The unworkable β-γ alloys were given preliminary treatment by sealing in Vycor tubes in vacuum and annealing for 4 hr at 800 C followed by cooling in air.

Samples of homogenized alloys were checked spectrographically for impurities, but the principal components were determined on samples subsequent to heat treatment. The impurities analyzed averaged approximately as follows: Ag, 0.0002 pct; Fe, 0.004; Si, 0.0008; Cd, 0.005; Mg, 0.0002; and Pb, 0.002.

For metallography, samples of appropriate composition were cut into rods $\frac{5}{8}$ in. long, sealed in pyrex tubes in vacuum and annealed for eight weeks at temperatures of 470 C and below, two weeks at 480 C, 500 C, and 600 C, and 4 hr at 700 C, followed by quenching in cold water. Temperatures were accurate to ±2 C. The cylinders were then machined to 8.7 mm diam and a slice weighing 1.5 g cut with a thin saw transversely from the center of each. This

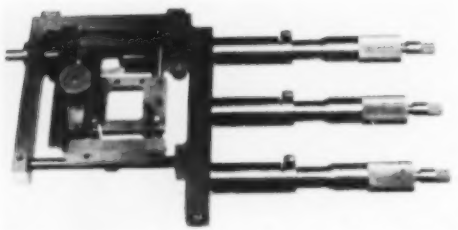

Fig. 2—Microscope stage with hydraulic traverse for quantitative linear analysis.

sample was dissolved in nitric and the copper content determined by the standard electrolytic method. The results are accurate to ±0.03 pct.

Metallography

Metallographic examination was done on both faces immediately adjacent to the slice cut for chemical analysis so that any slight gradient in composition would be appropriately averaged. The two half samples were mounted in bakelite, metallographically polished, and etched with dilute dichromate solution (copper alloy etchant No. 5, diluted to 20 pct normal concentration with water). The phases were clearly distinguished by color. Very light etching was used in order to give sharp delineation of the boundaries on a plane surface.

The volume fractions of the various phases were determined by measuring the relative length of traverse across the β phase and the other phase present. For this purpose a hydraulic traversing stage was used, Fig. 2, in which the cross-motion is provided by a hydraulic ram driven by oil forced by any one of three micrometer heads mounted with appropriate channels in the same framework. Observing through a microscope at an appropriate magnification (X50 to X500), the specimen was driven by one of the micrometer heads when the β phase was beneath the crosshairs and stopping and transferring to the other micrometer drive precisely at the boundary of the second phase.* The difference between the reading of each micrometer head before and after the traverse is, therefore, the integrated length of traverse across each phase, and hence proportional to the volume percentage of each phase allowing for a statistical fluctuation.

On each half sample, 18 traverses were taken entirely across the specimen. Closer spacing was used near the periphery of the circular sample in order to compensate for radial segregation if it existed, with appropriate geometric weighting of the results. Since both halves were measured (at right angles to each other) and averaged, the results are based on a total length of about 20 cm. The greatest uncertainty comes from the lack of sharpness of the boundary between the two phases. With

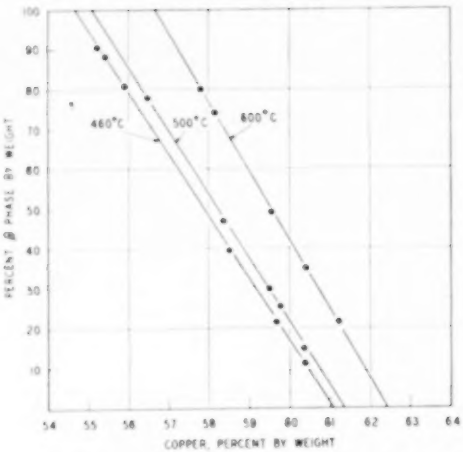

Fig. 3—Typical metallographic measurements of β fractions in $\alpha + \beta$ alloys.

Table I. Summary of Metallographic Results

Annealing Temperature and Time		Limits of Two Phase Regions in Copper, Wt Pct†			
		α Region		β Region	
°C	Weeks	α	β	β	γ
600	1	59.49	61.24	60.26	61.10
600	2	59.50	61.20	60.36	61.44
500	1	57.85	58.93	58.05	61.05
	2	57.87	58.86	58.09	61.04
460	1	57.53	58.68	58.05	61.96
	2	57.58	58.74	58.00	61.79
440	1	57.32	58.26	57.99	62.03
	2	57.50	58.49	58.20	62.10
420	1	57.07	58.32	58.09	62.20
400	1	57.19	58.06	57.74	62.07
	2	57.07	58.08	57.73	62.19
	repeat 2	57.20	58.09	57.79	62.13
470	2	57.58	58.88	58.19	62.25
480	2	57.56	58.85	58.04	62.19
500	2	57.54	58.83	58.01	62.29
550	2	57.44	58.68	58.02	62.19
700	1	58.00	59.47		

* The compositions represent the 0 and 100 pct intercepts of the straight lines best representing the fraction of β phase plotted as function of copper content.

Table II. Lattice Parameters of Homogeneous Solid Solution Alloys*

Phase	Lattice Parameter at 29.8°C, Angstrom Units	Copper Content by Analysis, Atomic Pct
α	3.6824 ± 0.0002	70.015 ± 0.003
α	3.6860 ± 0.00010	68.70 ± 0.03
α	3.6902 ± 0.0002	66.88 ± 0.02
α	3.6960 ± 0.0005	64.66 ± 0.02
α	3.6982 ± 0.0006	63.64 ± 0.02
β	2.9480 ± 0.0001	54.94 ± 0.03
β	2.9502 ± 0.0002	54.05 ± 0.02
β	2.95235 ± 0.00006	53.23 ± 0.02
β	2.9539 ± 0.0002	52.54 ± 0.03

* Alloys annealed 24 hr at 800°C, and 24 hr at 600°C in pump train, then cold and the filings annealed in evacuated Vycor glass ampoules for a further 24 hr at 500°C, and quenched.

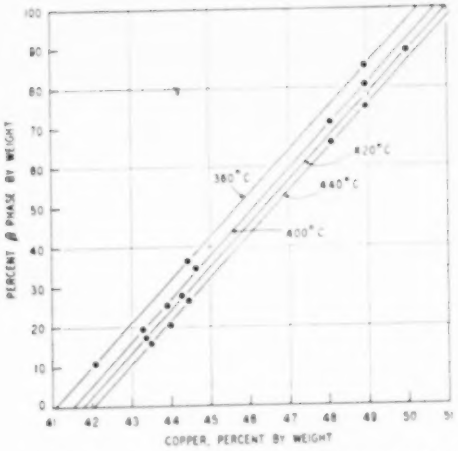

Fig. 4—Metallographic measurements of β fractions in $\beta + \gamma$ alloys

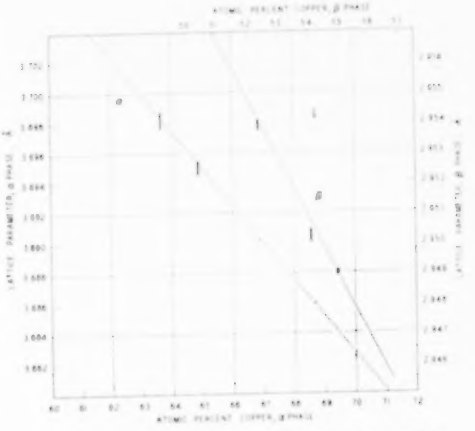

Fig. 5—Lattice parameters of homogeneous α and β phases

large well-defined particles of the various phases the error is negligible, but on specimens annealed at the lower temperatures where small particles of α or γ were concerned, appreciable errors could result. No measurements were attempted on samples annealed below 360°C.

The measured fraction of β phase in several samples of different composition after annealing at the same temperature were plotted against the analytical results and the best straight line drawn through the points, as in Figs. 3 and 4. The compositions corresponding to the intersections of this line with zero and 100 pct β, respectively, are the solubility limits at the temperature concerned.

A straight line on this method of plotting results only when the weight percentage of a given phase in the two-phase area is plotted against the composition on the same basis. In the present system the difference between volume and weight fractions is trivial, at most 0.15 pct, but the corrections were nevertheless applied. The results are listed in detail in the appendix, and the phase limits graphically derived from them in Table I.

Lattice Parameter Measurements

The separate series of alloys made for the lattice parameter measurements was given initial mechanical and heat treatment similar to the metallographic material. After homogenizing at 800°C, the series of single-phase alloys for the establishment of the standard α and β parameter curves were annealed in lump form for 24 hr at 500°C, quenched, sectioned, and (after microscopic inspection for uniformity and sampling for chemical analysis) filed. The filings were screened to −185 mesh, sealed in vacuo in small Vycor tubes, reannealed for 8 hr at 500°C, and quenched.

The duplex alloys had a composition of 60.4, 55.3, and 48.4 pct Cu, corresponding to a major amount of α, copper-saturated β, and zinc-saturated β, respectively. No suitable parameter measurements could be made of γ in the presence of β because of superposition of lines in the diffraction pattern. The alloys were first annealed in lump form at the desired temperature (for 1 week at 350° and 400°C or 5 weeks at 300° and 250°C) after which they were filed, and the sieved filings annealed for a further two weeks at 400°C or four weeks at 250°, 300°, and 350°C, followed by quenching.

X-ray diffraction patterns were made on a 9 cm radius Bradley camera thermostatically maintained at 29.8° ± 0.2°C. Cobalt radiation was used for measurements on the α phase and that of copper for the β phase studies. No filter was used. The parameter was calculated from the measurements made on the films by the use of the Hess modification of the Cohen procedure,[7] using the standard

Table III. Lattice Parameters of Alloys[*] in Two-Phase Fields

Temperature, °C	Lattice Parameter of γ Phase, in $\alpha + \beta$ Field, Angstrom Units	Equivalent Composition of α Phase, Atomic Pct Cu	Lattice Parameter of β Phase in $\alpha + \beta$ Field, Angstrom Units	Equivalent Composition of β Phase, Atomic Pct Cu	Lattice Parameter of β Phase in $\beta + \gamma$ Field, Angstrom Units	Equivalent Composition of β Phase, Atomic Pct Cu
400	3.7025 ±0.0006	61.95	2.95052 ±0.00009	54.16	2.9556 ±0.0002	51.53
					2.9557 ±0.0004	51.50
360					2.95608 ±0.00009	51.30
350	3.7000 ±0.0001	62.97	2.95143 ±0.00005	53.70		
300	3.6977 ±0.0005	63.90	2.95180 ±0.00003	53.50	2.95755 ±0.00004	50.58
250	3.6941 ±0.0002	65.30	2.9548 ±0.0004	51.96	2.95743 ±0.00009	50.63

* All alloys annealed 24 hr at 800°C and quenched, then given lump anneal at temperature stated for one week (400° and 350°C) or five weeks (300° and 250°C), filings made and filings annealed in evacuated Vycor glass tubes for an additional two weeks at 400°C or four weeks at 350°, 300°, or 250°C.

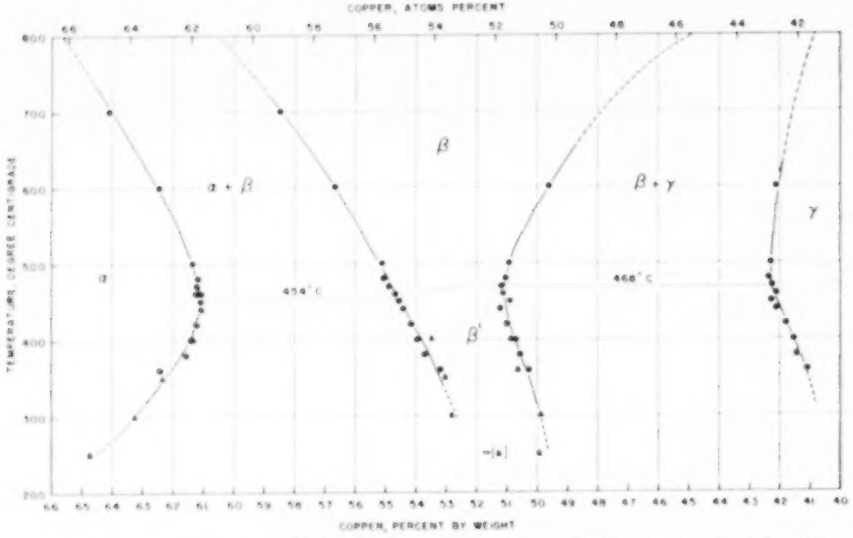

Fig. 6—Constitution diagram of Cu Zn alloys in the range 40 to 65 pct Cu showing new experimental points. Circle, metallographic results; triangle, X-ray results.

wave lengths as listed in the *Metals Handbook*,[7] converted to Angstrom units. The results are summarized in Fig. 5 and in Tables II and III. The latter table also shows the compositions corresponding to the observed parameters of the α and β phases in the two-phase alloys annealed at the various temperatures. These compositions, of course, correspond to the phase boundaries at the temperature concerned.

The Diagram

The results of the metallographic and X-ray studies are both plotted in the form of the constitution diagram, Fig. 6. No new features are observed, but the more precise location of the boundaries will be of value in connection with studies of the various thermodynamic properties of the alloys. The lines as redetermined are in close agreement with those chosen by Raynor as best representing previous data, except for the zinc-rich boundary of the β phase in the vicinity of the disorder point. This is 48.83 wt pct Zn compared with Raynor's point I (Fig. 1) which is 49.7 pct Zn. The width of the β phase at 434° becomes only 3.5 pct instead of 4.9 pct. The other fixed points are 38.9, 45.4, and 57.7 pct Zn for Raynor's points G, H, and J, which he gives as 39.0, 45.0, and 57.5, respectively. There is no evidence for a two-phase field between the β phase in the ordered and disordered conditions, which would show as a discontinuous composition displacement of the phase boundary at the transition temperature. Though the β boundary on the zinc-rich side does change slope at the disorder point, there is no discontinuity within the experimental error. The boundary of β in equilibrium with α suffers neither discontinuity nor apparent change of slope. The change in free energy resulting from ordering in the β phase does not result in increased width. Below 600° C the β phase field lies entirely on the copper-rich side of CuZn, and, though it bends in this direction at temperatures below 480°, it never attains the stoichiometric composition.

Summary

By quantitative microscopic measurement of the areas of each constituent in well annealed two-phase alloys, and by the precise measurement of lattice parameters, the $\alpha + \beta$ and $\beta + \gamma$ fields have been redetermined down to temperatures of 250° C. Although changes of slope are observed in the α, γ and zinc-rich β boundaries at the disordering temperature, there is no offset, and there is neither change of slope nor discontinuity in the copper-rich boundary of the β phase. The maximum extent of the α phase decreases from 49 pct Zn at 450° C to about 35.5 pct at 250° C. The β phase field retains approximately the same width at all temperatures below the transition and lies entirely at the copper-rich side of the composition CuZn.

Acknowledgment

The authors wish to express their thanks to the following individuals at the University of Chicago who provided assistance essential to the completion of this work: J. Getzholtz and J. Swies, who developed the details of design and constructed the integrating metallographic stage, A. Roman and A. Leoni, who performed all the chemical analyses, and James B. Hess, who helped to establish the roentgenographic procedure. For part of its duration the work was supported by the Office of Naval Research (Contract No. N-6ori-IV, NR 019 302); it would have been impossible, however, without the unrestricted funds supplied by the industrial sponsors of the Institute for the Study of Metals.

Appendix
Metallographic Measurements of β Phase Fractions

The numbers that are listed as pct α represent the fractions by weight corresponding to the volume fractions measured under the microscope.

Samples Annealed at 360° C for Eight Weeks: $\alpha + \beta$ series—61.24 pct Cu, 15.28 pct β, 60.37, 20.34, 58.73, 37.79, 57.71, 50.56, 55.94, 71.61. $\beta + \gamma$ series—48.93 pct Cu, 85.49 pct β, 44.44, 36.42, 42.09, 10.79.

Samples Annealed at 380° C for Eight Weeks: $\alpha + \beta$

series—55.18 pct Cu, 80.77 pct β; 39.69, 25.26; 58.65, 34.76; 35.88, 73.34. $\beta + \gamma$ series—48.59 pct Cu, 82.55 pct β; 47.86, 70.28; 43.22, 19.36; 43.07, 18.94; 43.12, 18.01; 44.66, 35.69.

Samples Annealed at 400°C for Eight Weeks: $\alpha + \beta$ series—60.40 pct Cu, 14.71 pct β; 59.62, 24.18; 58.94, 31.50; 55.95, 73.09; 55.30, 82.56. $\beta + \gamma$ series—48.94 pct Cu, 80.73 pct β; 48.07, 71.06; 43.91, 25.49; 44.64, 34.66; 43.31, 19.09.

Samples Annealed at 420°C for Eight Weeks: $\alpha + \beta$ series—60.36 pct Cu, 12.29 pct β; 59.41, 24.68; 55.91, 74.43; 55.23, 85.11. $\beta + \gamma$ series—49.99 pct Cu, 89.27 pct β; 48.98, 78.26; 44.29, 27.61; 43.37, 17.05.

Samples Annealed at 440°C for Eight Weeks: $\alpha + \beta$ series—60.38 pct Cu, 10.75 pct β; 59.72, 19.41; 58.21, 42.42; 56.53, 66.44; 55.45, 84.03; 55.27, 86.78. $\beta + \gamma$ series—48.97 pct Cu, 75.15 pct β; 48.08, 66.10; 44.47, 26.45; 44.00, 20.17; 43.51, 15.81.

Samples Annealed at 450°C for Eight Weeks: $\alpha + \beta$ series—58.73 pct Cu, 36.68 pct β; 58.04, 45.63; 55.85, 79.55; 55.28, 89.39. $\beta + \gamma$ series—49.66 pct Cu, 86.55 pct β; 47.85, 63.88; 44.42, 24.03; 43.24, 12.34.

Samples Annealed at 460°C for Eight Weeks: $\alpha + \beta$ series—60.39 pct Cu, 11.04 pct β; 59.70, 21.44; 58.51, 39.51; 55.46, 88.35; 55.93, 80.83; 55.26, 90.38. $\beta + \gamma$ series—48.97 pct Cu, 75.36 pct β; 48.07, 67.28; 45.49, 37.72; 43.44, 26.19; 43.93, 20.34; 43.35, 13.56.

Samples Annealed at 460°C for Eight Weeks (Repeat): $\alpha + \beta$ series—60.05 pct Cu, 17.84 pct β; 59.77, 22.54; 58.68, 38.73; 55.40, 89.65; 55.55, 81.79. $\beta + \gamma$ series—49.88 pct Cu, 85.33 pct β; 47.77, 62.51; 44.70, 29.17; 43.25, 12.04.

Samples Annealed at 470°C for Eight Weeks: $\alpha + \beta$ series—60.02 pct Cu, 18.09 pct β; 57.72, 55.88; 59.37, 28.52; 55.43, 90.48; 55.87, 84.01. $\beta + \gamma$ series—43.94 pct Cu, 19.14 pct β; 47.79, 61.58; 49.98, 86.79; 44.68, 27.21.

Samples Annealed at 480°C for Two Weeks: $\alpha + \beta$ series—60.40 pct Cu, 13.24 pct β; 59.48, 26.72; 58.30, 46.63; 56.41, 78.11. $\beta + \gamma$ series—48.03 pct Cu, 65.66 pct β; 43.67, 38.89; 43.96, 18.45; 48.53, 70.87.

Samples Annealed at 500°C for Two Weeks: $\alpha + \beta$ series—60.37 pct Cu, 14.90 pct β; 59.78, 25.47; 59.51, 29.75; 58.38, 47.00; 56.49, 77.80. $\beta + \gamma$ series—48.50 pct Cu, 72.38 pct β; 48.07, 67.18; 43.65, 37.89; 44.01, 20.65.

Samples Annealed at 600°C for Two Weeks: $\alpha + \beta$ series—61.25 pct Cu, 21.22 pct β; 60.41, 34.80; 59.57, 49.17; 58.19, 73.89; 57.83, 80.00. At 600°C for 4 hr for $\beta + \gamma$ series in air—44.66 pct Cu, 33.15 pct β; 43.26, 16.10; 46.94, 64.49; 47.82, 76.33.

Samples Annealed at 700°C for Four Hr in Air: $\alpha + \beta$ series—61.24 pct Cu, 50.90 pct β; 59.74, 77.24; 63.00, 19.07.

References

1. G. V. Raynor: The Equilibrium Diagram of the System Copper-Zinc. Annotated Equilibrium Diagrams, No. 3 (1944) Inst. Metals, London.
2. *Metals Handbook* (1948) p. 901. Cleveland, A.S.M.
3. R. T. Howard and Morris Cohen: Quantitative Metallography by Point-Counting and Lineal Analysis. *Trans.* AIME (1947) **172**, pp. 413-426; METALS TECHNOLOGY (August 1947).
4. Albert Sauveur: *Trans.* AIME (1896) **26**, pp. 863-906.
5. Heyn: *Ztsch. anorg. allgem. Chemie* (1904) **39**, p. 1; (1907) **52**, p. 129.
6. Huntington and Desch: *Trans.* Faraday Soc. (1908) **4**, p. 51.
7. E. P. Polushkin: *Trans.* AIME (1925) **71**, p. 669.
8. J. B. Hess: A Modification of the Cohen Procedure for Computing Lattice Constants from Powder Data. *Acta Cryst.* (1951) **4**, p. 209.
9. Ref. 2, p. 166.

Technical Note

Formation of Nitrides from Atmospheric Exposure During Creep Rupture of 18 Pct Cr-8 Pct Ni Steel

by E. J. Dulis and G. V. Smith

As reported several years ago, nitrogen may be taken up from the atmosphere by austenitic Cr-Ni steels during creep or creep-rupture tests. This was indicated by chemical analysis and by the appearance of a new microstructural phase, or phases, tentatively identified as chromium nitride(s), at the surface or at the intergranular cracks associated with fracture. The nitrogen pickup was observed to be dependent on time, temperature, and deformation.

In a more recent investigation, a sample was obtained in which there was sufficient of the precipitate to suggest that it could be readily identified by X-ray diffraction. This sample had been taken from a $\frac{1}{4}$ in. diam creep-rupture specimen of annealed, type 304L stainless steel of the following initial composition: C, 0.03 pct; Mn, 0.65; P, 0.010; S, 0.019; Si, 0.54; Cr, 19.50; Ni, 12.02; N, 0.031; and Al, 0.005. The specimen had ruptured after 10,470 hr at 1500°F (2000 psi). In this case nitrides were distributed across the whole section of the sample, Fig. 1. The precipitate occurred both at the grain boundaries and within the grains; the latter precipitate had in some cases the appearance of pearlite, and in others was distinctly Widmanstätten. Chemical analysis of the sample after test showed 0.64 pct "soluble" nitrogen (soluble in 1:1 hydrochloric acid: water) and 0.18 pct "insoluble" nitrogen (insoluble in the hydrochloric acid solution but dissolved by fuming sulphuric acid).

For identification of the precipitate by X-ray diffraction, the matrix in the surface layer of the specimen was dissolved by prolonged attack in an alcoholic solution of picric and hydrochloric acids. The appearance of the specimen surface after such etching is shown in Fig. 1c. The diffraction pattern of the surface-concentrated precipitate was obtained with a recording spectrometer in both the forward and back-reflection regions (the latter by adapting a special fixture to the conventional X-ray unit).

The observed X-ray diffraction lines, Table I, show the presence of Cr_2N and CrN; the agreement with interplanar spacings calculated from reported data[7] is quite good. Since it has been suggested[8] that CrN dissolves only in concentrated sulphuric acid, whereas Cr_2N dissolves in dilute hydrochloric or sulphuric acids, an effort was made to distinguish between the two nitrides. This proved possible, inasmuch as etching in a dilute solution of hydrochloric acid gave a sample in which microscopic examination showed that much of the Widmanstätten-pearlitic precipitate within the grains had been eaten out, leaving the grain boundary precipitate in relief, and which, when examined by X-ray diffrac-

E. J. DULIS and G. V. SMITH, Member AIME, are associated with Research Laboratory, United States Steel Co., Kearny, N. J.

TN 127E. Manuscript, May 20, 1952.

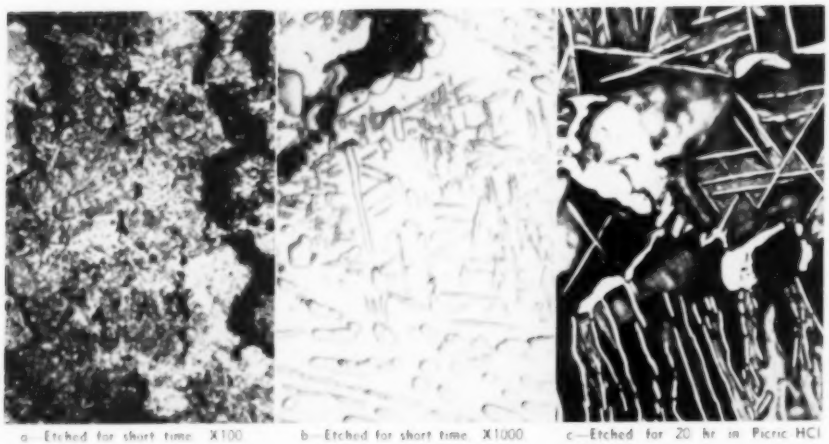

a—Etched for short time. X100 b—Etched for short time. X1000 c—Etched for 20 hr in Picric HCl X1000

Fig. 1—Longitudinal section near fracture of creep rupture specimen of 304L steel which ruptured after 10,470 hr at 1500°C.

tion, showed a substantial increase in intensity of the CrN lines relative to those of Cr$_2$N.

Although the relative coarseness of the precipitate particles suggests that they precipitated during the creep-rupture test, it is possible, since the fractured test specimen cooled in the furnace, that precipitation may have occurred during cooling. This possibility was refuted, however, by reheating a sample to 1500°F for 1 hr and quenching it, and finding no alteration in microstructure. Thus, the inward diffusing nitrogen is presumed to have combined with chromium in solid solution and precipitated as chromium nitride. It seems likely that Cr$_2$N formed first nearest the surface of the cracks, which had formed at the grain boundaries or at uncracked grain boundaries and with further diffusion, the Cr$_2$N reacted with nitrogen to form CrN at these sites. This would explain the experimental observations.

Depletion of chromium in the austenite by the formation of chromium nitride unbalanced the matrix composition so that much or all of the austenite transformed to ferrite, presumably by a martensite-like reaction, on cooling from the temperature of test.

References

1. G. V. Smith, E. J. Dulis, and E. G. Houston: Creep and Rupture of Several Chromium-Nickel Austenitic Steels. *Trans.* A.S.M. (1950) **42**, pp. 935-980.
2. S. Eriksson: X-Ray Investigation on the System Iron-Chromium-Nitrogen. *Jernkontorets Annaler* (1934) pp. 530-543.
3. R. Blix: Rontgenanalyse des Chrom-Stickstoff-systems nebst einer orientierenden Konstitutionsuntersuchung des stickstoffhaltigen Ferrochroms. *Ztsch. Physikalische Chemie* (1929) **3B**, pp. 229-239.
4. Moldenhauer and Groebe: *Ztsch. Angew. Chem.* (1914) **27**, p. 334.

Table I. X-ray Diffraction Identification of Precipitate Phases of 0.03 Pct C-18 Pct Cr-8 Pct Ni Creep-Rupture Specimen Tested for 10,470 Hr at 1500°F

Cr$_2$N			CrN			0.03 Pct C-18 Pct Cr-8 Pct Ni Creep Rupture Specimen (Phases Concentrated at Surface)			
Interplanar Spacing, d, Å	Intensity Observed[1]	(hkl)	Interplanar Spacing, d, Å	(hkl)	Interplanar Spacing, d, Å	Intensity Observed[1]	Phase	(hkl)
2.580	m	(101)			2.62	vvw	—	—
2.390	m	(006)	2.390	(111)	2.394	w	Cr$_2$N	(101)
2.208	vvw	(102)	2.070	(200)	2.07	w	Fe$_3$C[2]	(220)
2.114	vs	(105)	1.465	(220)	2.01	vw	—	—
			1.240	(311)	2.04	vvw	Fe$_3$C[2]	(311)
1.920	m	(107)					CrN	(111)
					2.39	s	Cr$_2$N	(100)
					2.23	vvw	Cr$_2$N	(002)
					2.11	vs	Cr$_2$N	(101)
					2.07	s	CrN	(200)
1.588	s	(110)			1.93	m	Cr$_2$N	(102)
1.260	m	(109)			1.46	s	CrN	(220)
					1.38	vvs	Cr$_2$N	(110)
1.189	s	(200)			1.265	s	Cr$_2$N	(103)
1.158	m	(112)			1.249	m	CrN	(311)
1.150	m	(201)			1.196	vvw	Cr$_2$N	(200)
					1.179	vvs	Cr$_2$N	(112)

* Calculated by the equation $\frac{h^2+k^2}{a^2}+\frac{l^2}{c^2}=\frac{1}{d^2}$ from unit values of ref. 2, based on hexagonal close-packed structure with a_0 = 2.742A, c_0 = 4.458A and c_0/a_0 = 1.709 (i.e., 4.47/2 representing whether low or high unit of the phase. The latter were used in this computation. For the equations in this unit the axial ratio of approximately characteristic oxidation S_{Cr} = 2.2845A, S_{Fe} = 2.2889A, S_{Ni} = 2.0804A, ref. 2.

† Calculated by the equation $\frac{h^2+k^2+l^2}{a^2}=\frac{1}{d^2}$ from a_0 = 4.140A, ref. 3, cubic with NaCl structure, face-centered cubic.

‡ M, medium; s, strong; w, weak; vw, medium weak; vvw, very weak; vs, very strong; vvs, very strong.

§ Listed as a "superstructure" line in ref. 2.

¶ Hadfield's Tables, ASTM Card Index.

Dynamic Formation of Slip Bands in Aluminum

by N. K. Chen and R. B. Pond

IN the study of slip band* formation, there have been many examples to show that they do not always appear as lines traversing the entire crystal, but as segments whose ends seem to vanish in their path through the crystal. This characteristic appearance of slip bands has been witnessed under the optical microscope at various magnifications[1] and also under the electron microscope.[2] A typical example of this behavior seen with the optical microscope is shown in Fig. 1.

* The terms "slip band" and "slip line" are used interchangeably in this paper and refer to those slip markings which cannot be resolved into fine lamellae with magnifications under 2000X.

However, the slip band studies were generally conducted on polished surfaces of single or polycrystalline metals which had been previously deformed, i.e., the load was generally released so that the observation could be made. Any picture of slip bands so obtained can represent the surface phenomenon only in a static state of the strained material. The conditions prior to their formation cannot be definitely and clearly assigned. Thus, while a segmented slip band may suggest that slip is a growth process as supposed by the theory of the nucleation of slip,[3] the usual appearance of suddenly and fully developed slip bands around the crystal has generally been considered as a consequence of uniform shear of the entire slip plane akin to a cataclysmic process.

Little clear-cut information is available with regard to the speed at which a slip band forms, its direction of motion, the geometry of its position with regard to its neighbors, and its dependence on orientation. A description is given in this paper of experimental apparatus by which the progressive formation of slip bands can be recorded while the specimen is undergoing deformation. Qualitative and quantitative data on the dynamic formation of slip bands will be presented with special interest concerning the propagation of slip bands, the spacing of slip bands, and their relations to strain hardening. Views on the formation of slip bands are discussed and a mechanism of the unit process involved in the formation of a slip band is proposed.

Preparation of Specimens

Single-crystal specimens of high purity aluminum (99.997 pct), $\frac{1}{8}$ in. square in cross-section and $1\frac{3}{8}$ in. long in gage length, were made by the method of gradual solidification from the liquid state. Since no machining work could be introduced in preparation of crystals of such small size, a special mold was designed for casting them to final shape. The mold consisted of two, separate, high purity graphite blocks. Generally, 20 molds were packed together in one container so that 20 specimens could be obtained by one casting operation. This was desirable since it was possible by this method to obtain groups of crystals with similar orientations.

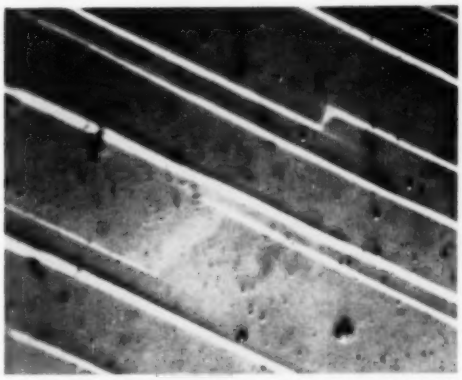

Fig. 1—Slip bands in extended aluminum single crystal A-311 viewed on a plane nearly perpendicular to the slip direction. X1000. Area reduced approximately 50 pct for reproduction.

The as-cast crystals were carefully clipped from the gate, etched, and homogenized for 24 hr at 600° C. They were then very gently polished using a 4/0 paper, re-etched, and finally electrolytically polished after the method previously described by Chen and Mathewson.[4] The crystallographic orientations were determined using a back-reflection, Laue method.

Tensile Testing and Photographic Method

The tensile testing equipment for these tests was composed of a specially designed microtensile machine, microload cell and microclip gage with necessary appurtenances. The members of the microtensile machine consisted of three parts, as shown in Fig. 2. The chassis is equipped with an oil cylinder, *A*, and piston, the piston being part of the movable crosshead, *B*. Pressure in the oil cylinder is controlled and regulated by an external pneumatic-hydraulic cell, *C*, which is connected to the cylinder by a $\frac{1}{8}$ in. high pressure copper tube. This cell is half filled with hydraulic oil and has a needle valve, *D*, on the oil exit side as well as a needle valve, *E*, on the gas inlet side. A quick-acting valve, *F*, as well as a pressure gage is provided for the gas side. The oil exits into the load piston on the microtensile machine. By connecting a tank of inert gas to the gas inlet, regulated pressures were provided over the oil so that the oil would leave the cell at a rate determined by the setting of the exit needle valve, the gas pressure, and the pressure of the oil in the load piston of the microtensile machine. With this pneumatic-hydraulic appurtenance it was possible to

N. K. CHEN, Junior Member AIME, and R. B. POND are Assistant Professors of Metallurgy, The Johns Hopkins University, Baltimore.

Discussion on this paper, TP 3365E, may be sent, 2 copies, to AIME by Dec. 1, 1952. Manuscript, April 14, 1952. Philadelphia Meeting, October 1952.

Fig. 2—Schematic arrangement of microtensile equipment

A—Oil cylinder
B—Movable cross head
C—Pneumatic hydraulic cell
D—Needle valve
E—Needle valve
F—Quick acting valve
G—Microload cell
H—Microclip gage

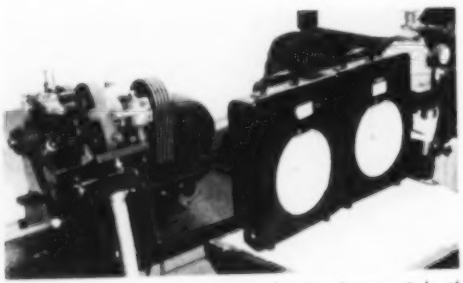

Fig. 3—Experimental apparatus used for the dynamic study of slip bands

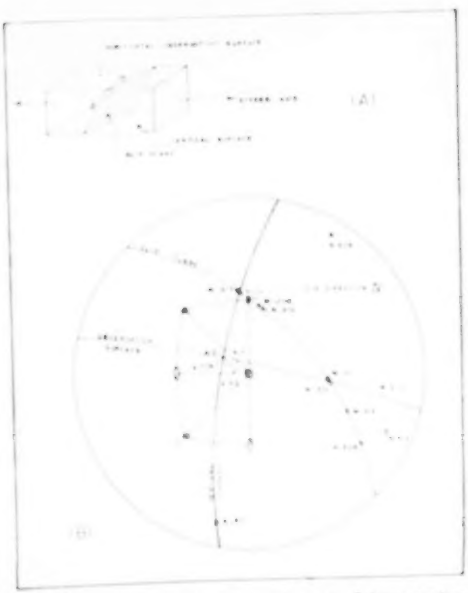

Fig. 4—Observation surface and slip plane. A—Relative position. B—Standard projection showing 1—orientation of crystals, 2—poles of observation surfaces, and 3—relative position of observation surface with respect to slip direction

control, within small limits, the strain rate of the specimen being tested.

Shoulder-type grips were attached to the movable cross-head as well as to the chassis through a centerless ball bearing race. These centerless bearings afforded axial loading on the specimen.

The microload cell, G, was constructed, utilizing the clip gage principle described by Marin.[7] In this load cell, two small flat elliptical springs were welded together at either end and provided with a shoulder grip at one end and a shoulder at the opposite end. SR-4 type A-1 strain gages were attached to the inner surface of one spring and the outer surface of the mating spring. This particular arrangement offered the smallest change in deflection due to an eccentrically placed load. A Foxboro Dynalog recorder was used to establish a continuous load-time record after the microload cell had been statically calibrated.

The best results obtained for recording strain were achieved by using a microclip gage, *H*, which was made in the form of a $\frac{3}{4}$ in. circle segment from very thin phosphor-bronze strip which was sufficiently wide to allow the permanent attachment of a type A-1 SR-4 strain gage on both sides. This clip gage was attached to the specimen in the following manner: two cotton strings were impregnated with Duco cement and tied around the specimen at a $\frac{1}{2}$ in. interval. When set and dried, these strings became holding blocks for the points of the clip strain gage. When the clip gage was compressed and its points set between these strings it was restricted from expanding until the specimen was elongated. By measuring the expansion, the elongation of the specimen was measured. It was possible with this clip gage to measure the percentage of elongation to a value of 0.05. Strain measurements were continuously recorded by means of a Foxboro Dynalog recorder.

A 16 mm motion picture camera was placed with its lens in intimate contact with one of the oculars of a binocular research metallograph on which the microtensile machine was placed, see Fig. 3. The focus was maintained through the free ocular while the specimen was being deformed. Since the photographic record was taken with a definite time interval, it was possible to coordinate phenomena with load and strain through time.

Orientations of Crystals

In the course of this investigation, more than 30 crystals of various orientations were extended in the microtensile machine. In this paper, documented data will be presented for four specimens together with observations derived from other specimens pertinent to the general interest outlined earlier.

It was found that the specification of orientation of a crystal by its stress-axis generally used on this type of research is not sufficient documentation. Rather, the relative position of the observation surface, i.e., the horizontal surface of the specimen, with respect to the slip direction is of primary importance. This can easily be seen in Fig. 4a, that if the slip direction in the slip plane *M-N* is parallel with the direction *M*, the shear of the slip plane would cast a maximum shadow on the observation plane to form the visible slip line. On the other hand, if the slip direction were to parallel the direction *N*, no visible slip band would be observed on the top surface.

Consequently, in addition to specifying the orien-

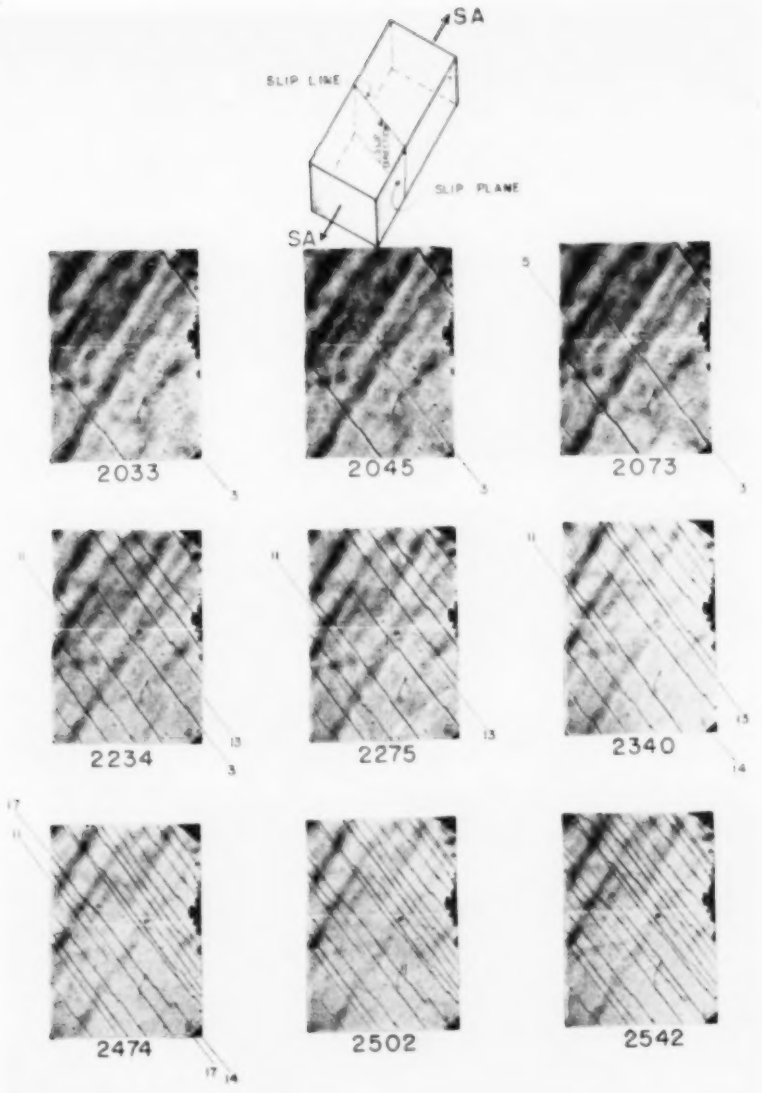

Fig. 5—Propagation of slip bands in A-311. Frame numbers are given. Speed of camera 32 ft per sec. Resolving power, 0.0022 mm.

tation of the crystals. Fig. 4b includes the positions of the observation surfaces (S-311, S-206, S-111, and S-313), and their relations to their slip directions. Here, the *M* and *N* directions in the projection (with numbers to designate different specimens) bear the same meaning as *M* and *N* used in the sketch, Fig. 4a. It can be seen that for crystals A-311 and A-206 the slip direction is only 6° from the direction *M* in both cases, yet for specimens A-111 and A-313 the slip direction is 6° and 7°, respectively, from the direction *N*. The vast difference in the progressive formation of slip lines in these two groups will be illustrated in subsequent sections.

Propagation of Slip Bands

In the extension of crystals A-311 and A-206, almost every slip line appeared first as a segment and then propagated through the field of observation. An example showing this type of propagation may be seen in Fig. 5, crystal A-311. Since the field was maintained in focus throughout the experiment, there could be little doubt as to the progressive

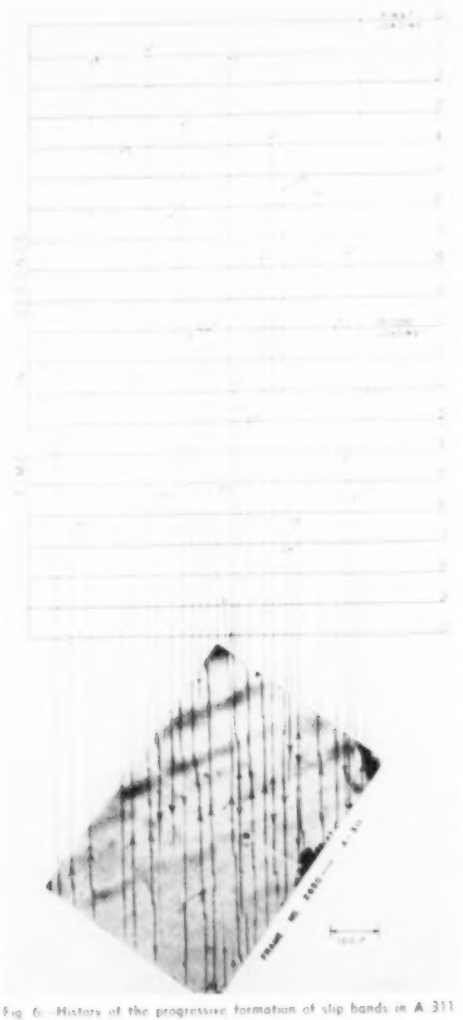

Fig. 6—History of the progressive formation of slip bands on A-311. Time-distance-sense plot.

propagation of slip bands, the optics used resulted in a resolving power of 0.0022 mm. The general appearance of the slip bands on the same specimen was observed statically at very high magnifications, i.e., the limit of the optical microscope, and segments of slip bands were also noted; see Fig. 1, for example.

Several important observations should be pointed out with respect to Fig. 5 and the formation of slip bands in general. Frame Nos. 2033, 2045, and 2073 were selected to show the propagation of slip band No. 3 from the lower right direction and that of slip band No. 5 from the upper left direction. The movement in opposite directions strongly suggests that their propagation is intimately associated with the fundamental process of plasticity of single crystals. It is to be noted that the propagation of the band was accompanied by an increase of its intensity which undoubtedly indicates an increasing amount of shear in the "slip zone" concerned. Since the observation in this specimen (A-311) is almost at the head of the glide lamallae, the increase in intensity of the slip band should be almost entirely due to shear in the slip direction.

The overlapping of slip bands is very preponderant, Fig. 5. For example, two such "overlappings" can be witnessed in frame No. 2073 of slip band No. 3 under the present resolution of the optics and the apparent width of the two overlapped "slipped zones" is of the order of about 1 to 3 microns. The "amount of the overlap" is probably governed by "the width of the overlap" and the extent of strain. In general, the amount of the overlap is too small to be measured under the present magnification. However, in frame Nos. 2275 and 2340, a faint segment can be observed that is added to slip band No. 3 at one end of the two overlapped "slip zones" as if it intended to continue the original path of propagation from the lower right direction. This characteristic appearance can be more clearly observed in Fig. 1, where the width of the overlap is 5 microns and the amount of overlap (a gradual disappearance on one side only) is about 10 microns. In this connection, it should be pointed out that the term "cross-slip" has been used to describe slip at the junction of two such overlapped slip bands in aluminum.[7] However, it is perhaps more appropriate to reserve the use of this term to its original sense,[1] i.e., a clearly-defined (111) [110], as the cross-slip system when the primary slip system is (111) [110]. This will be discussed later.

The propagation of slip line 13 is demonstrated in frame Nos. 2234, 2275, and 2340 of Fig. 5, while at the same time it may be noted that slip band No. 11 does not propagate in these same three frames; and, in fact, close examination of all the other frames in the film shows little or no propagation of this line beyond the point noted in frame No. 2340. In frame Nos. 2474, 2502, and 2542, the progressive formation and propagation of the overlapped slip bands, designated here as No. 14 and No. 17, is of particular interest. Here, the width of the overlap in frame No. 2474 is 20 microns, a much greater width of overlap than most others observed. With increasing extent of strain, this overlap was seen to develop into two distinct slip bands. Again, the direction of propagation of the initial slip band seems to have dictated the subsequent direction of continued propagation of the band which formed its mate.

It should be mentioned here that slip bands observed 90° away from the observation surface of A-311 after extension showed little overlapping. This is also true in the case of crystal A-206.

Quantitative Analysis of Propagation Data: In order to observe the overall panorama of slip band formation, propagation, geometry of position, and relations to stress and strain, it was found necessary to print the whole film of the first 30 to 35 slip bands to carry out detailed measurement frame by frame on the print. In the case of crystal A-311, 640 prints had to be investigated. Fig. 6 shows a time-distance-sense plot where time is the ordinate in seconds during loading; distance is the abscissa (actual spacing between slip bands) in microns; and sense is indicated by arrows on the bands. Each line is assigned a number, and is located at a position where and when it first appeared during the extension. Thus, the sequential addition of slip lines is known and their relative position can be determined. Most of the lines propagated into the field of observation

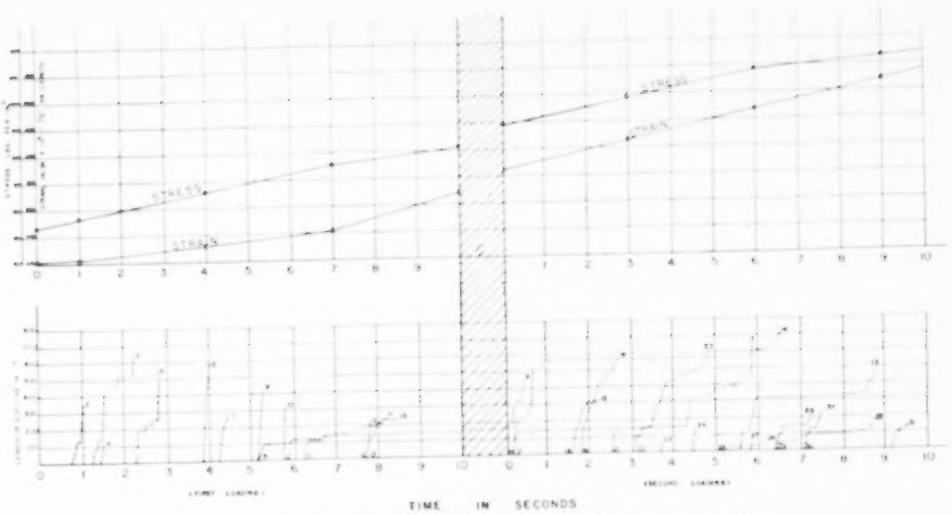

Fig. 7—Propagation of slip bands in A-311 with time as correlated with stress and strain.

from the sides, only a very few started to grow from the center of the field.

Fig. 7 shows the plot of the stress and strain vs. time used in the extension of crystal A-311. It should be pointed out that since the strain was measured over a ½ in. gage length it can be used only as an average strain indication in the study of the observed slip lines. The specimen was first loaded with a strain rate of about 0.00053 per sec and a stress rate of about 31.5 psi per sec until 10 slip bands were observed. After an intermittent time of about 5 min for a general survey on the total specimen surface (the load was held constant), the specimen was then reloaded with a strain rate of about 0.0007 per sec and a stress rate of 27.2 psi per sec until the end of the film was reached. At a camera speed of 32 frames per sec, the total spool of film of 100 ft would last 2 min. By then, a total of more than 40 slip bands was formed in the field of observation. However, in the analysis of the picture, only the first 30 slip bands were considered wherein distinct resolution of bands was assured.

In the lower part of Fig. 7, the length of each slip band is plotted against time during extension. The measurement was carried out frame by frame on the printed strip which had a magnification of 125X. The accuracy of measuring the length of the slip band is of the order of 10 microns. Again, it should be pointed out that the propagation here measured for crystal A-311 represents the growth process of slip bands not along the slip direction, but nearly perpendicular to the slip direction. It is seen that the rate of propagation is not uniform, since all the curves are discontinuous. However, several important points could be made regarding the nature of formation and propagation of slip bands. In the first place, considering the length-time curve for all the lines as a whole, there is a general trend of decreasing rate of propagation as the time increases, i.e., as the strain increases. This indicates that slip bands, such as Nos. 2, 3, 4, 5, etc., have hardened in some way the adjacent matrix material; i.e., the potential slip sites for slip bands, such as Nos. 18, 19, 22, etc., have been hardened. Another observation substantiating this viewpoint that slip in a particular slip band could harden its adjacent material will be discussed in the section under "Sequential Addition of Slip Bands."

Second, when the rate of propagation of an individual line is considered, there is the general tendency of decrease in rate with time, see, for example, line 18, 19, 22, etc. This implies that the propagation of a particular line has slowed down in its course in traversing the crystal due to some kind of retardation effect, i.e., strain hardening associated either within the slipped material itself or with the material immediately adjacent, or both. Since the overall external strain was continuously increasing at a constant rate, the variation of the rate of propagation of different slip bands at the same time interval also implies a "heterogeneous" strain hardening associated with various slip bands.

Thus, the rate of propagation of slip bands in crystal A-311 varies from zero as a minimum to about 7600 microns per sec as a maximum in the direction nearly perpendicular to the slip direction.

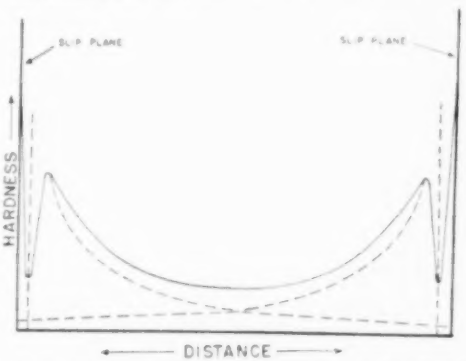

Fig. 8—Variation of hardness between two slip bands. From Brown.[7]

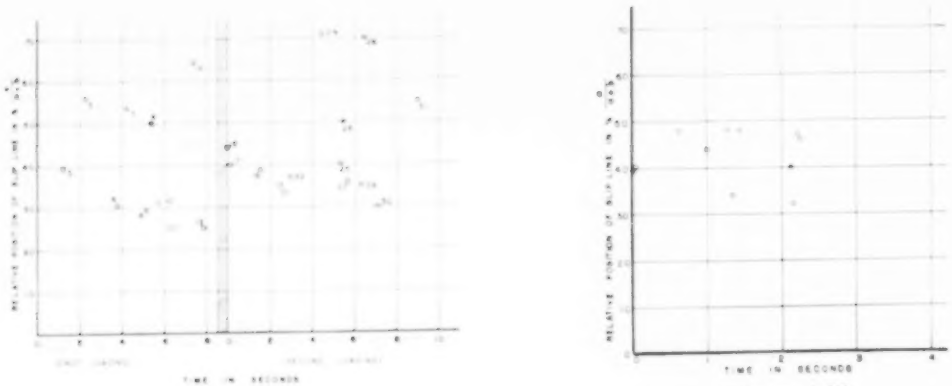

a—Specimen A-311 b—Specimen A-206

Fig. 9—Proximity of slip bands to their two closest neighbors

However, the rate of slip in the slip direction was not determined. Further work is contemplated in which the external strain rate will be changed, the camera speed will be increased, and the resolution of the optics will be increased in order to determine more accurately the rate of slip band propagation and the change of rate of slip band propagation as caused by the external strain rate.

Sequential Addition of Slip Bands. There have been many hypotheses to account for the occurrence and distribution of slip lines in extended single crystals. One assumes that there are surface irregularities, i.e., "macroscopic" variations in gage diameter along the length of the specimen which would determine the location of slip clusters.[7] Another one assumes that there are stress concentrations in the specimen of varying severity which are eliminated by slip, the most severe concentration is eliminated first.[8] A third assumption to explain the slip behavior of different metals, in general, is based upon the relative amount of strain hardening that results within the slip band during the straining. With respect to aluminum, in particular, recent work by Brown[9] has assumed a variation of hardness between two slip bands as shown in Fig. 8. According to Brown, the positions of lowest "hardness" are the positions where slip has been found to occur (i.e., either on planes approximately midway between, or on planes situated very close to, the existing slip bands—here, a self-annealing process is assumed). In the present investigation, since the addition of a slip band between two pre-existing bands can be actually observed, a plot to show relative position of the band with respect to the two pre-existing bands can be seen in Fig. 9a for slip bands in specimen A-311. In the figure, a refers to the spacing between the newest band and its immediate predecessor, while b refers to the spacing between the newest line and its second predecessor. The ratio $(a/a + b \times 100)$ is plotted as the ordinate, time as the abcissa. It is seen that there are more bands with an $a/a + b \times 100$ ratio smaller than 50 pct, suggesting that the subsequent slip band is frequently closer to the one of the two pre-existing slip bands on which less gliding has occurred. This relation is true in the case of crystal A-206, plotted in Fig. 9b, where the first 11 lines all show an $a/a + b$ ratio smaller than 50 pct. Thus, a logical deduction could be that, associated with each slip band, there is a hardening effect which extends some distance beyond itself and increases with the increasing amount of shear strain, shown schematically in Fig. 10. This hardening effect associated with a particular slip band seems to be a very important one of the many factors which can influence the geometry of the addition of slip lines.

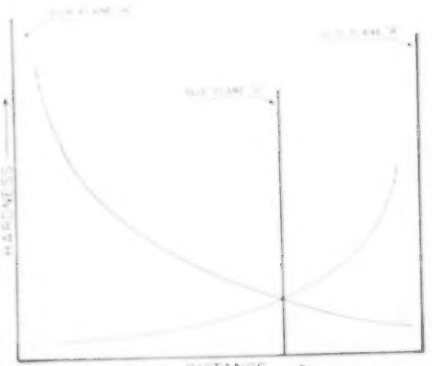

Fig. 10—Variation of hardness between two slip bands where band A has a greater shear strain than band B

Sudden Appearance of Slip Bands

In the extension of crystals A-111 and A-313, the propagation of slip bands, clearly observed in the cases with A-311 and A-206, could not be witnessed. Instead, each band, very weak and faint, but fully developed, appeared suddenly across the entire field of observation. An example showing this type of occurrence is seen in Fig. 11. Since the rate of deformation in all the experiments was almost equal, the vast difference in the appearance of formation of slip bands can be accounted for by a difference in orientation and in the plane of observation relative to the orientation. It is certain that since the observation surface in crystals A-111 and A-313 is only 6° from the plane containing the slip direction, see Fig. 4b, there is almost no upward displacement of one portion of the surface with respect to another, and thus, the lines are nearly invisible in the early

stage of deformation. Static observations after the extension showed that the appearance of slip lines in A-111 and A-313 in the vertical plane (i.e., 90° from the observation plane of Fig. 11) is analogous to that reported for crystal A-311 in Fig. 5. In this respect there is at present no evidence to support the assumption that slip in the slip direction is also by a process of propagation, or whether it is a catalytic process.

It should be pointed out that slip lines observed in the plane containing the slip direction are generally free from overlapping, except when they cross a deformation band. Since the deformation band formed in aluminum is perpendicular to the slip direction,[7] the progressive formation of a band in specimen A-111 in the horizontal plane can be easily observed, Fig. 12. The rotations involved are in accordance with the mechanism of band formation previously proposed.[7]

Discussion

Since the present experiment shows conclusively that a visible slip band is not formed suddenly around the entire crystal, the classical conception of the slip process, that slip is a uniform shear of a plane of atoms (i.e., the slip plane) in the slip direction must be modified. A definite modification, based on the observation of the propagation of slip bands at a position perpendicular to the slip direction (in specimens A-311 and A-206) would be that the unit process of slip is a shear of a row, or rows, of atoms in the slip direction. Thus, shear of each successive row of atoms in the slip direction would lead to the observed phenomenon of propagation of a visible slip band. This process is shown schematically in Fig. 13a, in which there is assumed a different amount of shear associated with each successive row of atoms from *AB* to *CD*. This is to account for the propagation of the slip band observed in the direction *BD* and also to represent qualitatively the tapering appearance generally observed at the growing front of a slip band. Consequently, the velocity, V_s, such as measured for slip bands in A-311 in this relative orientation represents only the rate at which additional rows of atoms participate in the slip process, and is not necessarily related to the velocity, V_r, at which slip takes place in the slip direction. At the present time the velocity, V_r, has not been measured owing to the inability to detect experimentally any visible slip band propagation in this direction (crystals A-311 and A-111).

It should be pointed out that the present consideration of a row of atoms as the unit of slip is quite similar to the early consideration of "rod slip"

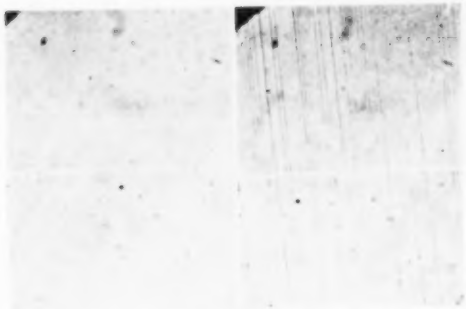

Fig. 11—Sudden appearance of fully formed slip bands in A 313. Note the absence of "overlap." Left, frame 1178; right, frame 1594.

or "pencil slip" which was proposed to explain the slip behavior in body-centered cubic metals. In the present model, however, the "rods" or rows of atoms, in the slip direction are definitely bounded by a simple (111) plane, the slip plane, and are shown to slip respectively in a progressive manner to form the visible slip band.

This model could also be interpreted from the general theory of dislocations. By definition of the two types of dislocations, it can be seen that V_s measures the velocity of the movement of the edge dislocations, whereas V_r measures the velocity of the propagation of the screw dislocations. In the present experiment, while V_s has been measured for slip bands in crystal A-311, and varies from zero as a minimum to 7600 microns per sec as a maximum at a strain rate of about 0.0007 per sec, a velocity of propagation of edge dislocations cannot be detected. The inability to detect a velocity of propagation in this direction may be interpreted as being caused by the fast-moving dislocations, approaching the velocity of sound.

The direction of propagation associated with V_r should be noted in Fig. 6, where most of the bands propagated into the field of observation from the sides and only a few started to grow from the center of the field. This seems to suggest that most slip planes were initiated at, or near, the specimen surface, containing the slip direction. It may be also that propagation of slip bands from opposite sides is a requisite in order to produce a macroscopically uniform strain of the crystal.

In Fig. 13b, the simple model of Fig. 13a is expanded to include the appearance of "overlap" of

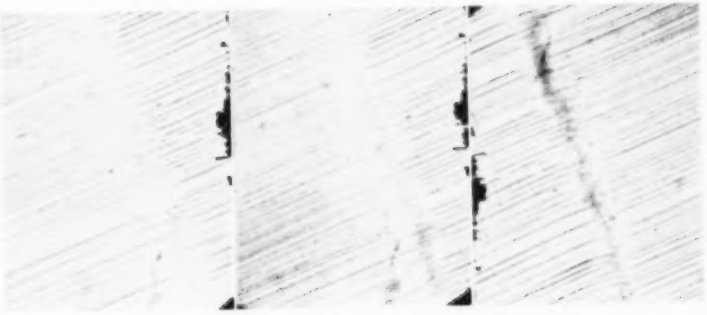

Fig. 12—Progressive formation of a deformation band in A 111.

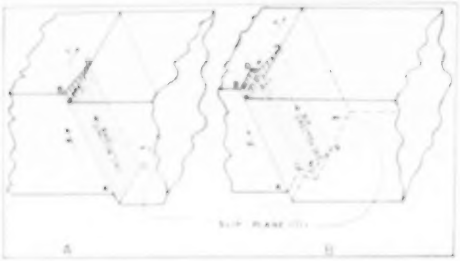

Fig. 13—Model for explaining the formation of a slip band. A—Growth of slip band. B—Overlap of slip bands.

slip bands. As shown in Fig. 13b, slip on plane *AB'C'D* may terminate quite abruptly at *CD* and proceed in another crystallographically equivalent plane, *EFGH*. The lattice region between *CD* and *EF* is here referred to as an "overlap." If this overlapped region consists of a (111) plane, different from the primary slip plane (111), and slips also in a [110] direction, then *CDEF* can be considered as a "cross-slip" plane. However, the visible band *DF* is generally very short and cannot be well resolved even under very high magnification. In many cases only a rumpled surface is observed, indicating no evidence of a slip plane, but a high distortion associated with the "overlapped" region, see Fig. 14. In this respect, the nature of the "overlap" may be very complicated and certainly may not be considered as "cross-slip" in its original sense.

The cause of the "overlap" or the "deflection of a dislocation" by different kinds of lattice disturbances such as the presence of impurity atoms, mosaic structure, lineage boundaries, etc., has been considered by Cahn.[7] In the present investigation, another possibility can be offered from the viewpoint of the progressive formation of the slip band. Since rows of atoms from *AB* to *CD* participate in the shearing process in a successive manner, there would be associated a continuous tendency of the slipped segment *AB'C'D* to rotate toward the stress-axis. The rotation may cause stress concentration near the region *CD* and thus activate slip on another slip plane *EFGH*. This explanation derives support from the rather unique relationship between the direction of slip band propagation, and the direction of the deflection of the "overlap" in crystal A-311, when analyzed from this viewpoint, see Fig. 6.

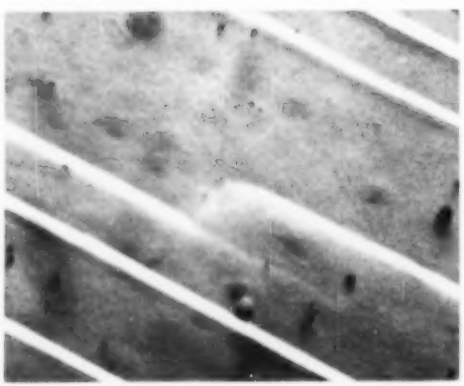

Fig. 14—"Overlap" of slip bands in A-311. X2000. Area reduced approximately 50 pct for reproduction.

Summary and Conclusions

1—An experimental apparatus has made possible the recording of the progressive formation of slip bands in a specimen which is undergoing plastic deformation.

2—Propagation of slip bands at finite rates from zero to 7600 microns per sec was observed at positions corresponding to the head of the slip direction. A similar propagation of slip bands at positions parallel to the slip direction has not been observed to date. In the former case, data of propagation of 30 slip bands has been presented together with stress rate and strain rate, Fig. 7. Strain hardening has been found to have the effect of retarding the rate of propagation of slip bands.

3—The unit process of slip is considered as a shear of a row, or rows, of atoms in the slip direction and the growth phenomenon of a slip band is considered as resulting from progressive participation in the shearing process by successive rows of atoms, see the proposed model in Fig. 13.

4—Characteristics associated with slip propagation such as the direction of propagation, the "overlap" of slip bands, and the sequential addition of slip bands are analyzed. It is concluded from the geometry of the addition of slip bands that one slip band can extend its hardening effect to its neighbors.

Acknowledgment

The authors would like to thank the Office of Air Research for support of their work under Project AF 33 (038) 12902, and the Aluminum Co. of America for supplying the high purity aluminum used in these tests. They also wish to extend their gratitude to J. H. Hoke for his assistance throughout the course of this investigation and to R. Maddin for his constructive criticism and helpful discussions.

References

1 C. Crussard: Slip in High Purity Aluminum Crystals. *Revue Metallurgie* (1945) **42**, p. 286; Figs. 3 and 5.

2 F. D. Rosi and C. H. Mathewson: A Study of the Plastic Behavior of High Purity Aluminum Single Crystals at Various Temperatures. *Trans.* AIME (1950) **188**, p. 1159; Figs. 13 to 18; JOURNAL OF METALS (September 1950).

3 R. W. Cahn: Slip and Polygonization in Aluminum. AERE Report, England (1950); Figs. 6, 10, 11.

4 H. Nishimura and J. Takamura: Effect of Strain Rate on the Plastic Deformation in Aluminum Single Crystals. *Memoirs of Kyoto University*, Japan (1951) **23**, p. 1; Figs. 8, 11, 12, 15, 20.

5 J. H. Hollomon: Nucleation of Deformation. *Trans.* A.S.M. Symposium on Cold Working of Metals (1948) p. 148.

6 N. K. Chen and C. H. Mathewson: Structural Studies of Plastic Deformation in Aluminum Single Crystals. *Trans.* AIME (1951) **191**, p. 653; JOURNAL OF METALS (August 1951).

7 Joseph Marin: Some New Testing Machines for Combined Stress Experiments. *Trans.* A.S.M. (1948) **40-A**, pp. 189-200.

8 R. Maddin, C. H. Mathewson, and W. R. Hibbard, Jr.: Unpredicted Cross-slip in Single Crystals of Alpha Brass. *Trans.* AIME (1948) **175**, p. 86; METALS TECHNOLOGY (February 1948).

9 C. S. Barrett: *Structure of Metals*, (1943) p. 294. New York: McGraw-Hill Book Co.

10 A. F. Brown: Slip Bands and Hardening Processes in Aluminum. *Journal* Inst. Metals London (November 1951) p. 115.

Mechanical Properties of Intermetallic Compounds At Elevated Temperatures

by Robert Lowrie

Nine intermetallic compounds were tested in tension at various temperatures. Seven exhibited extensive plastic deformation at elevated temperatures. Correlations of tensile strength and elongation are attempted with melting (decomposition) temperature, valence electron configurations of the component elements, heat of formation, crystal structure, density, and volume decrease accompanying compound formation.

ALTHOUGH intermetallic compounds have been known for many years, the study of their mechanical properties, particularly in tension, is just beginning. The problem has been unattractive because of the well-known, erratic behavior of brittle materials tested in tension. The strong influence of surface or internal flaws as stress raisers in nonductile materials and the effect of eccentricity of loading in superimposing bending stresses on the state of tension in the specimen are extremely difficult to mitigate and impossible to completely eliminate. Thus, tensile properties determined for brittle materials, such as intermetallic compounds at temperatures low in comparison to their melting points, are at best only general guides to the values to be expected in an ideal test of a perfect specimen of the material.

It is, nevertheless, surprising that apparently no attempt was made to follow up the pioneer work of Tammann and Dahl[1] in this field. Working with crude apparatus, these investigators succeeded in showing unequivocally that at temperatures sufficiently close to their melting points (from 75° to 400° C for the compounds tested) intermetallic compounds did exhibit plasticity. This was indicated by the appearance of slip lines on the surface of the specimen. No observations of strength were made in these tests, which were of a compressive or indentation type. Rossi[2] in 1932 attempted to study the physical and mechanical properties of single crystals of a group of intermetallic compounds. However, he was able to prepare only one material, Cu_5Zn_8, in the form of large, defect-free, single crystals. Thus, he was able to report only the relative fragility of the compounds at room temperature. He reported one compound, Ag_5Zn_8, to be somewhat plastic at room temperature and Cu_3Si to be friable, the latter in agreement with results reported herein.

Although test results are available only in classified literature, it has also been announced that MoSi$_2$ possesses some ductility at elevated temperatures.[3]

In 1948 and 1949 Savitskii[4] and Savitskii and Baron[5] published their work on the hot extrusion of Mg-Zn, Al-Mg, and Cu-Zn compounds. Under the favorable state of stress existing for this process $MgZn_2$, $MgZn_2$, Mg_2Zn_3, β (Al-Mg), γ (Al-Mg) and β (Cu-Zn) could be reduced by amounts up to 90 pct at elevated temperatures. These authors also report that hardnesses of Mg-Zn compounds decrease from room temperature values of about 300 kg per sq mm to 30 to 50 kg per sq mm at 325° C. They found that alloys consisting solely of one Mg-Zn compound were most resistant to softening on heating, mixtures of a compound and eutectic less resistant, and mixtures of two compounds least resistant. The more rapid softening of mixtures of

R. LOWRIE, Junior Member AIME, formerly Graduate Student, the Pennsylvania State College, is associated with the Lewis Flight Propulsion Laboratory, National Advisory Committee for Aeronautics, Cleveland.

Discussion on this paper, TP 3386E, may be sent, 2 copies, to AIME by Dec. 1, 1952. Manuscript, April 14, 1952; revised July 21, 1952. Philadelphia Meeting, October 1952.

This paper represents part of a thesis by R. Lowrie submitted in partial fulfillment of the requirements for the degree of Doctor of Philosophy to the Graduate School of the Pennsylvania State College.

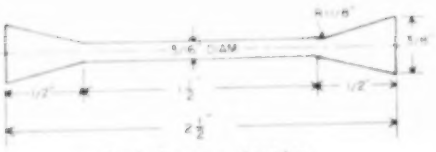

Fig. 1—Dimensions of test bar

compounds than of mixtures consisting of a compound and a terminal solid solution, is unexpected and may not be true in all or a majority of cases. Savitskii does not ascribe the great increase in plasticity of these compounds to an increase in amplitude of thermal atomic vibrations, but rather suggests that the operation of new slip systems, new types of chemical bonding, or other changes in the crystal are responsible.

In January 1947, a survey of promising lines of research for the development of improved high temperature alloys was begun by Gensamer, Larson, and the author[2] for the Bureau of Aeronautics, U. S. Navy Department. One of the recommendations of this report was that, inasmuch as no information was available on the behavior of intermetallic compounds in tension at elevated temperatures, an experimental study be made of a number of these materials. This work was begun by the author under a contract with the Bureau of Aeronautics and then continued with the assistance of an Atomic Energy Commission Predoctoral Fellowship.

The first purpose of this research program was to determine whether intermetallic compounds behave plastically when subjected to simple tension at elevated temperatures, and, if so, in what temperature ranges plasticity exists. Provided plasticity was found, it was then proposed to determine elongation and tensile strength as functions of temperature for a diverse group of intermetallic compounds. The final object of the program was an investigation of possible correlations between these mechanical properties and other physical properties of the individual compounds. Some properties which, it was believed, might correlate with strength and ductility were melting or decomposition temperature, heat of formation, valence electron configurations of the component elements, density, "volume shrinkage" upon formation from the elements, crystal structure, and the compositional range of homogeneous existence of the compound.

Specimen Preparation

Because of the well-known brittleness of intermetallic compounds at room temperature, no attempt was made to fabricate tensile specimens by machining or grinding bars of the material. Instead, the specimens were produced by casting directly to shape in special sand molds. The mold material consisted of sand, water, and a resin core binder. The molds were produced by ramming this material against precision matchplates. A sand of about 180-mesh average size was used for facing and a coarse sand for back-up. After baking, the molds were lightly painted with a zircon mold wash to prevent "burning in" and to improve generally the surface finish of the casting. The surface finish of the specimens was, in general, quite good. The irregularities were shallow and of relatively large radius of curvature. Eight test bars were cast at a

Table I. Description of Compounds

Compound	Analysis, Pct: Theoretical	Actual	Microstructure	Components
Al-Cr			Apparently single phase	99.99 pct pure Al* Electrolytic chromium
Al-Cr	(2.8 Cr)	(2.6 Cr)	Apparently single phase	Same as Al-Cr
Cr-Si			Apparently single phase	Chromium† with 0.6 pct Fe, 0.02 pct S, 0.2 pct Cr-Al-C.P. activities
Cu-Al	(16.66 Al)	16.8 Al	Single phase	99.9 pct Al, 0.04 pct Fe, 0.04 pct Si, 0.003 pct Mg* electrolytic copper, about 99.9 pct pure
Cu-Ca			Intergranular network of Cu — Cu_2Ca eutectic	Copper as in Cu_2Al_3 Calcium metal
Cu_2Al_3 I and II			Intergranular network of Cu — Cu_2Mg eutectic	Copper as in Cu_2Al_3 99.6 pct Mg (minimum)‡
Cu-P			Intergranular network of Cu — Cu-P eutectic	Commercial 15 pct P-Cu alloy
Cu-Si			Apparently single phase	Copper as in Cu_2Al_3 99.7 pct Si (minimum)‡
Ni-Si	(3.75 Si)	3.75 Si	Single phase	Electrolytic nickel,‡ nominally 0.75 pct Cu, 0.02 pct Cu, 0.01 pct Fe, traces Si, S, and C. Silicon as in Cu-Si
Ni-Si — Ni$_3$Si		14.6 Si	Two phase	Nickel and silicon as in Ni-Si
Ni-Si			Single phase	Nickel and silicon as in Ni-Si
Ni-Si			Single phase	Nickel and silicon as in Ni-Si

* Aluminum Company of America supplied the aluminum and made the Al-Cr master alloys.
† Material too brittle to be tested.
‡ The chromium was supplied by the U. S. Bureau of Mines.
§ International Nickel Co. supplied this material.

time. The dimensions of the test bar are given in Fig. 1.

The melting and casting of the compounds was accomplished in a special furnace built for the purpose. High frequency induction heating was used to prepare the compounds Ni_2Si, Ni_3Si_2, and $NiSi$. A graphite resistor of the slit-tube type[7] was used to melt the remaining alloys. This modification is shown in Fig. 2. The arrangement for withdrawing the stopper is the same as that of Parke and Bens,[7] who very graciously supplied their design, except that the activation is by hand through a sylphon bellows, J, rather than by a solenoid within the system. The melt is cast into a rotating mold, K, driven at 288 rpm by a motor reducer set. The power source was a bank of selenium rectifiers rated to deliver 1500 amp at 6 v. However, the available line voltage was considerably lower than that for which the rectifier was rated, and a maximum useful output of only 6 kw was obtainable.

The melting was performed under an atmosphere of 99.9 pct pure helium or nitrogen. Silica crucibles were used for the Ni-Si and Cr-Sb alloys, graphite crucibles for the Cu-Mg, Cu-Si, Cu-P, and Al-Cr alloys, and a stabilized zirconia crucible for the Cu-Ca alloy. Specimens of incongruently melting compounds were annealed close to their peritectic temperatures for times sufficient to complete the reactions, as determined metallographically. Descriptions of the metals used to prepare the compounds are given in Table I, as are some descriptions of microstructures and chemical analyses of the compounds.

Testing Procedure

The tensile testing was accomplished in a special furnace designed to permit testing in a neutral atmosphere, as shown in Fig. 3. The grips are of stainless steel and consist of conical inserts which fit the tapered end of the test specimen, and also a conical hole in the outer grip piece. Extension bars, which screw into these outer grip pieces, are connected to the heads of the tensile machine through spherically seated joints. A 60,000 lb maximum-capacity, Southwark-Tate-Emery hydraulic machine was used for testing. It was operated with the 1200 lb capacity range which has divisions of 1 lb each.

The electrical circuit of the furnace was a series connection of the furnace winding, a resistance equal to one-fourth that of the furnace winding, and a transformer, tapped at 10 v intervals from 10 to 110 v. A shunt across this resistance was operated by a Celectray indicating controller to maintain the temperature constant. The controlling, chromel-alumel couple was inside the alundum tube and at the approximate level of the center of the specimen. With the exception of two cases, where thermocouple trouble occurred, control appeared to be well within ±5°C. The electromotive force indicated by the controller was checked during each test with a Leeds and Northrup Type K potentiometer. The maximum deviation observed between the two voltages was 0.10 mv.

In testing, the furnace was evacuated and filled with 99.9 pct pure helium or nitrogen. The specimen was soaked at temperature for 30 min before testing. The tensile tests were conducted at approximately a constant rate by using the same setting of the loading and unloading valves of the tensile machine for all tests. The load on the specimen was read to the nearest ½ lb on the tensile ma-

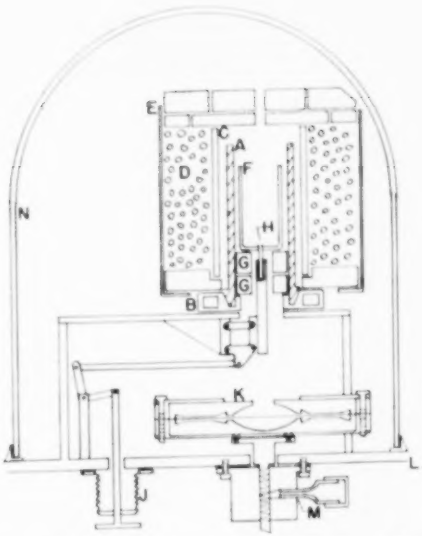

Fig. 2—Section view of furnace for melting and casting under a neutral atmosphere.

A—Slit graphite resistor
B—Water cooled electrodes
C—Alundum cylinder
D—Alumina bubbles
E—Aluminum casing
F—Crucible
G—Rings of insulating brick
H—Crucible plug
J—Sylphon bellows
K—Mold
L—Base plate
M—Grease seal
N—Bell jar

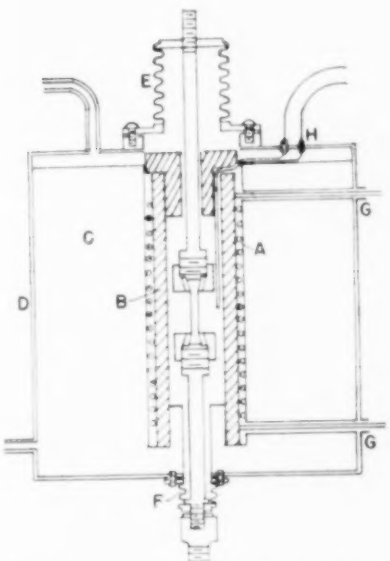

Fig. 3—Section view of apparatus for elevated temperature tensile testing.

A—Nichrome winding
B—Alundum tube
C—Insulating firebrick
D—Stainless steel shell
E—Sylphon bellows
F—Sylphon bellows
G—Kovar glass terminals, current leads
H—Kovar glass terminals, thermocouple leads

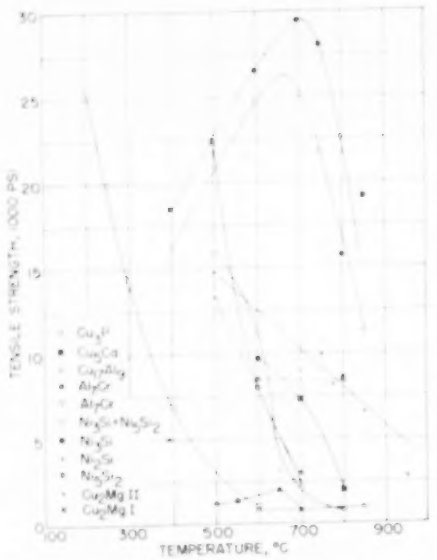

Fig. 4—Relationships between tensile strength and temperature for various intermetallic compounds.

chine. The major source of error, which amounted at most to 5 lb, was the load required to extend the upper syphon bellows. Only a general measurement of cross-head motion was taken as an indication of strain during the test. The overall length of the specimen was measured before testing and again on the re-assembled bar after fracture. The increase in length was assumed to have occurred in the 1½ in. reduced section, and the percentage of elongation was calculated accordingly. In a few

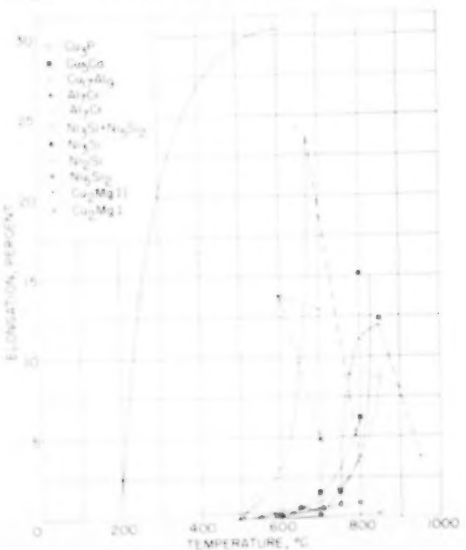

Fig. 5—Relationships between elongation and temperature for various intermetallic compounds.

cases where great elongations resulted in a poor fit of the re-assembled specimen, an appropriate correction was subtracted from the measured length before calculating the elongation. The tensile strength is calculated as the quotient of the maximum load and the original cross-sectional area.

Experimental Data

The tensile strength and elongation values of the various compounds tested are listed in Table II and are plotted vs. temperature in Figs. 4 and 5 and vs. homologous temperature in Figs. 6 and 7. The homologous temperature is defined as the quotient of the testing temperature and the melting temperature of the compound, (T/T_m), both expressed in degrees Kelvin. The critical homologous temperature is that value of T/T_m at which the elongation begins to increase rapidly from negligible values. This generally occurs at about 0.5 pct elongation. In the case of incongruently melting compounds the

Table II. Tensile Data for Intermetallic Compounds

Compound	Melting Temperature, °K	Testing Temperature, °K	T/T_m	Tensile strength, Psi	Elongation, Pct
Al_3Cr	1044*	500	0.741	1,250	0.00
		550	0.789	1,400	0.09
		650	0.885	2,000	0.60
		700	0.932	800	0.35
Al_2Cr	1294*	800	0.680	850**	0.04
		850	0.874	1,000	0.22
Cu_5Ca	1230*	500	0.598	16,000	0.29
		600	0.675	11,200	3.1
		650	0.714	3,200	24.2†
		700	0.752	2,300	22.6
		800	0.830	820	3.9‡
Cu_2Ca	1200	600	0.724	9,700	0.68
		700	0.808	3,300	1.82
		800	0.890	2,000	6.2
Cu_2Mg I	1090	500	0.706	22,400	Some elongation‡
		600	0.790	8,000	13.8
		700	0.890	3,000	4.9‡
Cu_2Mg II	1093	500	0.706	13,600	Little elongation‡
		700	0.890	2,400	13.0
Cu_3P	1295	200	0.365	25,400	1.5
		250	0.404	20,000	16.9†
		300	0.442	14,200	26.4
		400	0.520	6,900	16.5
		600	0.674	1,100	30.4
Ni_3Si	1443*	400	0.466	18,500	Little elongation‡
		600	0.605	26,000	Little elongation‡
		700	0.674	29,500	0.53
		750	0.710	28,100	1.6
		800	0.744	15,750	15.2
		850	0.779	19,200	12.4
Ni_3Si + Ni_5Si_2		400	0.466	16,300	0.37
		600	0.605	24,700	0.31
		750	0.710	21,800	1.85
		850	0.778	11,300	8.75
Ni_5Si_2	1554	600	0.565	8,500	0.68
		900	0.696	8,400	0.83
Ni_2Si	1592	500	0.485	14,800	0.04
		700	0.611	9,000	0.52
		750	0.643	9,900	0.85
		775	0.658	8,150	9.0
		800	0.674	8,600	11.1
		850	0.706	6,800	12.0
		900	0.768	2,800†	3.8*

* Denotes incongruently melting compound.
** Area used in calculation of tensile strength corrected for a blowhole.
† Length of re-assembled specimen corrected for poor fit before calculation of elongation.
‡ Intercrystalline fracture occurred.
§ Elongation not directly determinable. Qualitative result from curve of load vs. cross-head motion.
* Crack-like casting defect existed over about 1/3 of the fracture area.

melting temperature is replaced by the decomposition temperature of the compound in the definitions just given.

Two of the intermetallic compounds, CrSb and Cu_5Si, were so fragile that they could not be assembled into the grips for testing. Two others, AlCr and Al_7Cr, exhibited low strength and very limited ductility even at high melting-point fractions.

The seven remaining alloys exhibited quite similar behavior. The ductility of each is slight up to some "critical temperature" above which ductility increases rapidly. The specimens of Cu-Ca, Cu-Mg, and Cu-P contained small amounts of eutectic with copper solid solution at the grain boundaries. However, there were no indications that these eutectic networks appreciably influenced the mechanical properties of the specimens. The fractures of these specimens were, with one exception, transgranular. Thus, the full strength of the compound was developed in each case. The intergranular fracture occurred in a specimen of Cu-Mg tested at 700°C, very close to the reported temperature of the Cu + Cu_2Mg eutectic at 722°C.[7] Fig. 8 reveals that the fracture was intergranular and also that partial melting of the eutectic had occurred. This melting readily explains the course of the fracture.

The influence of these grain-boundary networks upon ductility is likewise apparently slight. While the very low "critical temperature" of Cu-P might be attributed to this structural feature, the very extensive elongations which it will undergo at slightly higher temperatures are surely evidence that the compound itself is taking a considerable part in the deformation. Cu-Mg and Cu-Ca do not become ductile until quite high testing temperatures are reached, which indicates that the plastic behavior of each of these alloys is controlled by, and representative of, the pure compound.

One case of intergranular fracture was encountered in a single-phase alloy. The Cu-Al specimen tested at 800°C broke in this manner as shown in Fig. 9. This specimen exhibited quite a low elongation.

Very pronounced maxima are present in the curves of tensile strength vs. temperature, or T/T_m, for Ni_2Si and $Ni_2Si + Ni_3Si$. The same phenomenon is apparently observable on a much smaller scale for AlCr. In each case, the maximum approximately coincides with the "critical temperature" for ductility. The maximum strength appears to be attained at the lowest temperature at which sufficient plastic deformation is possible to overcome stress concentrations and to permit the full strength of the material to be developed. The same type of behavior may exist for Cu-P, Cu-Al, Cu-Ca, and Cu-Mg for which data are not available below the critical homologous temperature. It definitely does not exist for Ni_2Si. At present no explanation is offered for this lower notch sensitivity of Ni_2Si.

The graphs of tensile strength vs. temperature and homologous temperature for Ni_2Si, Figs. 4 and 6, can both be plotted as straight lines. The scatter of points about these lines gives an indication of the approximate magnitude of the error (±1000 psi) to be expected in tests of this and other compounds in their plastic ranges. Such variability may be attributed to differences in the specimens, such as in surface finish or internal discontinuities, and to errors in determining the specimen area.

The tensile strength of the Ni_2Si specimen tested at 950°C (T/T_m = 0.768) lies somewhat below the line established by the specimens at lower temperatures. This is unexpected since usually such curves have a "toe" with curvature in the opposite direction. The elongation of this specimen is likewise unusually low. Examination of the specimen revealed a flaw in the fracture section covering roughly one-third of the area. A correction of the

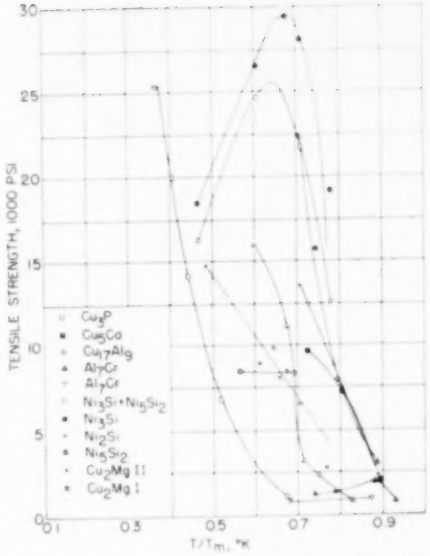

Fig. 6—Relationships between tensile strength and homologous temperature for various intermetallic compounds.

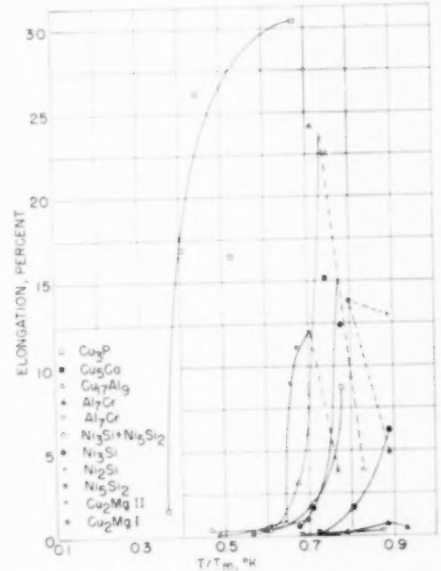

Fig. 7—Relationships between elongation and homologous temperature for various intermetallic compounds.

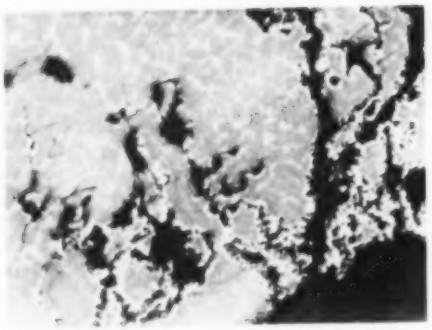

Fig. 8—Section normal to fracture surface of Cu-Mg specimen tested at 700 C and showing intergranular fracture and partial melting. 1 pct Nital etch. X100. Area reduced approximately 75 pct for reproduction.

tensile strength by the appropriate factor of 1.5 yields a value of 4200 psi, which lies very near the line established by other specimens.

The elongation vs. temperature, or T/T_m, curve is quite smooth and normal except for the value contributed by the specimen broken at 950 C (T/T_m = 0.768). The sharp notch created by the crack-like defect probably accounts for the low ductility observed.

Correlation with Melting Point

Basing their analyses upon an analogy between the fracture strength of a material and the thermal agitation required to melt it, Furth[7] and Saibel[8] have postulated theories of fracture based on thermal data. Similarly, consideration of the influence of thermal agitation upon the mechanical strength of intermetallic compounds suggests that the strength of each compound might be a common function of its melting or decomposition temperature. However it may vary at lower temperatures, the tensile strength of a material is substantially zero at its melting point, which indicates that such a correlation should exist at least at temperatures near the melting point.

The graph of tensile strength vs. T/T_m, Fig. 6, facilitates a comparison of this property for various compounds at corresponding temperatures. It is evident from this graph that the tensile strengths of intermetallic compounds are not a single-valued function of the melting point fraction. The only correlation appears to be the previously mentioned convergence toward zero strength at T/T_m = 1.0. On the other hand an unexpected correlation of melting point and ductility is observed. Five of the seven compounds which developed appreciable ductility had critical homologous temperatures in the range between 0.61 and 0.68. Cu-Ca had the slightly higher value of 0.73, while Cu$_3$P was a definite exception with a value of 0.35.

Correlation with Valence Electron Configuration

It seems reasonable to assume that the temperature dependence of the strength and ductility of intermetallic compounds should be a function of the type or types of interatomic binding present, for great differences exist between the behavior at elevated temperatures of metals, ionic compounds, and covalent materials. Since neither a quantum mechanical classification of the interatomic binding of intermetallic compounds nor an empirical one based on the percentages of ionic, covalent, and metallic binding has been made, the metal and metalloid elements have been divided into six classes of similar valence electron configuration. The assumption has been made that two elements from a given class should form compounds which possess similar interatomic binding with an element from another class. This, of course, implies the assumption that when several compounds are formed in a binary system the interatomic binding in each is of a similar character.

The classes of elements, which were chosen after consideration of groupings made by Wells,[9] Halla[10] (after Dehlinger), and Hume-Rothery[11] are: A_1, the alkali and alkaline earth metals; A_2, the transition, noble, rare earth and IB period metals; B_1, the IIB and IIIB period metals, boron and aluminum; B_2, the IVB, VB, and VIB period metalloids; N_1, the interstitial metalloids carbon and nitrogen; and N_2, silicon, phosphorus, and sulphur.

Two members of the group of compounds containing an A_1 and an A_2 metal were tested in this investigation, Cu-Mg and Cu-Ca. In addition, both materials are said to possess predominantly metallic binding.[12] and Nowotny[13] states that their crystal structures are very analogous. Structurally, both materials consisted of the compound with a grain-boundary network of copper plus the compound.

A remarkable correspondence of the strength of these compounds as a function of T/T_m is shown in Fig. 6. This would tend to indicate that intermetallic compounds which possess substantially the same type of interatomic binding and similar crystal structures will show essentially the same critical melting-point fraction and the same behavior of tensile strength as a function of T/T_m.

The three nickel silicides of group A_2N_2 all have critical melting point fractions of about 0.65. Their tensile strengths, however, are by no means such similar functions of T/T_m. While the values for Ni$_2$Si are close to the curve for Ni$_3$Si, both are far removed from the curves for NiSi and NiSi + Ni$_2$Si. In explanation of this behavior of the nickel silicides, it must be concluded that, although the types of atoms present in a compound possibly exert some influence upon the temperature dependence of the tensile strength, there must be other important factors, such as the crystal structure and the actual type of binding, in determining this relationship.

Correlation with Heat of Formation

The heat of formation, which closely approximates the free energy of formation in solid metallic systems, may be taken as a reasonable measure of binding energy. Where several compounds exist in a single binary system, the free energy or heat of formation should be an entirely satisfactory measure of their binding energies.

The only compounds investigated in this program for which experimental data on heats of formation are available are the nickel silicides, copper phosphide, and Cu-Al. Oelson and von Samson-Himmelstjerna[14] found the heats of formation of Ni-Si alloys to increase linearly from zero at pure nickel to −11.2 kcal per g-atom of alloy at Ni$_2$Si. Weibke and Schrag[15] determined the heat of formation of Cu$_3$P to be −8.0 kcal per g-atom ±4 pct. The heat of formation value reported for Cu-Al$_2$ is −5.35 kcal per g-atom,[16] considerably less than those found for Ni$_2$Si or Cu$_3$P.

From consideration of these experimental results it is evident that the heat of formation of a compound has little or no correlation with its strength at various temperatures or T/T_m levels. This complete lack of correlation may be understood by considering that the heat of formation is a quantity averaged over the entire material, while fracture is a highly localized phenomenon, and slip is generally confined to one or two sets of crystallographic planes. Thus, the details of the crystal structure as they relate to slip, cleavage, and fracture appear to be more important than the heat of formation in determining the strength of a compound.

Correlation with Crystal Structure

It appeared obvious upon initial consideration that crystal structure would be one of the factors which would influence ductility. Even pure metals show very considerable differences in the temperature dependence of their ductilities, as a result of their different crystal structures. The brittleness of intermetallic compounds has frequently been attributed to complexity of crystal structure, as compared to the simple lattices of most pure (and ductile) metals.

The crystal structures of six of the eleven compounds tested had been previously determined. Preliminary work on the remaining five had shown them to be relatively complex. Ni_2Si has perhaps the simplest lattice of any compound which was investigated. It is a simple superlattice of the Cu-Au type.[5] However, this does not result in its possessing a lower critical homologous temperature than those observed for less regular structures. Ni_3Si_2 and Ni_3Si, which are respectively hexagonal with 91 atoms per unit cell and orthorhombic with 48 atoms per unit cell, have approximately the same critical melting point fractions as Ni_2Si. Cu_3P with its extremely low critical homologous temperature of 0.360 does not have nearly so regular a lattice[6] as Ni_2Si. In the structure proposed by Steenberg[7] and substantiated by Haraldsen,[8] the atoms are found in "puckered" planes. This suggests that plastic deformation would be rather difficult to produce, which is far from the fact. However, Wyckoff[9] states that there is some evidence to show that the structure proposed by Steenberg is not correct. As a result, no final conclusions may be drawn with regard to the influence of the crystal structure of Cu_3P upon its mechanical properties.

The γ-brass type structure of Cu_9Al_4 may be thought of quite simply as an aggregate of 27 body-centered cubic cells.[10] However, because of the absence of two atoms, the resulting displacements of the remaining atoms from the true body-centered cubic positions render the structure quite complex in actuality. Nevertheless, the critical homologous temperature of Cu_9Al_4 is about the same as that of Ni_2Si.

Cu-Mg and Cu-Ca possess somewhat higher critical homologous temperatures than the compounds discussed previously. However, neither of these possesses a very complex structure. Cu-Mg has a cubic lattice[11] which approximates the closest packing for spheres with a radius ratio of 1.26. The distribution of atoms is quite regular, and it appears probable that (110) and [110] could constitute the slip system. Cu-Ca possesses a hexagonal structure[12] in which rows of contiguous calcium atoms run parallel to the c axis. Two different hexagonal nets of copper atoms are stacked alternately, enclosing these calcium rows.

The remaining four compounds are those which exhibited exceptional brittleness. The structures of Al_2Cr, Al_4Cr, and Cu_3Si have not been solved and are presumably complex. Thus, these compounds may be in accord with the idea that complexity of structure leads to brittleness. The structure of CrSb, however, as determined by Oftedal[13] and others is the rather simple NiAs structure. It consists of a layer lattice with alternate layers of chromium and antimony atoms. The chromium atoms alone would form a simple hexagonal lattice and the antimony atoms, a close-packed hexagonal lattice. So it appears that some property of the crystal lattice other than mere complexity must be called upon to account for the great differences in brittleness which exist between compounds.

Some single-crystal work to determine the cleavage and slip planes of various intermetallic compounds would be very valuable for elucidation of the influence of crystal structure upon mechanical properties. At present it can only be said that crystal structure appears to exert a profound influence on ductility, apparently determining whether the compound may become ductile at any temperature.

Correlation with Density

In general, among similar materials those having the greatest mass per unit volume would be expected to be the strongest. Accordingly, it appeared there might exist some correlation of the densities of intermetallic compounds with their strengths. Density values were obtained from the literature for ten of the eleven compounds studied. Since no data were available for Cu_3Si, a rough determination was made on a solid piece of the material.

Correlation tables were made of density and the following quantities: 1—tensile strength at the "critical temperature" for ductility; 2—maximum tensile strength observed at any temperature; 3—tensile strength at various constant homologous temperatures; and 4—tensile strength at various constant temperatures. Inspection revealed that only a very weak correlation could be said to exist between the tensile strengths and densities of intermetallic compounds.

The decrease in volume from the sum of the atomic volumes of the constituents to the molecular volume of an intermetallic compound might be considered to be a measure of the binding energy of the compound. This would be essentially true if all

Fig. 9—Section normal to fracture surface of Cu_9Al_4 specimen tested at 800°C and showing intergranular fracture. Acid ferric chloride etch. X50.

metals processed identical densities and compressibilities. However, as Biltz[7] has pointed out, metals vary greatly in the amounts of "volume shrinkage" which their intermetallic compounds exhibit. He further states that a given metal exhibits approximately a constant "volume increment" in its intermetallic compounds. Correlation tables were made of the ratio of the atomic to the molecular volume with the same quantities as those tried with density. The correlation was again so poor as not to be considered significant.

Summary and Conclusions

From tensile tests conducted on nine intermetallic compounds it can be stated that many intermetallic compounds are able to undergo extensive plastic deformation when subjected to pure tension at sufficiently elevated temperature. In general, the temperature of the onset of marked ductility lies in the range from 0.61 to 0.68 times the melting or decomposition temperature of the compound, expressed in degrees Kelvin. One compound was found which became ductile at a homologous temperature of 0.360, while two compounds did not become appreciably ductile at any testing temperature.

There is, in general, no correspondence of tensile strength and homologous temperature. However, in one case two compounds which were composed of metals of similar valence electron configurations and which were both reported to possess largely metallic binding, exhibit very close correspondence of their tensile strengths at given T/T_m values. These two compounds likewise show a close correspondence of the T/T_m values at which ductility arises.

No correlation could be found to exist between tensile strength and the heat of formation, density, or relative decrease in volume upon formation of intermetallic compounds. From this it appears that local conditions favorable to slip or fracture are more important than the overall energy of formation of the compound.

As evidenced by the four compounds of negligible ductility, there exists some factor which is related to the "degree of brittleness" of intermetallic compounds and which determines whether a given compound will become ductile at any temperature. The author suggests that this factor is intimately related to the crystal structure and proposes further work on single crystals of intermetallic compounds for its elucidation. It likewise appears probable that the tensile strength of intermetallic compounds is influenced strongly by the crystal structure.

The presence of small amounts of a eutectic containing a primary solid solution and located at the grain boundaries does not appear to appreciably influence either the strength or ductility value of an intermetallic compound at temperatures sensibly below the eutectic temperature.

Acknowledgment

The author wishes to acknowledge the assistance of an Atomic Energy Commission Predoctoral Fellowship and the loan of equipment built under Contract No. NOa(s)-9376 by the U. S. Navy, Bureau of Aeronautics. He would like to express his gratitude to Harold J. Read, to M. Gensamer, J. R. Low, Jr., and H. R. Larson in collaboration with whom this work was planned, and to the other members of the faculty and graduate students of the Division of Metallurgy of the Pennsylvania State College for their encouragement and assistance.

References

[1] G. Tammann and K. Dahl: *Ztsch. anorg. allgem. Chem.* (1923) **126**, p. 104.
[2] C. Rossi: *Ztsch. Physik* (1932) **74**, p. 707.
[3] I. E. Campbell, C. F. Powell, D. H. Nowicki, and B. W. Gonser: *Journal* Electrochem. Soc. (1949) **96**, p. 318.
[4] E. M. Savitskii: *Doklady Akad. Nauk SSSR* (1948) **62**, p. 349; Abstract *Metal Progress* (1949) **56**, p. 126.
[5] E. M. Savitskii and V. V. Baron: *Doklady Akad. Nauk SSSR* (1949) **64**, p. 693; Abstract *Metal Progress* (1949) **56**, p. 552.
[6] M. Gensamer, R. E. Lowrie, and H. R. Larson: Summary Report (Sept. 3, 1947). Contract No. N6-Onr-269, Task Order II, Office of Naval Research.
[7] R. E. Lowrie: Summary Report (Jan. 18, 1949). Contract No. NOa(s)-9376, U. S. Navy Dept., Bur. of Aeronautics.
[8] R. D. Evans: *Review of Scientific Instruments* (1933) **4**, p. 391.
[9] R. Kiessling: *Tek. Tidskr.* (1947) **77**, p. 586; *Engineer's Digest* (Amer. Edition) (1947) **4**, p. 578.
[10] W. J. Kroll, A. W. Schlechten, and L. A. Yerkes: *Trans.* Electrochem. Soc. (1946) **89**, p. 317.
[11] R. M. Parke and F. P. Bens: *Symposium on Materials for Gas Turbines* (1946) p. 80. A.S.T.M.
[12] R. Furth: *Proc.* Royal Soc. (1941) **177A**, p. 217.
[13] E. A. Saibel: *Trans.* AIME (1947) **171**, p. 639, METALS TECHNOLOGY (February 1947).
[14] A. F. Wells: *Structural Inorganic Chemistry* (1945) Oxford Univ. Press.
[15] F. Halla: *Kristallchemie und Kristallphysik Metallischer Werkstoffe* (1939) Leipzig, Verlag Barth.
[16] W. Hume-Rothery: *The Structure of Metals and Alloys* (1944) London, Inst. Metals.
[17] T. Heumann: Nachr. Akad. Wiss. Gottigen, Math-physik, Klasse, Math-physik-chem. Abt. (1948) p. 21.
[18] H. Nowotny: *Ztsch. Metallkunde* (1942) **34**, p. 247.
[19] W. Oelson and H. von Samson-Himmelstjerna: *Mitt. Kaiser-Wilhelm Inst. Eisenf.* (1936) **18**, p. 131.
[20] F. Weibke and G. Schrag: *Ztsch. Elektrochem.* (1941) **47**, p. 222.
[21] *Metals Reference Book* (1949) p. 424. London, Butterworths.
[22] *Metals Handbook* (1948 Ed.) Cleveland, A.S.M.
[23] B. Steenberg: *Arkiv Kemi, Min., Geol.* (1936-1938) **12A**, No. 26, p. 104.
[24] H. Haraldsen: *Ztsch. anorg. allgem. Chem.* (1939) **240**, p. 337.
[25] R. W. G. Wyckoff: *Crystal Structures* (1948) Vol. 1, New York, Interscience Publishers.
[26] A. J. Bradley, H. J. Goldschmidt, and H. Lipson: *Journal* Inst. Metals (1938) **63**, p. 149.
[27] J. B. Friauf: *Journal* Amer. Chem. Soc. (1927) **49**, p. 3107.
[28] W. Haucke: *Ztsch. anorg. allgem. Chem.* (1940) **244**, p. 17.
[29] I. Oftedal: *Ztsch. Physik. Chem.* (1927) **128**, p. 135.
[30] W. Biltz: *Ztsch. Metallkunde* (1934) **26**, p. 230.

Correction

In the May 1952 issue (TP 3305E, *Discussion—Institute of Metals Division*, P. 536, "On the Mechanism and Kinetics of the Scaling of Iron," Professor Paidassi's initial is incorrectly given as P. It should read J. Paidassi.

AIME OFFICERS

President—M. L. Hartman

Vice Presidents—O. B. J. Fraser, J. L. Gillson, Philip Hill, James E. Malcolm, L. P. Reinhardt, R. W. Thomas

President-Elect and Treasurer—Andrew Fletcher

AIME STAFF

Secretary—E. H. Robie

Ass't. Secretaries—L. B. Alford, H. N. Appleton, J. V. Beall, E. J. Kennedy, Jr., Ernest Kirkendall, R. E. O'Brien

Ass't. Treasurer—P. L. Agel

aime NEWS

X-Ray Studies Discussed By Fankuchen In Spokane

The importance of X-ray diffraction studies in scientific research and industrial development was explained by Prof. I. Fankuchen, head of the dept. of applied physics of the Polytechnic Institute of Brooklyn, N. Y. Speaking to a joint meeting of the Inland Empire Chemists, and members of local chapters of the American Institute of Mining and Metallurgical Engineers and American Society for Metals in Spokane, Wash., August 5, he stated that X-ray diffraction was not being used to its fullest extent. Before dinner, the Scientific Supplies Co. was host to the 80 persons attending the meeting.

Starting with the characteristics of X-rays, Prof. Fankuchen pointed out that 95 pct of their use in industry and university laboratories is for identification and analytical purposes. He called attention to their possibilities in development work, where they can be used in studying the preferred orientation of crystals, not only in metals, but also in rubber, rayon, nylon, and other modern fibers. X-rays are also useful in the study of organic compounds and in biological and clinical studies.

Prof. Fankuchen described three fields in which he is interested; small angle scattering, micro-camera techniques, and low temperature techniques. He commented that although simple crystal structure determination of solids have been made, interesting work remains in the study of materials which are liquid at room temperature, but which solidify into crystals with the proper low temperature technique.

Gift Received For Doherty Memorial Fund

The Henry L. Doherty Memorial Fund, established in 1945, has received a gift of $50,000 from the estate of the late Mr. Doherty. For several years the Cities Service Co. has contributed $5000 annually in lieu of income from the Fund, but this is the first large gift to the principal of the Fund. A further $50,000 is expected shortly from three other sources to establish a total Fund of $100,000.

This group from Bunker Hill & Sullivan Mining Co., Kellogg, Idaho, were among the 80 attending the August 5 meeting on X-ray diffraction at Spokane, Wash. Rear row: Fergus Strathie, Frank Sinclaire, A. Y. Bethune. Middle row: C. C. Papoff, Leo Baumeister, Walter Schmittroth, Glenn Blickensderfer. Front row: J. W. Johnson, Lamar Burgess, Kenneth Kirkpatrick, Donald Involdstad.

Mrs. Helen Lee Wessel, president of The Henry L. and Grace Doherty Charitable Foundation, Inc., made the gift in the form of Surface Combustion Corp. 5 pct debentures "as a contribution by this Foundation to American Institute of Mining and Metallurgical Engineers." Mrs. Wessel adds, "It is our further understanding you are contemplating that the income from the Fund will be used to finance the printing and distribution of publications, to grant scholarships, and for research in matters relating to the petroleum industry, all, to the extent feasible, within fields and along lines in which the late Henry L. Doherty was known to be deeply interested."

Heretofore, the annual contribution from the Cities Service Co. has been used for meeting the cost, in part, of the annual petroleum statistics volume and of the Buckley volume on *Petroleum Conservation*.

The committee administering the Fund has, since the Fund was established, consisted of John M. Lovejoy, Chairman, with Warren A. Sinsheimer and E. DeGolyer.

C. D. King To Deliver Howe Memorial Lecture

The Iron and Steel Div. has recommended, and the Board has approved, naming of C. D. King, chairman of operating committees of the U. S. Steel Corp., Pittsburgh, as Howe Memorial Lecturer for 1954.

Howe Memorial Lecturer for 1953 is Joseph Winlock, chief metallurgist of the Budd Co., Philadelphia.

AIME Membership Card No Longer Dues Receipt

Decision has been made to send out the 1953 membership card to AIME members, in good standing, along with the regular year-end bill for dues. Heretofore no membership card has been sent until payment has been received. This necessitated a second mailing and sometimes resulted in delay at peak periods or when it was impossible to identify a payment without further correspondence, as often happens when payment is made by a bank or by an employing company. A saving to the Institute of possibly $1000 should result.

The membership card will not, therefore, constitute a receipt for dues as it has in the past. Canceled checks of members will constitute a receipt. When payment is made by means whereby the member cannot be sure that his dues have been received by AIME headquarters, a receipt will be mailed if requested. An evidence that AIME headquarters lists a member as unpaid is the non-receipt of journals beginning with the April issues. Members are cut off the mailing list in March if their dues have not been received.

It is hoped that this new practice will meet with the approval of members and will result in prompt payment of dues.

Whatever Your Metallurgical Problem . . .

CM Metallurgical Microscope

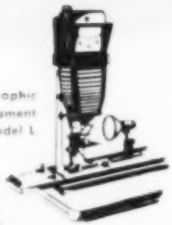

Photomacrographic Equipment Model L

Stereomicroscopes

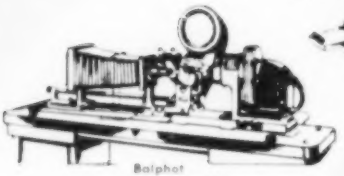

Balphot Metallograph

Research Metallograph

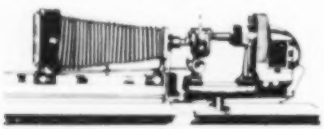

ILS Metallograph

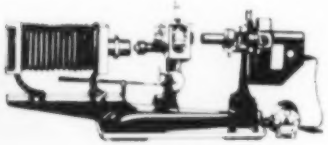

MILS Metallograph

the Bausch & Lomb COMPLETE LINE will help you solve it!

IN advanced research or in quality control, you'll get better results, faster, with the right instrument or combination of equipments from the Bausch & Lomb metallographic line—the most complete serving industry.

FOUR different metallographs—for routine bright field studies or advanced analyses requiring interchangeable phase contrast, bright field, dark field and polarized light.

- Photomacrographic Equipment Model L—widest low power range; no time lost in converting metallograph from high power set-up.
- CM Metallurgical Microscope—industry's standard.
- Stereomicroscopes—unequalled for 3-dimensional low power studies.

Let us help you select the equipment and set up the operating procedures that will most efficiently solve your problem. No obligation, of course.

WRITE for complete information. Bausch & Lomb Optical Co., 78710 St. Paul St., Rochester 2, New York.

Bausch & Lomb *Metallurgical* Equipment

Personals

Mark S. Lyons has accepted a position with the U. S. Vanadium Corp., Bishop, Calif.

Robert S. Lehto is now junior metallurgist in the smelting and refining div., Cerro de Pasco Corp., La Oroya, Peru.

Howard F. Martin, operations consultant in the office of the executive vice-president, production, Jones & Laughlin Steel Corp., has retired after 28 years with the firm.

S. J. SINDEBAND

S. J. Sindeband, executive vice-president of the Mercast Corp. and president of Alloy Precision Castings Co. was recently in Europe to study European production problems.

D. Levinger has retired from the Western Electric Co., Chicago.

Frank N. Speller has become an associate member of Management Counselors, Inc., New York.

Harry N. Elsey formerly with the Republic Supply Co., Kilgore, Texas has joined the Maloney-Crawford Tank & Mfg. Co., Wichita Falls, Texas.

Charles W. Hammond has been appointed head of the mechanical engineering dept., Walter Kidde Nuclear Laboratories, New York.

Edgar C. Bain, vice-president in charge of research, U. S. Steel Co., has been awarded the Grand Medal of the French Society of Metallurgy.

Cyril Stanley Smith has been named recipient of the Francis J. Clamer Medal by the Franklin Institute, for his metallurgical contribution to the development of atomic energy during and since World War II. Dr. Smith is professor of metallurgy and director of the Institute for the Study of Metals, University of Chicago.

H. P. Saxer, formerly assistant works manager, general services, Jones & Laughlin Steel Corp., Pittsburgh, has been appointed assistant works manager, production.

Harry L. Smith, Jr. has been made staff manager, product sales, Aluminum Co. of America.

Joseph H. Bach is section head, atomic energy div., Sylvania Electric Products, Inc., Bayside, N. Y.

A. G. Wolf, manager of the geological dept., **C. O. Stephens,** manager, gas dept., and **H. W. Strickland,** assistant to president, have been named vice-presidents of the Texas Gulf Sulphur Co.

James H. Lowe has been appointed product development director of the Steel Founders' Society of America. Mr. Lowe was formerly technical and research director of the Wehr Steel Co., Milwaukee.

W. Norman Sims has joined the American Cyanamid Co., New York. He recently resigned from the Philadelphia & Reading Coal & Iron Co., Philadelphia.

M. A. Ryan is now employed as a metallurgist by the General Electric Co., Richland, Wash.

Robert W. Crozier has been appointed regional manager in charge of the Pittsburgh and Cleveland offices of the Electro Metallurgical Co., div. Union Carbide & Carbon Corp.

Edward J. Duffy is assistant to the works manager, Kaiser Steel Corp., Fontana, Calif.

M. J. Day, formerly assistant metallurgical engineer with the U. S. Steel Co., Pittsburgh, is now manager, materials and processes div., Armour Research Foundation, Chicago.

Jess L. Belser is now production metallurgist of the sand casting foundry at the Watertown Arsenal.

J. K. Brooke has joined the chemical div., Kaiser Aluminum & Chemical Corp., Oakland, Calif., as senior engineer, raw materials dept.

Milton H. Fies was named vice-president in charge of mining for Alabama Power Co. Mr. Fies is a past Director of AIME.

Louis S. Castleman is supervisory scientist with the Westinghouse Atomic Power div., Bettis Field, Pittsburgh.

Robert J. Christ has accepted a position with John Deere & Co., materials engineering dept., Moline, Ill.

Hugh H. Bein has resigned from the AEC, Grand Junction, Colo., and is now with the American Cyanamid Co., Watertown, Mass.

Byron G. MacNabb has joined the research and development staff of Alloy Engineering & Casting Co., Champaign, Ill. as associate director. He had previously been assistant to the director of research, Pullman Standard Car Mfg. Co.

Leonard Frank is now metallurgist with the American Steel & Wire Co., Joliet, Ill.

Charles W. Walton has been appointed senior research analyst by Chemical Construction Corp.

Edward M. Lytle is now employed as a production assistant by the Kaiser Steel Corp., Fontana.

A. M. Gaudin recently presented the Sir Julius Wernher Memorial Lecture for the Institution of Mining and Metallurgy, London.

NORMAN PINTCHUK

Norman Pintchuk has joined Solar Aircraft Co., San Diego as foundry metallurgist. Mr. Pintchuk was formerly with the manufacturing research div. of International Harvester Co., Chicago.

L. F. Hickernell, chief engineer of the Anaconda Wire & Cable Co., Hastings-on-Hudson, N. Y., has been named chairman of the newly formed Committee on Technical Operations, American Institute of Electrical Engineers.

Richard E. Lindberg is with the U.S. Vanadium Corp., Bishop, Calif.

S. A. Goudsmit has been appointed chairman of the physics dept., Brookhaven National Laboratory, Upton, N. Y. and **G. N. Glasoe** has been named associate chairman. **Marvin Fox** will head the reactor dept. as chairman and **Clarke Williams** was appointed chairman of the nuclear engineering dept. These two departments had previously been grouped as one.

Advertisement

ELECTROMET Data Sheet

A Digest of the Production, Properties, and Uses of Steels and Other Metals

Published by Electro Metallurgical Company, a Division of Union Carbide and Carbon Corporation, 30 East 42nd Street, New York 17, N. Y. • In Canada: Electro Metallurgical Company of Canada, Limited, Welland, Ontario

How SILICOMANGANESE Saves Furnace Time . . . Produces Better, Cleaner Steel

Silicomanganese is used by the steel industry as a furnace block* and deoxidizer, and also for manganese additions.

The cleanness and quality of steel depend largely on how well it has been deoxidized. Deoxidation also greatly influences the physical properties of steel for rolling and subsequent fabrication. Silicomanganese combines two active deoxidizers in a single alloy and it has proved to be a more effective deoxidizer than silicon or manganese alloys added separately. This combination alloy contains silicon and manganese in the correct proportion — approximately 1 to 3.5 — to be most effective in reducing the oxygen content of the bath to a low level. The use of silicomanganese produces cleaner steel, saves furnace time, and gives high alloy recovery for manganese additions.

Gets More Oxygen Out of Bath

When silicomanganese is used for blocking and deoxidation, the combined effect of silicon and manganese lowers the oxygen content to a greater degree than silicon alone. This is due to the fact that the amount of oxygen in equilibrium with a given amount of silicon is lower in iron-silicon-manganese alloys than it is in plain iron-silicon alloys, as shown in Fig. 1.

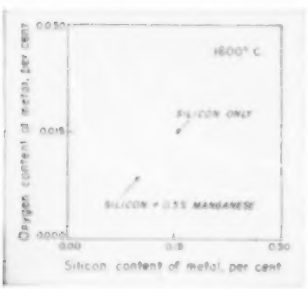

Fig. 1. Effect of addition of manganese to iron-silicon alloys. Alloys and with 0.30 per cent manganese at 1600° C.

The metal deoxidizer or steel frequently referred to as the furnace block, drops the carbon-oxygen reaction in the furnace. This arrests the carbon drop immediately and makes it possible to secure close control of analysis. If the oxygen content of the metal is reduced well below the level established by the carbon-oxygen reaction, metal deoxidation is accomplished.

Less Inclusions, Cleaner Steel

In addition to lowering the oxygen content, silicomanganese has a specifically beneficial effect on inclusions. The inclusions in a steel depend in large part on how low the carbon content (or how high the oxygen content) is before blocking. The lower the carbon, the dirtier the final steel, almost regardless of the subsequent deoxidation treatment. Since silicomanganese has a low carbon content, it is not necessary to drive the carbon as low (or make the oxygen as high), as when high-carbon or standard ferromanganese is used, so that the final steel is cleaner and has better working properties. The improved cleanliness resulting from silicomanganese is usually noticeable in higher carbon steels, but is outstanding in steels below 0.25 per cent carbon where inclusions and surface defects are a vital problem and where the time saved by blocking at a higher carbon level is significant.

Fast Solubility In Bath

Because of the high concentration of active elements in silicomanganese, less time is required to effect solution of this alloy than when equivalent amounts of silicon and manganese are used separately in the form of ferrosilicon and ferromanganese.

For example, compare these typical analyses of silicomanganese, standard ferromanganese, and 50 per cent ferrosilicon:

	Silicomanganese, %	Standard Ferromanganese, %	50% Ferrosilicon, %
Manganese	66.5	80	—
Silicon	19	—	50
Carbon	1.5	7	—
Iron, approx	13	13	50

From this it can be seen that 1,000 lb. of silicomanganese would contain 190 lb. of silicon and 665 lb. of manganese. These amounts of silicon and manganese would require 380 lb. of 50 per cent ferrosilicon and 840 lb. of standard ferromanganese, or a total of 1,210 lb. Obviously it is easier and faster to dissolve 1,000 lb. of the combination alloy silicomanganese than 1,210 lb. of these separate silicon and manganese alloys.

Lower Carbon Content

Silicomanganese contains less carbon than any combination of ferrosilicon and standard ferromanganese. Therefore, the carbon-oxygen reaction in the bath can be stopped earlier when silicomanganese is used for blocking. Heats can be blocked at higher carbon levels and hence lower oxygen contents, and the amount of deoxidation required is less.

Fig. 2. Charging silicomanganese into an open-hearth furnace.

Saves Furnace Time

Because of the advantages outlined, silicomanganese can save as much as 20 minutes per melt in the production of open-hearth steel. For low-carbon steel, an even greater saving in time can be realized.

For Producing Engineering Steels

Silicomanganese is also used for alloy additions of manganese, particularly in the production of engineering steels containing 0.10 to 0.50 per cent carbon.

When manganese or other oxidizable additions, such as chromium, must be made to the bath, the use of a block provides a higher alloy recovery. Silicomanganese introduces manganese with the silicon and the usual recovery of this manganese will range from 70 to 85 per cent.

Metallurgical Service Available

Ask to have one of our metallurgists call and explain more fully the advantages of silicomanganese as a furnace block and deoxidizer. He will be glad to help you with the use of ELECTROMET silicomanganese. This alloy contains 65 to 68 per cent manganese and is produced in maximum 1.50, 2.00, and 3.00 per cent carbon grades. All grades are furnished in a lump size of 75 lb. x 2 in. and in a crushed size of 2 in. x down. Write, wire, or phone the nearest ELECTROMET office.

The word "Electromet" is a registered trademark of Union Carbide and Carbon Corporation.

Obituaries

Appreciation of

Hugh M. Shepard

by T. D. Jones

The Extractive Metallurgy Div., AIME lost one of its most ardent supporters when Hugh M. Shepard died suddenly on May 30.

"Shep" as he was affectionately known to all his associates, assisted John Sullivan and Carleton Long in the organization of the EMD and served as its first secretary.

Mr. Shepard was born in Hamilton, Ont. in 1899 and majored in metallurgical engineering at the

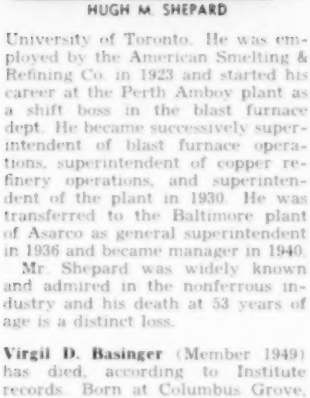

HUGH M. SHEPARD

University of Toronto. He was employed by the American Smelting & Refining Co. in 1923 and started his career at the Perth Amboy plant as a shift boss in the blast furnace dept. He became successively superintendent of blast furnace operations, superintendent of copper refinery operations, and superintendent of the plant in 1930. He was transferred to the Baltimore plant of Asarco as general superintendent in 1936 and became manager in 1940.

Mr. Shepard was widely known and admired in the nonferrous industry and his death at 53 years of age is a distinct loss.

Virgil D. Basinger (Member 1949) has died, according to Institute records. Born at Columbus Grove, Ohio in 1917, Mr. Basinger was a graduate of Bluffton College and Ohio State University. In 1939 he joined the Ohio Steel Foundry Co., Lima, Ohio as chemical laboratory technician. During World War II Mr. Basinger was in the Army and spent some time in England. After his discharge he accepted a position as metallurgical engineer with the Cincinnati Milling Machine Co. At the time of his death, Mr. Basinger was residing at Goshen, Ohio.

John C. Reed (Member 1947) vice-president in charge of research, American Radiator & Standard Sanitary Corp., died on June 14. Mr. Reed was born in 1902 at Glenfield, Pa. and graduated from Pennsylvania State College in 1928. After graduation he was employed by the Vesta Coal Co., and in 1929 joined the American-Standard firm at Louisville, Ky.

NECROLOGY

Date Elected		Date of Death
1947	Reginald K. Bailey	Dec. 16, 1951
1935	J. G. Bentin	Unknown
1920	Harold E. Boyd	June 24, 1952
1912	Thomas H. Clagett	July 23, 1952
1945	Jack W. Clark	Aug. 8, 1952
1933	W. T. Griffiths	July 30, 1952
1947	Fred B. Heath	July 25, 1952
1942	B. W. Jacobs	Unknown
1944	H. A. McAllister	Unknown
1929	George L. Richert	May 26, 1952
1899	H. Ries	April 1951

Proposed for Membership
— Metals Branch AIME —

Total AIME membership on Aug. 31, 1952 was 18,125, in addition 1555 Student Associates were enrolled.

ADMISSIONS COMMITTEE

T. D. Jones, Chairman; Thomas G. Moore, Vice-Chairman; Harold S. Bell, F. W. Hanson, R. H. Chadwick, T. W. Nelson, J. H. Senff, John T. Sherman, A. C. Bruker, Ivan Given, C. A. R. Lansley, G. P. Luljen, E. A. Prentis, and C. Leslie Rice, Jr.

The Institute desires to extend its privileges to every person to whom it can be of service, but does not desire as members persons who are unqualified. Institute members are urged to review this list as soon as possible and immediately to inform the Secretary's office if names of people are found who are known to be unqualified for AIME membership.

In the following list C/S means change of status; R, reinstatement; M, Member; J, Junior Member; A, Associate Member; S, Student Associate.

Alabama
Birmingham—Byrns, Howard A. (M)

Colorado
Rifle—Goth, John W. (J) (R, C.S—S-J)

Connecticut
Trumbull—Chudy, Frank S. (M)

Illinois
Barrington—Mathesius, Walther (M) (R, C.S—J-M)
Chicago—Hymes, Leslie C. (J)
Chicago Heights—Carruthers, Robert C. (J) (R, C.S—S-J)
Park Ridge—Glos, Edmond A., II (J)

Indiana
Fort Wayne—Knight, Donald P. (M)
Gary—Burt, Robert R. (J) (C.S—S-J)
Gary—Dickson, Ralph W. (M)

Michigan
Birmingham—Rundle, Donald F. (M)
Detroit—Carter, Roger V. (J)
Detroit—Holst, Henry V. (J)
Detroit—Sernka, Richard P. (J)
Highland Park—Schlachter, Herbert J. (J)
Midland—Roberts, C. Sheldon (J) (C.S—S-J)

New Jersey
Fords—Kapp, Hans R. (J)

New York
Ballston Lake—White, Donald W., Jr. (M) (R, C.S—S-M)
Levittown—Chynoweth, William (M) (R, C.S—S-M)

Brazil
Sao Paulo—Macari, Hanney (A)
Sao Paulo—Reginato, Jordao (A)

Germany
Oberhausen (Rheinland)—Dick, Walther H. (M)

New
METALLURGY BOOKS

METALLURGICAL ENGINEERING

By Reinhardt Schuhmann, Jr.
Massachusetts Institute of Technology

390 pp, 155 illus, 1952, $7.50

Presents metallurgical engineering according to basic principles and unit processes rather than according to metals treated. Stresses integration of physical chemistry with metallurgical engineering and emphasizes analysis and quantitative solution of engineering problems rather than descriptive treatment of current practices.

THERMODYNAMICS OF ALLOYS

By Carl Wagner
Massachusetts Institute of Technology

161 pp, 37 illus, 1952, $6.50

Summarizes principles of thermodynamics of binary and multicomponent systems, methods of experimental determination of characteristic thermodynamic quantities such as heat of mixing formation, partial free energies of mixing, activities, etc.; methods of calculating thermodynamic quantities from other quantities which have been measured, available experimental data and indirectly obtained values; atomic and electronic interpretation of data; treatment of equilibria between alloys, salt melts, oxide melts, silicate melts, etc.

ELEMENTS OF CERAMICS

By F. H. Norton
Massachusetts Institute of Technology

246 pp, 194 illus, 1952, $6.50

Presents principles underlying the various processes used in the ceramic field with illustrative applications. Emphasis is on unit processes rather than products. A complete reference for research workers and ceramic engineers, by one of the foremost authorities of the present time.

ELEMENTS OF PHYSICAL METALLURGY

By A. G. Guy, *Purdue University*

293 pp, 218 illus, 1951, $6.50

Fundamentals of physical metallurgy with emphasis on underlying ideas of the subject rather than applications. Important applications are introduced as illustrative examples. Examples are made quantitative rather than merely qualitative. A broad, unspecialized coverage of the whole field, including an unusual appendix of the literature of metallurgy.

The above books are part of

THE ADDISON-WESLEY METALLURGY SERIES

Morris Cohen, *Consulting Editor*

Detailed descriptions of above books are available upon request

ADDISON-WESLEY PRESS, INC.
CAMBRIDGE 42, MASS

NEW
Streamlined
AB
SPEED PRESS

The most advanced design in press equipment for speed, convenience, and economy in the production of Bakelite and Transparent Molded Specimen Mounts ever presented to the metallurgist.

A revolutionary feature introduced in this new press is preheated Premolds. The preheat compartment reduces the curing time of thermosetting molds to one-third of the time usually required. It enables the operator to produce perfect Bakelite Mounts in 2½ to 3½ minutes. All necessary indicators and controls including pressure gauge, pyrometer, thermostats, timer and pilot lights are provided. No experience is required to produce perfect mounts. Automatic ram retraction saves time and effort.

The hinged press head is made with a semi-automatic lock and a hand wheel screw to close the mold securely. Heating blocks are arranged with a magnetic closure to snugly envelop the mold assembly. The interchange of thermostatically controlled heating units of 600 watt capacity is facilitated by convenient supports. Cooling blocks are located in a practical position in front of the press cabinet.

This new speed press is the result of long exacting experiment, with every effort devoted to designing the finest modern specimen press we are able to engineer.

No. 1330 AB Speed Press, complete for 1" mountings $420.00

No. 1330-2 AB Speed Press, complete for 1¼" mountings $440.00

No. 1330-3 AB Speed Press, complete for 1½" mountings $460.00

THE BUEHLER LINE OF SPECIMEN PREPARATION EQUIPMENT INCLUDES . . . CUT-OFF MACHINES • SPECIMEN MOUNT PRESSES • POWER GRINDERS • DISC GRINDERS • HAND GRINDERS • BELT SURFACERS • MECHANICAL AND ELECTRO POLISHERS • POLISHING CLOTHS • POLISHING ABRASIVES.

Buehler Ltd.

A PARTNERSHIP

165 WEST WACKER DRIVE CHICAGO 1, ILLINOIS

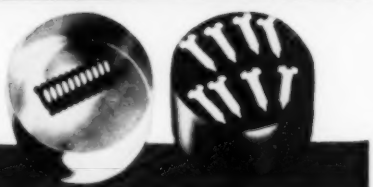

METALLURGICAL APPARATUS

Coming Events

Sept. 30-Oct. 3. Assn. of Iron and Steel Engineers, exposition and convention, Cleveland Public Auditorium, Cleveland.

Oct. 1-3. National Assn. of Corrosion Engineers, South Central Region, Jung Hotel, New Orleans.

Oct. 3. AIME, Southern Ohio Section, National Open Hearth Steel Committee, Deshler-Wallick Hotel, Columbus, Ohio.

Oct. 7-9. Iron and Steel Institute, Swansea, Wales, England.

Oct. 10. AIME, Eastern Section, National Open Hearth Steel Committee, Warwick Hotel, Philadelphia.

Oct. 10. AIME, Southwestern Section, National Open Hearth Steel Committee, Peoria, Ill.

Oct. 13-17. Canadian Institute of Mining and Metallurgy, annual western meeting, Royal Alexandra Hotel, Winnipeg.

Oct. 18-24. National Metal Exposition and Congress, Philadelphia.

Oct. 20-21. Special Libraries Assn., metals section, regional meeting, National Metal Congress, Philadelphia.

Oct. 20-22. AIME, Institute of Metals Division fall meeting with National Metal Congress, Hotel Adelphia, Philadelphia.

Oct. 20-24. American Welding Society, meeting with National Metal Congress, Bellevue-Stratford Hotel, Philadelphia.

Oct. 20-24. American Society for Metals, meeting with National Metal Congress, Benjamin Franklin Hotel, Philadelphia.

Oct. 20-24. National Safety Congress and Exposition, Conrad Hilton, Congress, Morrison, LaSalle, and Sheraton Hotels, Chicago.

Oct. 21-24. Society for Nondestructive Testing, meeting with National Metal Congress, Hotel Sylvania, Philadelphia.

Oct. 28. Assn. of Consulting Chemists and Chemical Engineers, Inc., open-door dinner meeting, Hotel Belmont Plaza, New York.

Oct. 30-31. AIME, Fuels Conference: Coal Div., AIME; Fuels Div., ASME, Bellevue-Stratford, Philadelphia.

Oct. 31. Metropolitan Brass Founders Assn., Inc., show and dance, Hotel New Yorker, New York.

Nov. 4. AIME, Morenci Sub-section, Longfellow Inn, Morenci, Ariz.

Nov. 7. AIME, Pittsburgh Section, National Open Hearth Steel Committee, off-the-record meeting, Hotel William Penn, Pittsburgh.

Nov. 18. AIME, Buffalo Section, National Open Hearth Steel Committee, Hotel Statler, Buffalo.

Nov. 19. AIME, Connecticut Section, Hartford, Conn.

Nov. 19. Institute of Metals, lecture theater, Royal Institution of Great Britain, London.

Nov. 20-21. American Society for Quality Control, Midwest Conference, Claypool Hotel, Indianapolis, Ind.

Dec. 1-6. AIME, Electric Furnace Steel Conference, Hotel William Penn, Pittsburgh.

Dec. 7-10. American Institute of Chemical Engineers, annual meeting, Hotels Cleveland and Carter, Cleveland.

Dec. 8. AIME, Arizona Section, all day meeting, Tucson.

Jan. 14, 1953. AIME, Connecticut Section, Hammond Metallurgical Laboratory, Yale University, New Haven, Conn.

Jan. 26-30. American Society of Heating and Ventilating Engineers, international heating and ventilation exposition, International Amphitheatre, Chicago.

Feb. 16-19. AIME, annual meeting, Statler Hotel, Los Angeles.

Mar. 8-11. American Institute of Chemical Engineers, Buena Vista Hotel, Biloxi, Miss.

Mar. 11. AIME, Connecticut Section, Waterbury, Conn.

Mar. 16-20. National Assn. of Corrosion Engineers, annual conference and exhibition, Hotel Sherman, Chicago.

Mar. 23-27. ASM, western metal congress and exposition, Pan-Pacific Auditorium, Los Angeles.

Apr. 12-May 23. Empire Mining and Metallurgical Congress, Australia-New Zealand.

Apr. 20-22. AIME, National Open Hearth and Blast Furnace, Coke Oven and Raw Materials Conference, Hotel Statler, Buffalo.

May 14-16. AIME Pacific Northwest Metals and Mineral Conference, joint meeting, Metals Branch and Industrial Minerals Div., Ben Franklin Hotel, Seattle.

June 3-7. Chemical Institute of Canada, Windsor, Ont.

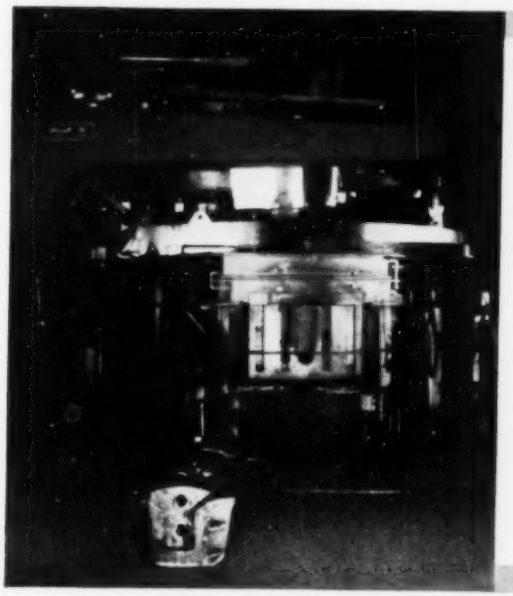

Heroult

ELECTRIC MELTING FURNACE

. . . as ever, the dependable furnace for the production of high-grade stainless, alloy and rimming steels.

Removable roof of new design now available for the larger furnaces.

AMERICAN BRIDGE DIVISION
UNITED STATES STEEL COMPANY

General Offices: 525 William Penn Place, Pittsburgh, Pa.
Contracting Offices in New York, Philadelphia, Chicago, San Francisco and other principal cities

AMERICAN BRIDGE

USS

UNITED STATES STEEL

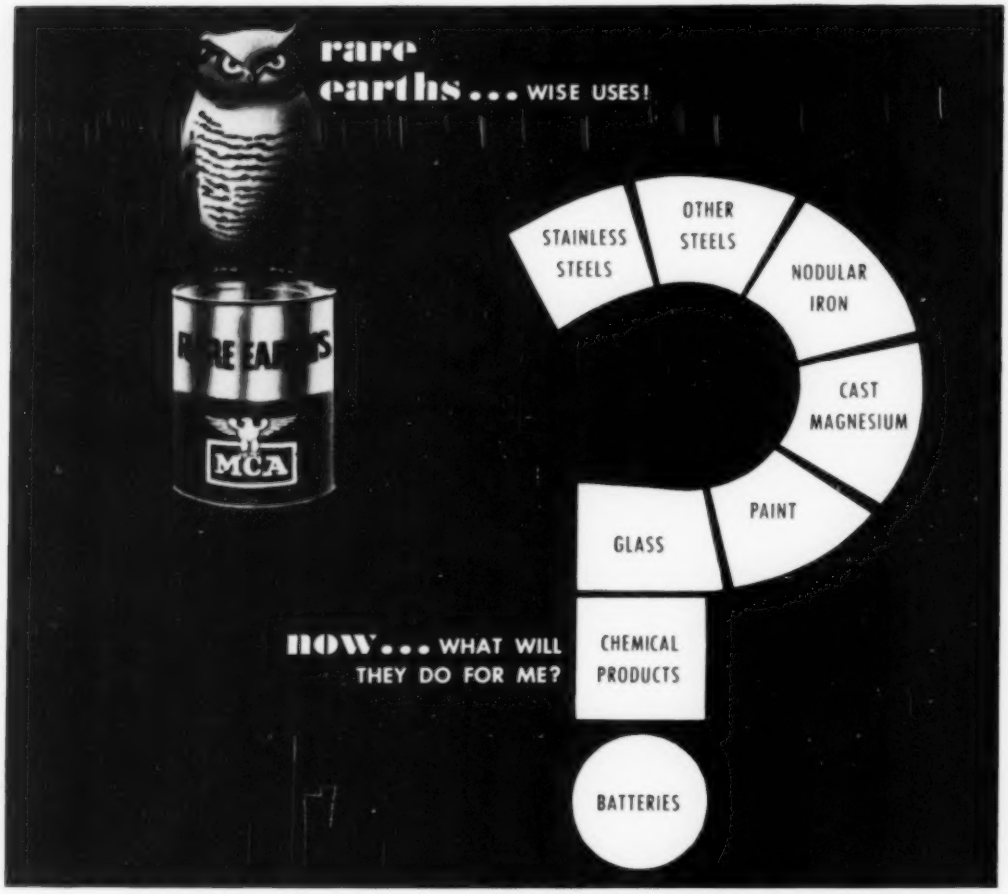

New abundance of raw materials obtainable within the United States, newly developed methods of refinement, new knowledge of the properties of Rare Earth substances, new uses tested and definitely proved by the Molybdenum Corporation:

. . . surely you will be interested in applying to your production the benefits of such discoveries. Ample test-records and other data are available, and are at the service of all who can put them to good use.

The Molybdenum Corporation invites and solicits your inquiry.

AMERICAN Production, American Distribution, American Control, Completely Integrated

Offices: Pittsburgh, New York, Chicago, Cleveland, Detroit, Los Angeles, San Francisco

Sales Representatives: American Steel and Supply Co., Chicago; Edgar L. Fink, Detroit; Brumley-Donaldson Co., Los Angeles, San Francisco

Subsidiaries: Cleveland-Tungsten, Inc., Cleveland, O.; General Tungsten Manufacturing Co., Inc., Union City, N. J.

Works: Washington, Pa.; York, Pa.

MOLYBDENUM

CORPORATION OF AMERICA
Grant Building Pittsburgh, Pa.

MCA

AJAXOMATIC

AN AUTOMATIC POURING UNIT FOR THE PRODUCTION OF ALUMINUM DIE CASTINGS

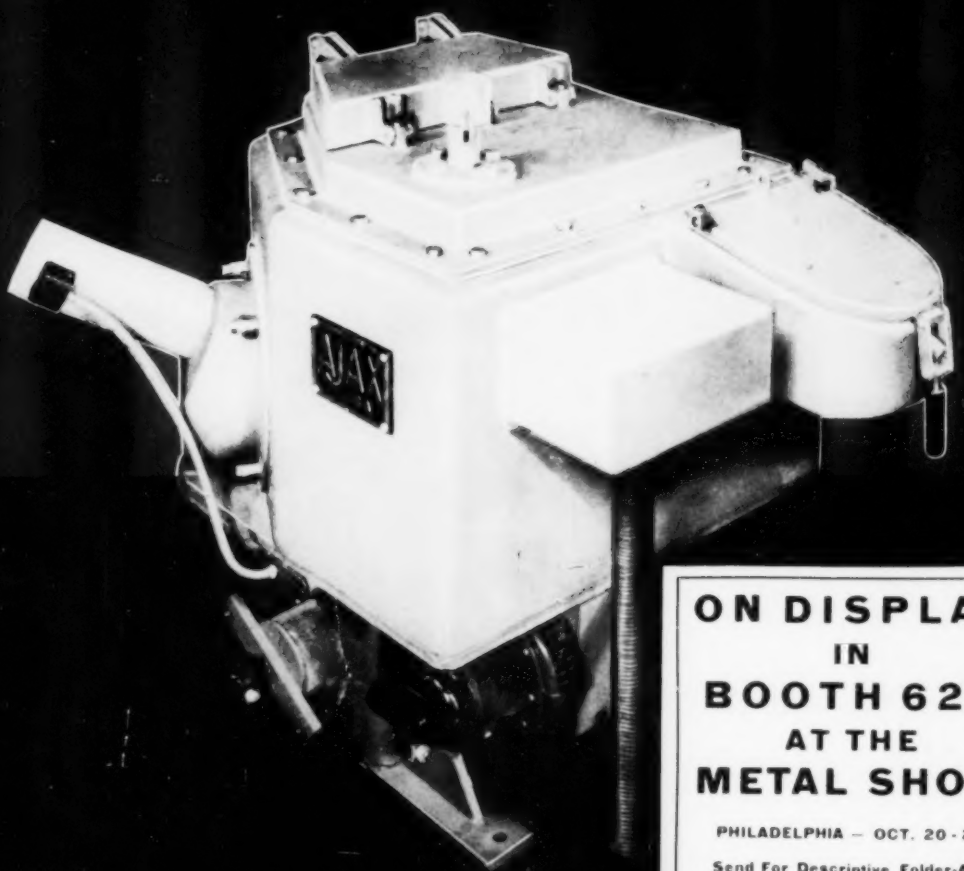

ON DISPLAY IN BOOTH 624 AT THE METAL SHOW

PHILADELPHIA — OCT. 20-24

Send For Descriptive Folder-A-1

AJAX ENGINEERING CORPORATION

TRENTON, N. J.

LEWIS

4 high reversing cold strip mills for Dependable Production

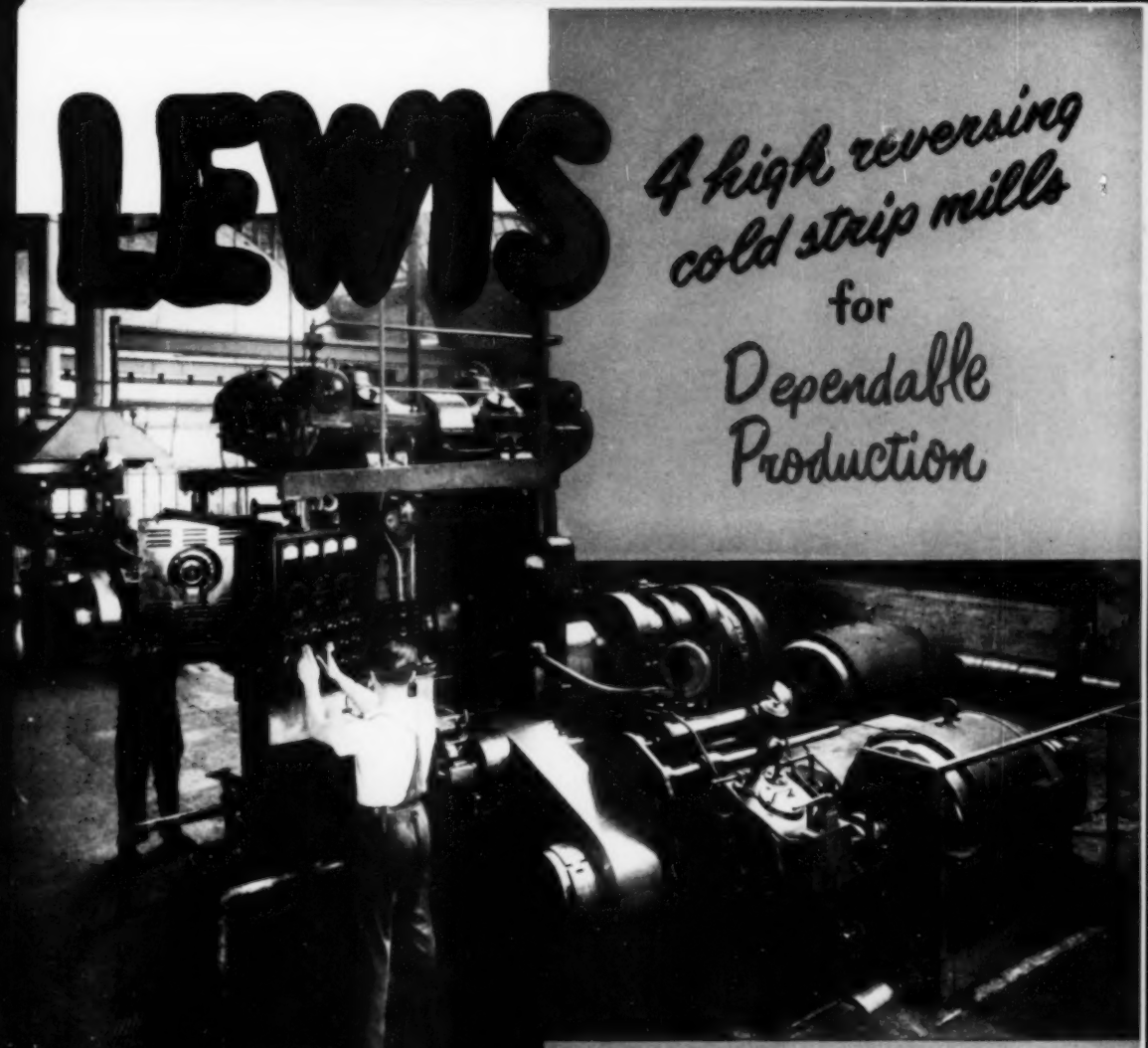

MANUFACTURERS OF
ROLLS AND ROLLING MILL EQUIPMENT
FOR THE IRON, STEEL AND
NON-FERROUS
INDUSTRIES

Two 7½" and 16½" x 18" 4-High Reversing Cold Strip Mills. One Stand (slow speed 285-570 f.p.m.) for roughing and One Stand (high speed 570-1140 f.p.m.) for finishing. Material rolled — medium and high carbon steel 12" wide — gauges .118" to .020". Flexibility provided in this equipment to accommodate a wide range of maximum and minimum gauges.

May we have the opportunity of studying your requirements and submitting our recommendations.
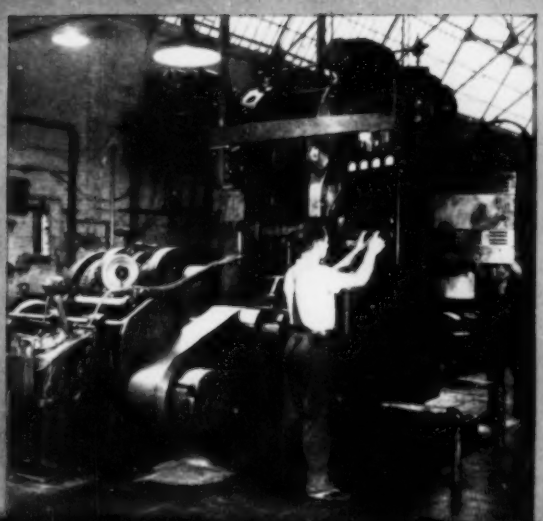
LEWIS FOUNDRY & MACHINE
Division of Blaw-Knox Company
Pittsburgh, Pa.